STRESS-STRAIN RELATIONSHIP IN CONCRETE

BY BENDING SIMULATION

ABSTRACT OF THESIS

Submitted by R.W. SMITHIES for the Degree of

Doctor of Philosophy of the University of London.

MARCH 1952

ABSTRACT OF THESIS

This work arose from the need of a thorough investigation of the factors involved in testing concrete specimens by Professor A.L.L. Baker's method of Bending Simulation. It was proposed to develop, from these investigations, a reliable technique for testing by Bending Simulation.

In Chapter I, a discussion of Bending Simulation explains how it may be used to obtain measurements of the stresses in a concrete specimen similar to an elemental length of a beam or column and subjected to the same linear strain-distribution.

The experimental work commenced with the installation of a hydraulic Bending Simulation machine. Numerous tests on the machine followed to determine the most accurate method of stress application. Two concrete specimens representing elements of beams were cast. Three types of strain gauges were used so that selection might be made of that type which proved most suitable for Bending Simulation tests.

Early attempts aimed at obtaining perfect linear strain-distribution across the compressive zone of the specimen. Linear stress-distribution in the elastic range produced strain distributions at various 'gauge banks' (transverse sections of the beam element where strain measurements were recorded) which showed, at each gauge, individual variations from a perfect straight line. These individual variations were repeated in a similar fashion under any linear stress-distribution in the elastic range. A perfect straight line strain-distribution on the gauge bank most

advanced in straining, however, could only be produced by an applied stress-distribution which was far from continuous. Also, because of strain-spreading along the length of the specimen, the ability of the recorded strain-distributions to indicate changes in the applied stress-distribution was limited. It was therefore necessary to take into account these repeated strain variations. Attempts were made to reduce this uneven straining. Results obtained by other experimenters from beam tests showed that these too repeated, up to failure, similar shapes only approximately linear. Further testing aimed at producing that strain-distribution which was found to exist under linear stress-distribution in the elastic range. The corresponding applied stress-distributions were accepted as representative of beam conditions.

To carry out this technique with the high degree of selectivity necessary to pin-point particular stress shapes, 'gauge factors' were evolved and 'corrected' strain diagrams graphed. A linear 'corrected' strain diagram indicated that the applied stress-distribution was of the same shape as that in a beam.

A basic technique for testing by Bending Simulation was thus discovered. Limited results indicated that the shape of the stress-distribution at failure for the particular combinations of crushing strength, rate of loading, etc..., corresponded closely to a cubic parabola. Values of constants required in plastic theories were evaluated for the particular case under test. Experimental evidence was collected to show that Bending Simulation copies closel those conditions which reliable measurement shows to exist in beams.

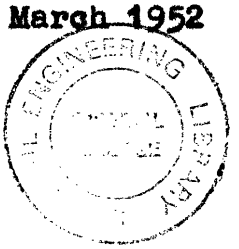
---//---

STRESS-STRAIN RELATIONSHIP IN CONCRETE

BY BENDING SIMULATION

A Thesis Submitted by R. W. Smithies for the Degree of Doctor of Philosophy of the University of London.

March 1952



INDEX.

	Acknowledgements.	(v)
	Notation.	(vi)
CHAPTER I.	Introduction.	1
	Summary of Professor A.L.L.Baker's	5
	Plastic Theory.	5
	Prototype Bending Simulation Machine. .	9
CHAPTER II.	Bending Simulation Machine.	13
	Multi-ram Hydraulic Loading Press. . .	13
	Control Panel.	15
	High Pressure Reciprocating Oil Pumps and Motors.	17
	Tensioning Device.	17
	Details of Construction of Specimens. .	20
	Construction of 1st. Specimen. . . .	20
	Arrangement of Specimen in Machine. . .	21
	Positioning of Strain Gauges. . . .	22
	Construction of 2nd. Specimen. . . .	24
CHAPTER III.	Electrical Resistance Strain Gauges.. .	25
	Equipment.	25
	Method of Construction.	28
	Calibration of Electrical Resistance Strain Gauges.	32
CHAPTER IV.	Optical Strain Gauges.	40

INDEX.

	Factors Governing Design.	40
	Optical Strain Gauge Lay-Out Developed and Adopted..	42
	Assembly and Adjustment of Gauges. . .	49
	Tests on Optical Gauges..	50
	Conclusions for Optical Gauge Tests.. .	54
	Metzger Strain Gauge.	58
CHAPTER V.	Pressure Gauge Calibration Tests. . .	59
	Tests on Automatic Cut-Outs for Pressure Gauges..	66
CHAPTER VI.	Investigation and Development of Technique on Concrete Specimen.	69
	Loading Technique.	70
	Observations of Strain Spreading. . .	75
CHAPTER VII.	Effect on Strain of Tension Application..	83
CHAPTER VIII.	Test of 1st. Specimen.	93
	Linear Strain Distribution on One Bank of Strain Gauges.	105
CHAPTER IX.	Experiments and Adjustments to Reduce Uneven Straining.	112
	I.) Two Proving Rings in Eccentricity Test.	112
	II.) Alignment of Specimen in Machine. .	116
	III.) Grouting of Specimen.	119
CHAPTER X.	Testing of 1st. Specimen Continued to Destruction..	120

INDEX.

	Changes and Improvements in Straining. .	123
CHAPTER XI.	Gauge Factors.	131
	Gauge Factor Determination.	133
	Application of 'Gauge Factors' to Results.	137
	Typical 'Corrected' Strain Diagrams.. .	138
CHAPTER XII.	Testing of 2nd. Specimen.	141
	Creep.	152
CHAPTER XIII.	Results and Conclusions.	154
	Stress-Distributions Corresponding to Those in a Beam Failing in Compression. . .	162
	Comparison Between Mathematical Figures and Stress-Distributions.	163
	Calculations Resulting from Stress Distribution at Failure.	168
	Stress-Strain Relationship at Points in The Compression Zone During Varying Load Stages.	171
	Discussions Arising from Test on Second Specimen.	183
	1): Tensioning.	183
	2): Type of Failure.	185
	Total Load against Strain at Different Fibre Depths.	188

(P.T.O.)

INDEX.

CHAPTER XIII.(Contd.)

Brief Summary of Conclusions. . . . 195

Further Research. 197

BIBLIOGRAPHY. 198

Appendix I. Sensitivity Factors. 200

Appendix II. Typical Result Sheet from Optical Gauge Tests. 201

Appendix III. Pressure Gauge Calibration. 202

Appendix IV. Table of Trial Run on Pressure Gauge No.2. Showing Comparison Between Estimated Load and Actual Load Given by Proving Ring. . 203

Appendix V. Pressure Gauge Indicator Readings. . . 204

Appendix VI. Results of Eccentricity Test Using Two Proving Rings. 205

Appendix VII. 'Gauge Factors' 207

Appendix VIII. 'Gauge Factors' for Central Bank of Second Specimen. 210

Appendix IX. General Assembly of H.P.Pump. . . . 211

Appendix X. Wire Stretching Frame. 212

Appendix XI. Strain Distribution in Beams. . . . 213

Appendix XII. Cylinder Block Assembly. 219

ACKNOWLEDGEMENTS.

The author gratefully thanks Professor A.L.L.Baker for his supervision, ready encouragement, and many helpful ideas given throughout the experimental work and during the preparation of this thesis. Gratitude is extended to all members of the D.S.I.R. Group at City and Guilds College and to fellow research students, particularly V.M.S.Ziauddin, K.A. Everard and A.H.Scott-Fleming, for their willing assistance and constructive criticism. The author is further indebted to A.H.Scott-Fleming for use of his apparatus in the manufacture of electrical resistance strain gauges, and to K.C.Productions for their part in the construction of the bending simulation machine. Thanks are also expressed to the C.E. Dept. workshop staff for their assistance.

NOTATION.

b Breadth of beam, or bending simulation specimen.

d Effective depth of beam, or beam element.

$n_1 d$ Depth of neutral axis.

T Total tensile force.

C Total compressive force.

C_u Cube crushing strength of concrete.

C_c Cylinder crushing strength of concrete.

t_y Tensile stress in reinforcement at failure.

C' Stress at extreme compression fibres.

e_m Strain at extreme compression fibres.

$\alpha n_1 d.C'$ Area of compressive stress-distribution diagram.

$\gamma n_1 d$ Distance of c.g. of compressive force from extreme fibres.

p_s Percentage of tensile reinforcement.

E'_s 'Secant' modulus of elasticity for steel.

E'_c 'Secant' modulus of elasticity for concrete.

e_x Strain at any point distant x(d) from extreme compressive fibres at failure.

C_x Stress at any point distant x(d) from extreme compressive fibres at faiure.

m' $\frac{E'_s}{E'_c}$

E_c Low stress, or elastic value, of E'_c.

M' Ultimate resisting moment of beam, or beam element.

In prestressed beams, the ratio of the stress in the steel, when the concrete stress adjacent to the steel is zero, to the stress in the steel at ultimate load. (P.T.O.)

NOTATION. (Cont'd.)

F — Ratio of the average strain in the concrete adjacent to the tensile reinforcement to the maximum strain in the concrete adjacent to that reinforcement.

Z — $\frac{F}{2\alpha(1-\beta)}$

CHAPTER I.

INTRODUCTION.

For many years conscientious engineers concerned with the design of structural members in reinforced concrete have shown much interest in the development of ultimate load theories. Because these theories take into consideration the experimental fact that the theory of elasticity does not apply for failing load, they have come to be referred to as the "plastic theories" for ultimate strength. The fundamental assumptions which have been adopted as a foundation for numerous plastic theories for the ultimate strength of reinforced concrete beams are similar up to a point. Two of these assumptions are just and equable; they are: strain is directly proportional to distance from the neutral axis: concrete has no tensile strength. With the particular exception of Professor A.L.L.Baker's plastic theory, a third assumption is then made, and a definite stress-distribution is assumed for the concrete in compression. It is in this third assumption that there is much controversy and difference of opinion. Up to the present, in the absence of a method of measurement of the stresses in the compressive fibres at different distances from the neutral axis, it has been necessary for theorists to make this third assumption for, without it, no correlation could be made between the ultimate strength of the beam and the cube, cylinder or prism strength of the concrete.

Specific assumptions of stress-distribution made by several theorists are as follows;-

C.S.WHITNEY[1] (1937). Assumes '... a simple equivalent (rectangular) stress block which closely approximates the effect of the real distribution at maximum load.' This assumption is made after a study of the stress-strain relationship in concrete cylinders, and is therefore, in effect, a corollary to the more basic assumption that the stress-distribution in a beam is of the same shape as the stress-distribution curve in concrete cylinders.

K.HAJNAL-KONYI[2] (1937) assumes that the stress-distribution in a beam is of the same shape as the stress-strain curve in concrete prisms.

K.C.FOX[3](1941) assumes that the stress-distribution in a beam, immediately before failure, is rectangular.

Some of the mathematical assumptions for the stress-distribution in a beam are:-

L.J.MENSCH[4](1914) Cubic Parabola.

H.KEMPTON DYSON[5] (1922) Quarter-Ellipse.

V.P.JENSEN[6](1943) Trapezium.

(For a more detailed study of the above theories see M.Sc.(Eng) thesis, 1949 by H.D.STEAD.[7])

The stress-distribution, except in cases where it is replaced by an equivalent stress block, extends from the neutral axis to the outer compression fibres

of the beam. Integration of the area of the particular stress-distribution assumed gives the total compressive force in terms of the neutral axis depth and cube, cylinder or prism strength. The neutral axis depth is generally computed, in under-reinforced beams, by equating the total compressive force to the total tension force, whilst in over-reinforced beams either a limiting value of the neutral axis depth is assumed or, alternatively, the neutral axis depth is determined by consideration of the steel and concrete strains. The line of action of the compression force passes through the centre of gravity of the area and can be determined by calculation. Thus an expression is derived relating the ultimate resisting moment of reinforced concrete beams to the cube, cylinder or prism crushing strength of the concrete.

If this controversial assumption of a specific stress-distribution could be avoided, and if instead, a method of measuring the stresses in the compressive fibres at different distances from the neutral axis could be utilised, then:-

(i). Differences of opinion regarding the shape of the stress-distribution diagram would be cleared up, and

(ii). The foundation would be laid for a plastic theory more closely representing actual conditions. With this in mind the idea of Bending Simulation was evolved.

The chief aim of Bending Simulation, therefore, is to obtain measurements of the stresses in a reinforced

concrete specimen which is similar to an elemental length of a beam and is subjected to the same linear strain-distribution. It is, however, clear that such tests can be extended to include columns subjected to bending and, since by this method of testing, values of the modulus of plasticity for the concrete are easily obtainable, it may also be applied with relation to plastic hinges in frameworks.

In 1949 PROFESSOR A.L.L.BAKER[8] brought forward a plastic theory which was well adapted to the solution of ultimate load problems not only in normal reinforced concrete beams but also in end-anchored and bonded pre-stressed beams. Because of this it was clear that the theory possessed a decided advantage over other plastic theories, and if the shape of the stress-distribution could be determined by bending simulation, the theory would be strengthened still further. It is felt that the student reader, if he is not already conversant with the details of Professor Baker's theory, should be strongly recommended here, to read Professor Baker's Paper to the Institution of Civil Engineers[8]. In this way references, made in this thesis to the details of that work, will become clear. This Introduction would not be complete, however, without the inclusion of the salient features of this plastic theory.

(P.T.O.)

Summary of Professor Baker's Plastic Theory.

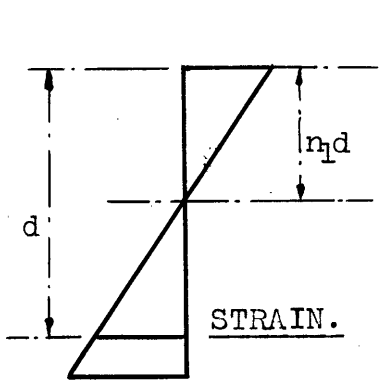


Fig. (i).

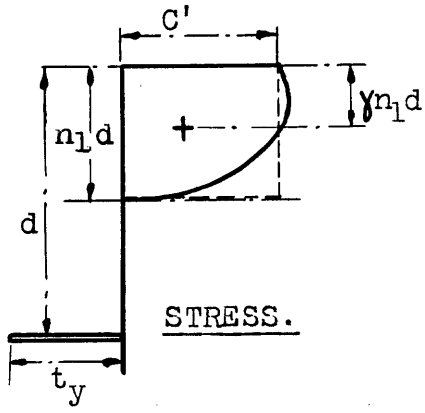


Fig. (ii).

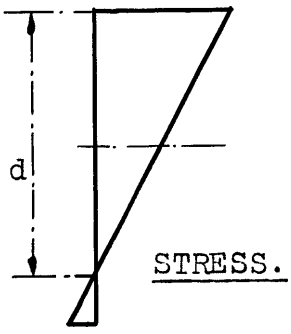


Fig. (iii).

Assumptions.

(i). Strain is directly proportional to distance from the neutral axis.

(ii). Concrete has no tensile strength.

(iii). The ultimate strength of a beam is the moment of resistance when, under increasing load applied at the worst rate likely to occur in practice, either:

(a). the concrete commences to crush, or it attains a stress at which a few repititions of load, or sustained load, would cause crushing, either without the tensile steel yielding or as a result of the steel yielding and causing the neutral axis to rise; or

(b). the steel fractures or attains a stress at which a few repititions of load, or sustained

load would cause fracture.

Notation. (See p. vi.)

Equating the total strain in the steel, which occurs under increasing load from the stage shown in fig.(iii) up to failure, to the total virtual tensile strain in the adjacent concrete over the length of the beam; and dividing by the beam length,

$$\frac{t_y(1-\beta)}{E'_s} = F.\ \frac{C'}{E'_c}\frac{(1-n_1)}{n_1}$$

$$\therefore \quad t_y = \frac{F.\ C'\ m'(1-n_1)}{n_1\ (1-\beta)} \quad . . (1).$$

Substituting for $Z = \frac{F}{2\alpha(1-\beta)}$ and transposing,

$$n_1 = \frac{1}{1 + \frac{t_y}{2\alpha Z m' C'}} \quad . . . . . (2).$$

In bonded pre-stressed beams $F = 1$; in ordinary reinforced concrete beams $F = 1$, $\beta = 0$, and $Z = 1$.

((for reinforced concrete beams, therefore, $n_1 = \frac{1}{1 + \frac{t_y}{m' C'}}$ ..(2)a.))

Equating total tension to total compression,

$$\frac{p_s bd}{100} . t_y = \alpha C' n_1 . bd$$

and substituting for t_y from eqn. (1),

(P.T.O.)

$$n_1 = \frac{-p_s + \sqrt{p_s^2 + \frac{200 \cdot p_s}{Zm'}}}{\frac{100}{Zm'}} \quad . \quad . \quad . \quad (3).$$

$$\text{or} \qquad p_s = \frac{50n_1^2}{Zm'(1-n_1)} \quad . \quad . \quad . \quad . \quad . \quad . \quad . \quad . \quad . \quad (4).$$

The ultimate moment of resistance of a rectangular section which fails by crushing of the concrete is given by:-

$$M' = \alpha C' b n_1 d^2 (1 - \gamma n_1) \quad . \quad . \quad . \quad . \quad . \quad . \quad (5).$$

Equation (2) may be used to find the value of n_1 for assumed simultaneous values of t_y and $\alpha C'$. The value of p_s which must be used, so that steel and concrete develop stresses t_y and C' simultaneously, i.e. balanced design, can then be determined from expression (4).

If, as is generally the case, failure occurs by steel fracture or yield causing concrete-crushing, the expression (4) may be used to find the value of n_1 when p_s is known, and hence the true value of the lever-arm. Since the lever-arm for a balanced design is smaller than for a case in which failure is due to steel fracture or yield, it is safe and generally convenient to assume the lever-arm to have the balanced design value when calculating the area of steel required direct from the applied bending moment.

Except for expression (2)a,

which is adapted for ordinary reinforced concrete beams, the fore-going equations are general and can be applied to rectangular sections whether of reinforced concrete or pre-stressed concrete (bonded or end-anchored); the constants F and β make possible true differentiation between these differing modes of construction.

---//---

Beam tests in which the required measurements of the steel strain and concrete strains at different fibre depths and of the applied bending moment (and conditions of pre-stress in the case of pre-stressed concrete beams) are recorded, enable many of the factors involved in Professor A.L.L.Baker's theory to be determined for a given combination of steel and concrete qualities and proportions. But careful consideration reveals that if no assumption or measurement of the stress-distribution in the compressive zone is made, recordings from beam tests alone are not sufficient to ascertain, either,

(i). the shape of the stress-distribution in the compressive zone, or,

(ii). <u>independent</u> values of α, C' and E_c', or,

(iii). any relationship existing between C', the extreme fibre stress, (or any other fibre stress) and the corresponding concrete cube, cylinder or prism crushing strength.

The relationship mentioned in (iii) might be investigated if E_c'

were known, but an assumption of E_c' from cube, cylinder or prism tests would be subject to the same uncertainty and controversy as is the assumption that the stress-distribution in beams is similar to the stress/strain curve in a concrete cube, cylinder or prism. Clearly a great advantage would be gained if the distribution of stress in the compressive fibres at different distances from the neutral axis could be measured. If this were achieved the essential points, (i), (ii) and (iii) mentioned above, and other additional factors required in 'plastic theory', would be readily resolved.

Bending Simulation endeavours to subject a concrete specimen which is similar to an elemental length of a beam to the same conditions of straining as are present, without question, in the fibres of a beam, and then to measure the distribution of applied stress which was required to produce these conditions of straining.

---//---

Prototype Bending Simulation Machine.

At City and Guilds College under the supervision of Professor A.L.L.Baker, the Department of Scientific and Industrial Research designed a mechanically operated Bending Simulation Machine the forerunner of the present hydraulic one. This prototype machine carried a specimen representing a beam element 14"deep x 12"long and 3"wide. Tension was applied by a steel bar threaded at its

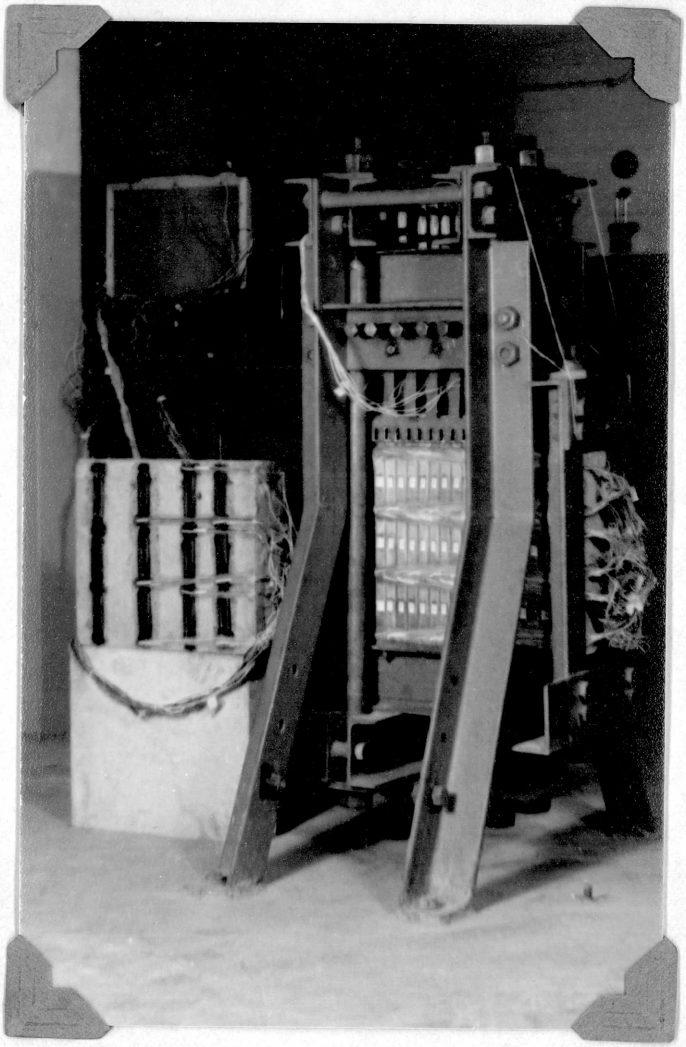


Fig.(i).

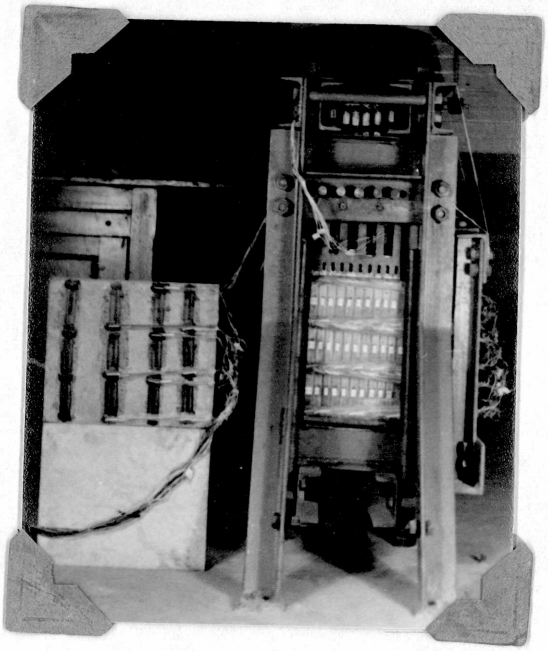


Fig.(ii).

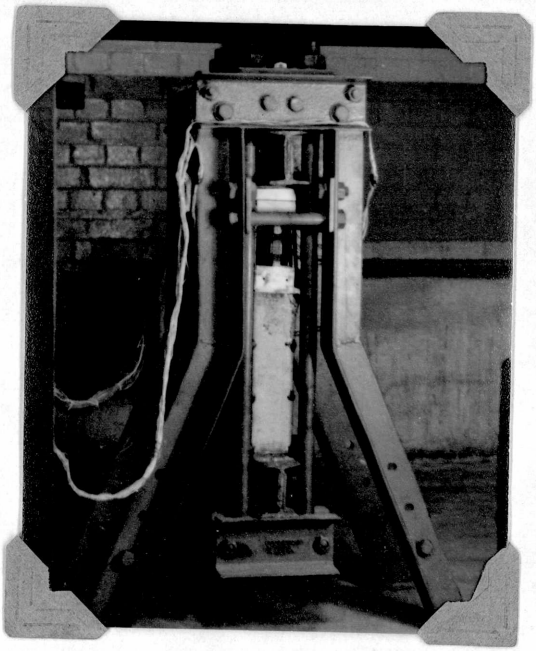


Fig. (iii).

Prototype Bending Simulation Machine.

ends running through the length of the element and stretched by tightening two nuts against a frame. See fig.(i), p. 10 The specimen was slung from the main frame of the machine by four long bolts and its lower loading face rested directly against a short length of steel 'I' beam. Stress was applied to the specimen by ten load points. Each load point was operated by forcing a wedge between the upper 'I' beam of the main frame and a short steel strut, each strut transmitted its load to the upper loading face of the specimen, see fig.(iii). The short steel struts acted as dynamometers measuring the load at each point, they were 'pin-ended' in an attempt to eliminate side thrust. The wedges were forced together by tightening set-screws (fig.(ii).).

The disadvantages of the machine were manifold. Firstly it was very difficult to attain high loads without lateral movement of the specimen causing the dynamometers to fall over; secondly there was no way of controlling the rate of loading; thirdly the applied stress-distribution at the top of the specimen was not repeated at the lower load face, consequently strain spreading and/or stress spreading was very pronounced.

A thesis by A.H.Scott-Fleming dealing with work on this machine is in the course of preparation.

---//---

The original experimental work to be recorded in this research set out firstly to discover methods of testing concrete specimens representing elemental lengths of beams or columns by Bending Simulation using a hydraulic Bending Simulation machine, and secondly, as a result, ultimately to produce a reliable technique for this testing by Bending Simulation. Clearly the method of measuring the loads stressing the specimen and that adopted for strain measurement should combine reliability with speed of operation. To ensure this the author tried various types of strain gauges and selected the most suitable. Attention was given to the system of load application and recording so that a high standard of accuracy might be achieved. The author then proposed to examine closely the results obtained as the tests proceeded and, by making strict comparisons with those conditions which reliable measurement has shown to predominate in beams, to develop a basically sound testing procedure. Precise measurements of straining at adjacent fibres in a beam are readily obtainable. Once these conditions could be accurately reproduced in all the compression fibres of the beam element by Bending Simulation, then the stresses producing these deformations would give the stress-distribution in a beam.

---//---

CHAPTER II.

BENDING SIMULATION MACHINE.

The main units of construction of the Bending Simulation Machine are :-

(i). Multi-ram hydraulic loading press.

(ii). Control panel with pressure gauges, oil-pressure relief valves, and electrical control switches.

(iii). High pressure reciprocating oil pumps and motors.

(i). Multi-ram Hydraulic Loading Press.

The loading press is illustrated on p. 14 and can also be seen diagrammatically on p. 113 . Mounted on a heavy baseplate are six cylinder blocks each containing five 1½in. dia. pistons connected in a line by an oil duct drilled along the cylinder block; each row of five piston rams operates one of the six lower loading blocks. The reaction from the specimen, when a load is applied, is transmitted from the upper part of the machine through four 3ins. dia. pillars to the baseplate. There is an independent oil pressure circuit, including pump, for each pair of upper and lower cylinders. The oil is delivered by the pump to a junction piece carried on the baseplate; here the pipe divides, one branch going direct to the lower cylinder



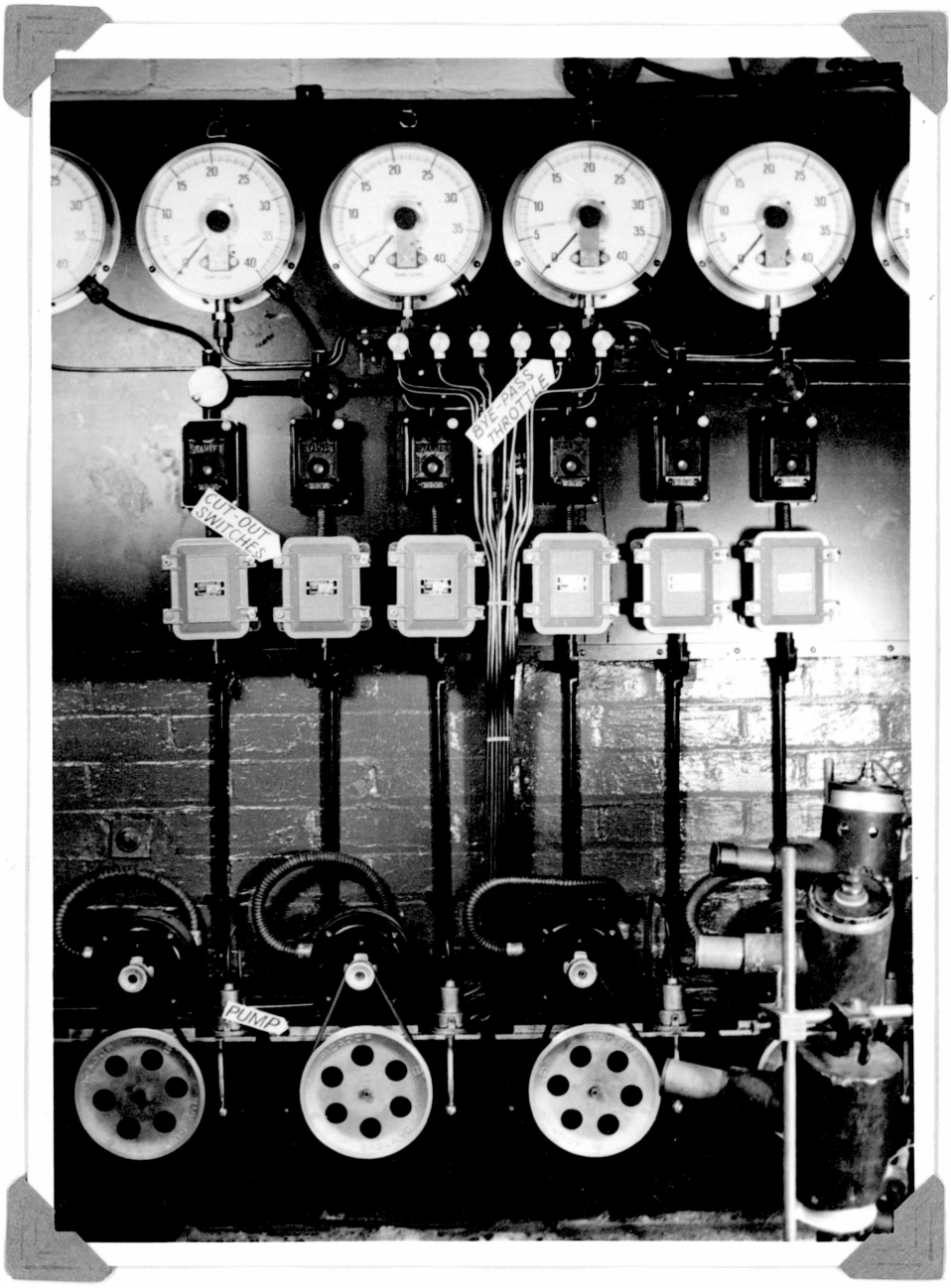
GENERAL ARRANGEMENT.

BENDING SIMULATION MACHINE AND SPECIMEN.

block, the other after looping to allow flexibility, is connected to the corresponding upper cylinder block.N.B. This latter arrangement is best seen on p.48.

(ii). Control Panel.

The control panel is mounted on the wall at a short distance from the loading press. Six 10"dia. Bourdon type oil pressure gauges run across the top of the control panel. Immediately under these gauges, and placed close together for ease of control, are six pressure relief or by-pass valves. Also mounted on the control panel are the press button 'start' switches for the motors, and the cut-out switches. (See p.16) On each pressure gauge there is a subsidiary pointer which can be set to any desired load on the scale of 40tons, by hand adjustment of a central knob. In the normal running position the electric circuit for the pump motor passes through a mercury-boat in the cut-out switches. This mercury-boat is carried on a crank lever the other arm of which is in close proximity to an electro-magnet. When the pressure indicator pointer of the Bourdon gauge reaches the adjustable pointer, the coil of the electro-magnet becomes energised and rotates the crank lever which in turn tilts the mercury-boat. The main circuit is then broken, as the mercury runs off one of the contacts, and the pump motor stops. Should the load, however, then fall off sufficiently to cause the pressure indicator pointer to break contact with the



CONTROL PANEL, PUMPS AND MOTORS.

adjustable pointer, the electro-magnet is de-energised, the mercury-boat returns to the horizontal position causing the main motor circuit once more to be completed, and the pump motor starts once more.

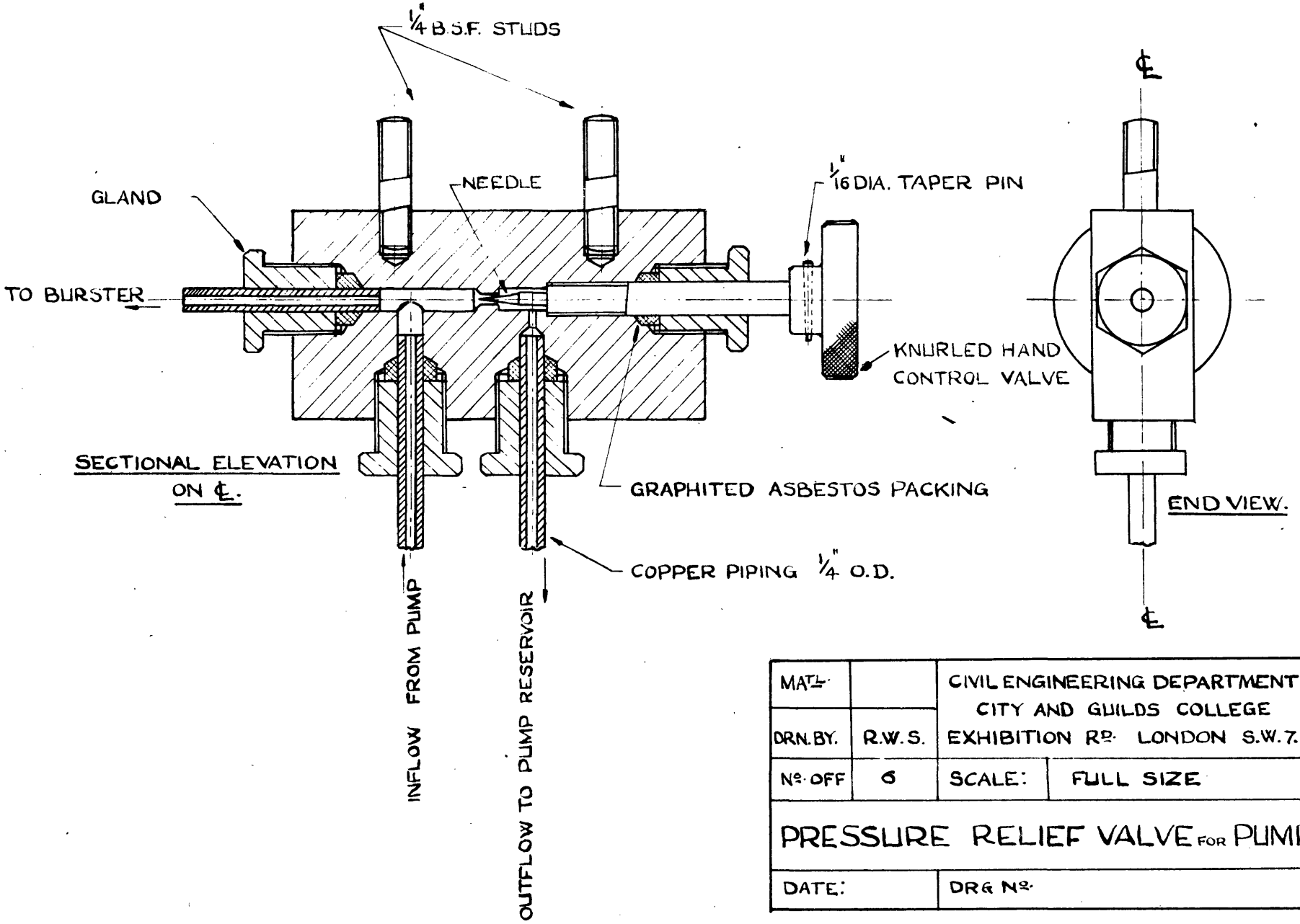
(iii). High Pressure Reciprocating Oil Pumps and Motors.

The six pumps and motors for the six pairs of loading blocks were mounted on an inverted channel iron at the foot of the control panel. The electric motors were ¼H.P., 50c.p.s., single phase A.C. motors running at 1425R.P.M. off the mains supply. The pumps (see Appendix IX) are two cylinder, single acting, reciprocating high pressure pumps driven by a Vee belt, reduction about 5 to 1, from the motor pulley. One revolution of the pump drive, therefore, completes a cycle of each cylinder, the delivery stroke in one cylinder taking place during the suction stroke of the other. The pump body itself acts as an oil reservoir, and the pressure relief or by-pass valve bleeds oil from the delivery side back into this reservoir when being used to reduce the load or control the rate of loading. See p.18.

Tensioning Device.

A drawing showing the components of the apparatus used to apply a tensile force to the specimen is shown in appendix X.p.212.

Two 3"x 3" 'I' beams formed the main



MAT'L.		CIVIL ENGINEERING DEPARTMENT CITY AND GUILDS COLLEGE EXHIBITION Rd. LONDON S.W.7.	
DRN. BY.	R.W.S.		
No. OFF	6	SCALE:	FULL SIZE
PRESSURE RELIEF VALVE FOR PUMP			
DATE:		DRG No.	

members of the tensioning frame. At the ends were two steel blocks 3" wide by $2\frac{1}{2}$" deep through which passed three groups of 2mm. high tensile steel wires. Each group of wires was anchored at both ends by an S.W.R. cone and tapered conical wedges. The outside group of wires had stretching bolts fixed on them which were prevented from rotating by means of a key held in position by the upper end block. The central group of wires was tensioned from the lower end in the same way. This was necessary to enable a spanner to be placed on the stretching nut of the central group of wires; also by having adjustment at both ends, more even application of tensile load to the specimen was achieved.

The end blocks butted up against 3" x $\frac{3}{8}$" steel plates welded to the inner faces of the 'I' beams. Four studs were screwed through the B.S.B. flanges into the block to prevent any tendency for the beams to spread. The stretching bolts were cupped at one end to carry the bearing ends of the cones. Two templates were made from $\frac{3}{16}$" plate to align the high tensile steel wires in the specimen during construction. The wires were grouped in three sets of twelve wires, the centre of the tensile force being $1\frac{1}{2}$" from the edge of the specimen.

The maximum theoretical load which could be applied by the wires when fully stressed was $16\frac{1}{2}$ tons.(breaking strength.) The load at the limit of

proportionality was 12½ tons.

-"- -"-

DETAILS OF CONSTRUCTION OF SPECIMENS.

Construction of First Specimen.

In choosing the dimensions of the specimen it was remembered that wherever possible the specimen should represent an element of a beam. With this in mind, the following dimensions were selected.

Dimensions of Beam Element (Specimen.)

Length of element	24"
Overall depth	21"
Width	8"
Effective depth	19½"
Weight	350lbs.

The mould for the specimen was constructed from seasoned ¾" timber with heavy 1" x 4" battens on both the large faces and the end faces. Special end plates, allowing clearance for the mould, were constructed out of ¾" plate so that the wire tensioning frame could be used to hold the wires in position during the pouring of the concrete. A wire spacing plate, similar to that shown on p. 212 , and made from strong pressed card was threaded over the wires and adjusted in the centre of the beam element. This formed an artificial crack which was designed to assist the tensioning device to crack the concrete.

The specimen was cast with the high tensile steel wires running horizontally along the bottom of the mould box.

This test, being the first to be carried out in the Bending Simulation machine, it was decided to choose a strength of concrete which would produce failure fairly well up the range of the machine. In this way it was hoped to minimize errors introduced by pressure gauge inaccuracies.

MIX.

1:2:4 by weight. $\frac{3}{8}$" aggregate. Water/cement ratio 0·6

Cube strength at time of testing: " " 4100lbs/sq.ins.

Cylinder strength at time of testing " 3500lbs/sq.ins.

Arrangement of Specimen in Machine.

The weight of the specimen including tensioning frame was of the order of 400lbs. and as two of the main faces of the block were covered with gauges, it was necessary to arrange a block for lifting purposes which did not interfere with the gauges. This was done by using two 4"x2" channel irons 12" long arranged back to back and bolted to one another by long $\frac{3}{8}$" dia. bolts sandwiching the specimen between them. The specimen could then be lifted by means of a block and tackle hooked into a shackle carried on the upper channel iron. In this manner the specimen was rotated through 90 degrees from its casting position and the tensioning device became vertical. (N.B. All further references to portions of the specimen apply to this, its position in the machine.) Two

thicknesses of felt packing paper were placed between the specimen and the hydraulic rams.

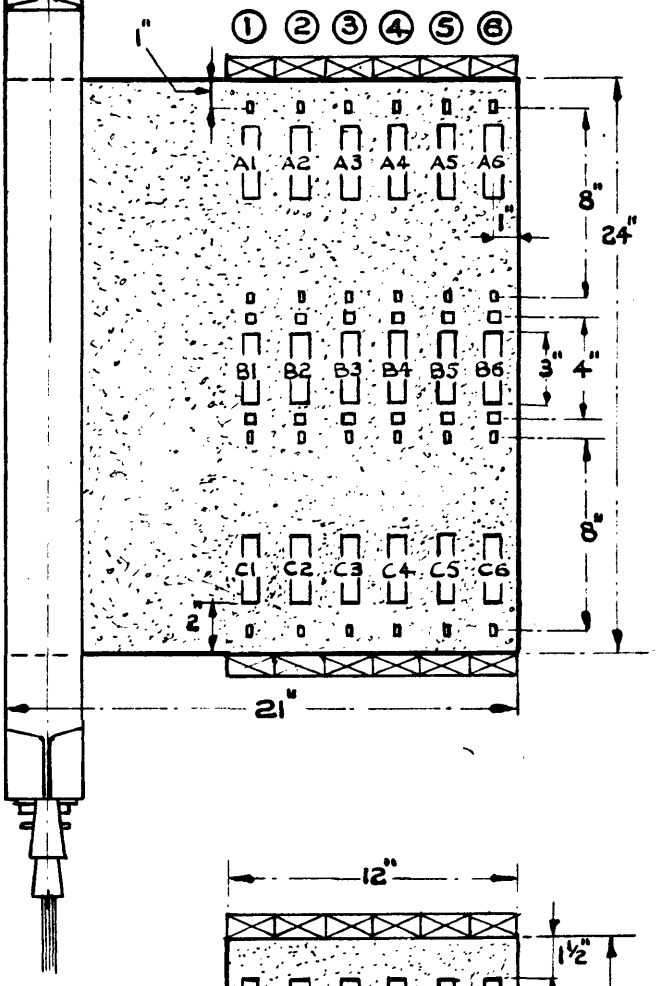
Positioning of Strain Gauges.

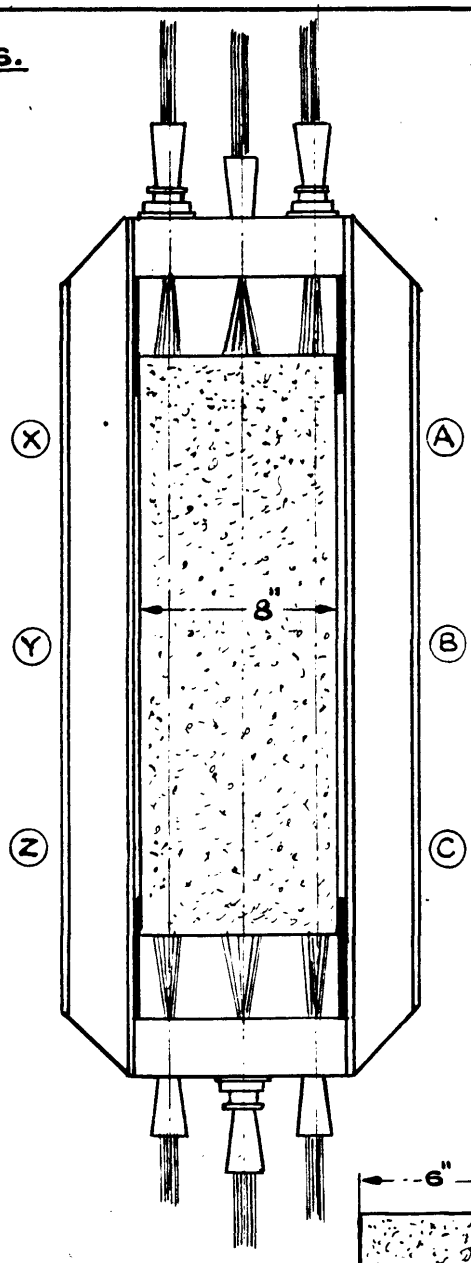
The position of the strain gauges was arranged as follows. See p. 23 . Three banks of six electrical resistance strain gauges were arranged on each side of the specimen, the upper section nearest to the top hydraulic rams being designated BANK 'A' on one side and BANK'X' on the other; the central bank, BANK'B' on one side and BANK'Y' on the other; the lower bank, BANK 'C' on one side and BANK'Z' on the other. Each gauge was numbered '1' to '6' commencing with number '1' under the hydraulic ram nearest to the tension side (and therefore nearest to the neutral axis) and finishing with number '6' nearest to the outer compressin fibres. The reader is requested to observe this method of notation carefully, as a picture of the position of any gauge on the specimen can then readily be obtained from its reference. E.G. 'A6' is the top gauge farthest from the neutral axis and on the first side of the specimen. 'Y2' is the second gauge away from the neutral axis in the central bank on the second side of the specimen ... etc. ... This system proved most useful and was retained during the second test.

The gauge length of the optical gauges was so arranged that they fitted conveniently over the electrical gauges. The six optical gauges

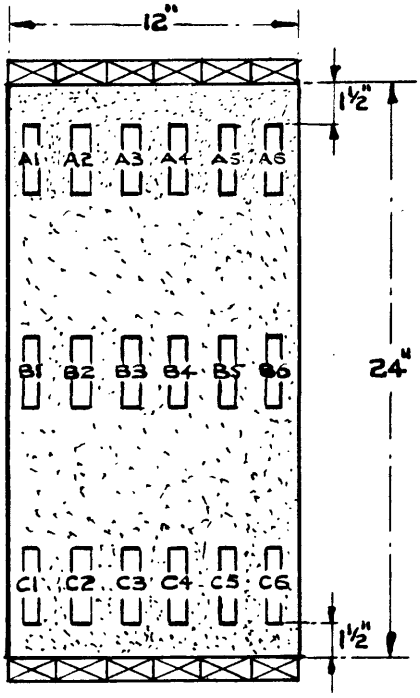
ARRANGEMENT OF STRAIN GAUGES.

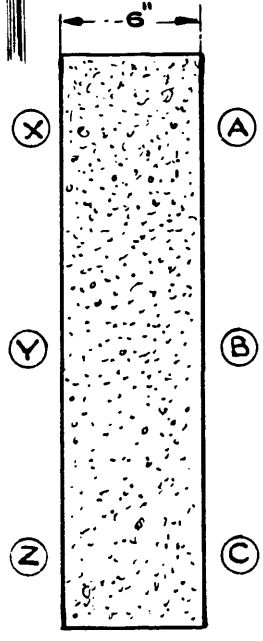
1ST. SPECIMEN.





2ND. SPECIMEN.





used on the first specimen were arranged over the central bank of electrical resistance strain gauges corresponding to 'B1'.....'B6'.

The Metzger gauge could not be used on the central portion owing to that position being taken up by the optical strain gauges, but 8" gauge length points were set up corresponding to banks 'A' and 'X', and 'C' and 'Z'.

Construction of Second Specimen.

In view of information gathered from the first test, the following modifications were made to the second specimen.

(i). Weight kept down to more manageable amount.

(ii). Electrical resistance gauges retained.

(iii). Tensioning device omitted.

Dimensions of Second Specimen.

Length of specimen	24"
Overall depth	12"
Width	6"
Weight	150lbs.

The end pieces of the mould were replaced by steel shuttering precision squared. The specimen was not artificially cracked.

MIX. 1:1½:2¼ by weight.

⅜" aggregate. Water/cement ratio 0·45

Cube strength at time of testing . .. . 6270 lbs./sq."

Cylinder strength at time of testing .. .. .. 5310 lbs./sq."

CHAPTER III.

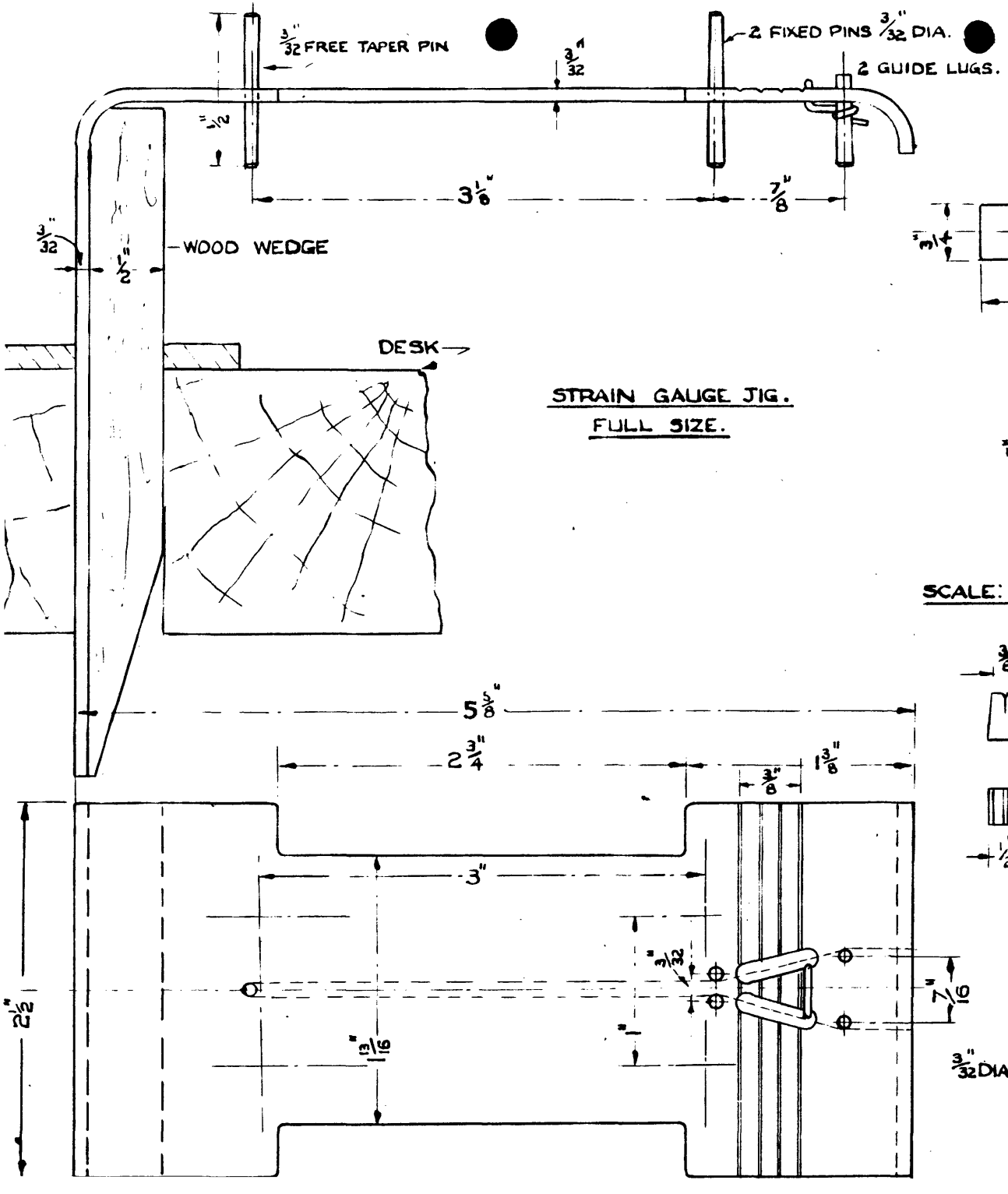
ELECTRICAL RESISTANCE STRAIN GAUGES.

Experiments carried out at Imperial College by R.D.Binns and H.S.Mygind[9] have shown that the maximum error of strain measurement increases directly with aggregate size and inversely with gauge length. Thus with an aggregate size of $\frac{3}{8}$" the maximum errors for gauge lengths of 1cm., 2cms. and 4cms. would be 40%, 12% and 6%, respectively. It was decided, therefore, to use gauge lengths as long as possible in order to reduce this error. No electrical resistance strain gauges with long gauge lengths could be obtained commercially, so the author undertook to make 3" electrical resistance strain gauges of a similar type to those made by Scott-Fleming.

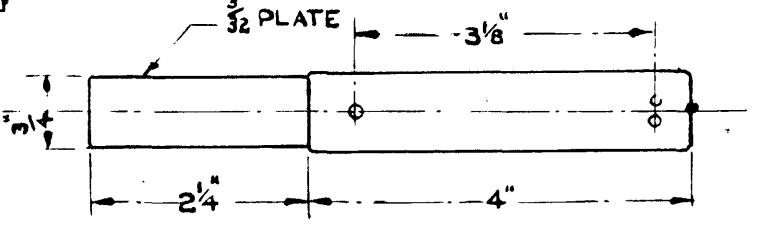
Equipment.

The following equipment was used in the construction of the electrical resistance strain gauges, drawings of which are shown on p. 26.

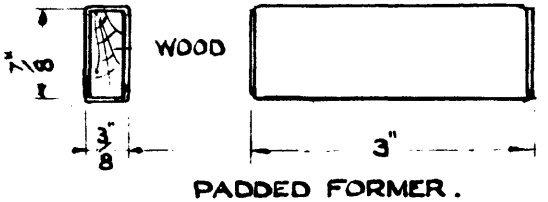
(i). A jig comprising a duraluminium plate $\frac{3}{32}$"nds. thick with a vertical and horizontal portion $2\frac{1}{2}$" wide. On the surface of the horizontal portion, guide lines were marked so that the gauge backing paper 3" x 1" could be accurately centred before clamping in position. A number of taper pins were fixed in the jig to hold the gauge wire in place. To prevent the lead wires becoming soldered to the jig, slots were cut in the jig at the position where the gauge wire joined the gauge



STRAIN GAUGE JIG.
FULL SIZE.

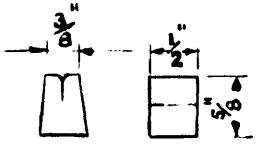


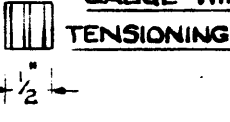
WETTING PAD.



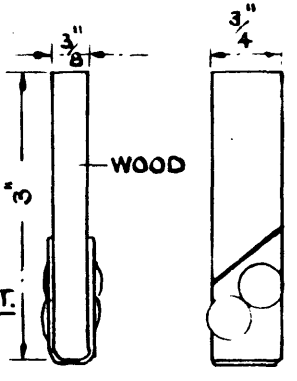
PADDED FORMER.

SCALE: HALF SIZE.

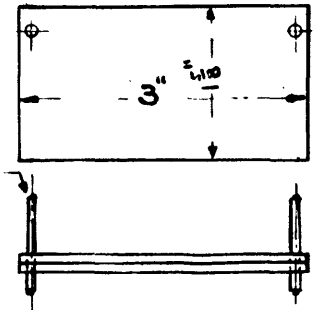




GAUGE WIRE TENSIONING WEIGHT.



SMOOTHING TOOL



GAUGE TEMPLATE

3/32" DIA. TAPER

lead wires. At right angles to the gauge wire a number of grooves were cut to carry the gauge lead wire during assembly. The second groove, which proved most convenient, was used for all but the first few trial gauges. A central taper pin at the rear end of the gauge was made, so that it could be removed quite easily from its position; by this means the gauge under construction could be removed from the jig. The jig was secured to the desk by means of a wooden wedge clamping the vertical portion into a rectangular slot in the desk.

(ii). A gauge template consisted of two duraluminium plates $\frac{3}{32}$" thick by $1\frac{5}{8}$" x 3" holding between them the gummed paper strip used to make the gauge backing. The plates were held together, during the cutting to size of the paper, by two taper pins located at the top corners of the template.

(iii). A wooden former covered with soft chamois-leather was used to carry a thin strip of insulating paper which 'sandwiched' the gauge wire against the backing paper.

(iv). A wetting pad, with holes drilled to allow it to be pressed close against the backing paper, when the gauge was in position on the jig, had its working surface covered with chamois-leather which was kept moistened with water.

(v). Gauge wire tensioning weights were cut from an india rubber and were suspended over the edge of the jig from the gauge wire.

(vi). A smoothing tool, padded at one end, was utilized to remove any wrinkles formed in the thin insulating paper.

(vii). Bulldog clips held the gauge and accessories in position at various stages during construction.

(viii). Two types of resistance wire were used in the construction of the gauges. The first type was annealed copper nickel wire 50 S.W.G.. In calibration tests carried out by A.H.Scott Fleming on gauges constructed from this wire it was found that the sensitivity factor of 1·85 changed by approximately 3% when the wire had been strained sufficiently to become work hardened. To overcome this difficulty - or rather added complication - the author also constructed gauges from hard-drawn copper nickel wire 0·001"dia.. This wire, being already hard, could not work-harden with straining and could not produce subsequent changes in sensitivity. N.B. The disadvantage of hard-drawn wire, however, was that being more brittle than annealed wire, there was a higher percentage of failures of gauges during construction. On the other hand, once the gauges were completed this difficulty waspassed. Both types of wire were supplied by Johnson, Matthey and Co.,Ltd..

(ix). Gauge lead wire was ordinary 12·5amp. fuse-wire.

Method of Construction.

A strip of gummed paper was placed in between the plates of the gauge template, squared up parallel

PROGRESSIVE STAGES IN STRAIN GAUGE MANUFACTURE.

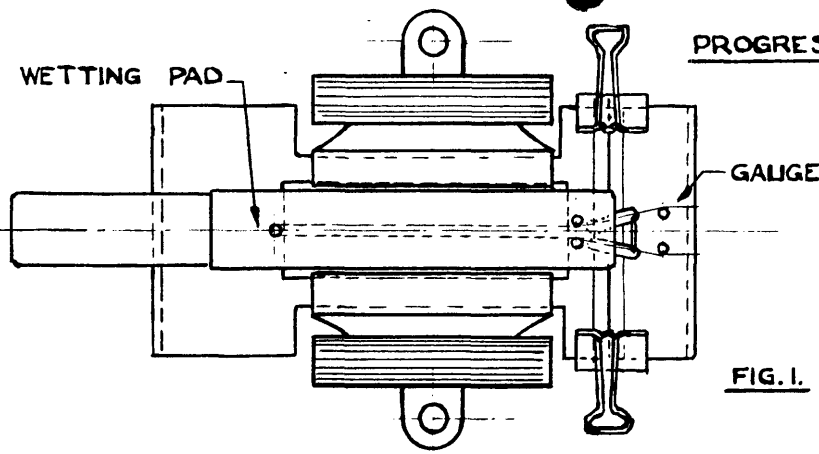


FIG. 1.

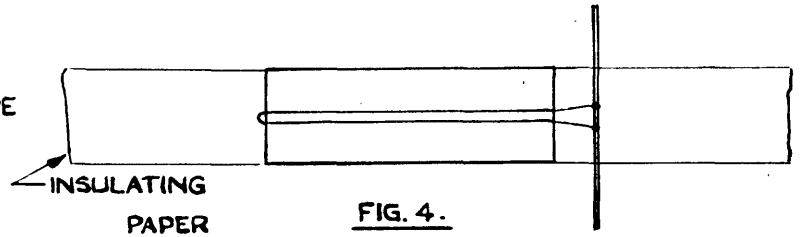
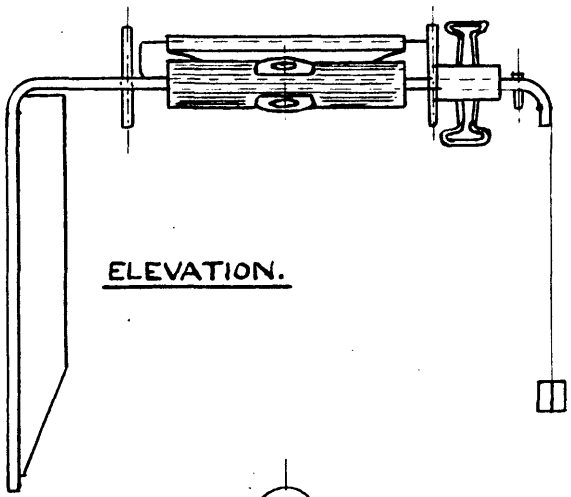


FIG. 4.



ELEVATION.

FIG. 2.

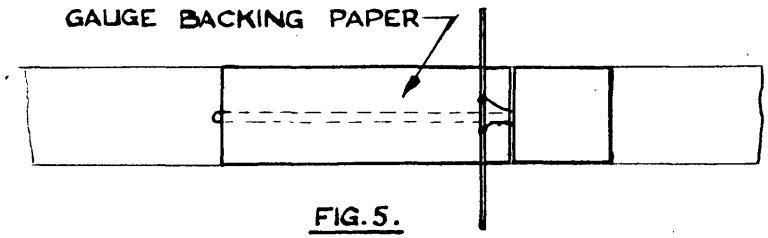


FIG. 5.

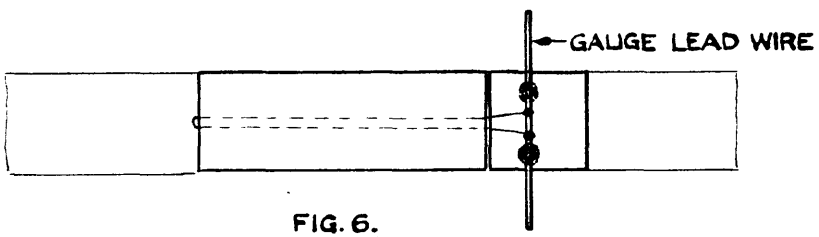


FIG. 6.

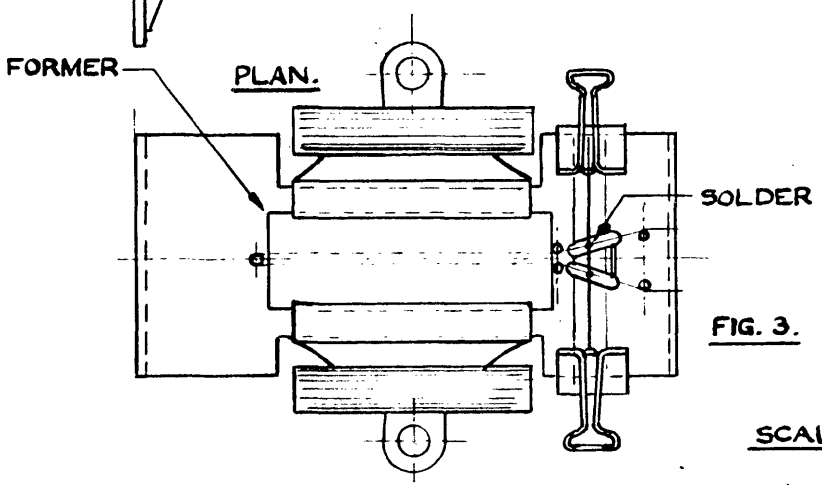


FIG. 3.

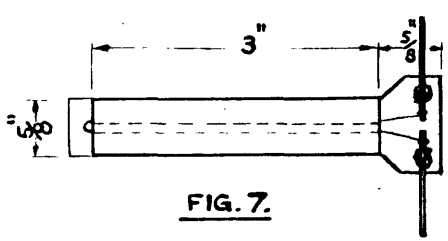


FIG. 7.

COMPLETED GAUGE.

SCALE: HALF SIZE.

to the long edge, and clamped tight by the two taper pins. The ends of the strip were trimmed with a razor-blade. The gummed paper, which now formed the gauge backing, was centred on the jig platform by the centre-lines marked for the purpose, and held temporarily in position by the Bulldog clips. A short length of fuse wire was cut and secured in the second groove at right-angles to the gauge wire, to form the gauge lead wire. A length of gauge resistance wire (crossing the gauge lead wire) was loaded with two rubber weights and positioned over the gauge backing paper. The weights thus gave to the resistance wire a standard tensioning. A strip of insulating paper was wound over the padded former and held loosely in place by moistening the top surface of the former. The wetting pad was pressed onto the gummed paper, being centered by the projecting taper pins. The apparatus at this stage of construction is shown in fig.1. p.29. Immediately after the removal of the wetting pad, the padded former and insulated paper covering were pressed onto the tacky surface of the gauge and clamped in position by the Bulldog clips. Whilst the gauge was held in this position, the soldering of the gauge resistance wire to the gauge lead wire was completed at the two points where these wires crossed one another. This was facilitated by using flux-solder and by employing a short piece of stout wire formed round the two guide lugs to act as a steady for the soldering-iron bit. See fig. 2 (elevation) and fig. 3 (plan) p. 29.for this stage in

gauge manufacture.

The removal of the gauge from the jig was done in the following way. First the electrical strain gauge resistance wire was trimmed at both ends close to the soldered joints. Secondly, the central taper pin, around which the resistance wire had been looped, was removed. Thirdly, all the Bulldog clips were released. Finally the gauge and wooden former were lifted bodily from the jig and transferred to the desk top, where the insulating paper was unwound from the wooden former and the gauge placed face downward as in fig.4. The smoothing tool was then used to even out any irregularities in the joint between the gauge backing paper and the insulating paper. The gauge was turned over and a small square of gummed paper attached to carry the gauge leads, see fig. 5. The gauge leads were stuck down to this paper-stiffener with 'Semmentum', (a tile glue) . See fig. 6. The gauge was then placed under weights and allowed to dry out. The final trimming of the gauge included nicking the gauge lead wire into two halves to prevent any shorting of the circuit. A final drawing of a completed gauge is shown in fig. 7. p. 29.

..././/.../.

Calibration of Electrical Resistance Strain Gauges.

In the first test carried out in the bending simulation machine the gauges used were manufactured by the writer from annealed copper nickel wire. The sensitivity factor of these gauges was, as already mentioned, known to be 1·85 with a 3% variation due to work-hardening. In the second test, however, hard drawn copper nickel wire was used, to avoid work-hardening, and calibration tests to determine the sensitivity factor were therefore necessary.

Four gauges with their resistances varying from 185·4ohms to 186·6ohms were selected for the test. These gauges were stuck with Araldite to a duraluminium beam 3'-3" by 2"x$\frac{3}{4}$", dried, and waxed in the normal way. Four other gauges were selected to act as dummy gauges and applied to a second duraluminium beam in precisely the same manner as the active gauges. The duraluminium beam carrying the four active gauges was placed in a loading frame. See p. 33. This loading frame had a short length of R.S.J. carried upon rollers which rested on the duraluminium beam at the quarter points. A hand wheel actuated a vertical screwed spindle which pressed a steel ball down upon the R.S.J., thus transmitting load to the beam and deforming it in circular bending. The vertical deflection of the beam at mid-span, relative to its deflection at the quarter points, was measured by a dial gauge carried by clamps fixed to the beam. Deflection readings of the dial gauge were, therefore,



CALIBRATION OF ELECTRIC RESISTANCE STRAIN GAUGES.

directly proportional both to the strain at the outer fibres of the duraluminium and to the strain in the electrical resistance strain gauges. A deflection of 0·271" on the dial gauge gave a strain in the extreme fibres of 0·00250ins./in..

Thus knowing the mechanical strain taking place in the duraluminium under the gauges, and measuring the 'electrical strain' in the gauges by means of the Parsons strain gauge box to which they were wired, the operator could determine values of the sensitivity factor, $\frac{\text{electrical strain}}{\text{mechanical strain}}$, at various load stages.

Calculation of mechanical strain.

L = length of beam between load points.

d = depth of beam in inches.

δ = deflection at mid-span in excess of quarter points.

R = radius of curvature.

θ = angle between tangents at quarter points.

$$L = R\theta$$

$$(2R - \delta) = \left(\frac{L}{2}\right)^2 = \frac{L^2}{4}$$

$$R = \frac{L^2}{8\delta}$$

Strain at outer fibres $= e = \dfrac{(R - \frac{d}{2})\theta - R\theta}{R\theta} = \dfrac{d}{2R}$

Substituting for R; strain $e = \dfrac{d}{2}\cdot\dfrac{8\delta}{L^2} = \dfrac{4.d\delta}{L^2}$

$$\text{or } \delta = \frac{eL^2}{4d}$$

Now $d = \frac{3}{4}"$; $L = 1'-6"$

Therefore for a strain of $0{\cdot}25 \times 10^{-4}$ corresponding deflection would be $\frac{eL^2}{4d} = \frac{0{\cdot}0025 \times 18^2}{4 \times 0{\cdot}75} = 0{\cdot}271$

Determination of Gauge Sensitivity Factor, λ.

η variable factor for Parsons box.

λ gauge sensitivity factor.

R original gauge resistance.

ΔR change in original gauge resistance.

d_r dial reading.

e mechanical strain.

Let 'X' be the scale reading given by the box when balanced for dial reading d_r.

Then $X = \eta(\frac{100\Delta R}{R})$

$$\frac{\Delta R}{R} = \frac{X}{100\eta}$$

and $$\lambda = \frac{\Delta R/R}{e} = \frac{X/100\eta}{e}$$

Now dial gauge reading of 2710 divisions gives a strain of :- 25×10^{-4} ins./in.

For a dial reading d_r,

$$\lambda = \frac{X}{100\eta} \div \frac{25 \times 10^{-4}}{2710} \cdot d_r$$

$$= \frac{10840.X}{\eta\, d_r}$$

Now $\eta = 2$; $\lambda = 5420. \frac{X}{d_r}$

If the graph of 'X' against 'd_r' is plotted for different beam

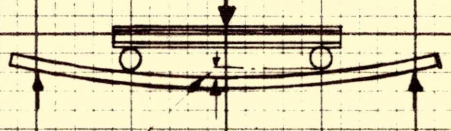
ELECTRIC RESISTANCE STRAIN GAUGE CALIBRATION TEST.

TYPICAL CURVES FOR GAUGE No: ① IN COMPRESSION.

KEY.

- 1ST. LOAD UP
- 1ST. LOAD DOWN
- 2ND. LOAD UP
- 2ND. LOAD DOWN

TEST ARRANGEMENT.



DEFLECTION.

$\frac{\%(100\Delta R)}{R}$

0·900
0·800
0·700
0·600
0·500
0·400
0·300
0·200
0·100
0

STRAIN %.

0·05 0·10 0·15 0·20 025 0·30

0 500 1000 1500 2000 2500 3000

DEFLECTION IN INCHES × 10

ELECTRIC RESISTANCE STRAIN GAUGE CALIBRATION TEST.

TYPICAL CURVES FOR GAUGE No. 1. IN TENSION.

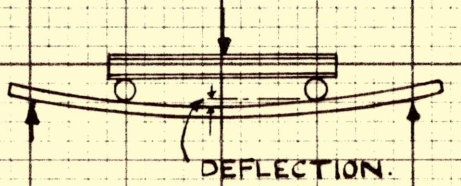
KEY.

- 1ST. LOAD UP
- 1ST. LOAD DOWN
- 2ND. LOAD UP
- 2ND. LOAD DOWN

$\frac{100\,\Delta R}{R}$

0·900
0·800
0·700
0·600
0·500
0·400
0·300
0·200
0·100
0

TEST ARRANGEMENT.



STRAIN %.

0·05 0·10 0·15 0·20 0·25

0 500 1000 1500 2000 2500

DEFLECTION IN INCHES × 10^{-4}

deflections, λ may be obtained from the slope of the graph.

for, $\lambda = 5420 . \frac{X}{(d_r)}$.

.../.../...

It was observed from the graphs of electrical strain plotted against mechanical strain, that with increasing deflection the sensitivity factor decreased slightly after a strain of 0·11% had been reached. On the other hand, when the deflection was decreasing, the graphs showed a higher sensitivity factor at the higher deflections and a lower sensitivity factor below a strain of 0·11%.

From the results it may be seen that the initial loading showed a small deviation from the subsequent loading curve. But in both the tests with the gauges in compression and in that in which the gauges were tensioned, the changes in the sensitivity factor became less, once an initial load had been carried. The average of four gauges gave a sensitivity factor of 1·93.

The graphs obtained from gauge No.1 with the first and second load applications both in tension and in compression, are given as an example. E.G. Gauge No. 1. Compression 2nd. load application:-

From zero up to $e = 0{\cdot}0013$ ins./in.

$$\frac{X}{d_r} = \frac{0{\cdot}448 - 0{\cdot}089}{1400 - 400} = \frac{0{\cdot}359}{1000} = 3{\cdot}59 \times 10^{-4}$$

(P.T.O.)

Now $\lambda = 5420 \times \frac{X}{d_r}$

$\therefore \quad \lambda = 5420 \times 3{\cdot}59 \times 10^{-4} = 1{\cdot}95$

By calculating λ for all the gauges, a table of results given in Appendix I. p.200 was compiled.

CHAPTER IV.

OPTICAL STRAIN GAUGES.

Of the three types of strain gauges which were used in the experiments, the optical gauges were the only type which was capable of giving direct comparison between the strain measured by one gauge and that measured by another. By direct comparison is meant the ability to be able to observe simultaneously, by some means or other, the strain at one point relative to another, as opposed to having to plot a graph of seperate readings. Direct comparison was attained by observing the relative positions of points of light upon a white screen placed a short distance from the specimen. In view of this advantage which optical strain gauges have over other types, it was considered to be well worth while doing searching tests on the apparatus used, so that the best accuracy which could be expected from the equipment available, might be obtained.

Factors Governing Design.

(i). Sensitivity.

The magnification factor, governed by gauge length, knife-edge dimensions and light lever-arm, should be sufficient to enable the smallest changes in strain to be easily detected.

E.G. Given,

$\frac{1}{8}$" Knife Edge.

4" Gauge length.

(P.T.O.)

10'-0" Light lever.

$\frac{1"}{50}$ Smallest observable movement of light on screen.

e Strain under gauge length.

Angle turned through by knife edge = $\frac{4e}{0{\cdot}125}$ = 32e radians.

Light deflection at screen = 10 x 12 x 2 x 32e

= 7680e

Magnification factor would be 7680

i.e. strain of 0·1% gives deflection of $\frac{0{\cdot}1}{100}$ x 7680 = 7·68"

Minimum strain detectable = $\frac{1}{50} \times \frac{1}{7680}$ = $2{\cdot}6 \times 10^{-6}$

This corresponds to a stress of 10·4lbs./sq.in. with an assumed 'E' for the concrete of $4{\cdot}0 \times 10^{6}$ lbs./sq.in..

A sensitivity of these proportions would be well within the limits of accuracy required.

(ii). Direct Comparison.

The light spots on the image screen should be so arranged that when they are adjusted to a straight line under no-load conditions, they will remain in a straight line for all subsequent load stages which produce straight-line strain-distribution across the face of the specimen.

(iii). Compensation.

Some method should be supplied to make allowance for irregular changes in the image position taking place due to:-

(a). Body movement of specimen or gauge.

(b). Temperature changes.

Optical Strain Gauge Lay-out Developed and Adopted.

The chief components of a complete unit were:-

(i). Gauge, including knife edge and mirrors.

(ii). Projector and stand.

(iii). Clamping device.

(iv). Image screen.

(i). Gauge.

The gauge body consisted of $\frac{1}{8}$" mild steel strip $\frac{5}{8}$" wide cranked at one end to form a fine 'claw' which was hardened and ground to give a firm, two-point contact at the fixed end of the gauge. At the 'gauge length' of 4" from this claw a fine groove was cut on the under-side of the gauge body. Into this groove fitted a ground steel knife-edge, carried on a spindle. Two highly polished steel concave mirrors, aperture diameter $\frac{5}{16}$", were fixed, one to the spindle of the knife-edge and the other to the upper face of the gauge immediately over the knife-edge groove. See fig.2. p. 43. A pin was screwed into the end of the gauge to assist in assembling the gauge into position.

(ii). Projector and Stand.

Considerable difficulty was met with in obtaining suitable types of projectors for the gauges. The chief difficulty was that of obtaining enough light concentration on the small concave mirrors to enable the light spot on the

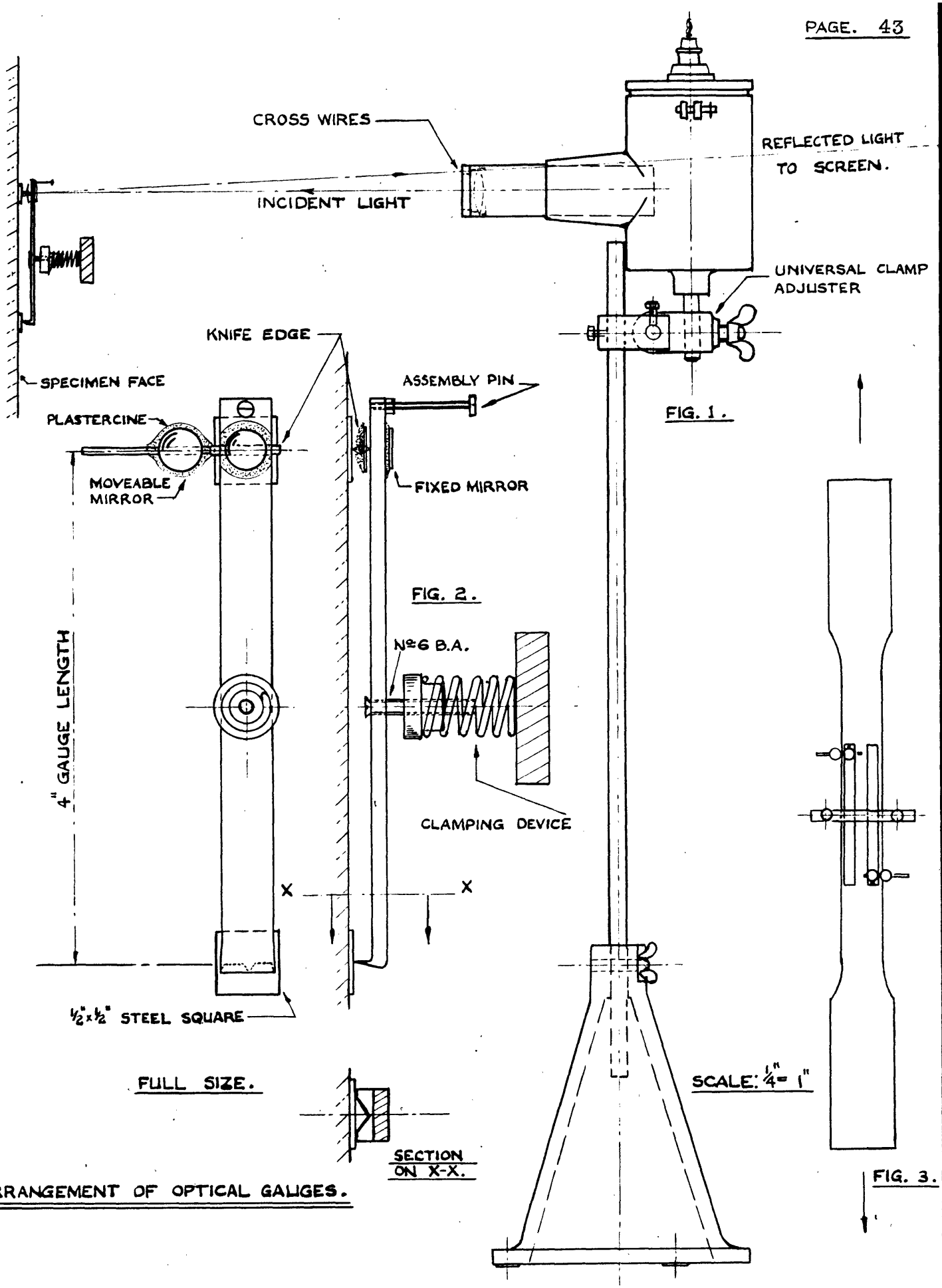


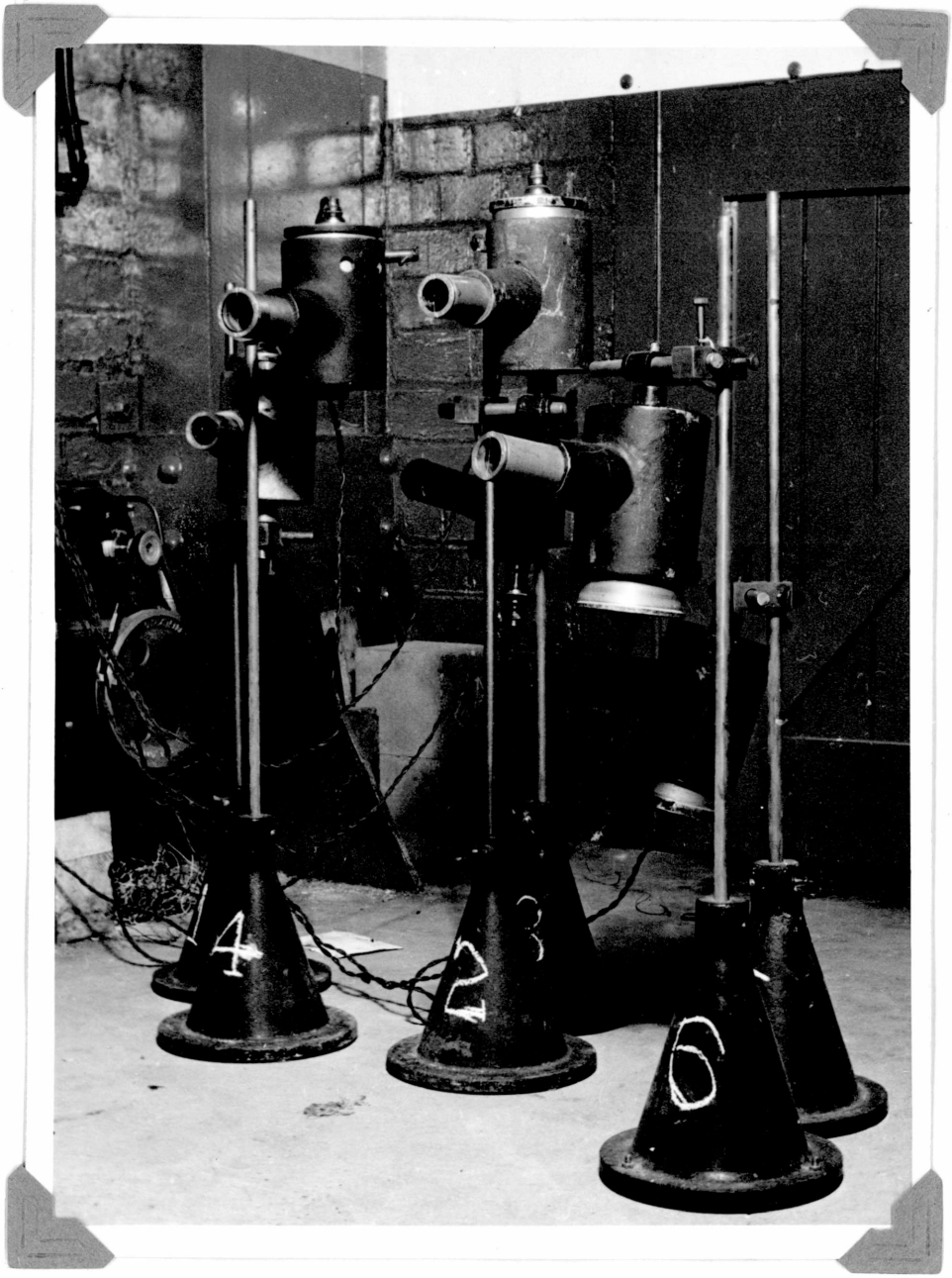
FIG. 1.

FIG. 2.

FIG. 3.

ARRANGEMENT OF OPTICAL GAUGES.

screen to be visible without having the room in total darkness. Finally, galvanometer projector units were used modified by the author to suit the particular needs of the case. In order to give an accurate 'spot'on the image screen, cross-wires were soldered over the aperture of the projector lens. Instead of a normal lamp, a 40watt, 20v. coiled coil filament lamp was fitted to each projector. Working off the 230v. mains supply, these gave an intense light which was focussed through the lens of the projector so that the image of the filament from one projector fell on both the fixed and moveable mirrors of the corresponding gauge. By this means two images were thrown on to the screen by each gauge projector. Movements of the first image - that from the moveable mirror mounted on the knife-edge - showed rotation due to straining under the gauge plus rotation and translation due to movement of the specimen and/or the gauge; whilst movement of the second image recorded rotation and translation due to movement of specimen and gauge only. By adjustment of the readings of the first image by the correction from the second, accurate strain measurements were obtainable. Unless, however, these corrections indicated by the fixed mirror could be applied <u>automatically</u> to the image thrown from the moveable mirror, direct comparisons of strains would be prevented as corrections would have to be added to all readings once any movement of the fixed mirror image had occured. The first idea was to re-zero the moveable mirror, when movement



ADJUSTABLE OPTICAL GAUGE PROJECTORS.

of the specimen was shown by the fixed mirror image, by adjusting it in its housing on the knife-edge spindle. This method of adjusting the zero proved too difficult as very small adjustments to the mirror angle by disturbing the plastercine mounting, besides being rather risky, proved to be impracticable. The solution adopted was that of mounting a universal clamp adjuster between the projector and its stand. See fig.1. p.43. and the photograph on p.45. This allowed fine adjustments to be made to the angle and position of the incident ray falling on the mirrors. In this way both the initial zeroing of the moveable mirror images on the screen, and any subsequent re-adjustment of zeros warranted by the movement of the fixed mirror images over the screen, could be obtained.

When the first projector lamp to be tried out in this way had been assembled, it was found that when the projector was supported on a normal retort-stand, its weight was too much and caused the image spots to waver. Heavy cast conical bases were substituted for the retort-stands and more robust pillars were made. These remedies were successful and by taking care that all the components were good fits, no further trouble was experienced from unreliable supporting arrangements.

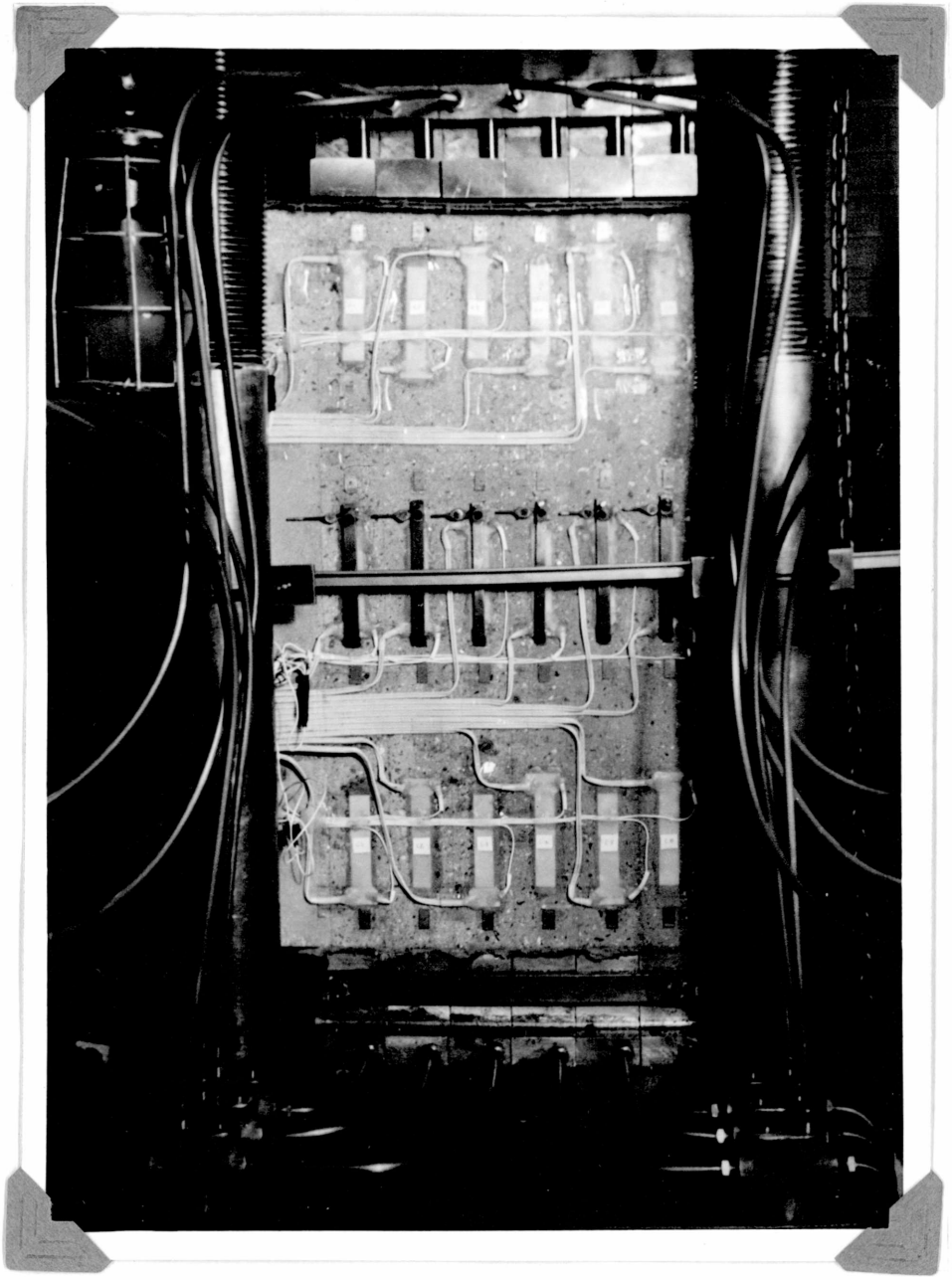
(iii). Clamping Device.

The following method was adopted for securing the gauges to the surface of the concrete specimen.

Small $\frac{1}{2}$"x$\frac{1}{2}$" by $\frac{1}{16}$" thick steel squares were firmly fixed to the surface of the concrete specimen. They were spaced 4", the gauge length, apart. There were six optical gauges in all, placed in a vertical position across the centre of the specimen. (The optical gauges can be seen in the photograph on p. 48.) The claw end of each gauge rested on the lower of the small steel squares and the knife-edge rested on the upper square. Through a tapped hole in the centre of each gauge protruded a screw which carried an adjustable knurled collar upon which was centred a stocky compression spring. Each compression spring served to hold the whole gauge against the vertical specimen face. These springs reacted direct against a heavy 1"x$\frac{1}{2}$" steel flat clamped to the specimen and running horizontally across the front of the gauges. This steel flat replaced an earlier idea, seen in the photograph, of a brass angle iron fixed to the vertical columns of the machine. The latter proved unsatisfactory as when relative movement occurred between specimen and machine, the gauge was disturbed on its seating.

(iv). Screen.

The image screen was fixed to the wall about 10ft. from the specimen. Care was taken to see that the screen was tilted to the correct angle so that the reflected rays falling on it did so normally. A large sheet of squared paper was mounted on the screen, so that if recordings of deflections



FIRST SPECIMEN IN MACHINE: OIL PRESSURE DELIVERY SHOWN TO UPPER AND LOWER CYLINDER-BLOCKS.

were required they could be noted without having to measure them with a rule.

Assembly and Adjustment of Gauges.

As future experimenters in this field may make use of this type of gauge, the author thought it worth while to make a note here of the method finally adopted by him for the assembly and adjustment of the gauges.

First the two mirrors were firmly housed in plastercine in their respective positions on the knife-edge spindle and on the gauge back. Secondly the heavy steel flat to be used as a carrier was clamped to the specimen. Thirdly the gauge, with compression spring and collar in the slackest position, was placed between the specimen and heavy steel flat, and the knife-edge fitted into its groove and rested against the small steel square provided on the specimen. With the gauge thus assembled, the knurled collar was adjusted to bring heavier thrust onto the gauge from the compression spring so that the knife-edge should be held firmly in position.

Adjustment of the position of the images thrown onto the screen was obtained in two ways. The initial coarse adjustment was obtained by moving the mirrors slightly in their housings. Final adjustment was done by moving the projector lamp and directing the incident light accurately by means of the universal clamp

(adjuster.

TESTS ON OPTICAL GAUGES.

Preliminary tests were carried out on the optical gauges to determine with what accuracy small changes in strain could be measured. The method employed was to set up two gauges, side by side, on a standard steel tensile specimen as shown in fig.3. p. 43. The tensile specimen was then loaded in a Buckton testing machine. By comparing the resulting load/strain graphs obtained from different optical gauges and calculating a value of Young's Modulus for the steel, the amount of variation which could be expected to be met with when using the gauges in experimental work could easily be ascertained.

In order that two gauges might be tested simultaneously, without the knife-edge spindles interfering with one another, one gauge was placed upside down. The only effect this had was to make the image spot move in the opposite direction, hence scale readings on some of the graphs can be seen to decrease with increased straining.

The sensitivity or magnification factor of the type of optical gauge used, depends upon the following:-

(i). Gauge length.

(ii). Knife-edge width.

(iii). Lever arm. i.e. distance between the scale on the image screen and the gauge mirror.

The 'magnification factor' is the ratio between the scale deflection in inches and the strain in the material under test.

Test No. 1.

To compare the relative behaviour of two gauges, one with an $\frac{1}{8}$" knife-edge and the other with a $\frac{1}{4}$" knife-edge.

Gauge No.'0'.

Gauge length 4"

Knife-edge width $\frac{1}{4}$"

Lever arm 9' - $2\frac{1}{2}$"

Magnification factor $= 4 \times \frac{110 \cdot 5}{0 \cdot 25} \times 2 = 3535$

Gauge No. 1.

Gauge length 4"

Knife-edge width $\frac{1}{8}$"

Lever arm 9' - $2\frac{1}{2}$"

Magnification factor $= 4 \times \frac{110 \cdot 5}{0 \cdot 125} \times 2 = 7070$

The two gauges were set up side by side on the tensile steel specimen. The specimen was then loaded up to a maximum stress of 8tons/sq.in. and unloaded. The loading cycle was repeated. Graphs were plotted of load against deflection readings, and load against percentage strain.

See p. 55 .

Apart from the first few readings of the first loading, both $\frac{1}{8}$" and $\frac{1}{4}$" knife-edge gauges showed reasonable

agreement. The graph of the $\frac{1}{8}$" knife-edge had a slightly more consistent slope. Because of this, and also because the $\frac{1}{8}$" knife-edge gives a greater magnification factor, it was decided to use $\frac{1}{8}$" knife-edges. Values of Young's Modulus determined with $\frac{1}{8}$" and $\frac{1}{4}$" knife-edges were 31·3 x 10^6lbs./sq.in. and 31·4 x 10^6lbs./sq.in. respectively taken over the upward part of the second loading cycle.

Test No. 2.

To compare gauges '1' and '2' both with $\frac{1}{8}$" knife-edges, with repeated loads and to see if the hysteresis loop gets less. Magnification factors of gauges '1' and '2' were respectively 6910 and 6650.

As in test No.1. the largest variation from a straight line occurred during the earliest readings taken immediately after the start of the test. At the second load cycle - up and down - the load/strain line traced out a flatter loop which was followed closely by subsequent load stages. The maximum variation of readings from a true straight line was 3% in the case of gauge No.1. and 2½% in the case of gauge No.2. See graphs on p. 55 and 56. Points on the graph obtained beyond the second load cycle have not been plotted on this graph as their inclusion would blur the graph due to their close proximity to the points on the second load cycle.

(P.T.O.)

Test No. 3.

It was noticed, during the setting up of the gauges, that the knife-edges usually contacted the specimen at only one point. Some anxiety was felt lest this should make a marked change in the reliability of the gauges, depending upon the particular way in which the knife-edge happened to lie at the time of setting up. The object of test No.3. was to remove the gauges from the specimen and replace them, then to carry out loading tests to see if the same loop would be traced out.

On plotting the results of this test, it was observed that the percentage variation of readings from a straight line was very much the same as before, but that the hysteresis loop was reversed. Calculated values of Young's Modulus were $31{\cdot}6 \times 10^6$ lbs./sq.in. for gauge No.1. and $33{\cdot}0 \times 10^6$ lbs./sq.in. for gauge No.2. As a result of the reversal of the hysteresis loop, the slope of the increasing load line was greater than that of the decreasing load line. No change was observed in the results after reversing the specimen in the machine and reloading.

Test No.4.

All previous tests had been carried out on an unpolished steel specimen, and with the knife-edge of the optical gauge resting in a milled groove at the normal gauge length of 4" from the claw end of the gauge body. In testNo.4.

the surfaces of the specimen and of the gauge were polished and a fine line scribed on the polished gauge surface. The knife-edge was set up resting in the scribed line and against the polished specimen. The results obtained were poor, due, it is believed, to the knife-edge resting at different points in the scribed line during the various stages of loading. This belief was confirmed when the experiment was repeated with the knife-edge resting between two polished surfaces, not in any groove, for then the best results of all were obtained. Calculated 'E' was $32{\cdot}5 \times 10^6$ lbs./sq.in.

Summary.

	CALCULATED VALUES OF 'E'	
	GAUGE No.1.	GAUGE No.2.
TEST No.1.	$31{\cdot}3 \times 10^6$	- -
TEST No.2.	$31{\cdot}0 \times 10^6$	$32{\cdot}7 \times 10^6$
TEST No.3.	$31{\cdot}6 \times 10^6$	$33{\cdot}0 \times 10^6$
TEST No.4.	- -	$32{\cdot}5 \times 10^6$

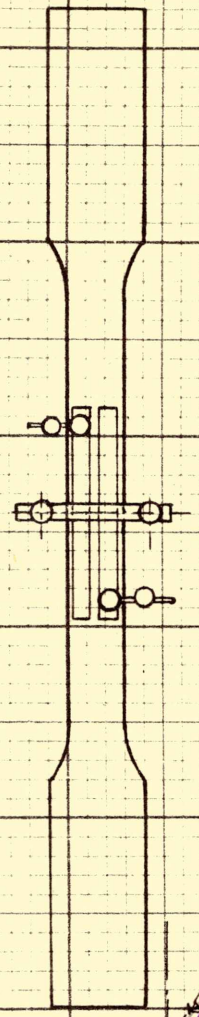
All figures in lbs./sq.in.

General Conclusions from Optical Gauge Tests.

Though the best results were obtained in the test No.4. where the knife-edge was placed between two highly polished surfaces, it was decided to utilize the milled grooves to carry the knife-edges.

(P.T.O.)

TEST COMPARISON OF 1/8" AND 1/4" KNIFE EDGE OPTICAL GAUGES.



KEY.

1ST LOAD UP

1ST LOAD DOWN

2ND LOAD UP

2ND LOAD DOWN

GAUGE Nº ①
1/8" KNIFE EDGE.

MAGNIFICATION FACTOR
7070

E = 31·3 × 10⁶ LBS/□"

GAUGE Nº ②
1/4" KNIFE EDGE

MAGNIFICATION FACTOR
3535

E = 31·4 × 10⁶ LBS/□"

LOAD IN TONS

2·8
2·4
2·0
1·6
1·2
0·8
0·4
0

STRAIN %

0·01 0·02 0·03 0·04 0·05

1·0 2·0 3·0 4·0

SCALE READINGS (INS.)

STRAIN %

0·01 0·02 0·03 0·04 0·05 0·06 0·07

3·5 3·0 2·5 2·0 1·5 1·0

SCALE READINGS (INS)

PAGE 33

TEST OF OPTICAL GAUGES Nos. ① AND ② ON STEEL TENSILE SPECIMEN.

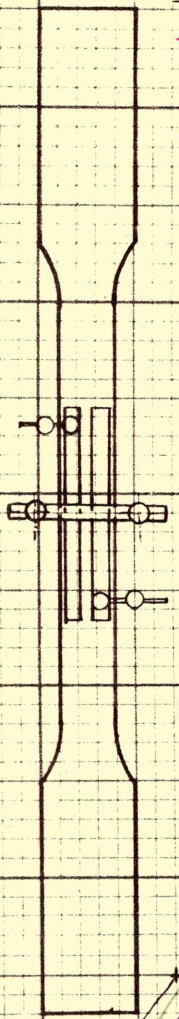
KEY.

1ST. LOAD UP

1ST. LOAD DOWN

2ND LOAD UP

2ND LOAD DOWN



LOAD IN TONS.

2·8
2·4
2·0
1·6
1·2
0·8
0·4
0

GAUGE No. ①.

1/8" KNIFE EDGE.

LEVER ARM. 9'-0".

MAGNIFICATION FACTOR 6910.

$E = 31{\cdot}0 \times 10^6$ LBS/□".

STRAIN %

0·01 0·02 0·03 0·04 0·05 0·06

5·0 4·0 3·0 2·0 1·0

DEFLECTION READINGS.

GAUGE No. ②.

1/8" KNIFE EDGE.

LEVER ARM 8'-8"

MAGNIFICATION FACTOR 6650.

$E = 32{\cdot}7 \times 10^6$ LBS/□".

STRAIN %

0·01 0·02 0·03 0·04 0·05 0·06

1·0 2·0 3·0 4·0 5·0

DEFLECTION READINGS.

PAGE 56.

The reasons for this were the following:-

(i). Standard gauge length of 4ins. assured.

(ii). No necessity to keep the surfaces polished and clean, which might prove difficult once the gauges were set in position.

(iii). Less probability of slipping occurring at high strains.

The mean deviation of the values of Young's Modulus calculated during the tests were $\pm$ 1% for the individual gauges, and $\pm 3 \cdot 1$% for all the gauges. The gauges may therefore be expected to read strains as small as $2 \cdot 6 \times 10^{-6}$ ins./in. corresponding to a stress of about 10lbs./sq.in. in concrete of 'E' = 4×10^{6} lbs./sq.in. with an accuracy of ± 3 to $\pm 3\frac{1}{2}$%.

Comparisons of strains recorded by optical gauges and electrical gauges are given in later pages in this thesis.

For typical result sheet of these tests see Appendix II.p. 201.

METZGER STRAIN GAUGE.

The third and last type of strain gauge which the author used in the test on the first specimen was the Metzger strain gauge, an American mechanical device introduced into this country by Professor A.L.L.Baker. This type of gauge has been used a great deal in experiments involving the measurement of strain in concrete structures in the laboratory at City and Guilds College. A detailed account of it will not, therefore, be given in this work. Briefly it consists of two fine conical points, one fixed, the other acting as the short arm of a crank-lever which converts horizontal strain movement under the gauge length into vertical movement at the other end of the long arm of the crank-lever. Situated above the end of the long crank-lever arm is a dial-gauge reading direct to $\frac{1}{10,000}^{th}$ of an inch. Changes in the 8" gauge length are thus first magnified by the crank mechanism, and then accurately measured by the dial gauge. 1 division on the dial gauge represents a strain of $11{\cdot}5 \times 10^{-6}$ ins./in.

Two small metal squares, with small holes drilled into their centres by a No. 60 drill, are stuck onto the surface of the concrete at 8" intervals. To measure the average strain between these two points, the Metzger gauge is held so that the two conical points fit into the holes in the metal squares. A reading is then taken of the dial gauge. Using the conversion factor given above, the operator may thus deduce the strain.

CHAPTER V.

Pressure Gauge Calibration Tests.

As can be seen from the drawing of the cylinder block assembly (Appendix XII p. 219.) each loading block is equipped with five $1\frac{1}{2}$" dia. plungers arranged across the width of the machine. Though the tolerances on the plungers were as small as possible, a certain amount of loss of load due to friction may reasonably be expected, particularly as the oil seal is in the form of 'U' packing to prevent oil leakage past the pistons. Also changes in section and bends in the delivery though, in theory, having no effect once the oil is stationary, might, in practice, partly account for discrepancies between the pressure gauge readings and the actual loads applied to the specimen.

To determine the variation, due to friction and any other causes, between the Bourdon type pressure gauges (reading directly in tons) and the actual pressure transmitted to any specimen placed in the machine, the following tests were carried out.

A 50 ton. proving ring was placed in the machine between the two loading blocks of the first load point. Commencing at zero, loads were applied to the proving ring in increments of approximately 5tons up to the maximum of 40tons. The load was then

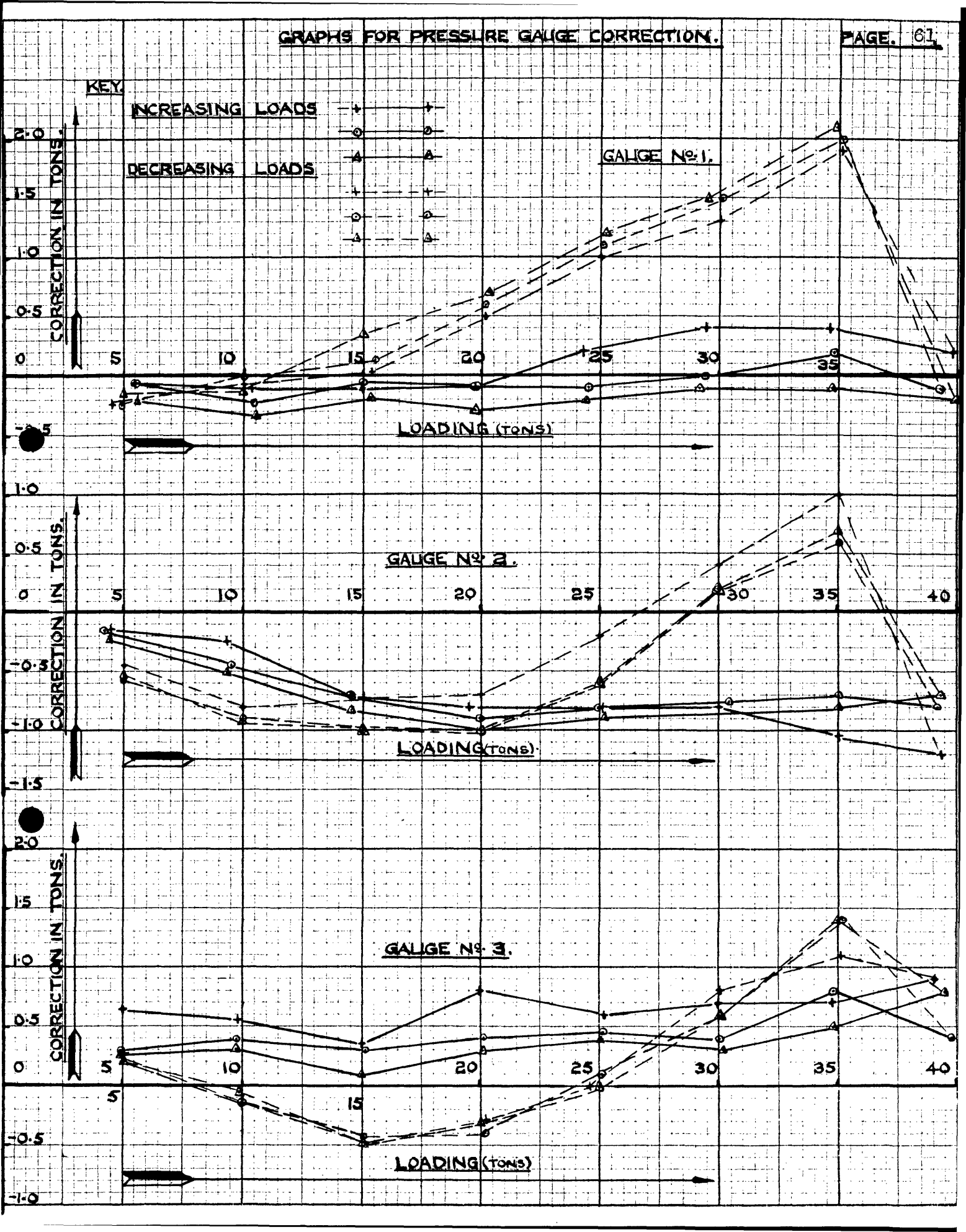
run off, again in increments of 5 tons. At each load, readings were taken of the dial gauge on the proving ring, and of the pressure gauge. Care was taken to see that the 'cut-out' pointer on the Bourdon pressure gauge in no way prevented the pressure gauge from giving its true reading. This was repeated a number of times, in order that the mean variation of the pressure gauge readings from the true load(proving ring load) might be determined.

The whole experiment was repeated for all six loading points, and graphs were plotted as on p.61 and 62 showing the corrections required, in tons, to the pressure gauge readings to give the true load.
N.B. This refers to the pressure gauge pointer being unrestricted by the automatic 'cut-out'.

From observations of the graphs, which show the first three loading cycles completed in this test, the largest inaccuracy was shown to occur at gauge No.4, being from 0·75 tons. at a load of 15 tons to -2·3tons at a load of 40tons. For decreasing loads the largest variation from true load was -2·3tons again on gauge No. 4. at 20tons load, whilst a correction of 2·0tons was required on gauge No. 1. at 35tons load.

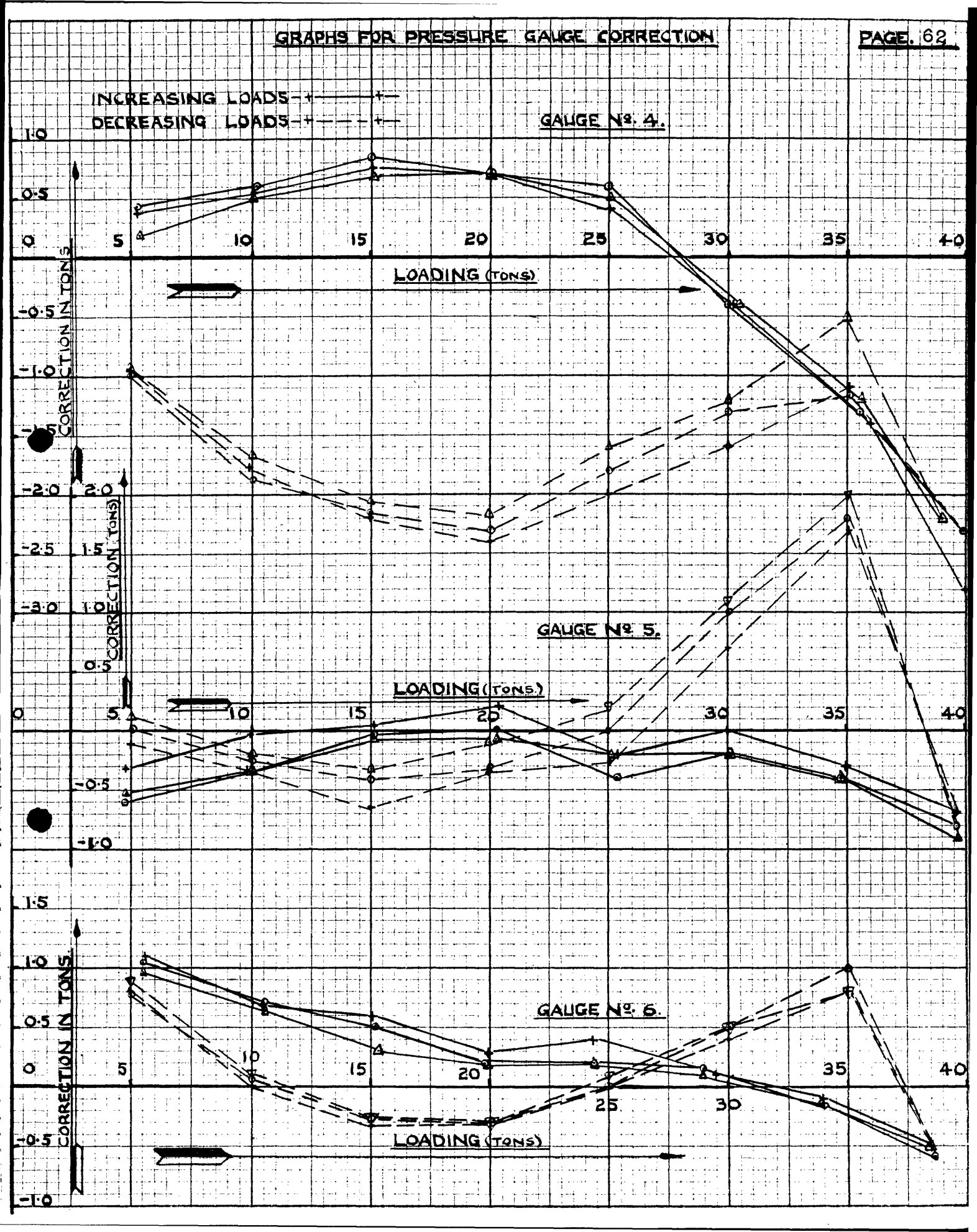
One major point which was brought out by these graphs and merited further tests, was the great change which took place in the load corrections

GRAPHS FOR PRESSURE GAUGE CORRECTION.



GRAPHS FOR PRESSURE GAUGE CORRECTION

INCREASING LOADS -+———+—
DECREASING LOADS -+— — —+—



immediately after the reversal of loading. An explanation of this phenomenon given by the writer was that during increasing loads, since the pistons' frictional resistances must act in the opposite direction to their movement, i.e. against the oil pressure, a drop in the load transmitted to the specimen or proving ring was caused. During decreasing loads, obtained by opening the pressure relief valve, the specimen or proving ring forces the oil through the pressure relief valve and friction acts in the reverse direction causing the load on the specimen or proving ring to be higher than that registered by the pressure gauges.

During an actual test on concrete specimens it was expected that the load on any given load point would have to be varied, either up or down, quite a number of times before the required straining would be obtained on the concrete. If, then, each reversal in loading was going to cause a sudden change in the correction required, to obtain those corrections from curves which were of purely increasing loads or decreasing loads over the whole range of the pressure gauges would be a policy likely to lead to grave errors. The only way to enable corrections to be made for small adjustments of load seemed to the author to be to have graphs showing the effect of reversals of loading direction occurring at all levels of loading, (not just at the maximum) and to obtain the required

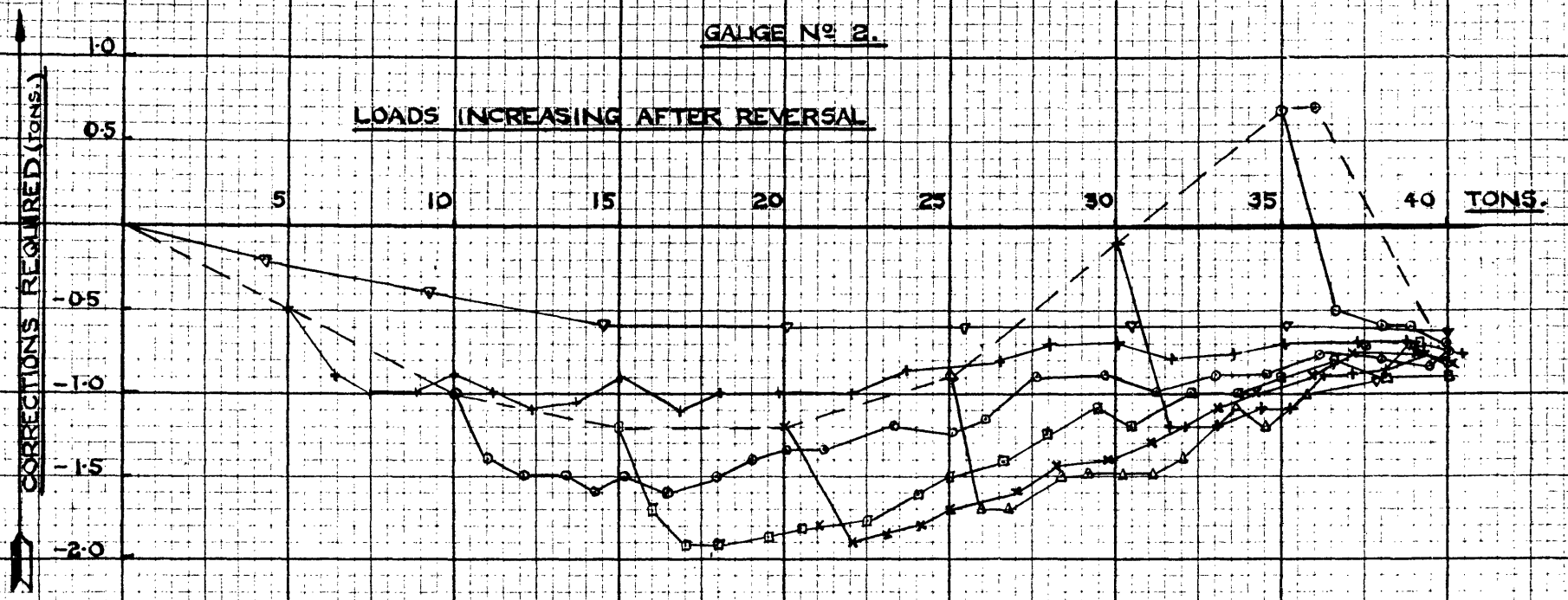
correction, stage by stage, from these graphs.

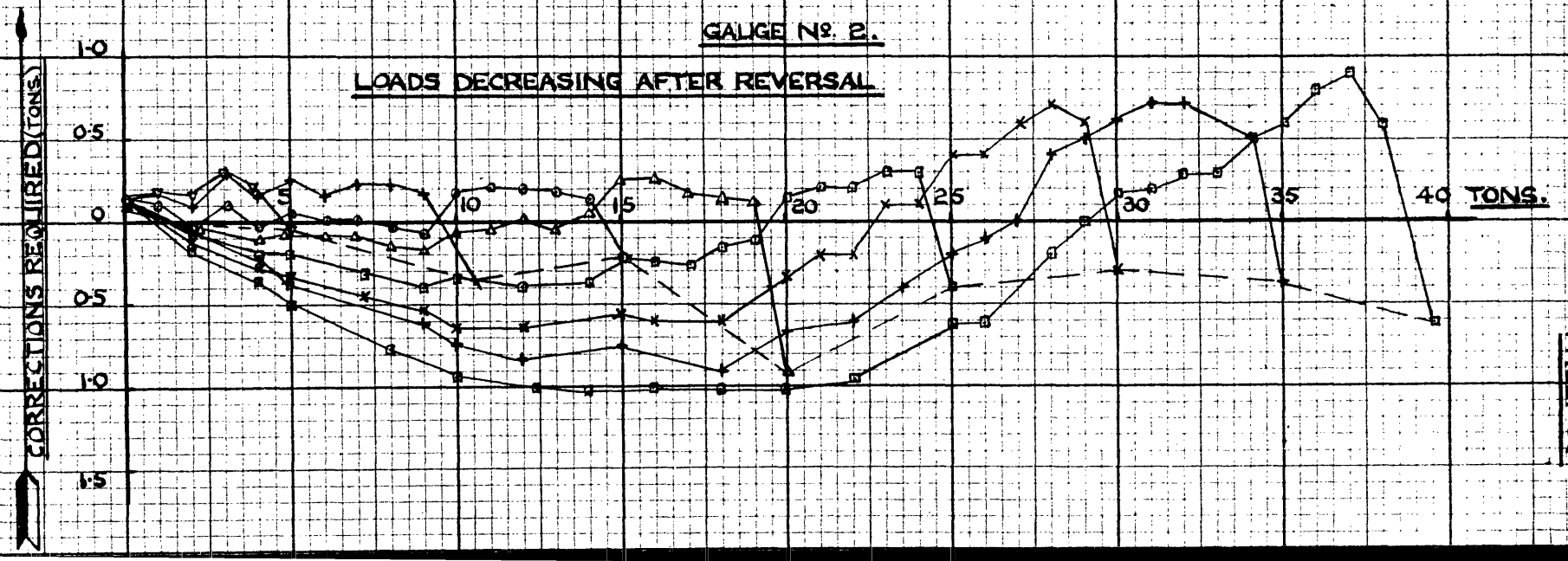
As a result testing was extended, on No.2. gauge, with a view to trying out this idea on one gauge before calibrating all six as the test necessarily required many readings. With the proving ring set up as for the previous test, load was run up to 40tons and then decreased to 5tons and readings taken at small intervals of further increasing load up to the maximum load. The load was then run completely off before commencing the next part of the test. The load was again run up to 40tons and then decreased this time to 10tons and readings taken at small intervals of further increasing load up to the maximum. This was repeated until reversals of load had been plotted every 5tons. See graph on p. 65 .

The whole experiment was then repeated readings being taken at small intervals of <u>decreasing</u> loads after reversal.

From these graphs it was possible to trace out the course of a varying load with a high degree of accuracy. To check this the load was varied on gauge No. 2. and a comparison made between the estimated loading - as obtained from the graphs- with the true loading, as given by the proving ring. The estimated and true loading showed good agreement, (see Appendix IV.p. 203.). This latter method of gauge correction, though very accurate for obtaining

EFFECT OF REVERSAL OF DIRECTION OF LOADING ON PRESSURE GAUGE READINGS.





gauge corrections on load changes done by either motor or relief valve, proved rather laborious. Also no check could be kept by this or any other method on load corrections required for a particular load point when the changes were due to stress transference to or from adjacent load points. Because of these last two reasons it was decided that possibly the simplest way of overcoming these difficulties was to attempt to keep all the pressure gauges controlled in such a way that they always had an increasing load applied to them - so far as the motor and relief valve were concerned - right up to their required loading. If it were necessary to decrease the load on a certain point, then the procedure should be to return all pressure gauges to zero by opening the relief valves and then to re-load up to the new load. This method was adopted, and by using the automatic cut-outs to stop the motors just short of their required loading the time occupied in attaining a given stress-distribution was reduced to a minimum.

Tests on Automatic Cut-outs for Pressure Gauges.

The method of operation of the automatic cut-out device attached to each oil pressure gauge is described on p. 15 . Tests were carried out on these cut-outs to determine the degree of accuracy of a load attained by their use. The original idea was that all six automatic cut-outs should be set at

the particular stress-distribution required, the motors started and the loading stopped by these cut-outs once the correct loads had been reached. This proved to give inaccurate values of the stress-distribution for:-

(i). Each cut-out had a different place, relative to the gauge pointer, at which electrical contact was made.

(ii). Due to motor and pump inertia some oil was still pumped into the system after the cut-out had stopped the motor power supplies, thus tending to cause over-shooting of the required load.

(iii). The pump inertia was likely to have a greater effect at low loads, as the retarding effect of the oil pressure tending to keep the delivery valve closed was less, than at high loads.

(iv). The automatic cut-out device impeded, slightly, the free operation of the gauge indicator needle. It was necessary to move the cut-out pointer away (with the motor switched off) to obtain the 'free' pressure gauge indicator reading.

Adequate control of these inaccuracies was attained by carrying out load tests on all the gauges and comparing the loads reached by the pressure gauge indicator with the setting of the automatic cut-out. These

tests were carried out on a concrete specimen - up to 25tons - and on a steel specimen up to the maximum load of 40tons. See table in Appendix V. p. 204 for these results.

CHAPTER VI.

INVESTIGATION AND DEVELOPMENT OF TECHNIQUE ON CONCRETE SPECIMEN.

The earlier tests carried out on the first specimen ever to be tested in the Bending Simulation machine were confined chiefly to the elastic stage in the loading range of the particular concrete used. The reasons for this were twofold. Firstly there were preliminary investigations dealing with such questions as, the technique of loading with the machine; the most satisfactory method of obtaining strain recordings; the effect of the tensioning device employed; and the spreading out of strains in the specimen; and it was intended to obtain the information required about these points during the stage of testing where relations bwtween stress and strain were, to a large extent, already known. i.e. during the elastic range. Secondly it was hoped, that these preliminary investigations having been successfully accomplished and any difficulties arising from them being overcome, to continue the test beyond the elastic range into the plastic range and finally to obtain the stress/strain relationship at failure in this specimen loaded as a beam element. These latter tests would, naturally, require everything to be in smooth working order and also the employment of a tried technique, as once in the plastic range there is no turning back.

As it transpired much benefit was reaped from the employment of this procedure, but, as can be observed from this report, a great deal of care and attention to detail was required not only in the preparation of the specimen but also in the preliminary investigations mentioned in the preceding paragraph. Some idea of the amount of work required can be gathered from the fact that over thirty complete sets of readings, (with loads well down in the elastic range) each involving seventy-eight individual gauge recordings, were taken before serious testing of the specimen itself commenced. In the test of the first specimen alone, upwards of one hundred complete sets of readings were recorded, whilst on the subsidiary eccentricity investigations which were undertaken during the test, over two hundred sets (averaging twelve readings each) were noted.

Loading Technique.

Some of the difficulties likely to arise in any attempt to obtain a method of loading which could be reproduced reliably have already been discussed in the paragraphs dealing with automatic cut-out trials and pressure gauge calibration tests. The various methods of loading tried out, and the one finally adopted will now be explained fully.

It was not practicable to decide

on a loading technique from tests carried out using one loading point only, even had such tests been done on a concrete block instead of a proving ring, because when there is a specimen in the machine, considerable inter-action takes place between neighbouring load points. This inter-action between load points causes a given point to relieve or intensify, through deformation of the specimen, the stress on its neighbours, and is most pronounced during the loading and unloading of the specimen.

The first loading technique to be tried out was to set the cut-outs (due account having been allowed for their individual inaccuracies) to the required stress-distribution, close the pressure relief valves and start the pump motors. When any particular gauge reached its load first, the cut-out stopped the motor. However, other load points, with oil systems which took longer to develop a stress-carrying oil pressure, or which had cut-outs set at higher values, were still building up load to their cut-out pressures and caused -by inter-action - a relief of loading on the first load point. This relief of load on the first point caused, in turn, a breaking of the electric control circuit of that gauge and the motor re-started. This action was repeated by other gauges, resulting in a stress-distribution which had been attained by a series of increases, then decreases and subsequent increases, of (stress.

As was shown previously in the tests on pressure gauge calibration, this type of load application is liable to introduce grave frictional errors.

The second loading technique, therefore, which was tried has as its object the attainment of a stress-distribution without any reversals in the direction of loading of any gauge. The pressure relief valves were first closed and all the pump motors switched on. As each pump produced enough pressure to show a movement of the pressure gauge indicator, its corresponding relief valve was opened so that there was no further increase in load. This was continued until all the pumps had begun to hold a little load. Gradually each valve was shut until, with the motors still running, the required stress-distribution had been obtained. In theory this may sound a reasonable method, but in practice it was very difficult firstly to make fine adjustment to any one valve without effecting the others and secondly to maintain all six load points at a steady value at one and the same time.

Variations on the above two loading techniques were given a trial and, subsequently, the following method, considered by the author to be the most practical and adopted in all further applications of stress-distribution, was evolved.

(P.T.O.

(i). The automatic cut-outs were set just the least fraction below the desired stress-distribution setting. (Due account having been allowed for individual inaccuracies.)

(ii). The pressure relief valves were closed and the pump motors started.

(iii). As each gauge began to show load, the pressure relief valves were slackened until all pumps were carrying a little load.

(iv). The pressure relief valves were then adjusted, care being taken to avoid reversals in loading, until all six gauge indicators were almost at the cut-outs, and the pumps were still running.

(v). The valves were then quickly shut tight, the indicators moved simultaneously over the short distance to the cut-outs, the motors stopped automatically and, first the main switch (controlling all six motors) and then each individual pump motor switch was turned off.

(vi). The cut-out pointers were now moved well clear of the gauge indicators and the latter brought up, successively, to their final required values either by a turn, by hand, of the pump driving pulley or a rapid flick (on and off) of the individual pump switches, the main switch having been returned to the 'on' position for this purpose.

Repetitions of the same initial stress-distribution were tried out using these various loading

techniques, and the final method described proved to give strain repetitions (at low loads in the elastic range) most nearly equal to one another. (N.B. The three different sets of stress-distribution, shown in the tests investigating the spreading out effects of strain on p. 77 , were obtained from exactly similar automatic cut-out settings following the first method of loading technique described in this chapter.) Use was made of the tables derived in the experimental work on the automatic cut-outs, and also of the graphs plotted for pressure gauge correction, to obtain the necessary settings in stages (i) and(vi). Operations (iv) and (v) were much facilitated and more efficiently executed if two persons were employed in operating the pressure relief valves at this point in the loading method. The technique may appear a little involved, but in practice this is not so. The time taken, from the moment of starting the first motor to having the desired stress-distribution applied even in the case of heavy loading, was not more than two minutes. Experience was gained, naturally enough, at lower loads and this reduced the effect of heavier loads tending to take longer application.

The obvious advantages of the method were the ability to bring the indicators very finely up to the required setting, and the elimination of any reversal of loading occurring during application and hence by use

of the pressure gauge calibration graphs, the production of a reliable method of correcting frictional resistance losses in the loading point cylinders.

Observations of Strain Spreading.

In a portion of a beam over which there is a constant bending moment the neutral axis may, at a given load well before failure, be reasonably expected to be at a distance from the extreme fibres which is constant along the length of the portion considered. As strain is directly proportional to distance from the neutral axis and the lever arm will, necessarily, be the same at points along the length of the portion (with a constant total tension force) , not only does it seem likely that the strain-distribution at all cross-sections of this portion will be similar -viz. a triangle - but it appears also probable that the stress-distribution will be similar (though of course not necessarily triangular) for all cross-sections of the element. It must be stressed that this argument is only brought forward as a possibility of the state of affairs existing in the beam portion before a sufficiently high intensity of loading has been reached (coupled with local conditions of the concrete) to cause excessive straining over a small length of the beam and/or local changes in the position of the neutral axis, which would produce failure.

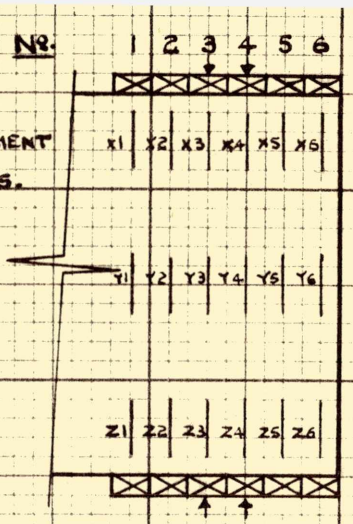
With this in mind, a true simulation

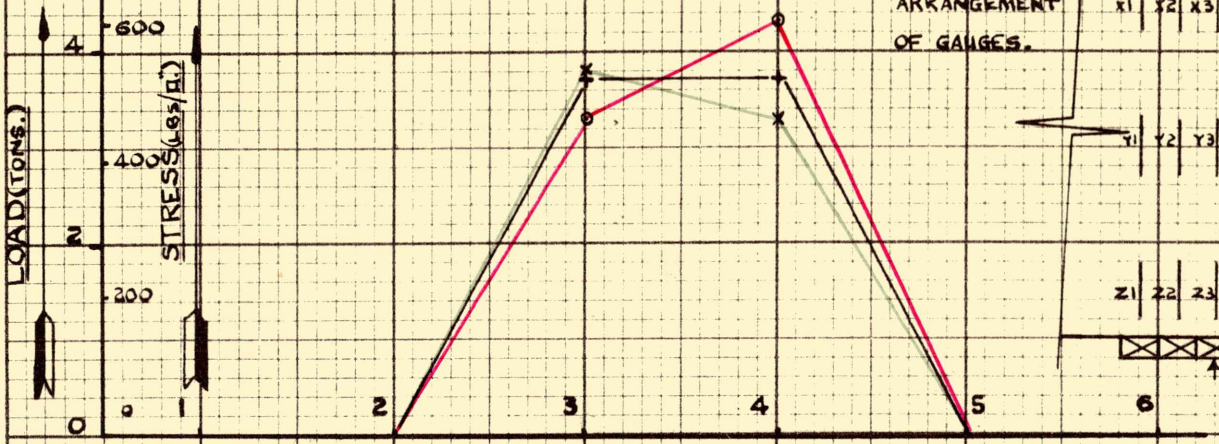
of the conditions pertaining in a beam might seem to include the condition that, at a given load stage, a particular stress-distribution should remain the same at all beam cross-sections throughout the length of the portion considered.

Applying this argument to the specimen in the bending simulation test would mean that the stress-shape should remain constant, for a certain load stage, (particularly for a low load stage) over the 'length' of the specimen.

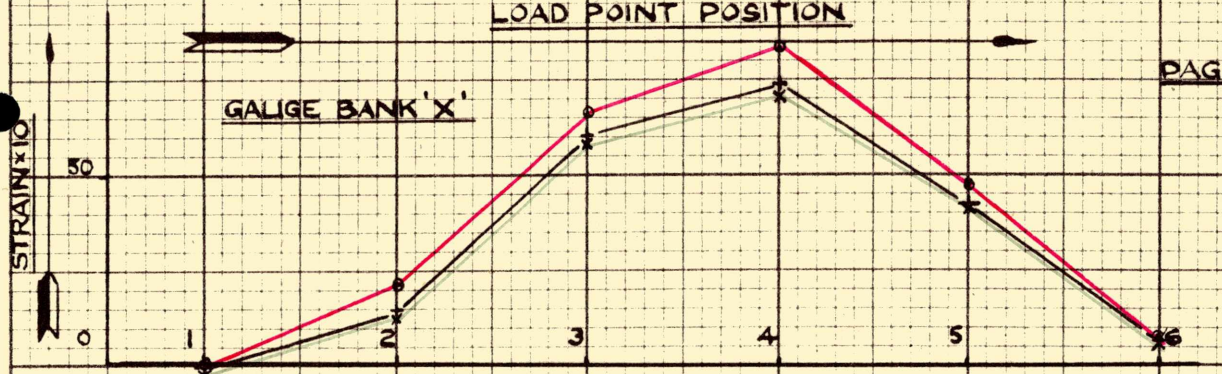
This was experimented with in the following manner. At low loads stress may be assumed to be proportional to strain, and hence it is possible temporarily to utilize the strain gauges as stress gauges at points in the specimen which are not close to the load points and where direct stress measurement is not as reliable as it is close to the load points. A stress-distribution which was easily identifiable by its particular shape was applied to the specimen in the bending simulation machine. The particular stress chosen was trapezoidal, being merely two loads on the central gauge numbers 3 and 4 , and this stress-distribution was applied by the first method shown under'loading technique' on p. 70 . Readings of the strain gauges were taken and graphs plotted. See p. 77 and 78 . The experiment was repeated three times with the same cut-out settings for the loads on gauge numbers 3 and 4, hence theoretically the

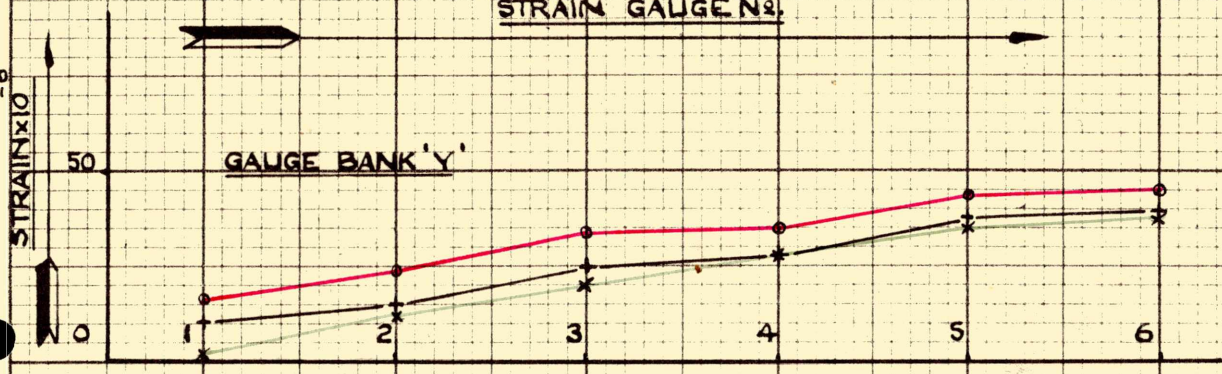
GRAPHS SHOWING SPREADING OUT OF STRAIN ACROSS LENGTH OF SPECIMEN.

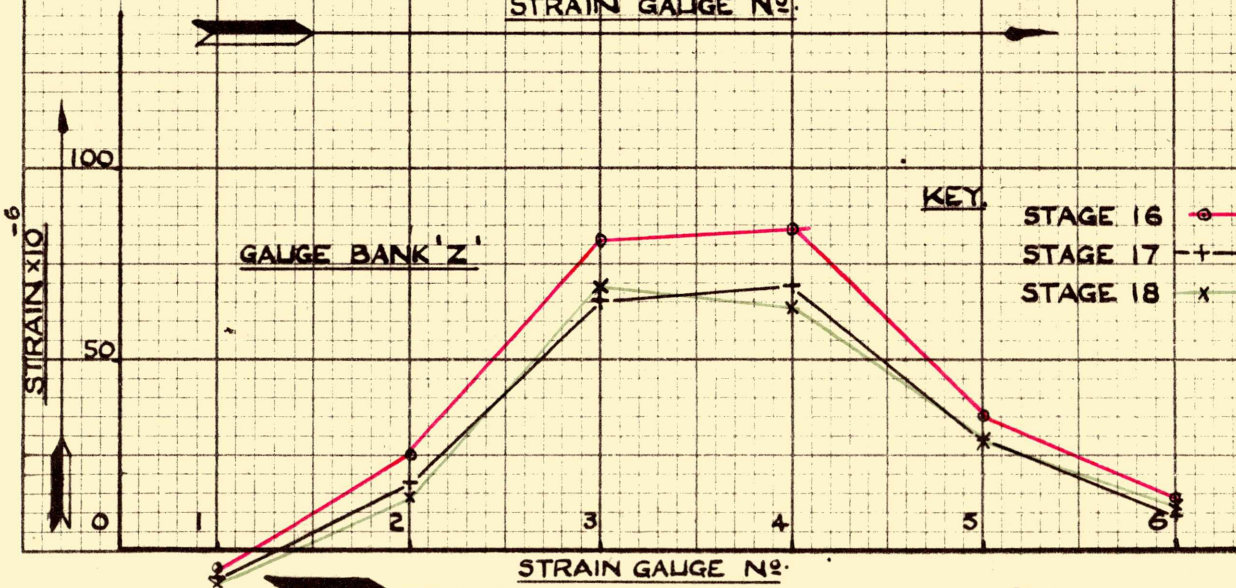




PAGE. 77



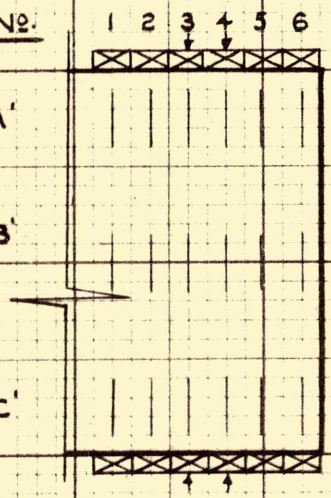




PAGE. 78

GRAPHS SHOWING SPREADING OUT OF STRAIN ACROSS LENGTH OF SPECIMEN.

ARRANGEMENT OF STRAIN GAUGES.



LOAD AT TWO POINTS ONLY.

GAUGE BANK 'A'

STRAIN x 10^{-6}

150
100
50
0

1 2 3 4 5 6

STRAIN GAUGE Nº.

GAUGE BANK 'B'

STRAIN x 10^{-6}

100
50
0

1 2 3 4 5 6

STRAIN GAUGE Nº.

GAUGE BANK 'C'

STRAIN x 10^{-6}

100
50
0

1 2 3 4 5 6

STRAIN GAUGE Nº.

KEY.

STAGE 16.
STAGE 17.
STAGE 18.

strain readings should be the same. Once the pumps had stopped, the motors were switched off and readings of the indicated loads were taken with the cut-out pointers moved so that they did not impede the true readings of the gauges. The actual stress-distributions which had been applied in each case, with corresponding pressure gauge corrections already added, are given at the top of p. 77.

It can be seen that greater straining occurred on the side 'A','B','C' of the specimen than on 'X','Y','Z', the latter being roughly 70% of the former. (This particular phenomenon is observed and discussed in detail later on in the thesis.) The strain, and consequently the stress in this case of low loading, can be seen to have spread out from a shape corresponding to that of the applied stress-distribution at the ends of the specimen, (i.e. on banks 'A' and 'X', and 'C' and 'Z') until at the central sections of the specimen (i.e. banks 'B' and 'Y') it has become linear.

At first sight it would appear that in this particular respect, the bending simulation machine fails to reproduce the conditions existing in a beam. But on further consideration of the question, the author came to the conclusion that the foregoing experiment was not a fair test of the ability of the machine to simulate bending in a concrete specimen. The reason for coming to

this conclusion was as follows. In a beam, at any particular cross-section which one may choose, the strain will be of a linear nature in the compressive zone. Hence the stress-distribution, at this cross-section, must be that which corresponds to straight line strain-distribution. It may be found by proceeding to neighbouring cross-sections in the beam that this strain-distribution, and possibly also the stress-distribution, remains unchanged. Any comparative test on the bending simulation specimen should, therefore, be done with a stress-distribution corresponding to a linear strain-distribution, if a fair comparison is to be made, and not by some arbitrary stress-distribution with a similar shaped corresponding strain-distribution. This type of comparative test, however, cannot be achieved, because when a non-linear stress-distribution, which has a corresponding straight line strain-distribution in the end strain gauge banks of the specimen, is applied, the loading has necessarily reached such limits that the strain gauges can no longer be assumed to act as stress gauges; therefore no check can be made on the shape of the stress-distribution existing at the centre of the specimen. Further, to apply a straight line stress-distribution with corresponding linear strain-distribution would prove nothing, as it has already been shown that non-linear stress-distributionsat the ends of the specimen produce linear stress and linear

strain distributions at the centre, it could hardly be expected that linear stress-distribution would produce anything different.

One point on this subject which resulted from the type of failure which occurred in the second specimen, might, with advantage, be mentioned here. Failure of the specimen took place at the central section where continual linear strain-distribution was observed throughout the test (irrespective of the stress shape applied). Presumably, therefore, the stress-distribution at this section was of a curved nature at this particular stage. (i.e. failure). The stress-distribution, giving linear strain-distribution, at the ends of the specimen, had barely begun to depart from its straight line form when failure occurred at the centre. This appears to indicate that the stress-distribution at the centre may not necessarily be the same as it is at the ends even when (as in this case) straight line strain-distribution is maintained throughout the specimen. Bearing this in mind, the pressure gauges will only register true stress-distribution conditions at failure, when that failure occurs sufficiently close to the ends of the specimen to allow no change in the stress-distribution to take place between the section at which failure occurs and the load points.

In the opinion of the author, the

departure of the stress-distribution from a constant shape (at a given high loading) at different cross-sections, produces in the bending simulation specimen the same conditions as are present when a plastic hinge forms in a beam.

It would appear, then, that in the second specimen a plastic hinge formed in the central portion of the specimen, and continued loading produced failure there, before the concrete in the ends of the element had more than just commenced plasticity.

CHAPTER VII.

Effect on Strain of Tension Application.

One of the early difficulties encountered with the tensioning frame (see Appendix X. p. 212.) was the high frictional resistances set up between the top and bottom end blocks and the stretching nuts. This resistance was sufficient to make any application of a high tensile force in the wires impossible with a normal spanner. To lessen this effect, ball-races were inserted between the stretching nut and the end blocks thus reducing the frictional resistances and enabling maximum load to be transmitted to the wires. A second difficulty, however, which it was not possible entirely to overcome, was to ensure that each wire was equally loaded. The orientation of the wires when passing through the specimen was governed by two steel templates. This arrangement allowed sufficient space between the wires to enable efficient bond to be attained between each wire and the surrounding concrete. But in the re-arrangement necessary to pass the wires through the holes in the end blocks and into the conical thimbles holding the wedges, a rapid change in the positioning of the wires inevitably led to some being a little slacker than others. It was estimated that due to these losses the maximum load which could be reached by stressing the wires until one failed, was

approximately 12tons.

In the part of the testing of the first specimen in which experiments were being done on the best methods of applying load, tests were also carried out to determine the effect of tensioning the high tensile steel wires in the specimen. It is proposed only to publish here those results obtained using the loading technique which was finally decided upon as being the best, since other tests carried out with earlier loading techniques will suffer from the inclusion of the greater inaccuracies inherent in the earlier methods.

Graphical results of a test investigating this tensioning effect are shown on pages, 86, 87 and 88. The test commenced by taking 'no-load' readings on all the electrical, optical and Metzger strain gauges. Load stage 43 was then applied using the loading technique developed from the load tests.

LOAD STAGE. 43.

Load Point.	1.	2.	3.	4.	5.	6.
Distance From Extreme Fibres.	11"	9"	7"	5"	3"	1"
Indicated Load. (Tons.)	0	1·9	3·3	5·1	6·6	9·3
Correction. (Tons.)	0	-0·1	0·3	0·3	0·6	-0·3
True Load. (Tons.)	0	1·8	3·6	5·4	7·2	9·0

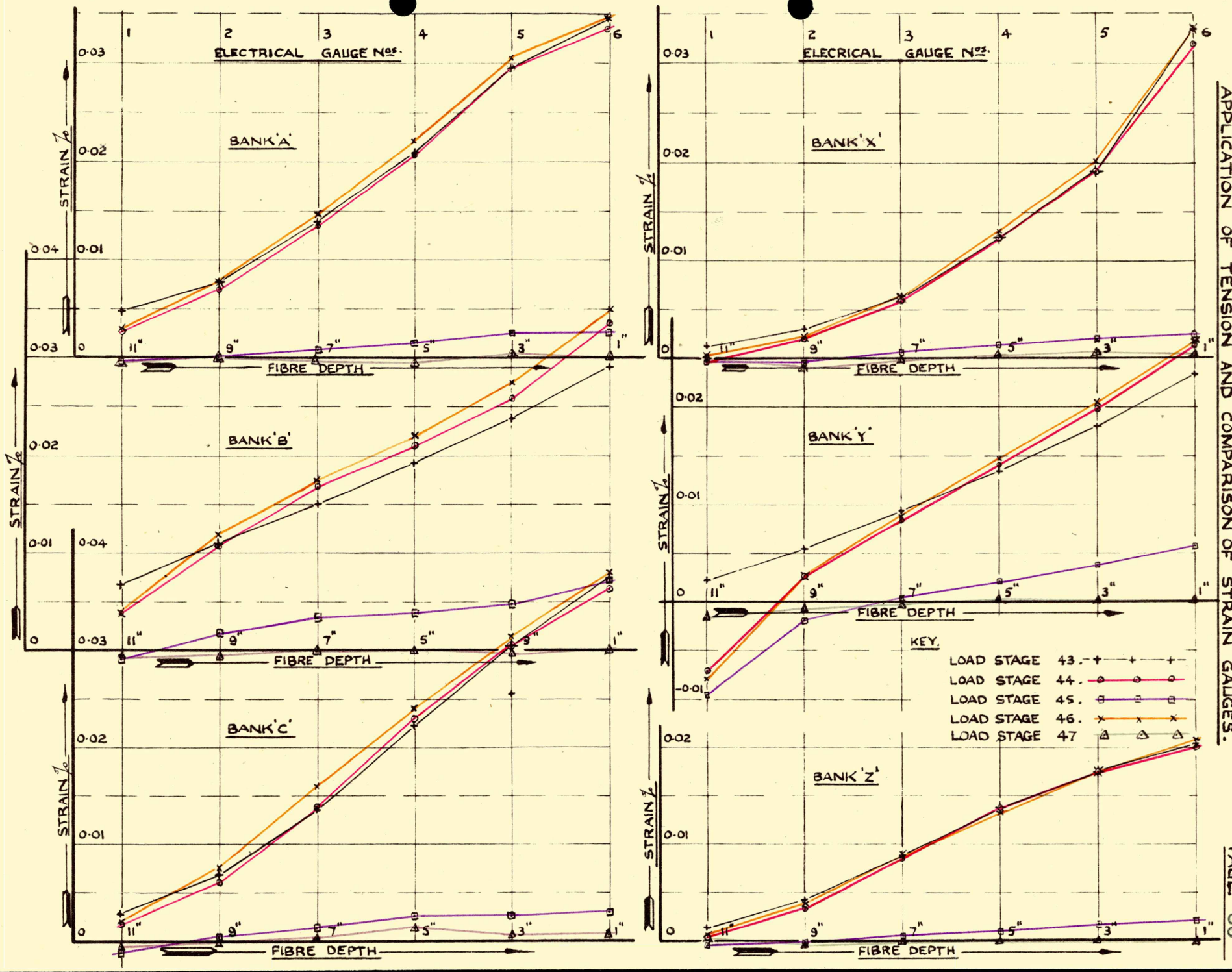
Tension was then applied by the stretching nuts. The specimen

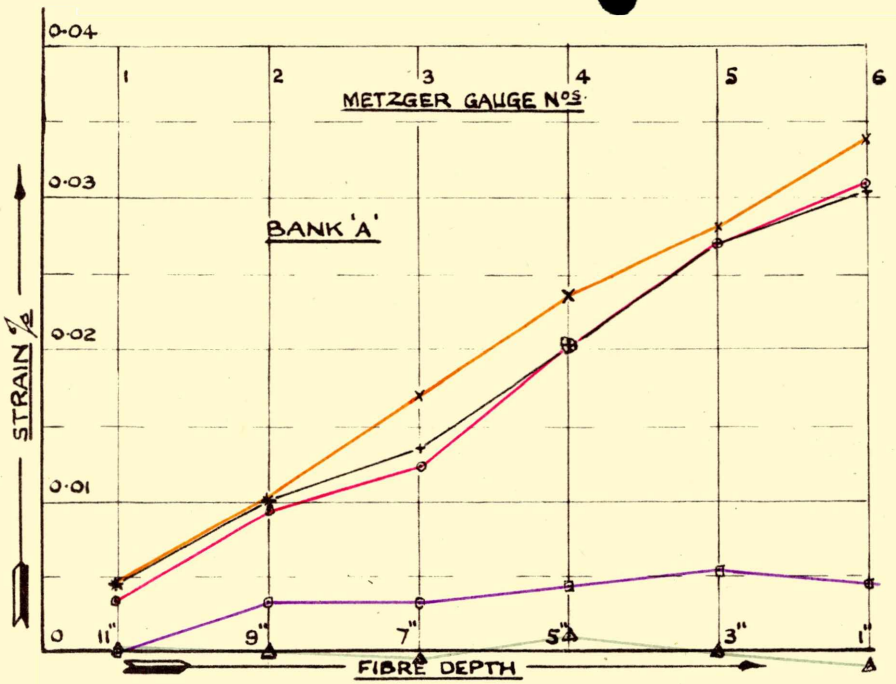
was loaded before tensioning in order that it should not be twisted in the machine by the reaction set up by the spanner load. Readings were again taken of all strain gauges -load stage 44-. In order that the effect of tensioning alone might be observed, the load was now run off completely, and readings taken without slackening the tensioning-frame.- stage 45. Upon unloading, a tension crack was seen to develop in the specimen at the point were the pressed card had been inserted. This crack extended across the width of the specimen and for a depth of 1" towards the neutral axis and the compression zone. Load stage 46 was next applied, being the same loading as for stage 43 but with tension already existing in the tension wires. Readings of the strain gauges were noted. Finally the tensioning nuts were slackened and the loading removed and 'no-load' readings of all the strain gauges recorded on load stage 47.

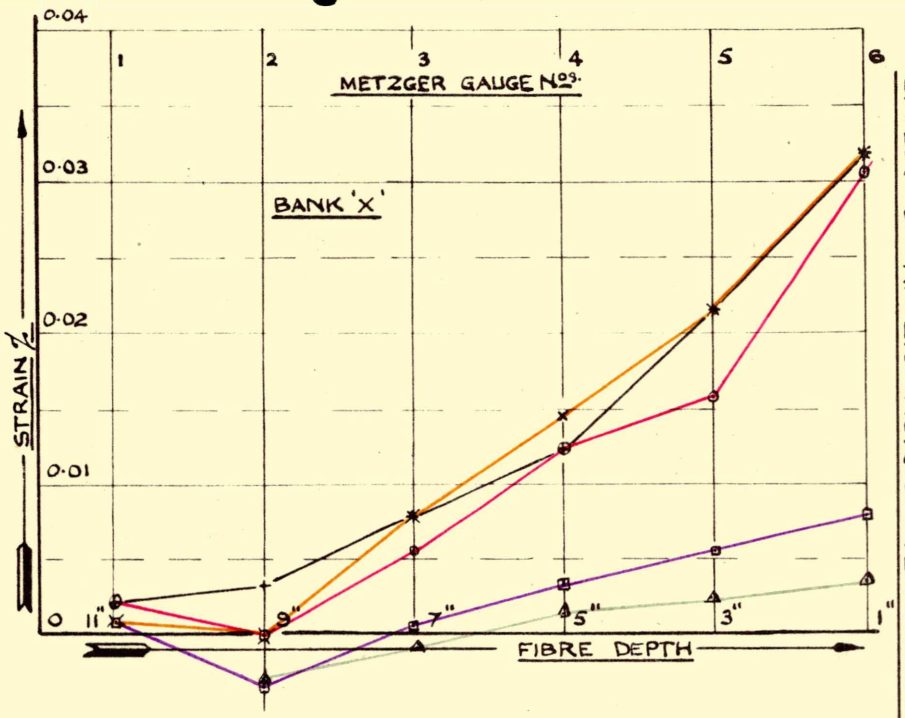
Summary of Load Stages.

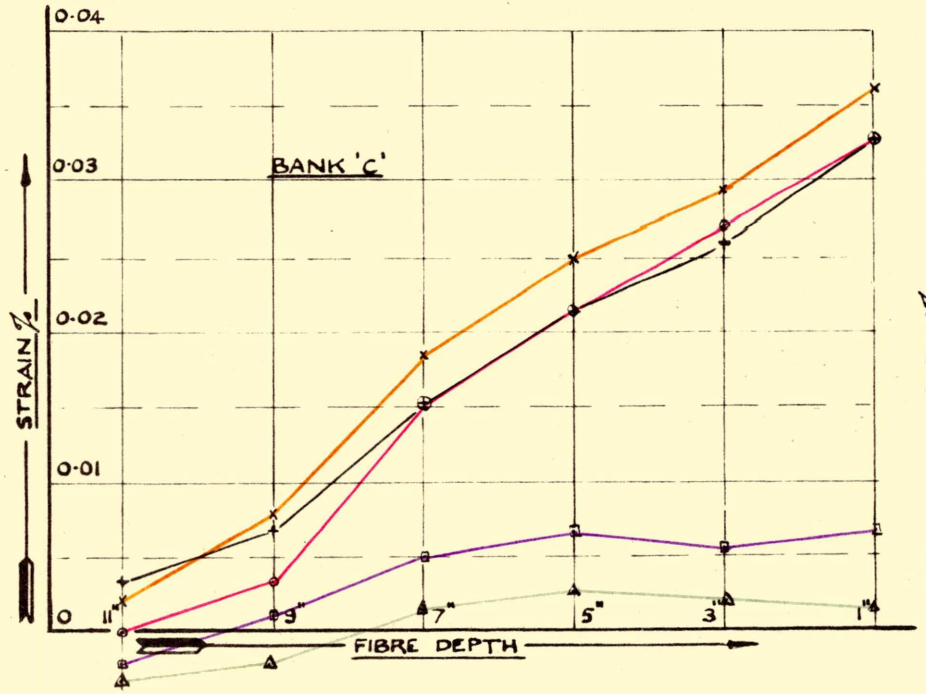
Load stage 43 . .	.Compressive load only
Load stage 44 . . .	" " + tension force
Load stage 45 . .	Tension force only
Load stage 46 . .	Compressive load 43 + tension force
Load stage 47 . .	No-load, no tension.

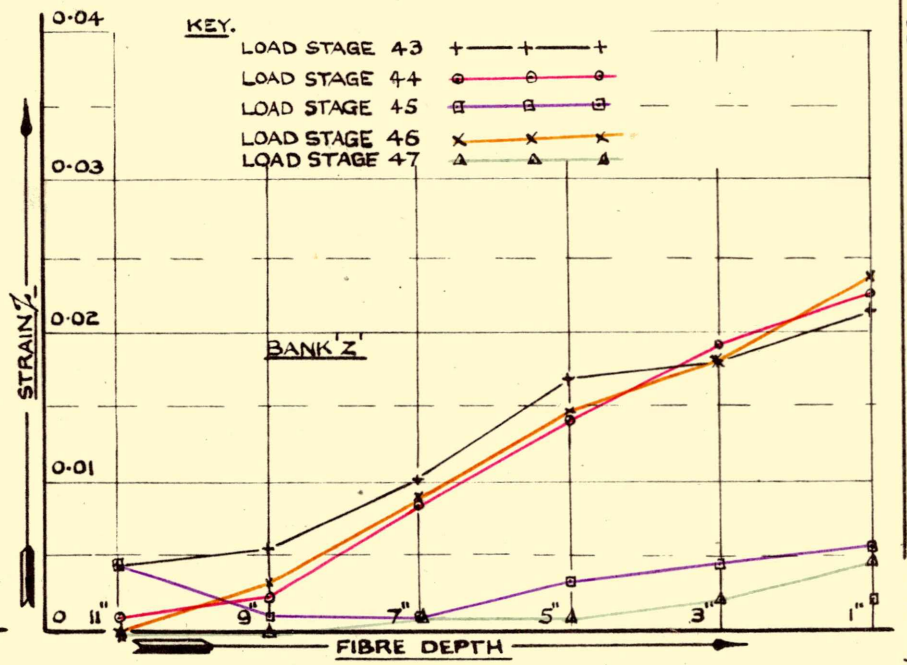
When comparing the graphical results given by the different types of strain gauges in this and in subsequent tests, it must be remembered that the positions

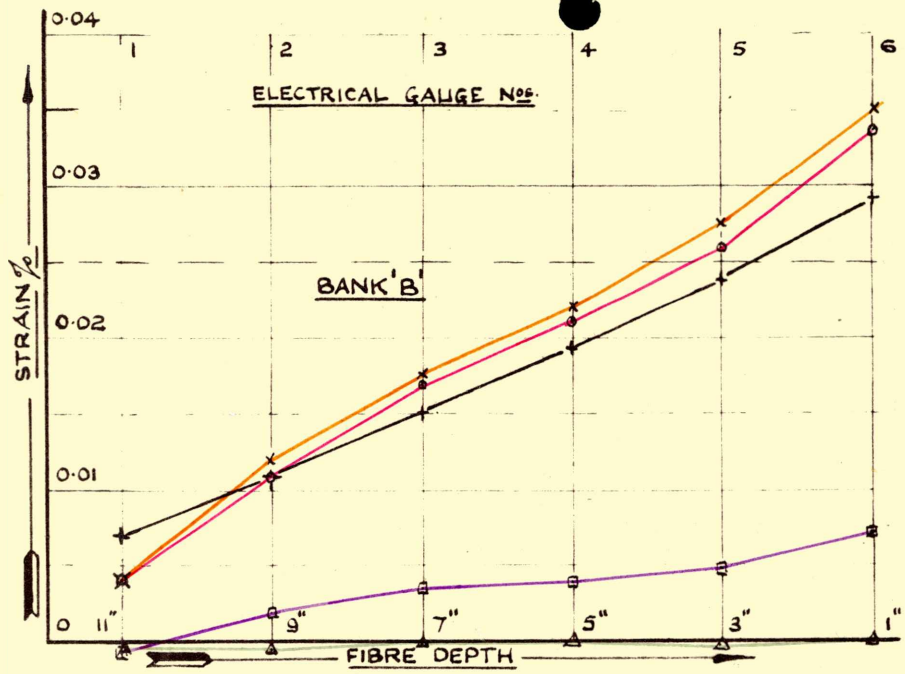

ELECTRICAL GAUGE Nos.
1
2
3
4
5
6
BANK 'A'
BANK 'B'
BANK 'C'
BANK 'X'
BANK 'Y'
BANK 'Z'
STRAIN %
0.03
0.02
0.01
0.04
0
-0.01
11"
9"
7"
5"
3"
1"
FIBRE DEPTH
KEY.
LOAD STAGE 43.
LOAD STAGE 44.
LOAD STAGE 45.
LOAD STAGE 46.
LOAD STAGE 47

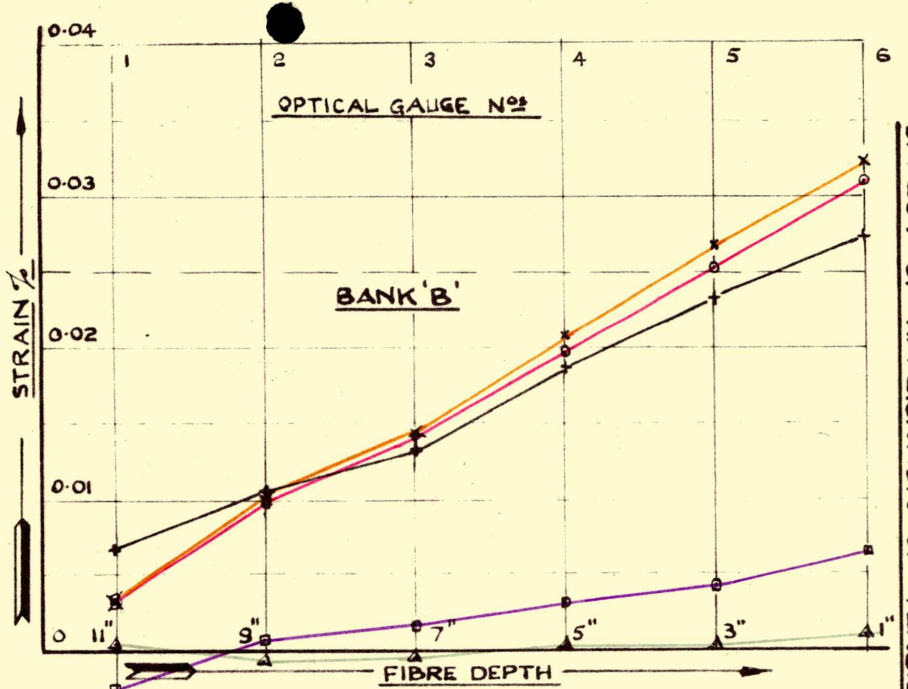

METZGER GAUGE Nos.
1
2
3
4
5
6
BANK 'A'
STRAIN %
0·04
0·03
0·02
0·01
0
11"
9"
7"
5"
3"
1"
FIBRE DEPTH


METZGER GAUGE Nos.
1
2
3
4
5
6
BANK 'X'
STRAIN %
0·04
0·03
0·02
0·01
0
11"
9"
7"
5"
3"
1"
FIBRE DEPTH


BANK 'C'
STRAIN %
0·04
0·03
0·02
0·01
0
11"
9"
7"
5"
3"
1"
FIBRE DEPTH


KEY.
LOAD STAGE 43
LOAD STAGE 44
LOAD STAGE 45
LOAD STAGE 46
LOAD STAGE 47
BANK 'Z'
STRAIN %
0·04
0·03
0·02
0·01
0
11"
9"
7"
5"
3"
1"
FIBRE DEPTH





KEY.

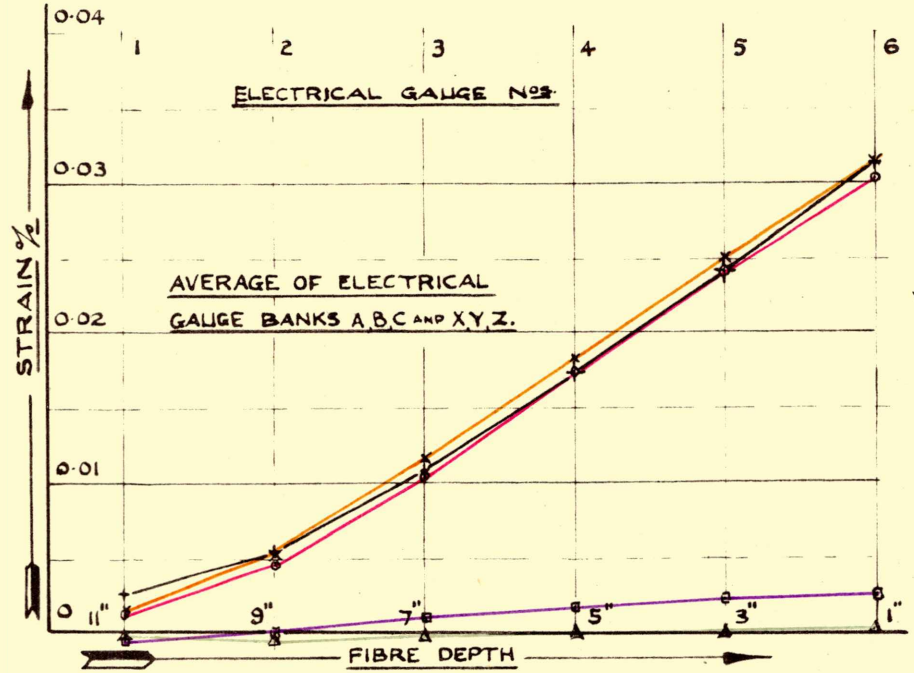
LOAD STAGE 43 —+—+—+—

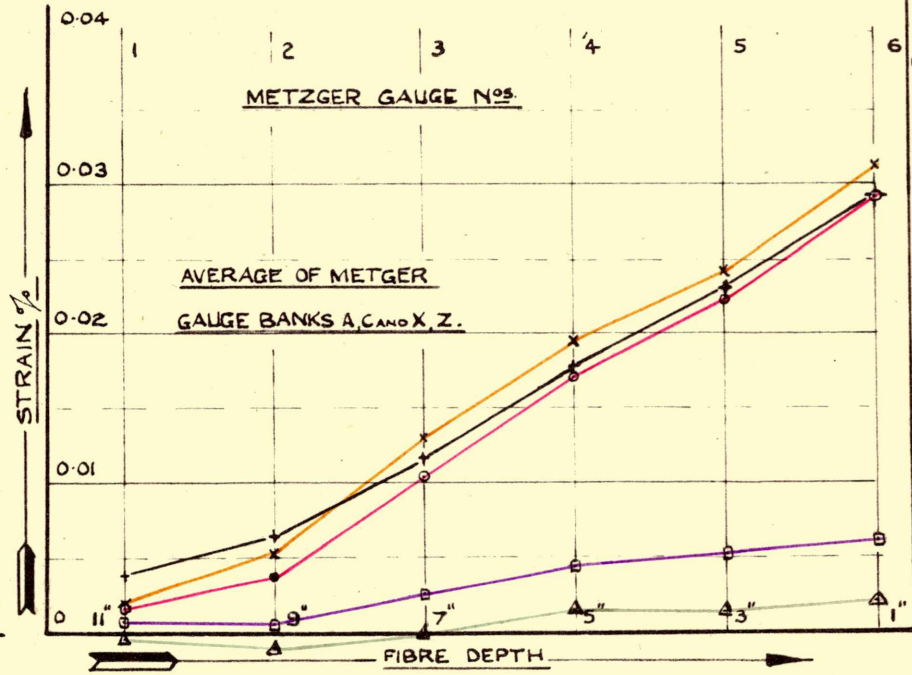
LOAD STAGE 44 —o—o—o—

LOAD STAGE 45 —□—□—□—

LOAD STAGE 46 —×—×—×—

LOAD STAGE 47 —▲—▲—▲—





of the gauges on the specimen vary slightly. It was considered best, for purposes of comparison, to place one type of gauge over another; the difference in gauge lengths made this easy to accomplish. In the case of the Metzger gauge a choice had to be made between two instruments, one with a two inch and the other with an eight inch gauge length. The eight inch gauge length was selected as being the most suitable; firstly it could be located over the electrical resistance strain gauges, and secondly it gave a greater degree of sensitivity. A detailed diagram showing the relative positions of the gauges and their particular gauge lengths has been given on p.23.

The following observations were made from the results of the foregoing tension test. In none of the strain gauge banks was the effect of the tension force greatly marked. The central gauge banks,'B' and 'Y', showed the effect of the tensioning most, the compressive strain under gauge 'B6' due to tension force only being 0·0072%, as measured by the electrical resistance strain gauge, and 0·0066% measured by the optical strain gauge. The general effect of the tensioning was to cause an increase of compressive strain near to the extreme compressive fibres, and a decrease in the compressive strain under the loading points nearest to the neutral axis. As a result of the tensioning, the strain curve 'pivotted' about a point,

all sections to one side of this point showing an increase in compressive strain and to the other side, a decrease. The point about which the strain curve 'pivotted' varied with the particular gauge bank considered, but on the average this point was 8" from the outer compression fibres. The tendency was, therefore, for the tensioning to shift the neutral axis over towards the compression zone. A sound explanation of why a greater effect was noted at the central sections of the specimen than at the ends, appears to the author to be that this was due to the particular way in which tension was applied. As the stressed high tensile steel wires enter the specimen, the bond of the concrete will gradually transfer more of the load from the steel into the concrete; this will increase with the distance of the wires in the concrete. It is probable that the high tensile strain induced in the wires at their ends caused a local break-down of the bond there. Evidence of this was seen, after the tensile force had been fully applied, by the flaking of the concrete occurring where the tensile steel entered the specimen. This would mean that very little tensile force was present in the concrete at the end sections, causing, as a result, only a small effect on the strain recorded there. On the other hand, at the central section the heavier tensile force induced in the concrete would have its effects increased by the existence there of an artificial crack.

In theory load stage 44 being composed of the compressive load and the additional tensile force should show the same strain figures as does load stage 46. However in general the strains recorded under stage 44 were less than those for stage 46. This difference was caused by the greater length of time elapsing between the application of the compressive load and the reading of the strain gauges in the case of load stage 44 (it being necessary to spend some little time in the application of the tension force) than in load stage 46. During this time slight leakage of oil from the oil pressure circuits would cause the drop in strain observed. This drop is very small compared with the strains recorded, but it does tend to emphasize the need for speed in reading the gauges, once the load has been applied. The best comparison between a load without tension and the same load with a tension force applied, was given, therefore, by load stages 44 and 46.

On investigation of the results obtained in this test by the three different types of gauges, it can be seen that the electrical resistance strain gauges do, in general, give the most consistent results. Bank 'B' of these electrical strain gauges compares closely with the results obtained by the optical strain gauges, their gauge lengths being 3" and 4" respectively. The results obtained by the Metzger gauges show a little irregularity, but give

similar results, for various positions of the gauge points on the specimen, to the readings obtained by the electrical resistance strain gauges. Allowance should be made, when comparing these latter types with one another, for the large difference in gauge length, the Metzger's gauge length being 8". This would cause, in theory, the readings on the Metzger gauges to fall between those registered on the electric gauges at the end bank considered and at the corresponding central bank. This was found also to be the case in practice, after observation of the results obtained.

---//---

N.B. In the many graphs throughout the thesis in which strain is plotted against fibre distance from the neutral axis, the orientations of the axes are as for the beam element standing in the machine. The more familiar form of the strain-distributions as they appear from actual beam tests, can be gathered by turning the book through ninety degrees so that the axis of strain is horizontal.

CHAPTER VIII.

Test of First Specimen.

Having completed the preliminary investigations, given in detail in the preceding chapters, testing of the first specimen was commenced. The first routine to be followed was that of loading the specimen with a linear stress-distribution. It was expected that, being in the elastic range with stress proportional to strain, the resulting strain-distribution obtained from readings would be linear. The resulting strain-distributions recorded at the gauge banks approximated to a straight line, but they each showed individual variations from a true straight line (some more markedly than others).

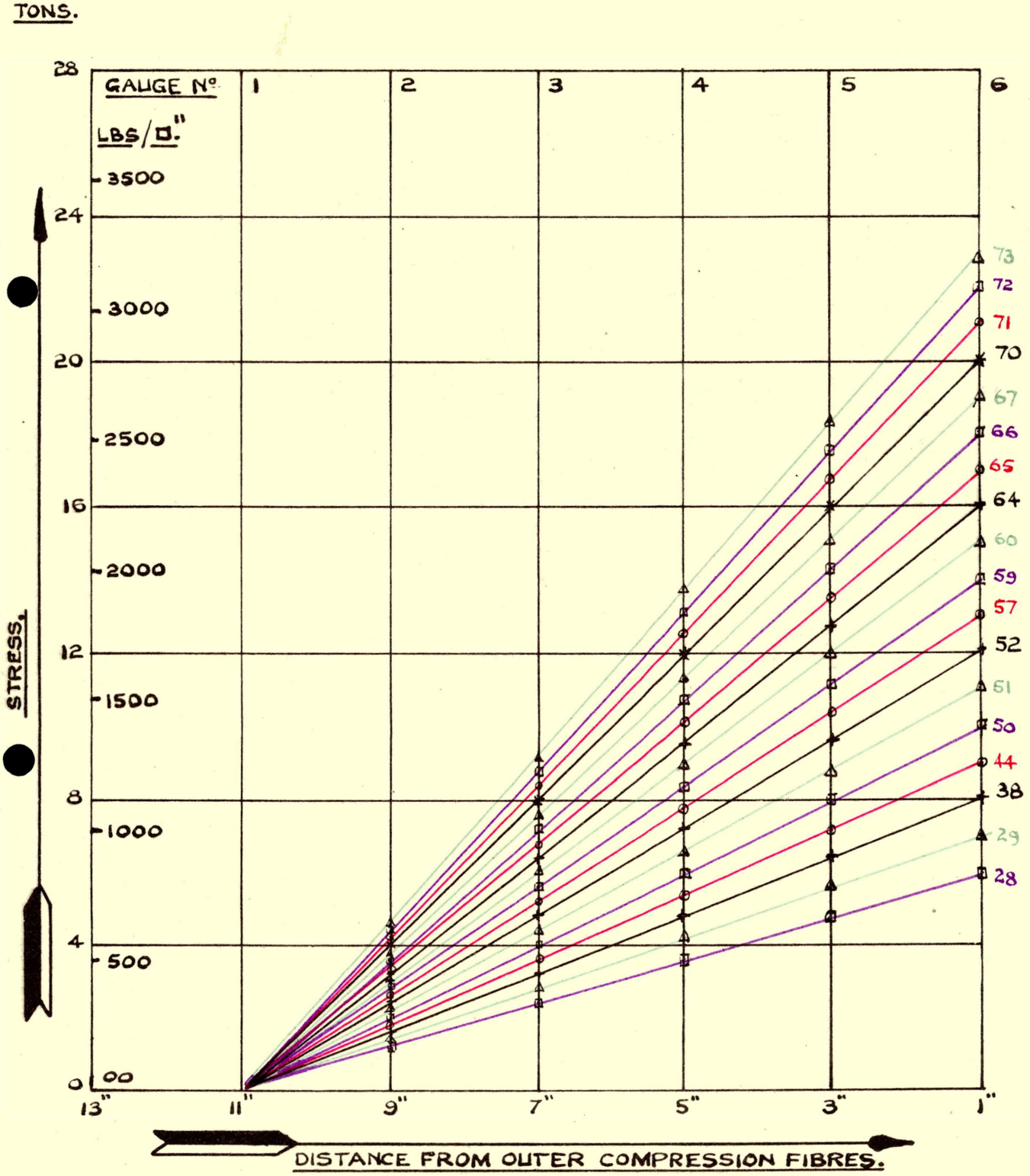
Readings of all the strain gauges, electrical resistance, Metzger and optical were taken and graphs plotted, p.95 to100 showing the strain-distributions at the various gauge banks. Corresponding stress-distributions are also given on p. 94 . The strain-distributions recorded at banks 'B' and 'Y' were nearer to a perfect straight line than those recorded at the other banks.

It was significant that the individual variations from a perfect straight line, which any one gauge bank showed under a particular linear stress-distribution in the elastic range, were repeated in a similar fashion

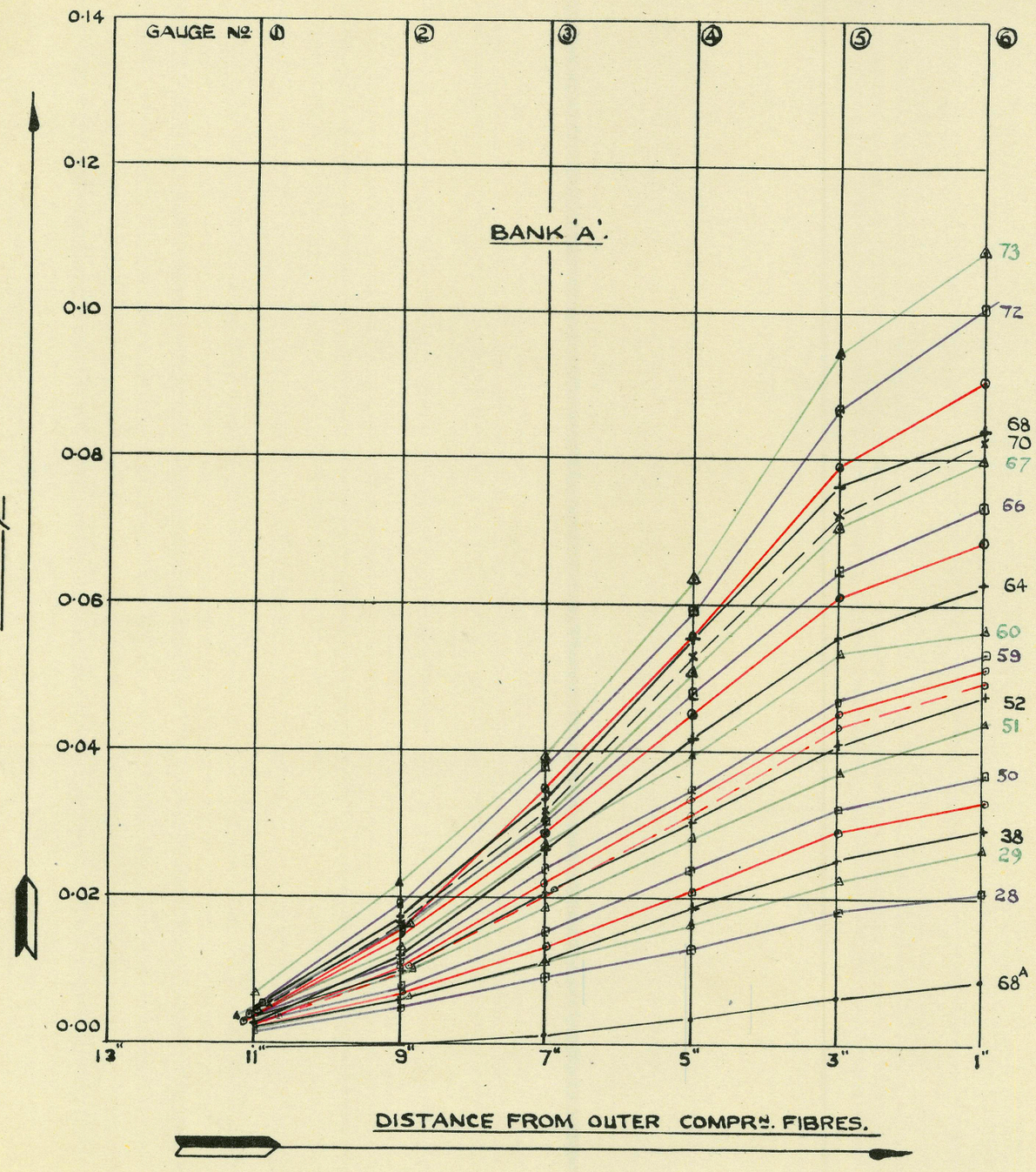
LOAD STAGES UP TO PLASTIC ZONE.

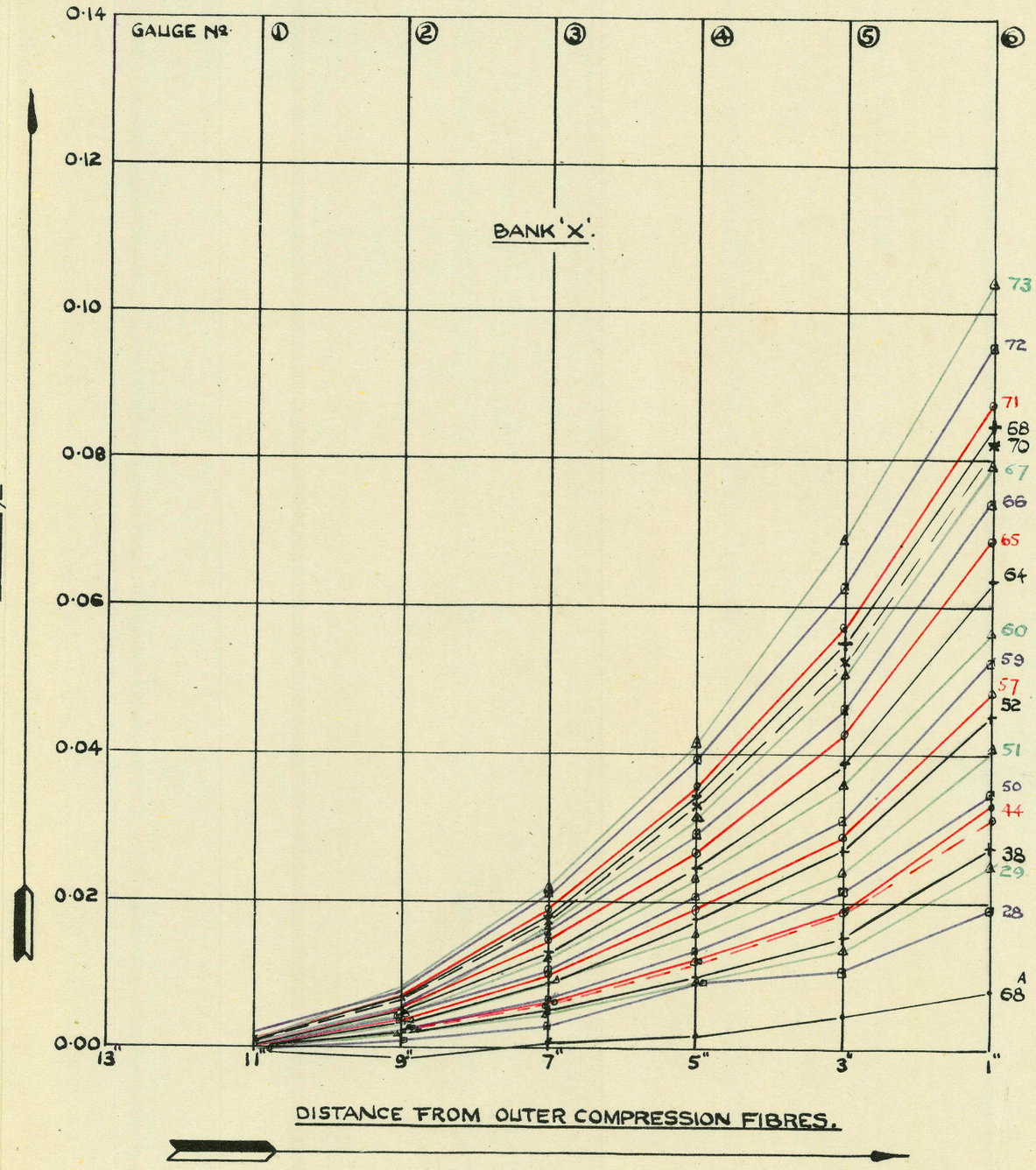
1ST. SPECIMEN.

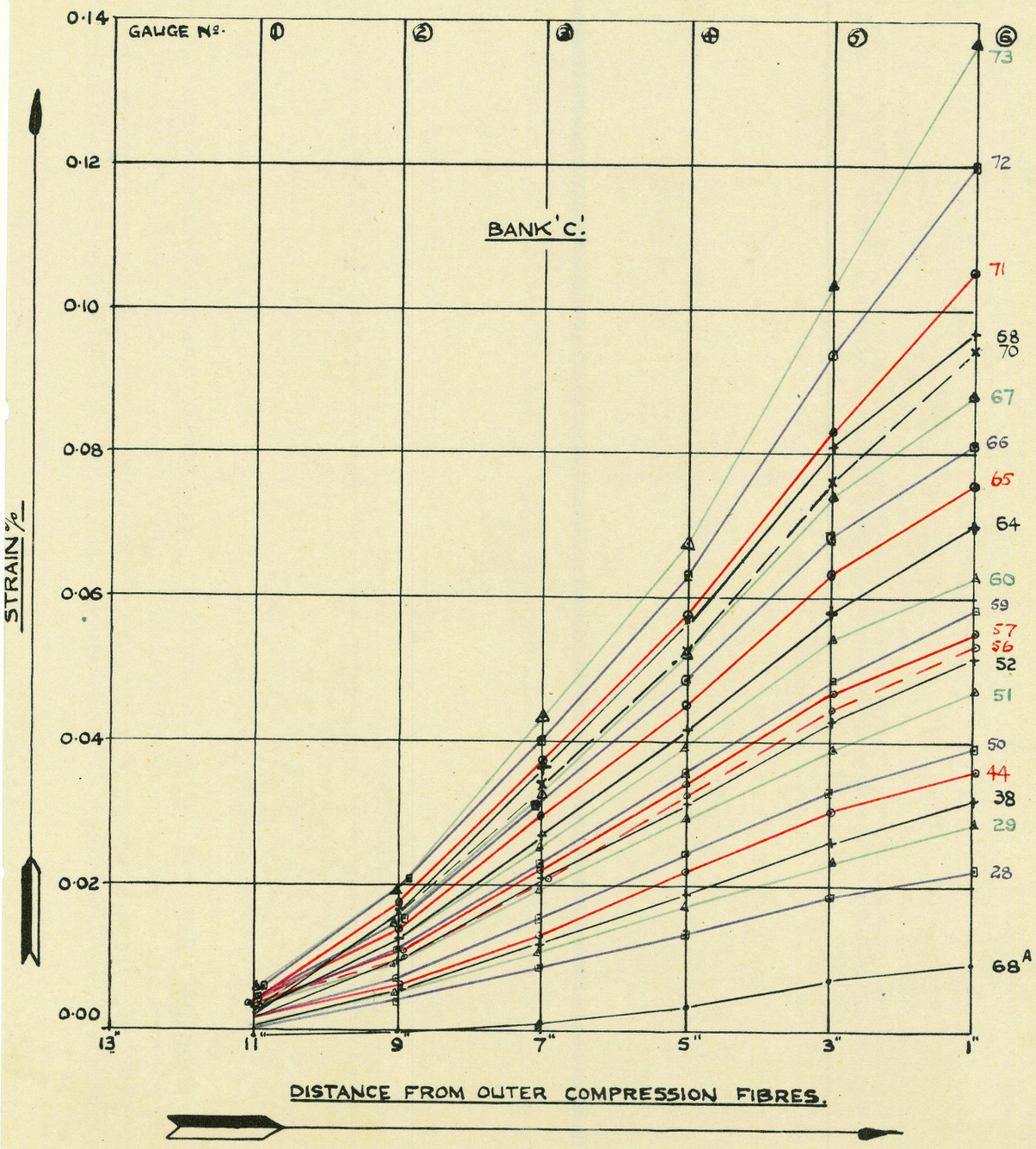
STRESS DISTRIBUTION.

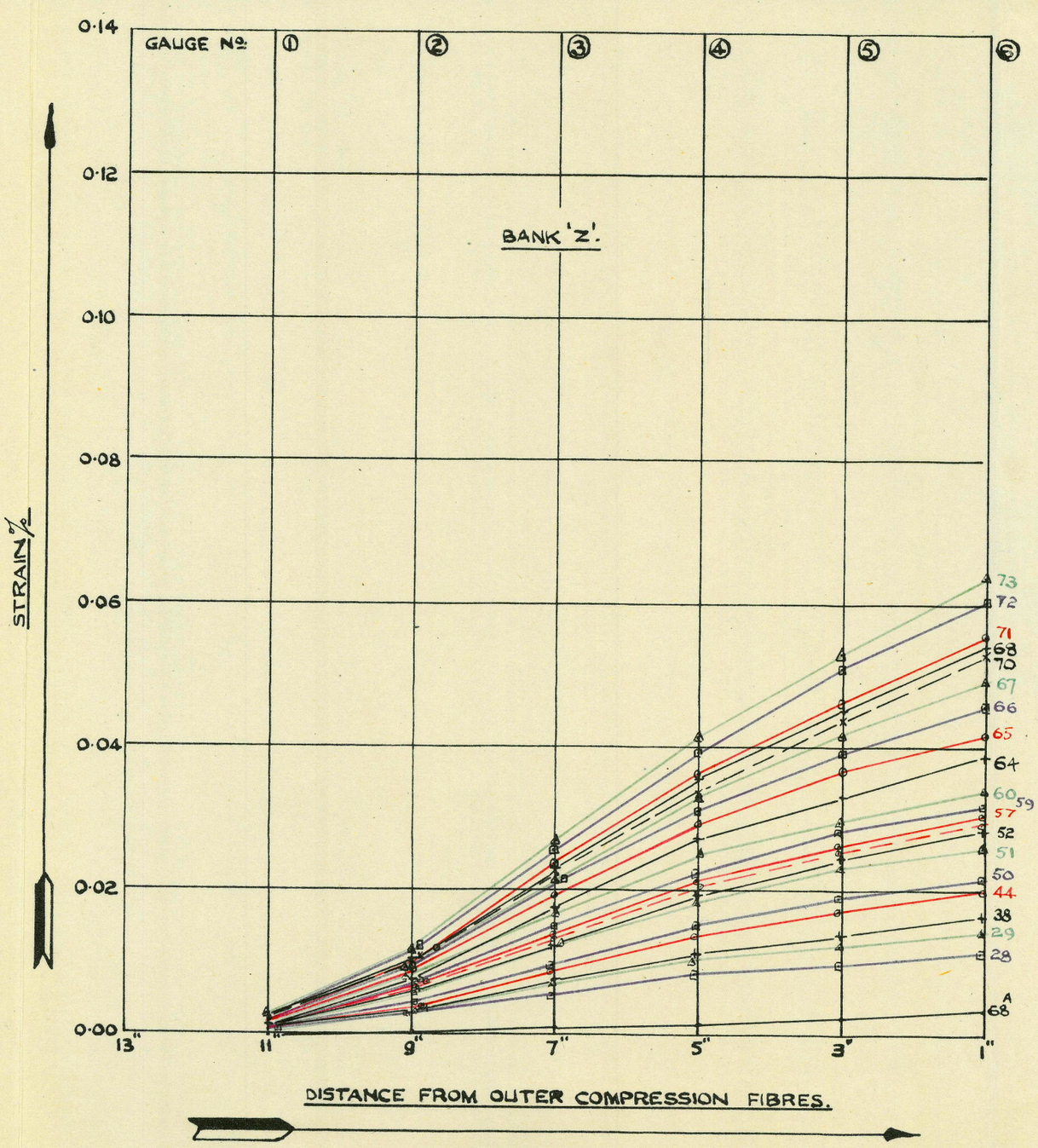


STRAIN DISTRIBUTION AT END SECTIONS OF 1ST. SPECIMEN FOR LOAD STAGES UP TO THE PLASTIC ZONE USING ELECTRICAL RESISTANCE STRAIN GAUGES.

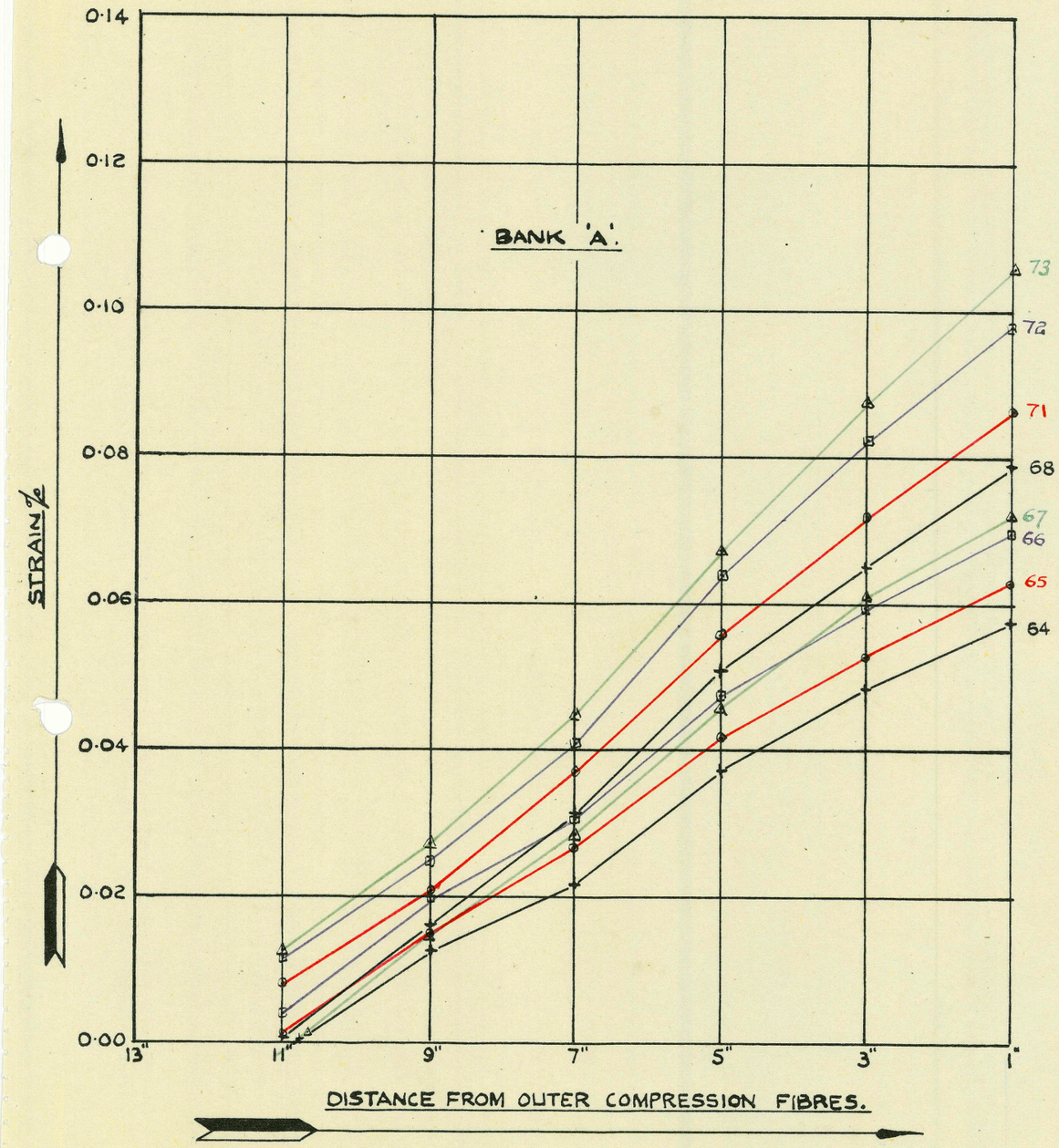


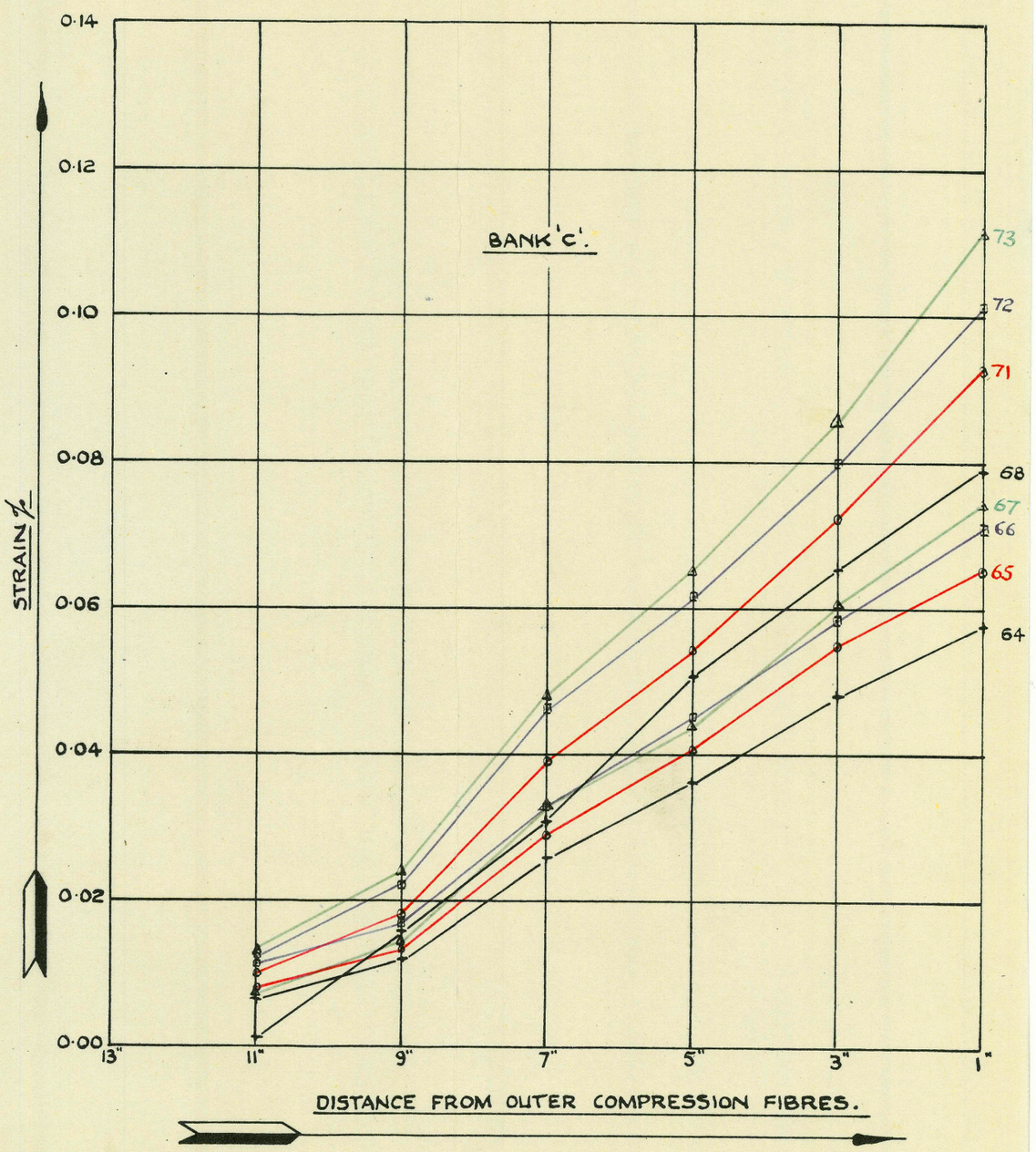


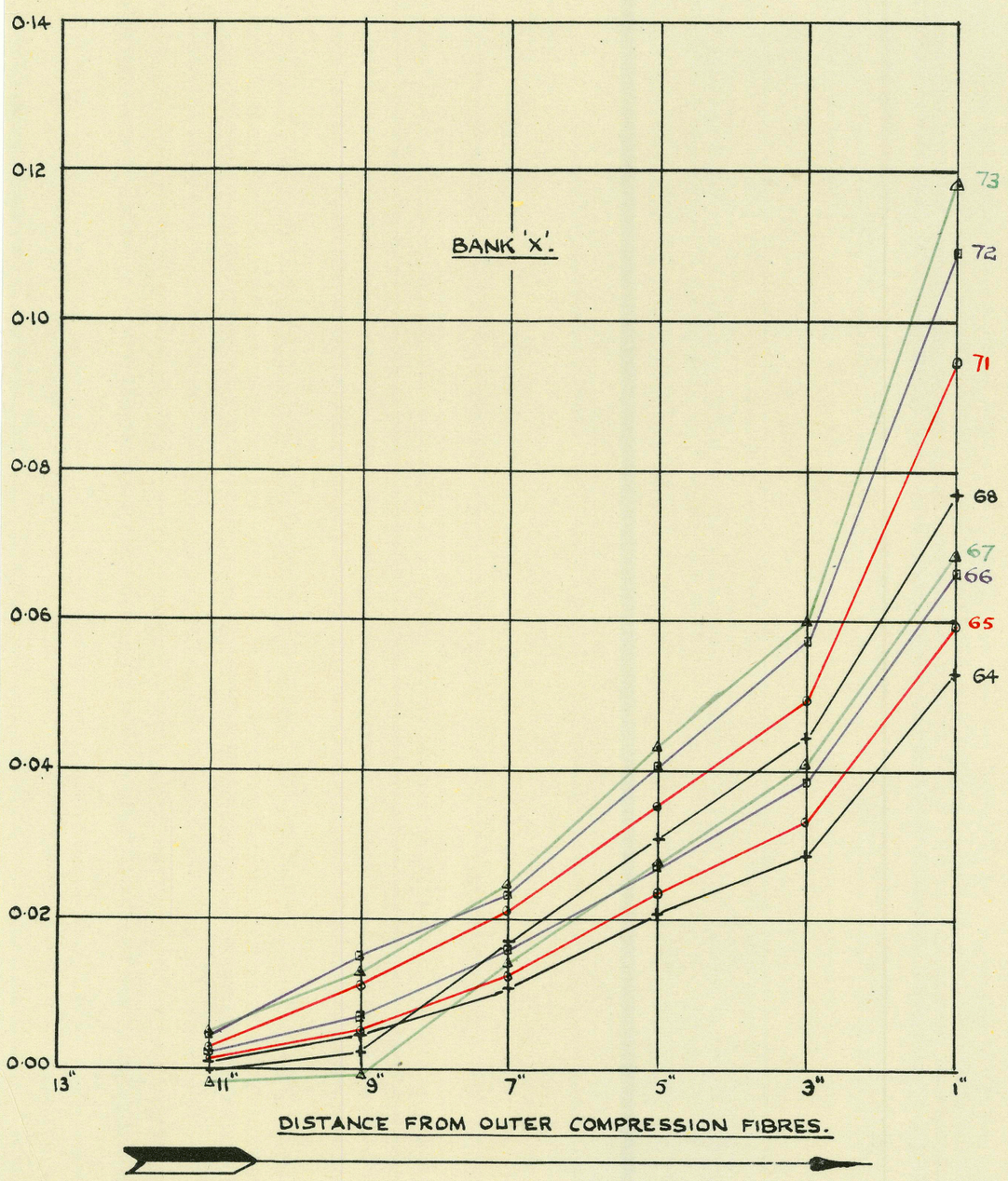


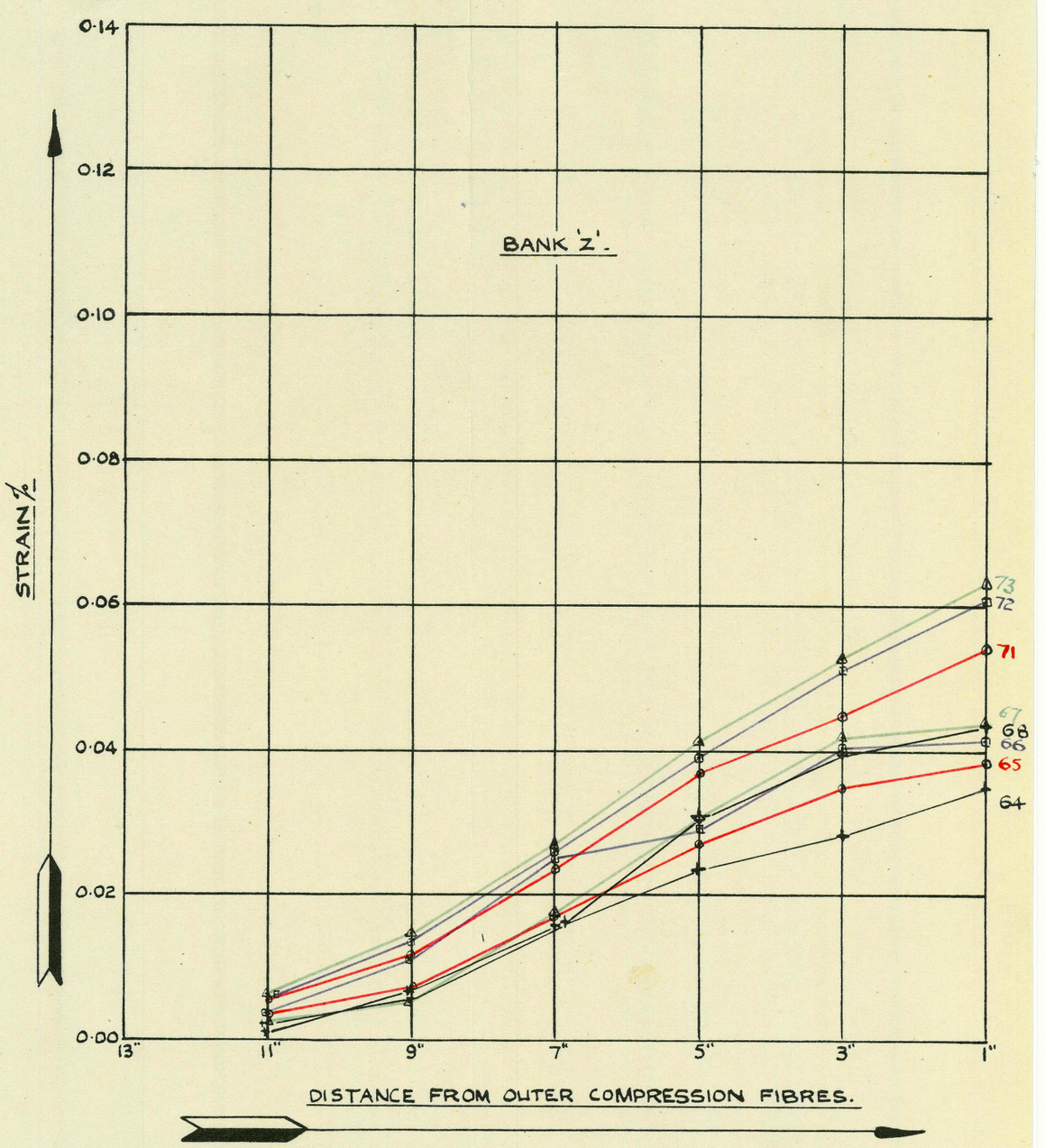


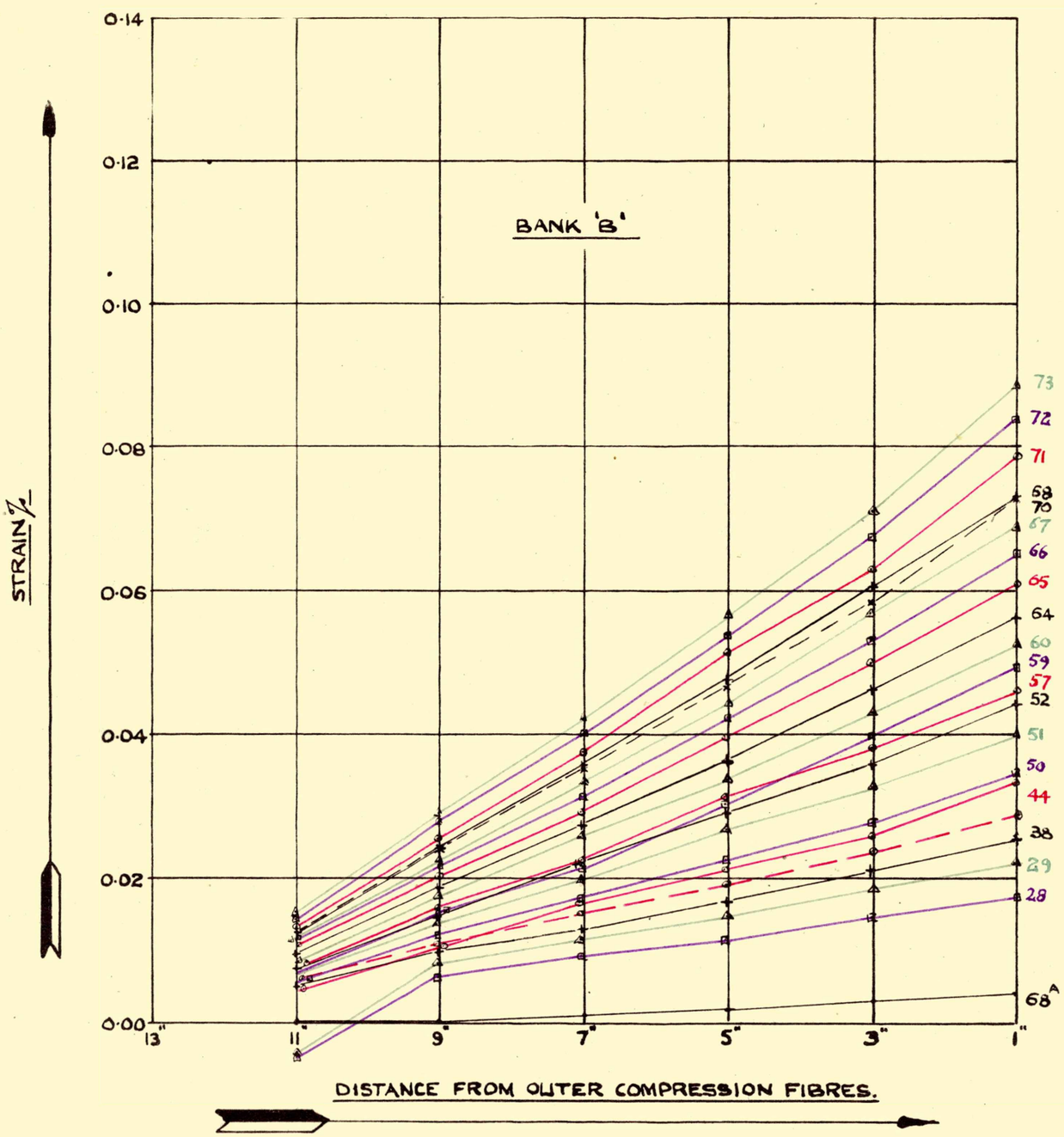
STRAIN DISTRIBUTION AT END SECTIONS OF 1ST SPECIMEN FOR LOAD STAGES UP TO THE PLASTIC ZONE USING METZGER STRAIN GAUGE.

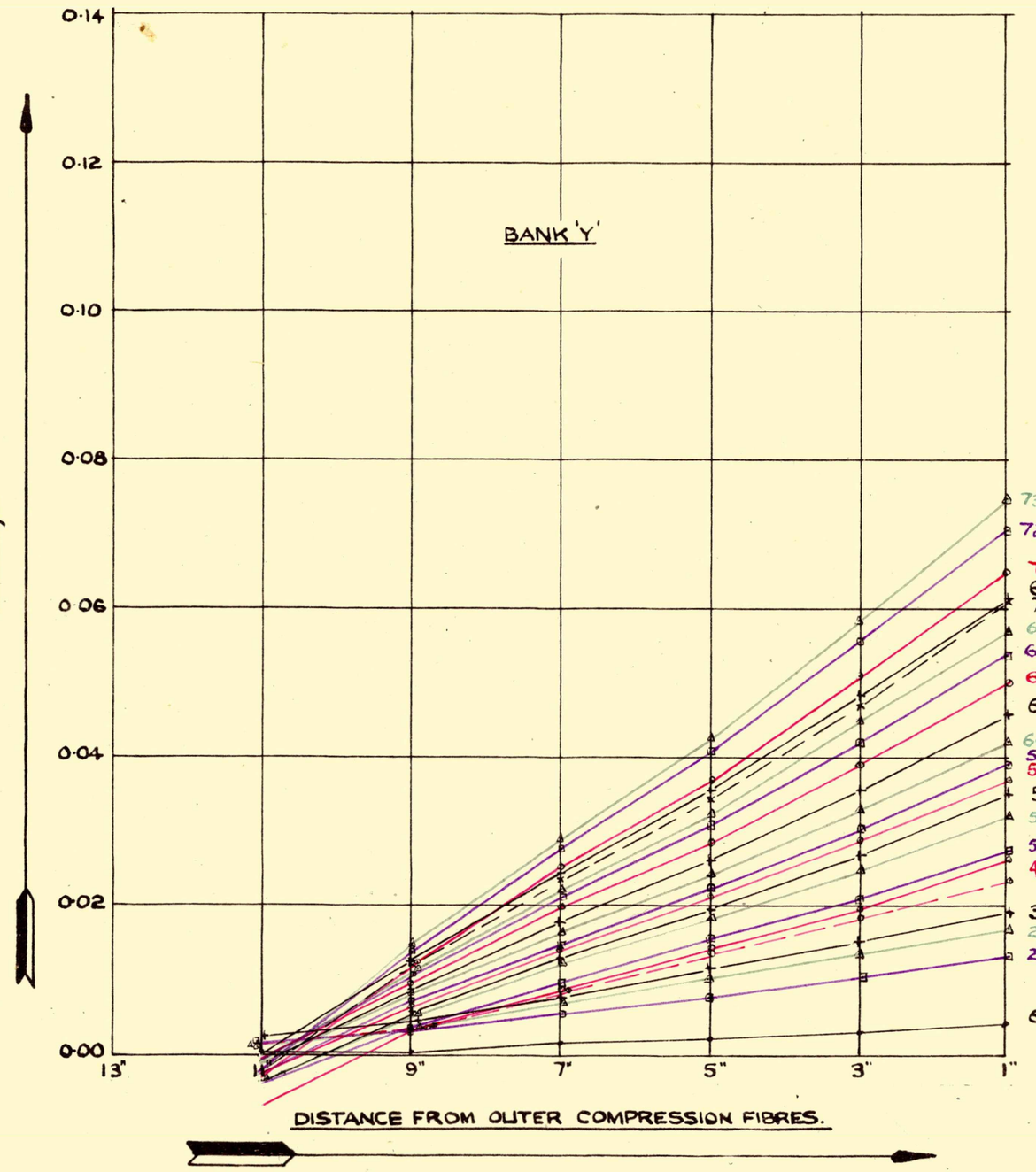












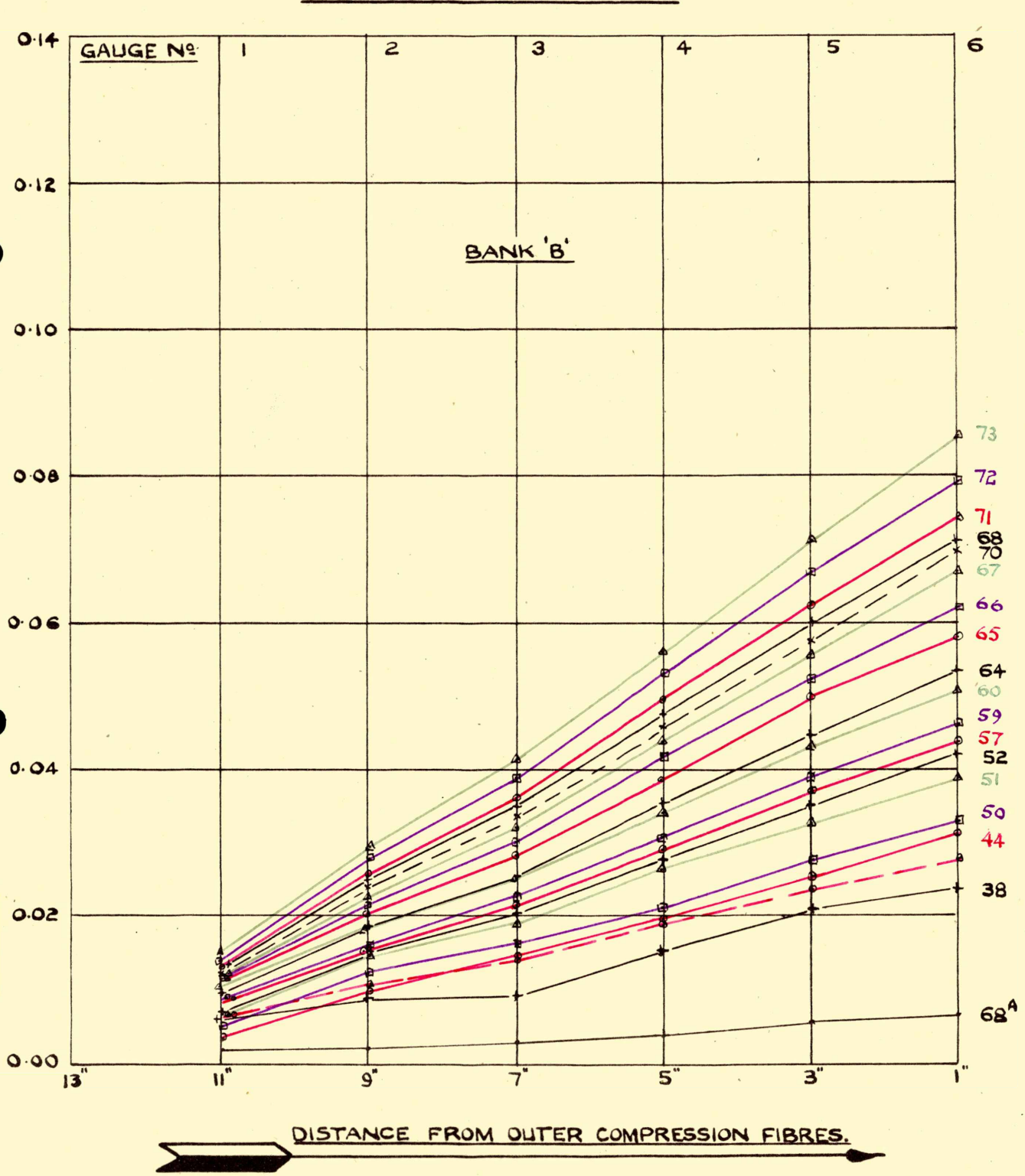
STRAIN DISTRIBUTION AT CENTRAL SECTION OF 1ST. SPECIMEN

FOR LOAD STAGES UP TO THE PLASTIC ZONE

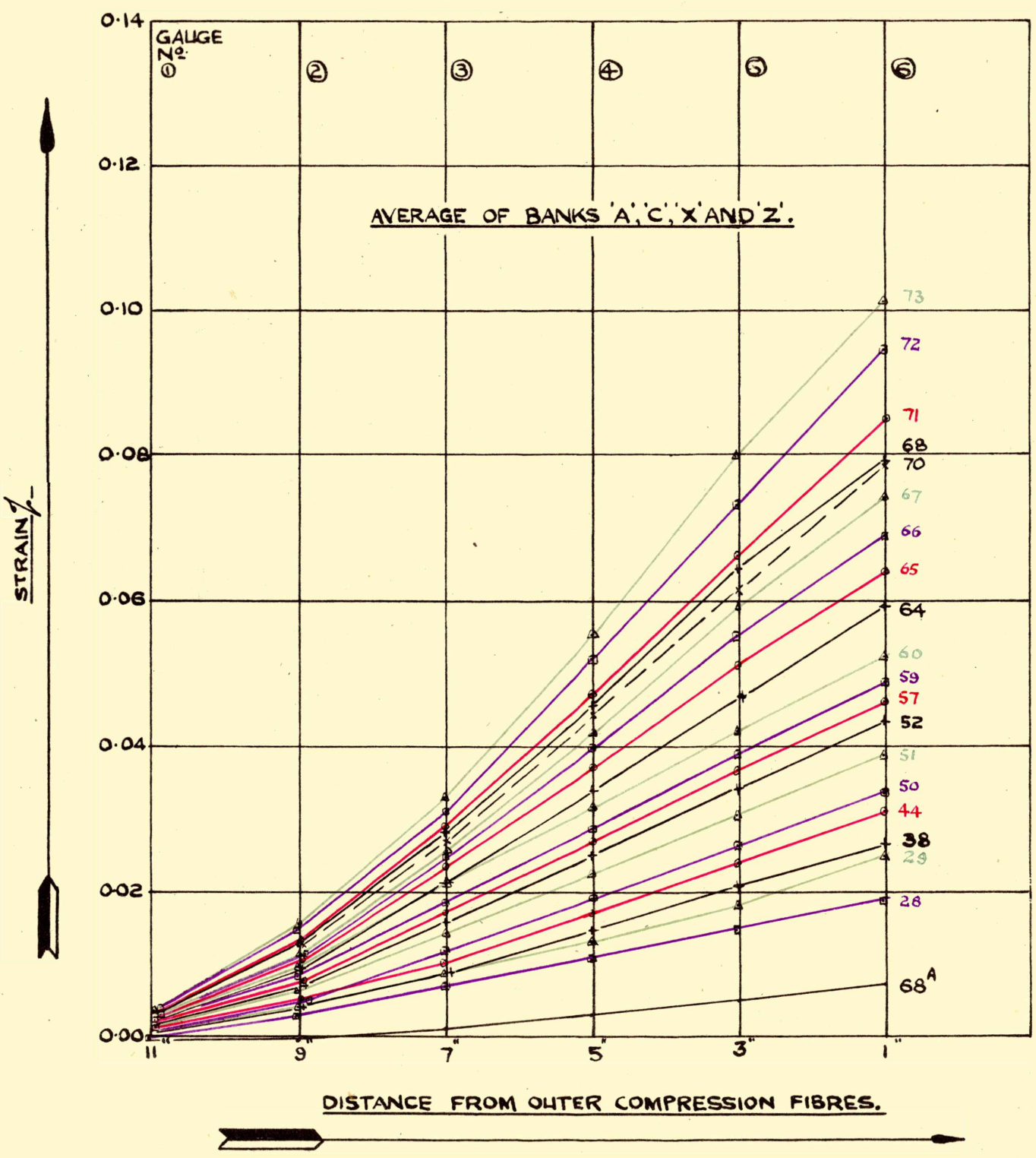
USING ELECTRICAL RESISTANCE STRAIN GAUGES.

STRAIN DISTRIBUTION AT CENTRAL SECTION 1ST SPECIMEN

FOR LOAD STAGES UP TO PLASTIC ZONE.

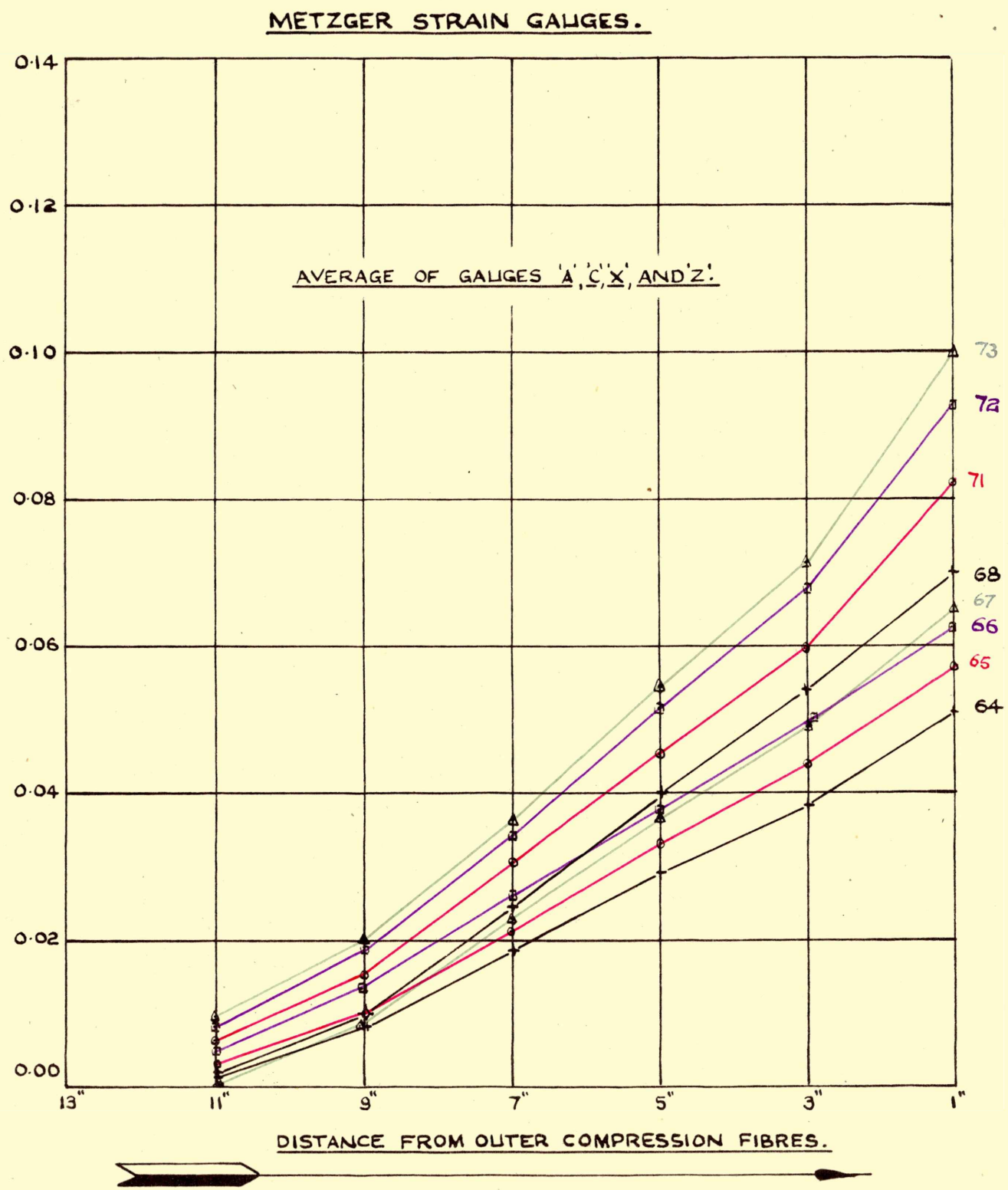


STRAIN DISTRIBUTION IN 1ST. SPECIMEN FOR LOAD STAGES UP TO PLASTIC ZONE.



STRAIN DISTRIBUTION IN 1ST SPECIMEN

FOR LOAD STAGES UP TO THE PLASTIC ZONE.



under any other linear stress-distribution in the elastic range.

The question which was now foremost in the mind of the writer was:- What strain shape should be aimed at during the further testing of the specimen through the elastic range and on into the plastic range? To say that the achievement of a straight line strain over the central banks 'B' and 'Y' would give true stress shape, when the preliminary testing had shown that linear strain could be produced at these points by almost any stress-distribution, was most certainly not the answer. Obviously if any reasonable degree of discrimination between different stress shapes was to be maintained by the testing machine, the gauge banks which should be watched and adjusted to a given shape, whether linear or otherwise, were the gauge banks nearest to the load points. viz. 'A' and 'X' at the top and 'C' and 'Z' at the bottom. But to obtain a perfect linear strain-distribution on all four end banks simultaneously proved to be impossible. It seemed that the most satisfactory thing to do was to consider all the probable causes of these non-linear strain shapes being produced by a linear stress-distribution in the elastic range, and either to correct them or to arrive at some compromise.

(P.T.O.)

Non-linear strain-distribution in the gauge banks could be caused by :-

(i). Inaccuracy of the strain gauges.

(ii). Incorrect loads on the various load points.

(iii). Eccentricity of loading at any load point.

(iv). High spots on the loading surfaces of the specimen.

(v). Variation in the value of 'E' for the concrete under certain gauges due to compaction, aggregate, etc. ...

Point (i). could hardly be worth considering because the results obtained by the Metzger and optical gauges confirmed the shapes obtained by the electrical resistance strain gauges.

Point (ii). might have some effect, but using the loading technique which had been carefully developed, it seemed very doubtful that this inaccuracy could cause more than a small percentage of the variations shown.

Point (iii). A probable cause of uneven straining.

Point (iv). A further possible contributory cause of local effects which could be transmitted to the strain gauges. The fact that the specimen was made in a wooden mould would increase the possibility of there being unevenness in spite of the care taken in smoothing the end faces with emery-stone.

Point (v). An obvious factor causing local differences which was reduced, to a certain extent by the selection of a long gauge length.

Points (ii), (iii), and (iv) would have greater effects on the end gauge banks than on those gauges at the centre of the specimen.

On careful consideration of these factors which when combined resulted in local differences in the strain distribution, it was decided by the author that averaging the results obtained by gauges in corresponding positions on the specimen would serve as a means of overcoming these local discrepancies. Averaging both sides of the specimen would tend to eliminate causes (iii), (iv), and (v), whilst if averages were taken for corresponding gauges in the upper and lower banks, further elimination of causes (iv) and (v) would be effected. Experiment showed that this, indeed, occurred and further testing was continued the strains being observed not only individually, but as average values. Results obtained using this procedure are shown on pages 99 and 100. By careful study of these results the following points, which influenced further testing, were noticed. Each load stage, as plotted, represented an increase on the preceding load stage of 1ton. on the highest load point (No.6.). As the load increment was constant, therefore, the relative positions of the

strain-distribution lines, for any one gauge bank, should be equally spaced (so far as experimental error will allow) during the elastic zone. But so soon as plasticity is reached this spacing would be expected to increase. This was in fact the case and can be seen occurring in bank 'C' for, after a strain of about 0.10% has been reached, the increments of strain become larger for equal increments of stress.

The vastly varying amounts of straining which were found to occur at different sections of the specimen are easily recognisable from the results. On the 'A', 'B', and 'C' side of the specimen there is more straining than on the other, 'X','Y', and 'Z' side, whilst at the end corresponding to 'A' and 'X' there is more straining for a given loading (at points in the same position relative to the outer compression fibres) than at the other, 'C','Z' end. Again the reasons for this undue discrepancy of straining must be put down to the causes outlined earlier in this chapter.

The consequences, resulting from this localisation of non-elastic straining, were such that further testing, by assuming correct stress-distribution to occur when the average of the four end banks of gauges gave linear strain-distribution, had to be abandoned and a more satisfactory method evolved; for the effect of increased straining due to plasticity at one bank only,

would not be great enough to cause much change to the shape of the average strain-distribution of the four banks, 'A','X', 'C',and'Z', and failure could occur at, say, bank'C' with an applied stress-distribution lagging far behind that really required for true agreement with the straining at bank 'C'.

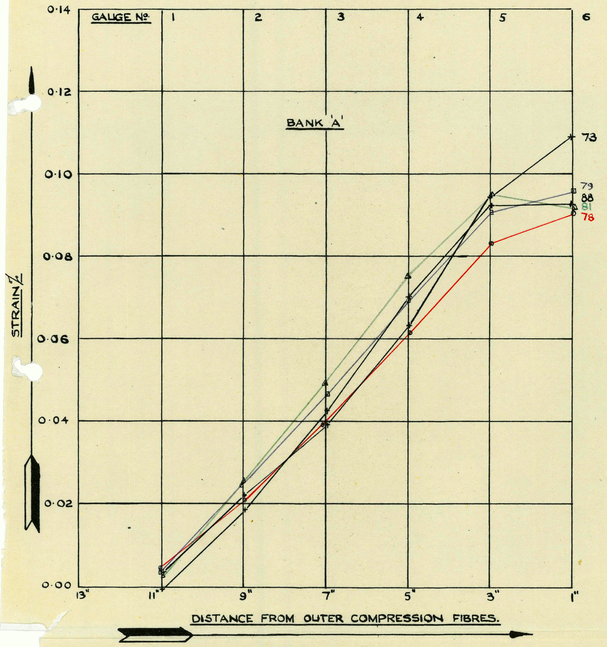
At the stage of loading now reached, differently shaped stress-distributions were applied and the corresponding strain-distributions plotted. (see p. 106.) Except to condemn load stage 81, however, there seemed to be no way of determining which of these applied stress-distributions was the most accurate.

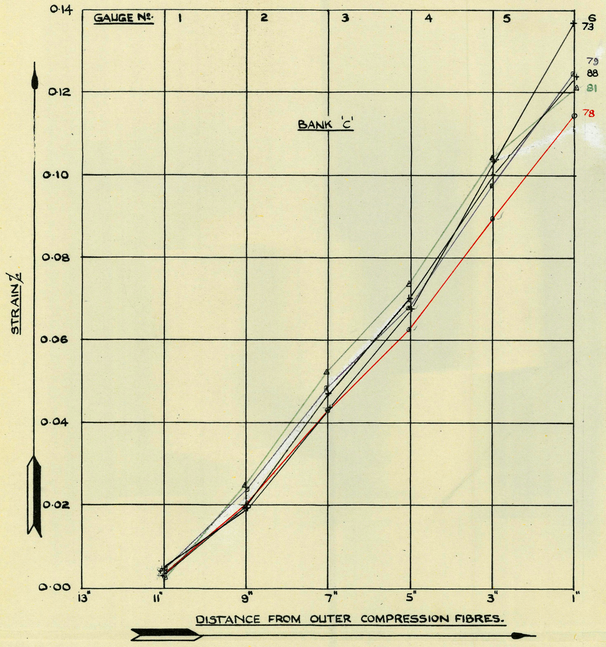
It appeared, therefore, that as bank'C' was the furthest advanced, a strain-distribution which was linear should be produced here, and the corresponding stress-distribution determined. Page 107 shows the results of an attempt to obtain linear strain-distribution (at this stage reached in testing) on bank'C' alone. Gauge No. 1, 11" from the outer compression fibres, has been ignored in these attempts as it was realised, from previous tests, that this reading was too readily susceptible to changes in the tensioning and, if included, would only misguide the tests as the tensioning could not be brought up to the full amount of the compressive load.

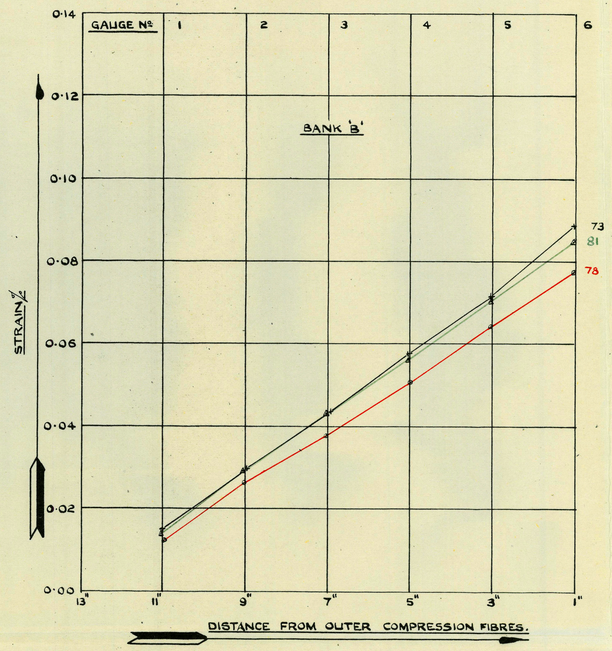
Linear Strain-Distribution on One Bank of Strain Gauges.

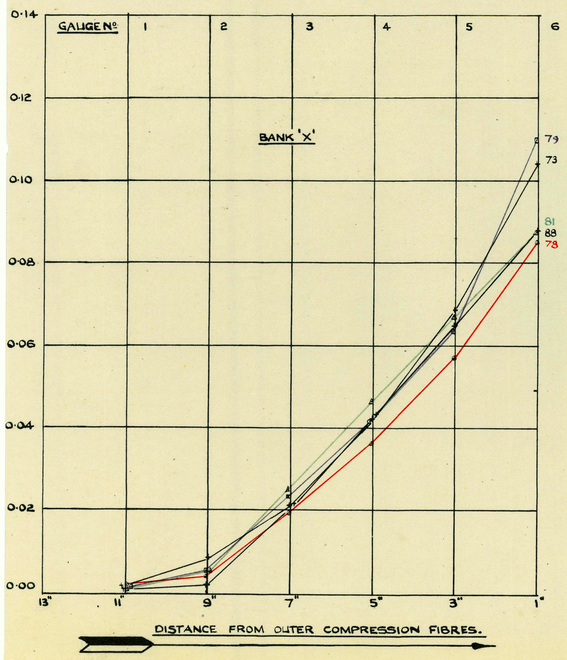
Load stage 72 showed that

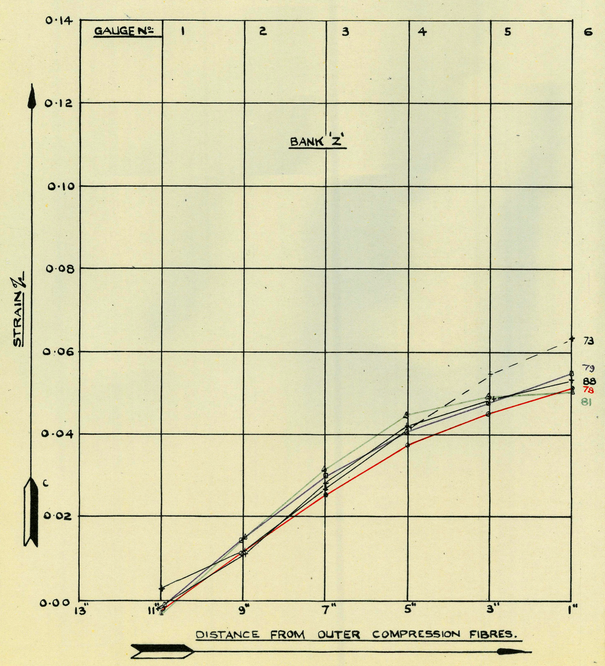
STRAIN DISTRIBUTION AT ALL SECTIONS OF 1ST. SPECIMEN.
FOR LOAD STAGES DURING COMMENCEMENT OF PLASTICITY.

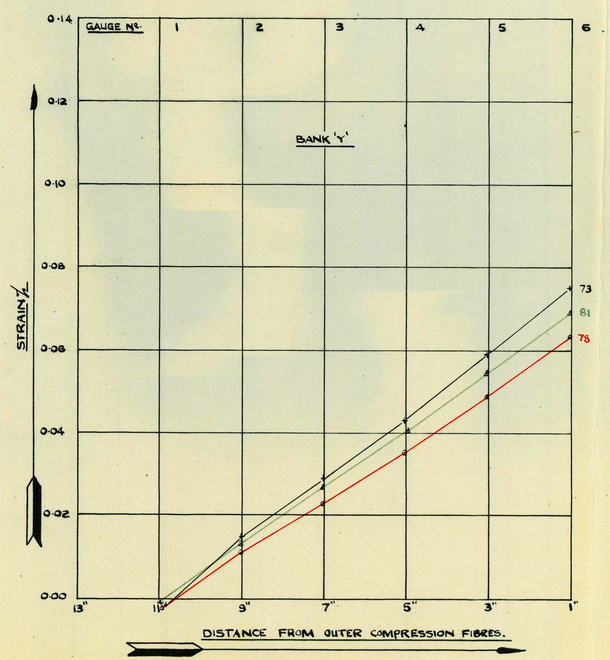




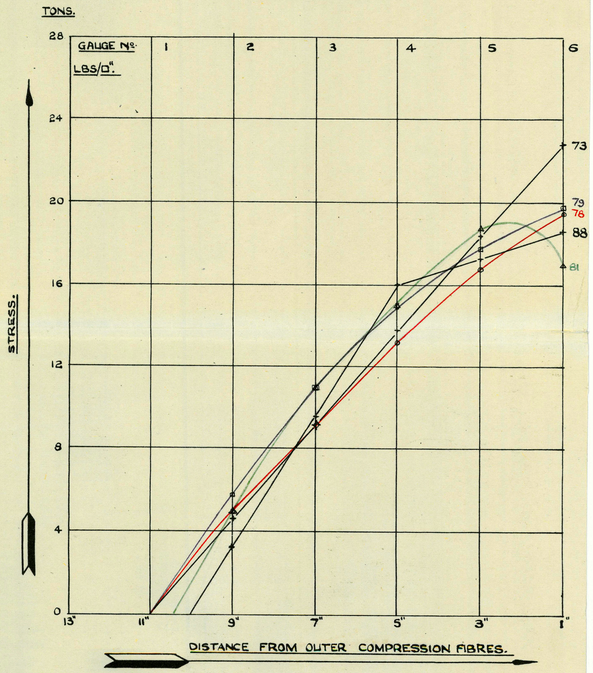






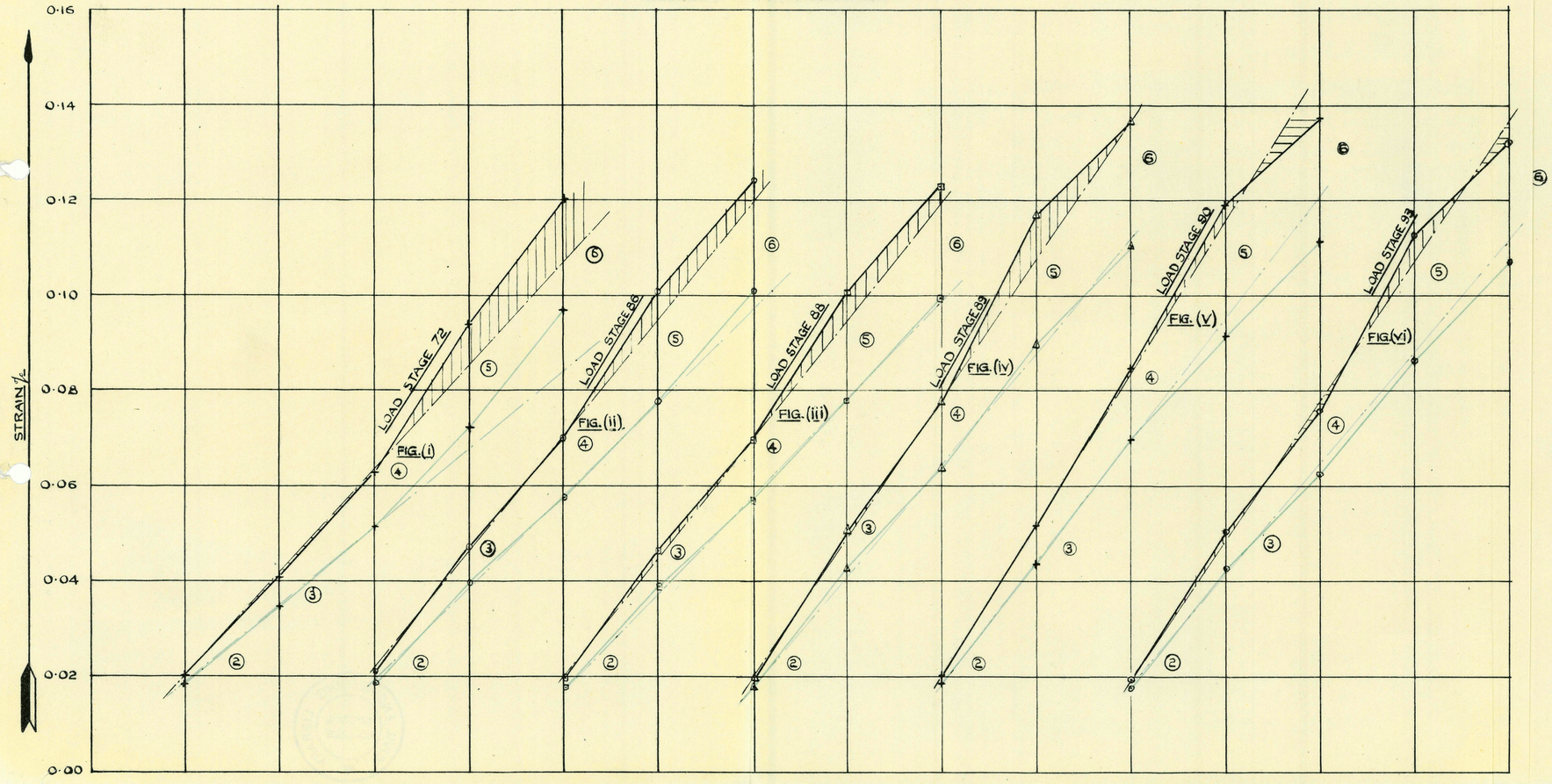


STRESS DISTRIBUTION.



PROGRESSIVE STAGES IN ATTAINMENT OF PERFECT LINEAR STRAIN DISTRIBUTION ON ONE BANK ONLY.

BANK 'C'. STAGES 72 – 93.



KEY.

ACTUAL STRAIN DISTRIBUTION: ——————

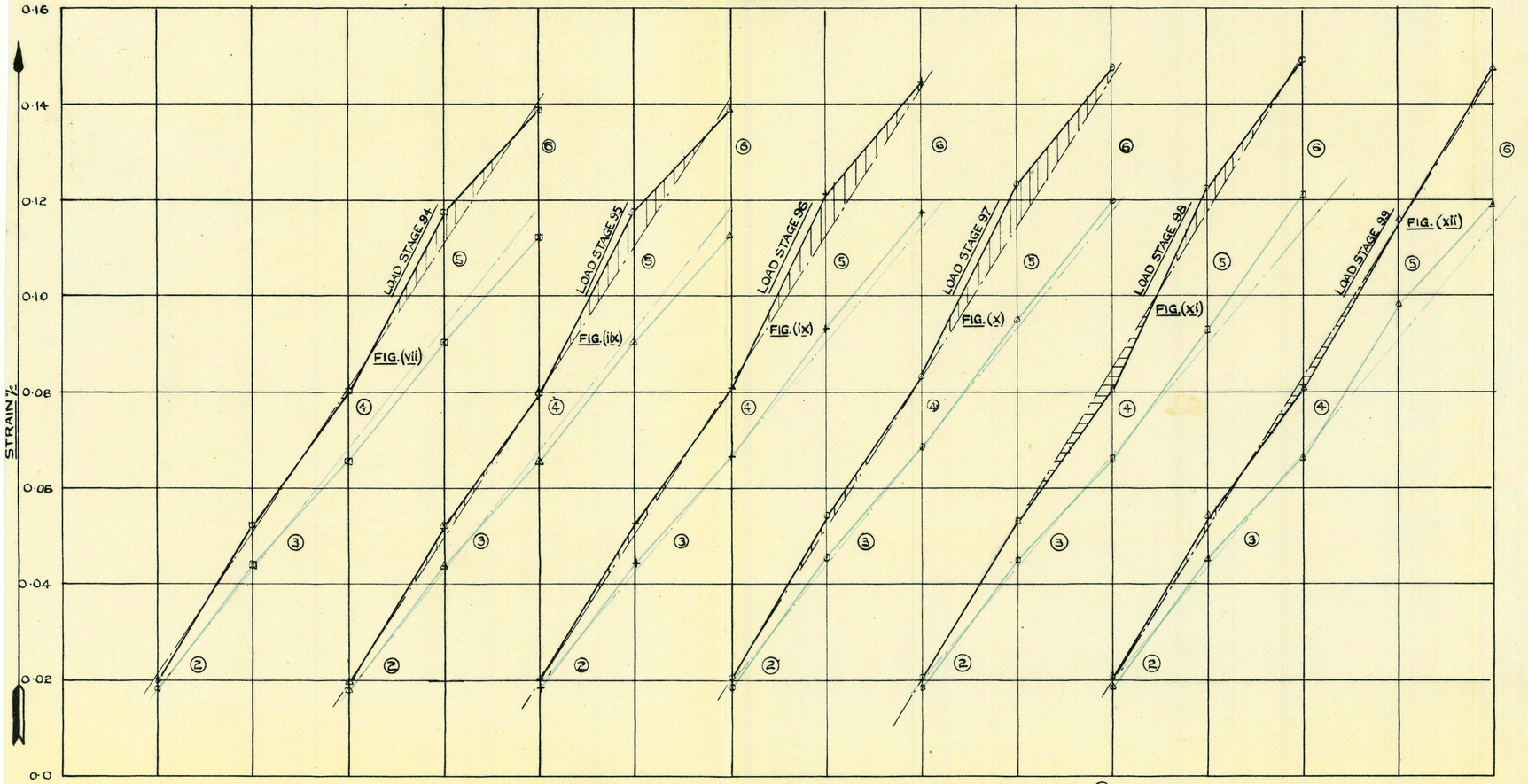
MEAN LINE THRO' ACTUAL STRAIN DISTRIBUTION: —— - ——

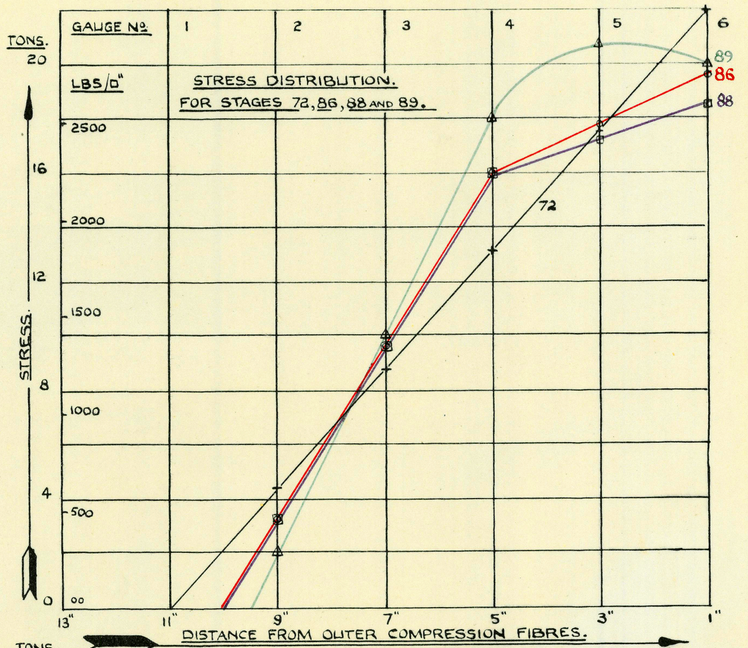
'CORRECTED' STRAIN DISTRIBUTION: ——————

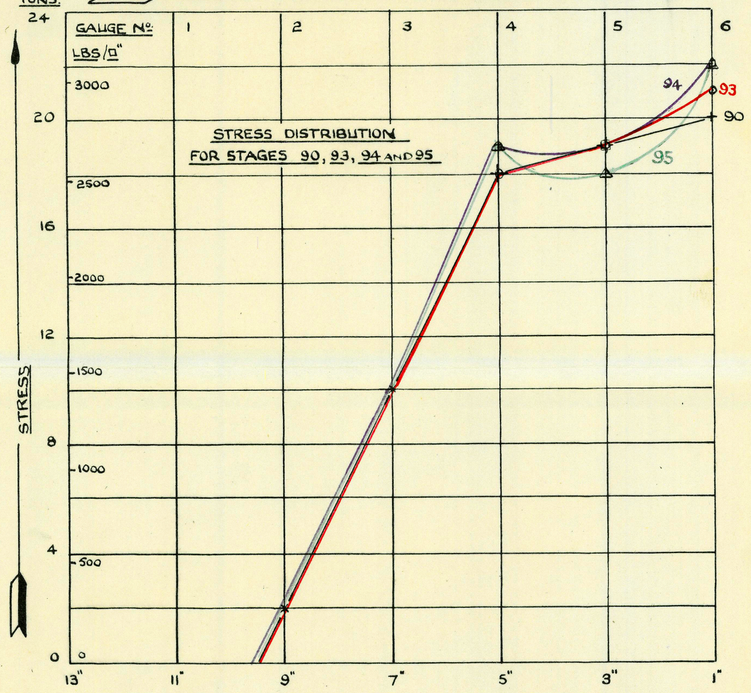
MEAN LINE THRO' CORRECTED STRAIN DISTRBN.: —— · ——

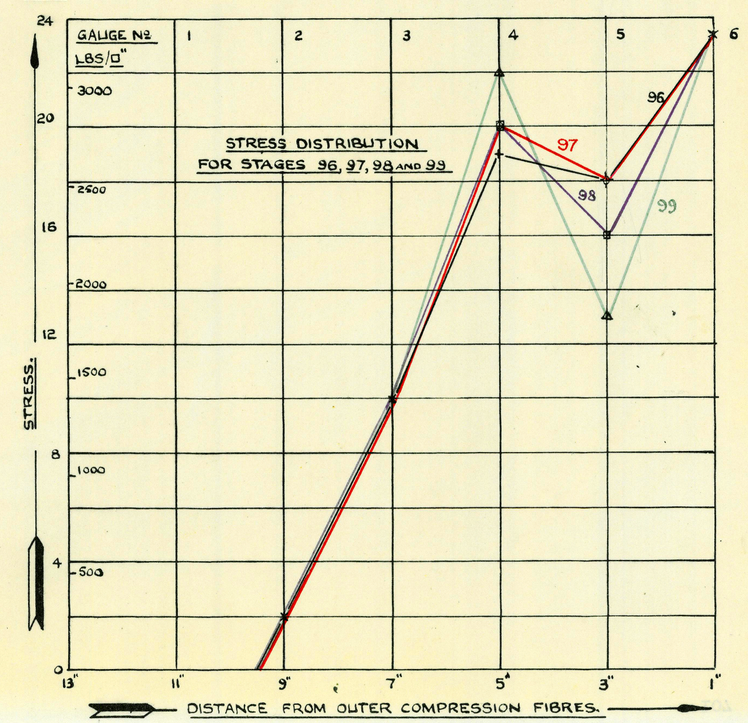
CORRECTION REQUIRED:

BANK 'C'. STAGES 94 – 99.









the straining over gauge No.5 and 6 was too much. See fig.(i) p.107. The load was reduced over 5 and 6 and increased, to compensate, over gauges 3 and 4. This gave stage 86, but high strain was still shown under gauges 5 and 6, fig.(ii), and a further reduction was made at stage 88, fig.(iii). In an attempt to reduce the straining over gauges 5 and 6 further tests as shown in figs.(iv) to (xii) were carried out. The trouble encountered was that gauge number 5 appeared to have excessive strain even when the loading over both points 5 and 6 had been reduced sufficiently to bring point No. 6 onto the linear strain-distribution line as was achieved in stage 89. It was not until unique stress-distributions, which had non-continuity of loading, particularly over gauge No.5, had been tried that the strain distribution was brought very close to a perfect straight line. This is shown in the progressive stages up to load stage 99.

After considering very carefully the results of this test and of the strain-distributions produced earlier by linear stress-distributions in the elastic range, the writer began to believe that perfect reproduction of linear strain-distribution across the specimen, whether on individual gauge banks or not, was not necessarily the best guide for obtaining the true stress-distribution in the beam element under bending simulation conditions.

At all stages of loading, the true strain-distribution on any given gauge bank, which should be aimed at and attained, before any corresponding stress-distribution be accepted as representative of beam conditions, is that strain-distribution which follows, exactly, the shape of the strain-distribution existing under linear stress-distribution in the elastic range. Under ideal conditions this would, of course, be a perfect straight line, but due to the inconsistencies existing in concrete, whether in beams or bending simulation specimens, this strain-distribution will normally be only of a form approximating to a straight line, and its deviations from a perfect straight line must be taken into account if reasonably good results are to be obtained.

The author was anxious to examine other people's results showing the distribution of strain in concrete beams, so that some further light might be thrown upon this point.

The evidence which was examined showed without doubt that whilst the distribution of strain across a beam section is practically linear, there do exist small irregularities in the straining occurring at different distances from the neutral axis which, in any particular case, are repeated at all levels of loading.

Some of this evidence was

included in the thesis, and reference to Appendix XI.p.213 et sec. shows results of:-

(a). Test on full-scale rectangular reinforced concrete beam 19ins. deep carried out by the D.S.I.R. at City and Guilds College;

Strain-distributions at centre of beam using:-

(i).Electric resistance strain gauges. Side'A' p. 213.

(ii). " " " " Side'B' p. 214.

(iii).Mean electric resis.gauge readings p. 215.

(iv). Mean of optical gauge readings p. 216.

(b). Test on end anchored pre-stressed 'T'section beam. (For permission to reproduce these results the author is indebted to A.H.Mattock, M.Sc., D.I.C.)

(i). Strain on side 'A' by Metzger gauge p. 217.

(ii). " " " 'B' " " " p. 217.

Further evidence in support of this idea may be seen in the strain recordings given by both Professor A.L.L.Baker[8] and Professor R.H.Evans[10] in their respective Papers.

N.B. The irregularities are not so well marked in small scale beams as they are in full-size beams; this is attributed to the fact that in a small scale beam there is less possibility for a variation in the Modulus of the concrete taking place.

After it had been decided that the shape of the strain-distribution corresponding to linear

stress-distribution in the elastic range should be copied, there still remained the fact that the amount of straining at various gauge banks varied considerably. Being anxious about the bad effects this fact might have on the test, and suspecting eccentricity of loading due either to the machine or unevenness in the shape of the specimen or both, the author postponed further loading so that testing of the machine and improvements to the loading faces of the specimen might be carried out.

CHAPTER IX.

Experiments and Adjustments to Reduce Uneven Straining.

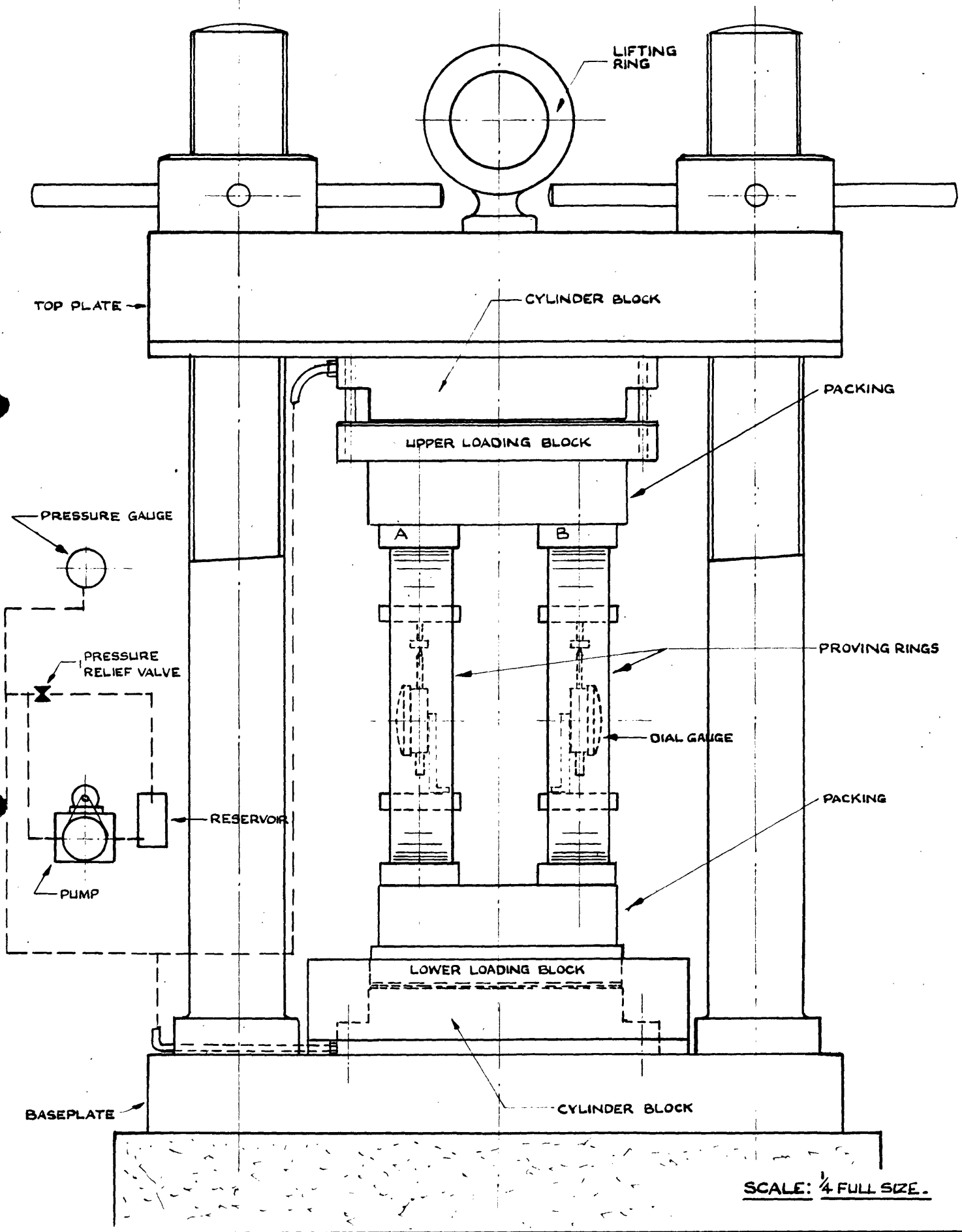
I: Two Proving Rings in Eccentricity Test.

During investigations carried out to determine the reason for unequal straining occurring on either side of the first specimen, considerable doubt existed in the mind of the writer as to whether or not the machine was producing eccentric loading. There was a possibility that higher frictional resistances existing at any of the plungers of a particular loading block -especially one of the plungers at the end of the row and therefore more off centre - might be sufficient to cause considerable eccentricity of loading and consequently uneven straining. Further it was thought highly probable that the positioning of the top plate (which is governed by the relative places to which the four heavy column nuts are screwed down) would have some effect on the eccentricity or otherwise of the load.

The following test procedure was therefore tried out to investigate this problem.

Two 10ton proving rings were mounted, on rectangular packing pieces, between the upper and lower loading blocks of one of the six loading points. See drawing on p.113 . Great care was taken to see that the two proving rings were exactly equidistant from the centre-line of the machine, as inaccuracies in this detail

PROVING RING TEST FOR ECCENTRICITY.



SCALE: ¼ FULL SIZE.

would quickly lead to wrong conclusions being drawn. Load was then applied and readings taken of the proving ring dial gauges. No.6 load point, nearest to the motors, was the first to be tested. The top block was simply lowered down by its supporting tackle until the weight was carried by the proving rings, the column nuts were then screwed down firmly against the top plate. This meant that the top plate was not necessarily horizontal or in the plane of the base-plate. The resulting readings, Appendix VI p.205 showed an eccentricity such that the load on Ring'A' -on the oil delivery side of the load blocks- was 20% less than that on Ring'B'. The top plate was then raised slightly on the side over Ring'B' by unscrewing the column nuts half a turn. This resulted in the loading being 23% greater on Ring'A'. Alternatively when the top plate was lowered slightly on the side over Ring'B' by screwing down the column nuts half a turn, the resulting load was 17% less over Ring'A' than'B'.

Obviously the positioning of the top block is of importance in obtaining a concentric load. On testing the slope of the base-plate with a spirit level it was found that it tilted upwards slightly at the end corresponding to proving ring 'B'. The remaining part of the test was carried out on all the load points.

This time the top plate was 'set' by the spirit level. Two sets of load readings were taken, one with the top plate horizontal,,

and the other with the top plate in the same plane as the base plate (of the machine); i.e. perpendicular to the centre-line of the machine. The results are tabulated and given Appendix VI. p. 206 . In the tables in addition to all load readings there are recordings of the ratio of the loads on the two proving rings, of the total load and of the difference, for calibration purposes, between the total load and that registered on the pressure gauge.

Conclusions.

From the results it was seen that:-

(a). The eccentricity was much effected by the positioning of the top plate, and that, therefore, the top plate should be positioned so as to lie in a plane parallel to the baseplate of the machine.

(b). Within the limits of experimental accuracy the positioning of the top plate did not effect the total load.

(c). Eccentricity appeared to exist even when the top plate was correctly positioned, but the resulting unevenness of loading was reduced to approximately 6%

(d). The check now given on the original pressure gauge calibration test showed that on some of the gauges there had been a re-adjustment of the corrections required at various loads. As these differences were not great, however, it was decided to use the figures obtained with the 50ton proving ring for the pressure gauge corrections,

as these covered the whole range of possible loading. Two proving rings of the same dimensions which together were capable of carrying 40tons were not available.

II:Alignment of Specimen in Machine.

Would any small adjustment in the centering of the specimen between the top and bottom loading points of the bending simulation machine over come strain discrepancies on either side of the specimen? The possibility seemed worth investigation. Further with the specimen in its original form, it was noted, on detailed examination, that the loading faces were out of square by $\frac{1}{16}$"; this caused the upper face to be $\frac{3}{16}$" off the centre line of the lower loading face, once the specimen had been set up in the machine. Clearly re-alignment of the specimen would seem desirable.

Theoretical Investigation.

Assuming the specimen to be homogeneous and elastic:-

Let W be total load exerted on one load-point.

e, eccentricity of load W .

l, length over which W is applied (i.e. specimen width)

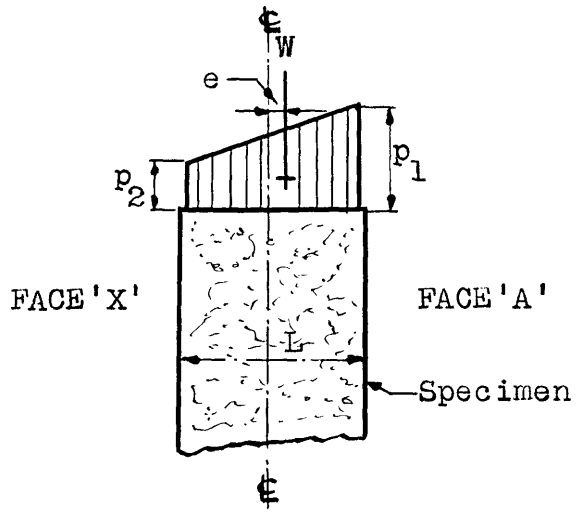
b, breadth " " W " " (load point breadth)

p_1 and p_2 stresses produced on either specimen face.

e_1 and e_2 strains corresponding to p_1 and p_2.

With a uniform change from a stress p_1 on face 'Y' of specimen to a stress p_2 on face 'X' :-

(P.T.O)



Equating vertical forces.

$$\frac{p_1 + p_2}{2} \cdot bL = W$$

$$(p_1 + p_2) = \frac{2W}{bL} \quad \ldots\ldots 1.$$

Equating moments about the centre line,

$$We = (p_1 - p_2) \cdot \frac{bL}{2} \cdot \frac{L}{6}$$

$$(p_1 - p_2) = \frac{12.We}{bL^2} \quad \ldots\ldots 2.$$

From equations 1. and 2.,

$$\frac{(p_1 - p_2)}{(p_1 + p_2)} = \frac{12.e}{bL^2} \cdot \frac{bL}{2} = \frac{6e}{L}$$

$$e = \frac{(p_1 - p_2)}{(p_1 + p_2)} \cdot \frac{L}{6}$$

If investigations are carried out at low loads well within the elastic range it may safely be assumed that stress is proportional to strain,

hence, $$e = \frac{(e_1 - e_2)}{(e_1 + e_2)} \cdot \frac{L}{6}$$

Let the ratio of the strains on opposite faces be 'k'.

$$\text{Then } k = \frac{e_1}{e_2}$$

$$e = \frac{k - 1}{k + 1} \cdot \frac{L}{6}$$

$$k = \frac{L + 6e}{L - 6e}$$

$L = 8"$ $\quad e = \frac{3"}{16}$;

$$k = \frac{8 + \frac{9}{8}}{8 - \frac{9}{8}} = \frac{73}{55} = 1{\cdot}33$$

Hence an eccentricity of $\frac{3"}{16}$ would cause a difference in strain of 33% to be registered on opposite faces of the specimen. Experiments were carried out on the specimen by loading one point at a time and observing the strains registered at either end of the loading block. Marked changes were noted in the ratio of these strains when the specimen was moved slightly in the machine. Many different positions of the specimen were tried in an attempt to equalize the strains on both faces. However, no really satisfactory position was found, for when one loading point gave a good result the next one to it was often found still showing differences of straining on either face.

It was therefore decided that grouting of the ends of the specimen should be carried out:-

(a). To square the ends of the specimen.

and (b). To eliminate local high spots.

III.) Grouting of Specimen.

The specimen was rested on the lower load points of the machine and adjusted by wedge-shaped packing pieces until both vertical faces were parallel to the centre-line of the machine. The upper loading face was roughened to act as a key and a thin layer of mortar was spread evenly over the surface. By means of a thick glass plate and a spirit-level, the new surface was smoothed off truly square to the vertical faces of the specimen. When this grouted surface had hardened, the specimen was reversed in the machine, the new surface resting on the lower loading points. The second loading surface was similarly grouted, and made square to the vertical faces of the specimen. The grouting can be seen in the photographs on p. 129 and 130. The specimen was now centred accurately (to within $\frac{1}{32}$") ready for further testing.

CHAPTER X.

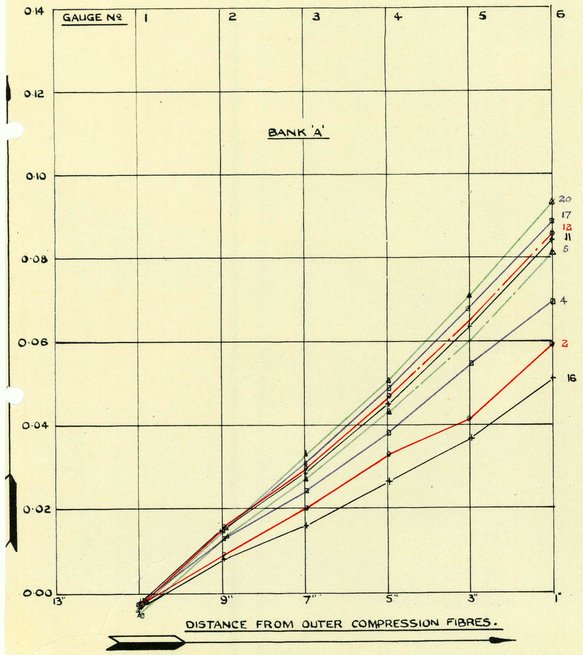
Testing of First Specimen Continued to Destruction.

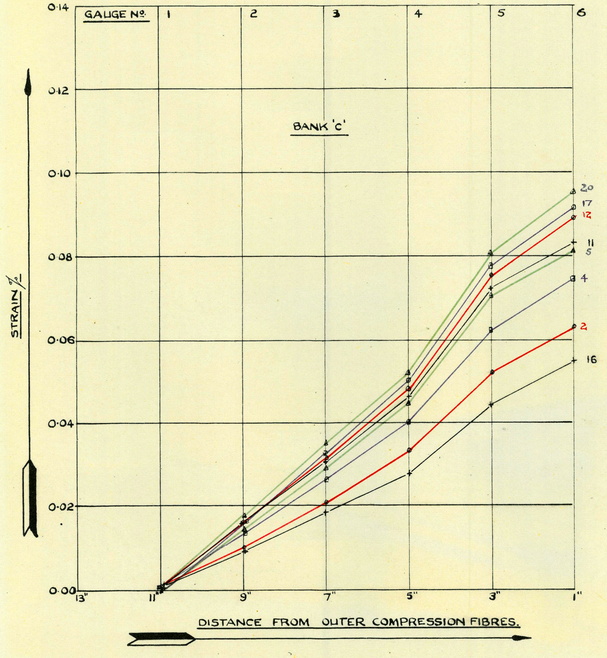
Loading of the specimen was recommenced with high hopes that the combined effects of grouting the loading surfaces and of the realignment of the specimen in the machine would produce straining at the gauge banks of a more uniform nature. In order to observe whether differences had occurred, the specimen was once more subjected to loads giving a linear stress-distribution -some of the load stages being identical with those applied in the first test- and of such magnitude that the elastic range was not exceeded. The graphs showing strains recorded on all the electrical gauges during this investigation are shown on p. 121 together with the corresponding stress-distributions at the various load stages. These graphs were compared with the earlier ones (pages 94,95,97.) obtained before the above improvements had been carried out. N.B. Care was taken when comparing these graphs to select results obtained under similar loading conditions, i.e. like stress-distributions, and to avoid confusion between differing gauge banks. (To assist, all graphs have their particular gauge bank letter printed upon them.) A new series of numbers was started for the load stages with the specimen in its second position in the machine. This series bears no relation to the original series of load stage numbers.

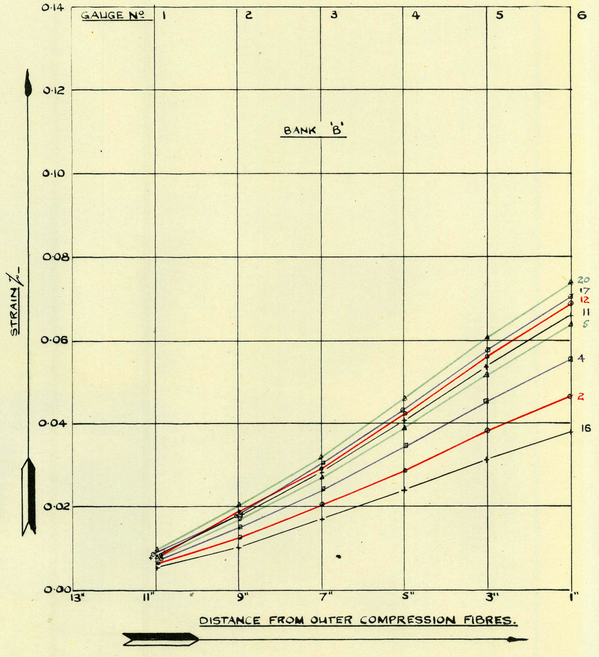
STRAIN DISTRIBUTION AT ALL SECTIONS OF 1ST. SPECIMEN.

2ND POSITION IN MACHINE.

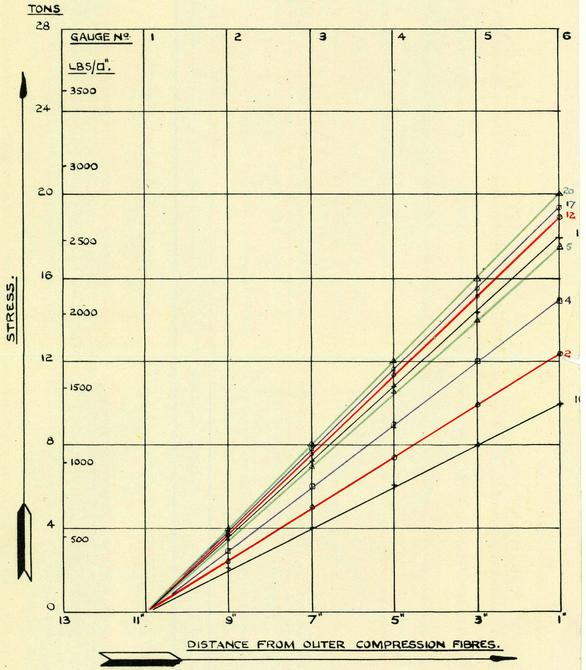
FOR LOAD STAGES IN THE ELASTIC ZONE.

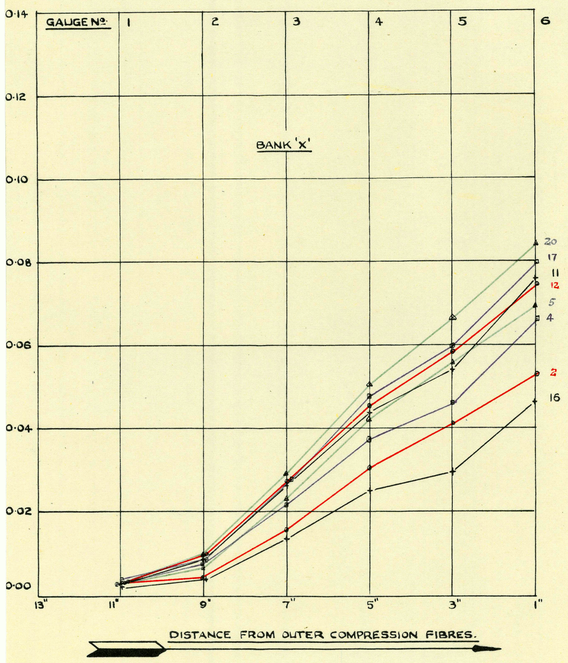


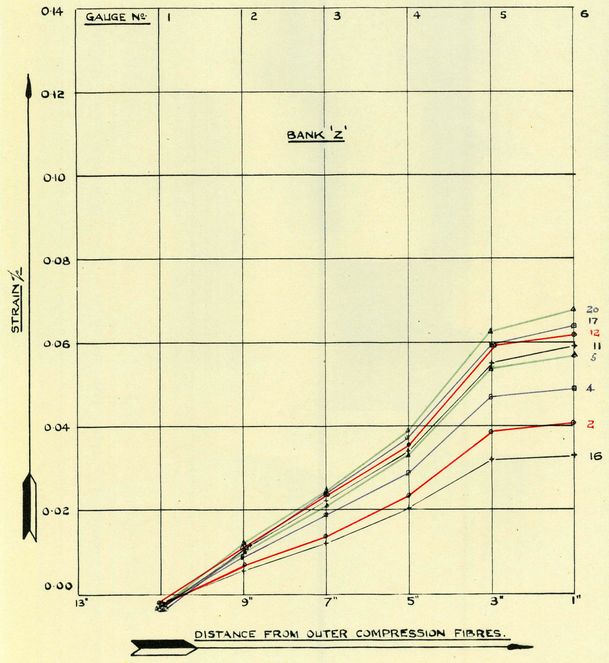


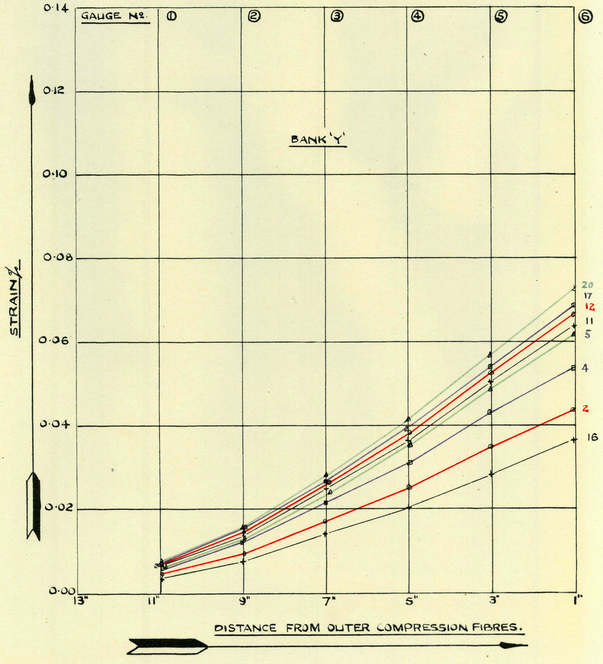


STRESS DISTRIBUTION.





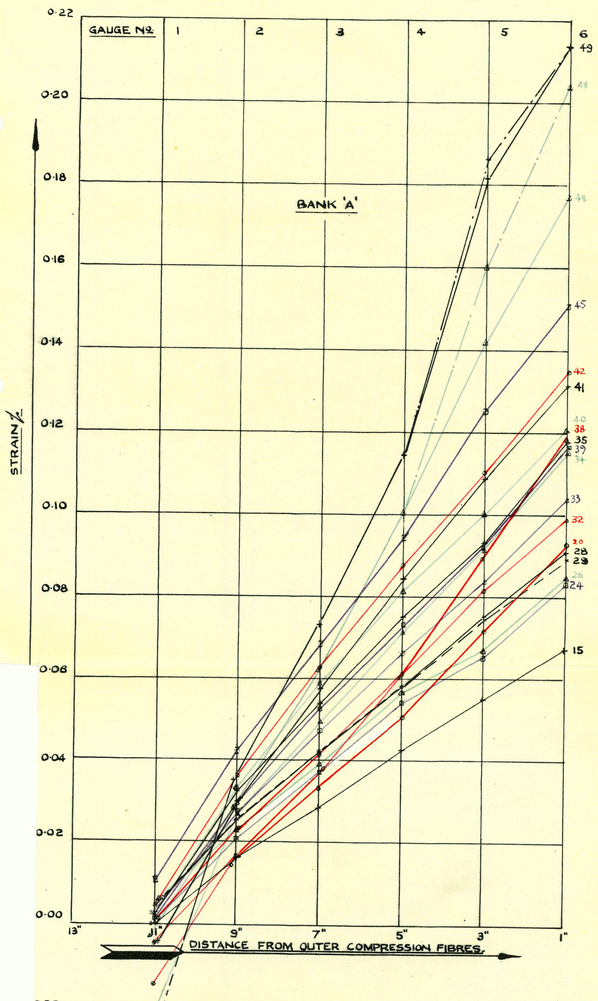


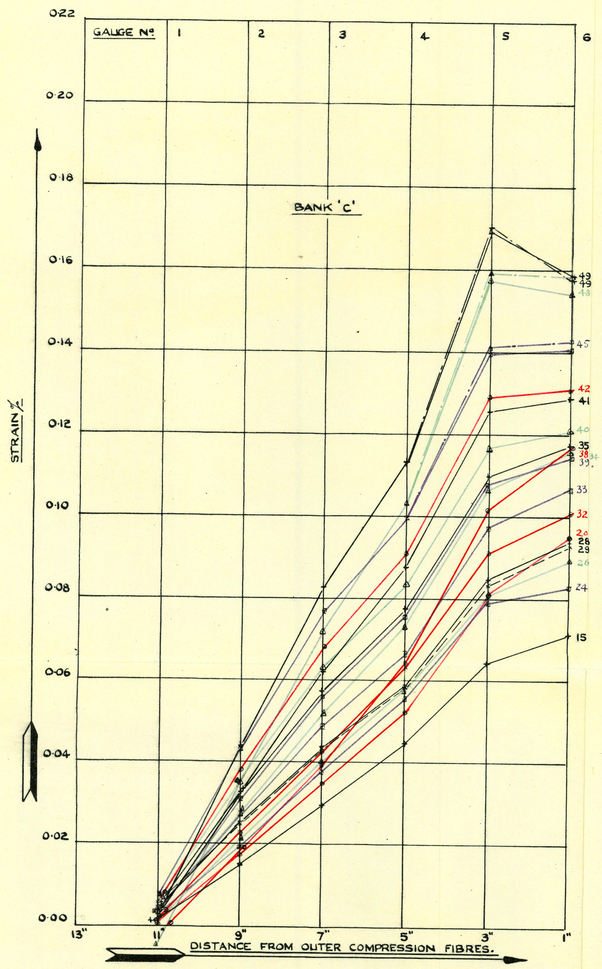


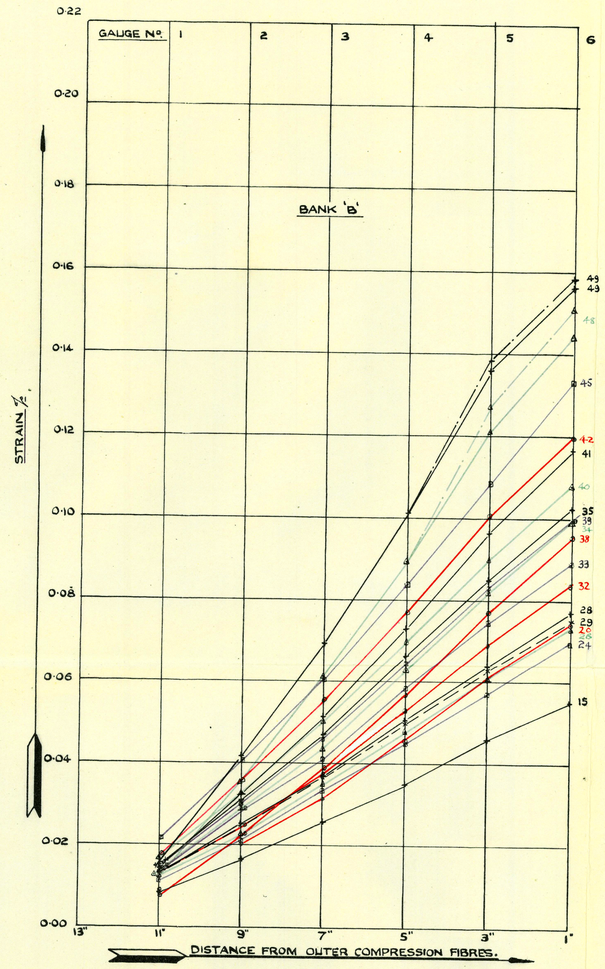
STRAIN DISTRIBUTION AT ALL SECTIONS OF 1ST SPECIMEN.

2ND POSITION IN MACHINE.

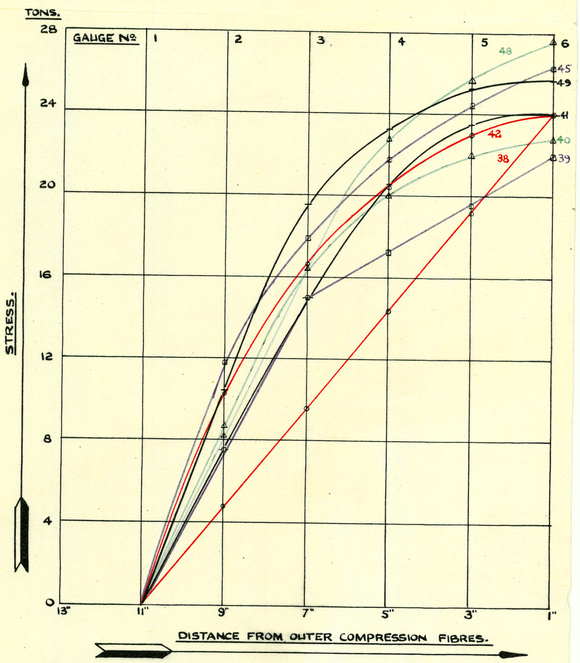
FOR LOAD STAGES IN THE PLASTIC ZONE UP TO FAILURE.

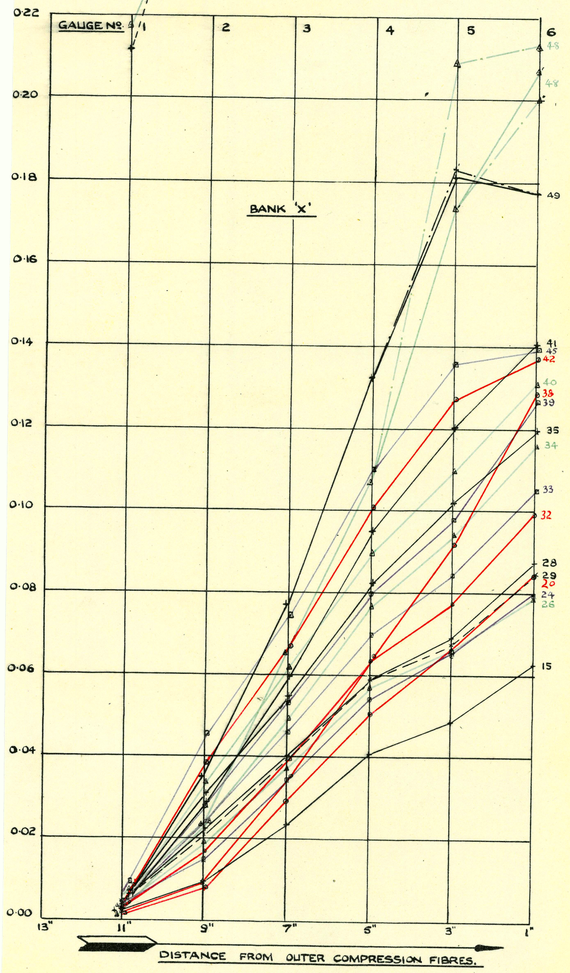


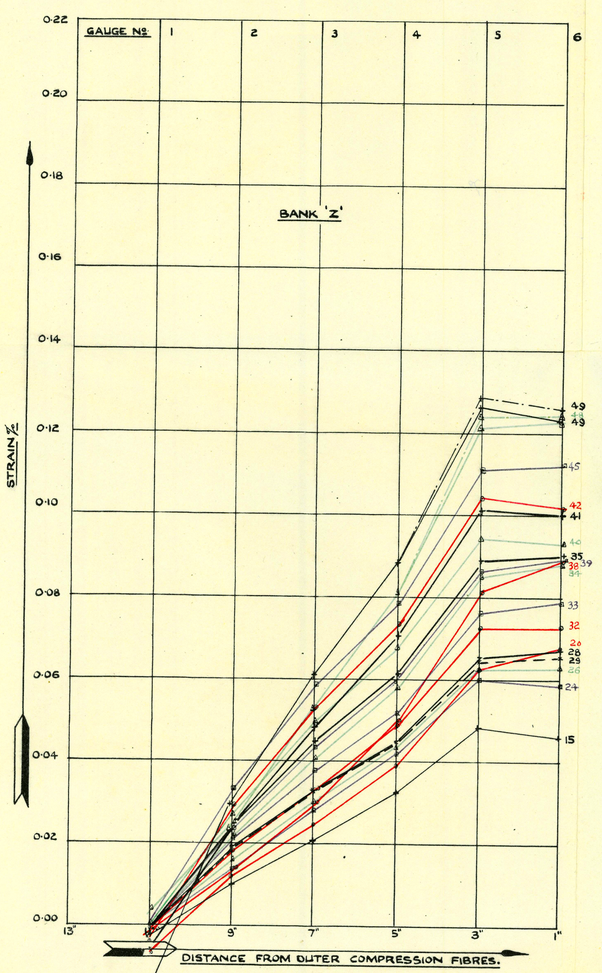


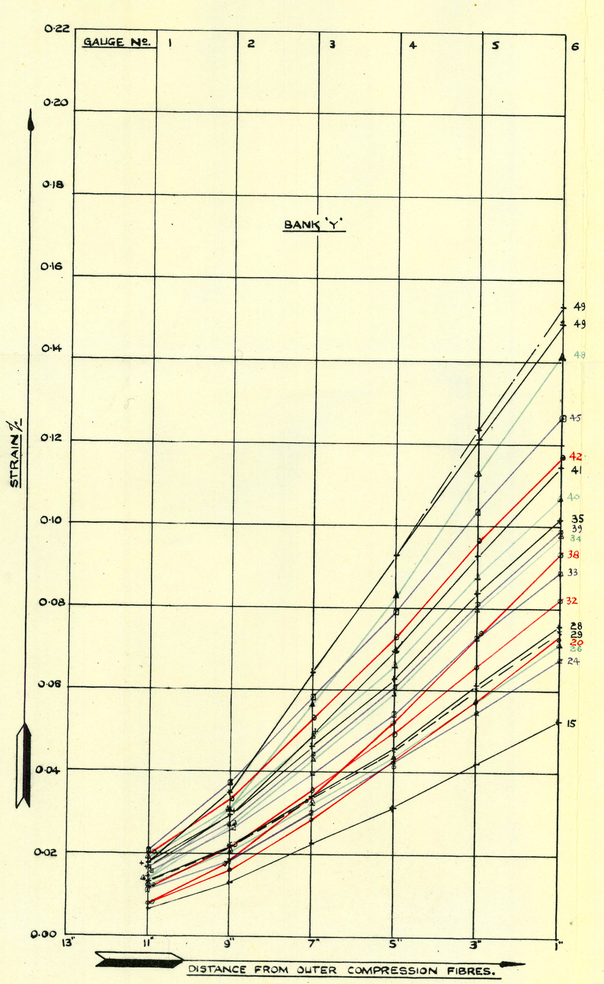


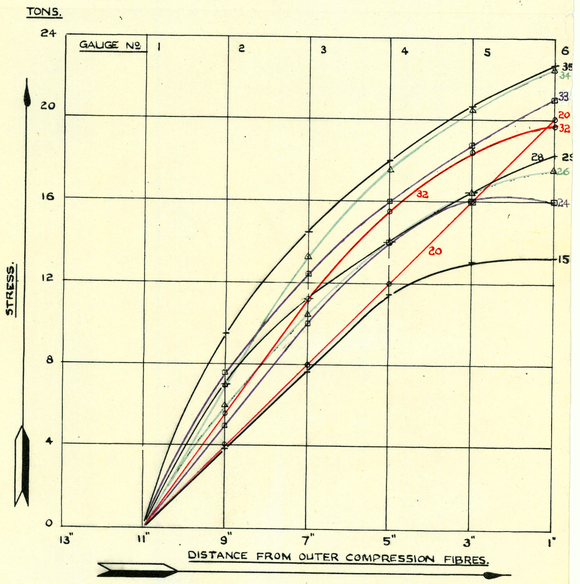
STRESS DISTRIBUTION.











Changes and Improvements in Straining.

Changes and improvements in the straining at different points on the specimen were observed as a result of grouting and re-alignment.

Bank 'A'.

A marked improvement of the linear form of the strain-distribution was achieved as a result of an increasing of the strain under gauge A6 and a decreasing under gauge A5.

Bank 'C'.

Straining of the gauges in this bank now almost identical with corresponding gauges in bank 'A', except in the case of gauge C5 which remained relatively high.

Bank 'X'.

Most of the curved 'concave upwards' shape observed previously has been improved by a relative increase of straining under gauges X3, X4, and X5.

Bank 'Z'.

Individual gauges have departed to some extent from the original straight line, but, in general, the straining has increased at this gauge bank so bringing its behaviour nearer to that of the other banks. In spite of this, Bank 'Z' remained still markedly less strained

under any given stress-distribution than did the other gauge banks.

Bank 'B'.

Straining under these gauges remained practically unaffected.

Bank 'Y'.

An increase of the straining at this part of the specimen caused the straining in corresponding gauges in Banks 'B' and 'Y' to be almost identical.

Taking due account of the improvements which had been accomplished by the alterations to the specimen, the author was now convinced that the earlier conclusions, which were drawn after the test producing perfect linear strain on one bank of gauges only, were valid and should be adhered to. Namely:-

' At all stages of loading, the true strain-distribution on any given gauge bank, which should be aimed at and attained, before any corresponding stress-distribution be accepted as representative of beam conditions, is that strain-distribution which follows, exactly, the shape of the strain-distribution existing under linear stress-distribution in the elastic range.'

With this rule as a guide, the specimen was loaded into the plastic range and on up to failure.

The strains recorded on all the gauge banks and the corresponding stress-distributions are given on p. 122 . As the test progressed it became more difficult to copy the strain shape accurately because at that time the only method of control was that of visual comparison between the earlier strain-distribution graphs, obtained in the elastic range under linear stress-distribution, and the strain shape which had just been recorded. Adjustments were made to the stress-distribution between each load stage and if it transpired that the strain-distribution was not in agreement with the desired form, other distributions, composed of approximately the same total load, were tried out until agreement was achieved, before the total load was increased. In this way it was hoped to obtain true stress-distributions at all stages of loading. N.B. A different 'number' to any given 'load stage' always implies a change of stress-distribution but not in all cases a change in the total load.

The first visible cracks to be seen in the compressive fibres of the beam element were adjacent to strain gauges C6 and X6 and ran vertically from the load blocks for a short distance, $\frac{1}{2}$" - $\frac{3}{4}$", over the main faces of the specimen, corresponding in a beam to horizontal cracks on the sides of the beam and high up in the compression zone. This occurred at load stage 33. After load stage 42 vertical cracks - 2 to 3 inches

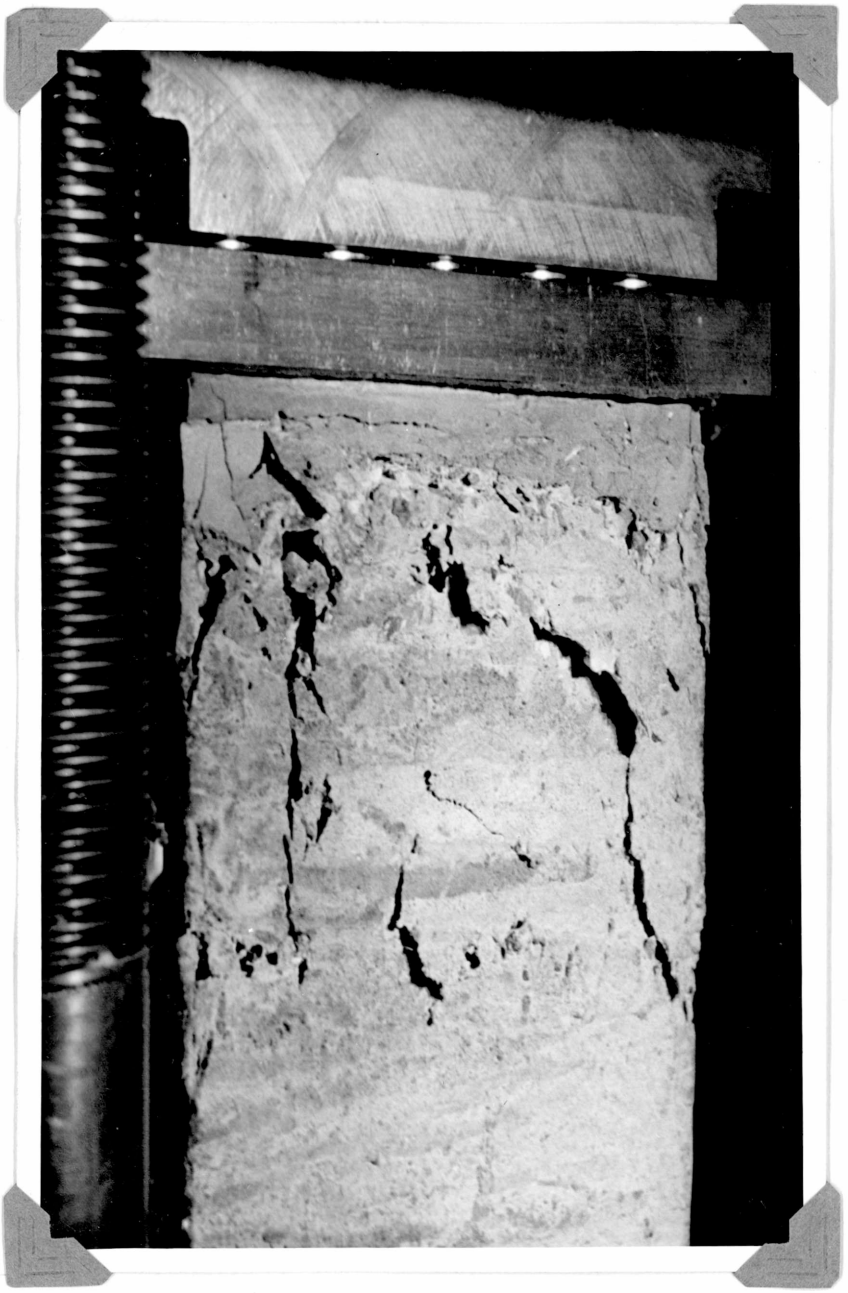
long - developed on the end face of the specimen under gauges X6 and Z6 approximately $\frac{1}{4}$" in from the gauge-carrying faces of the specimen. This position represents the top of a beam near to the sides. After the application of load stage 45 the vertical cracks on the gauge face of the specimen at X6 , $\frac{1}{8}$" and $1\frac{1}{4}$" from the outer edge of the concrete, were extended in length and began to increase in width and in apparent depth.

The time required, at every load stage, to record the strains on all the electrical resistance gauges was approximately 12 minutes. At the load stages near to failure, movements of the load points during this 12 minutes due to straining of the concrete were sufficient to cause a marked falling off in the oil pressure and a subsequent drop in the load. It was necessary, therefore, to use the automatic cut-out device on the switches to enable this load to be restored by the motors. In connection with this, it will be remembered that the loading technique adopted after preliminary experiments (devised to reduce frictional inaccuracies to a minimum) attained a given stress-distribution with the motors switched <u>off</u> in the final stage. If any of the cut-outs were to be used to boost a falling load, the motor concerned must be switched on. In practice this proved at first rather inconvenient; because though the cut-out setting might be adjusted to operate immediately (by setting

the cut-out pointer so that it touched the pressure gauge indicator) , once the switch was depressed the pump turned over a little before coming to rest thus increasing the load and altering its value. Fortunately after a little thought about the electrical process involved, the writer managed to solve this difficulty. The reason why the motor flicked over before stopping was because until the switch was in the 'on' position the solenoid operating the cut-out was not energised and therefore the main motor circuit was uninterrupted. For the solenoid to become energised and rotate the mercury contact to break the main circuit, only a short time was required, but in this time current flowed to the motor. The remedy was to hold the circuit breaker 'open' by hand whilst switching on the motor button, then no current flowed to the motor before the solenoid could become energised to hold the contact in the 'open' position. By this simple process the same loading technique could be used as before, but in addition, should any of the heavier loads begin to fall off, the cut-outs would operate, the motor start and the load be recovered to its original setting.

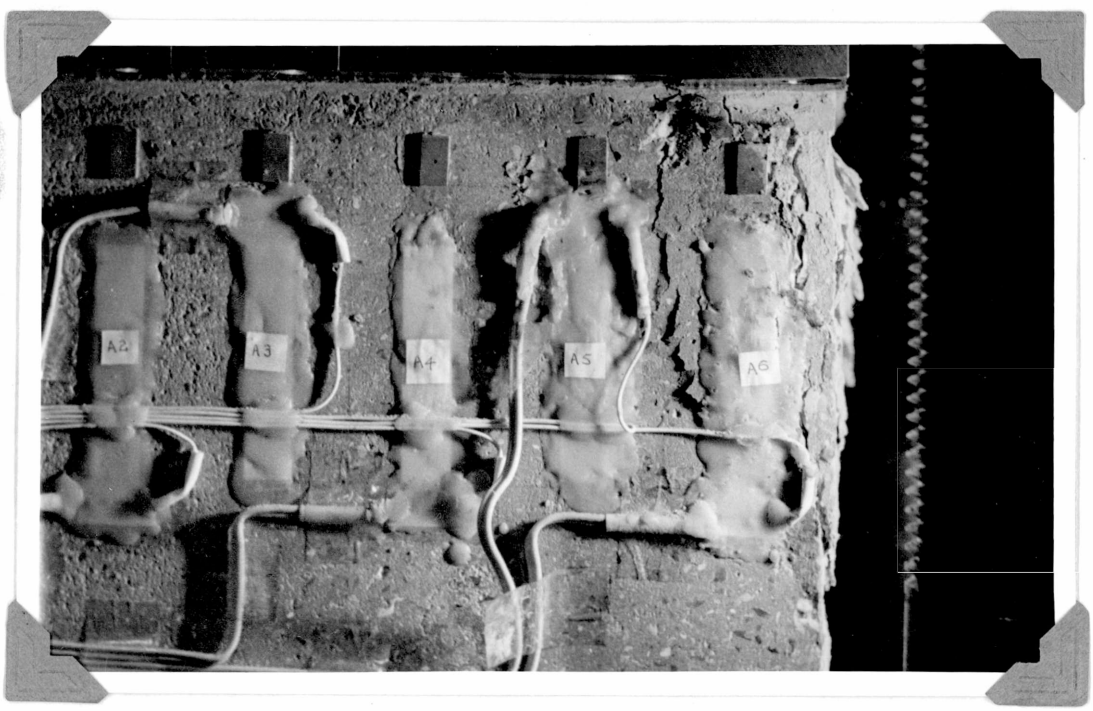
During the last few load stages the strain gauges which were under load points 5 and 6 were read first - and in some cases re-read after all gauge readings had been recorded - owing to their growing tendency to become unsteady.

Load stage 49 was only just carried by the specimen, and when a further stage was attempted, the load could not be withstood and failure occurred. Close-up photographs of the failed part of the specimen are shown on pages 129 and 130 .



FAILURE OF FIRST SPECIMEN.





DETAILS OF FIRST SPECIMEN FAILURE.

CHAPTER XI.

Gauge Factors.

When all the results obtained from the first specimen had been plotted collectively, much thought was concentrated upon the development of a method whereby more accurate selection of the stress-distributions corresponding to those in a beam might be made than could be obtained from judging by visual comparison the extent to which a strain-shape in the plastic range corresponded to that obtained on the same gauge bank in the elastic range under linear stress-distribution. The reasons for the small variations from a true linear strain-distribution at the various gauge banks for an applied linear stress-distribution during the elastic range, had by now been narrowed to:-

(i). Heterogeneous composition of the concrete.

(ii).Slight differences in gauge sensitivity,

(iii).Possible load-point inaccuracies.

(N.B. Item (iii). could be expected to be more pronounced at the end gauge banks than at the centre and was the only item peculiar to the bending simulation machine and not, therefore, operative in a beam. It was, nevertheless, reduced to a minimum by the application of the carefully developed loading technique.)

The method adopted was to obtain, from the strain shapes in the elastic range under linear stress-distribution,

'gauge factors' which when multiplied by the actual strain readings of their particular gauges, produced perfectly linear 'corrected' strain-distribution. Next, these 'gauge-factors' were applied to all the strain gauge recordings and so the 'corrected' strain-distributions for all load stages were calculated. Selection of those load stages whose 'corrected' strain-distributions were nearest to a perfect straight line then gave the stress-distributions corresponding to those in a beam.

It will be easily recognised that the validity of this method depends upon the 'gauge factor' remaining constant throughout the range in which it is applied. The condition which must be satisfied for this to be so is that the strain reading inaccuracies should be proportional to the actual strain. On re-examination of the three items which govern these strain reading inaccuracies (given on the previous page) it will be seen that item (ii) most certainly satisfies the required condition and it seems almost certain, in view of the evidence shown in Appendix XI. p.213etc. where the strain shape is repeated up to failure, that item (i) also fulfills the required condition. Now item (iii) cannot easily be assessed. If item (iii) is due to <u>frictional</u> resistances, one would expect that inaccuracies caused by it would most likely be proportional to the stress, and therefore the 'gauge factor' would

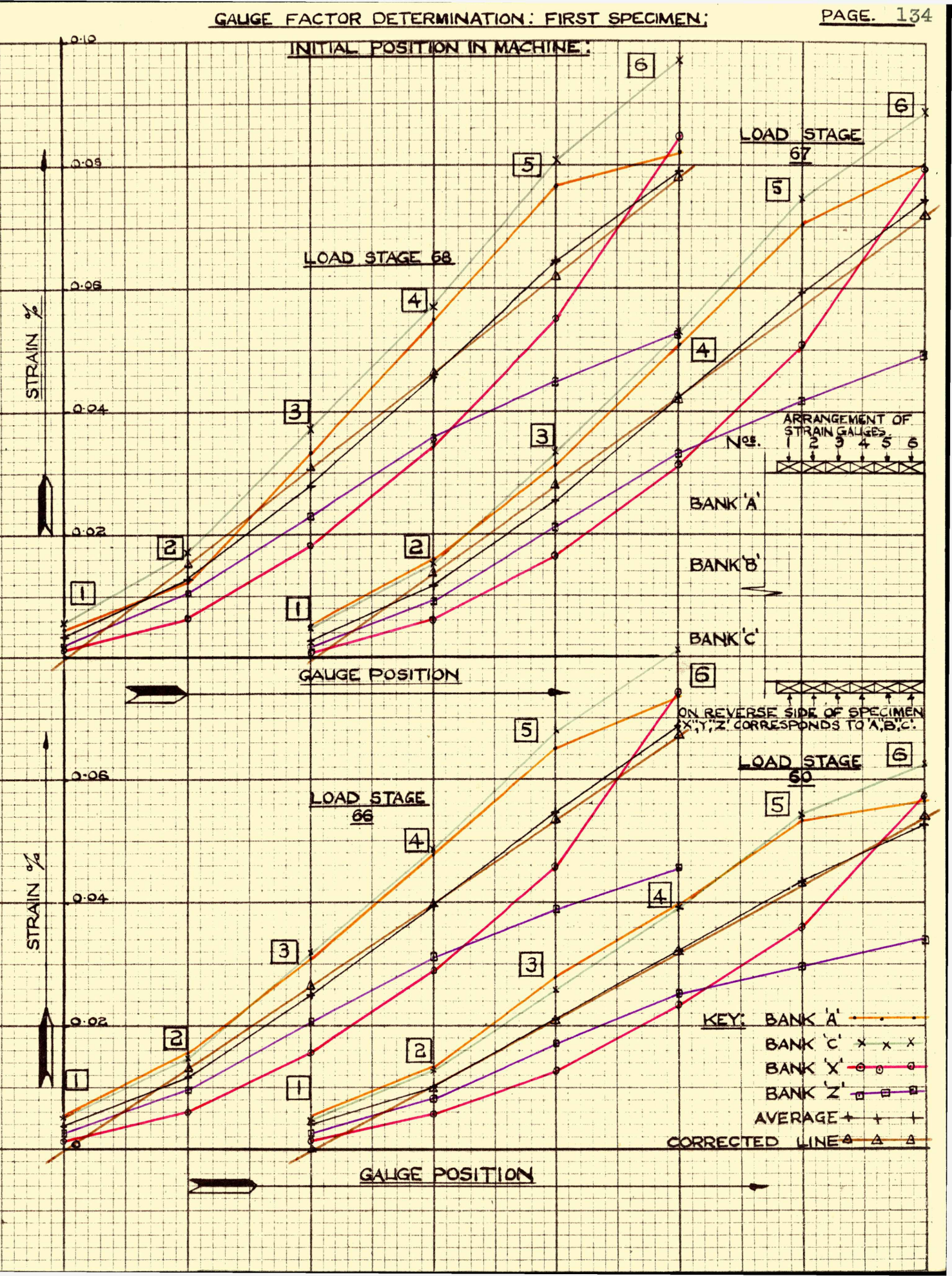
hardly be influenced. On the other hand it might be that the load point inaccuracies remain the same throughout the test, and if that were so its effect upon the 'gauge factor' would diminish with increasing load. In either case, item (iii), as mentioned before, has been reduced to a minimum and so the author was confident that its effects could not impair the use of the method suggested.

Gauge Factor Determination.

Two easy ways of calculating the 'gauge factors' from the strain recordings presented themselves. In both methods typical strain-distributions corresponding to linear stress-distributions in the elastic range, were plotted for all gauge banks. Care was taken to select stress-distributions which covered as wide a range as possible. In the first method a 'corrected' straight line was drawn for each gauge bank, but in the second method one 'corrected' straight line was used for all the gauges. As no particular significance was to be attached to individual 'corrected' strain readings, the second method was employed, being the most straightforward of the two. On pages 134 and 135 graphs of strain recordings at all gauge positions are plotted, and the 'corrected' strain line shown. The 'gauge factor' for any one gauge was calculated as the ratio:-

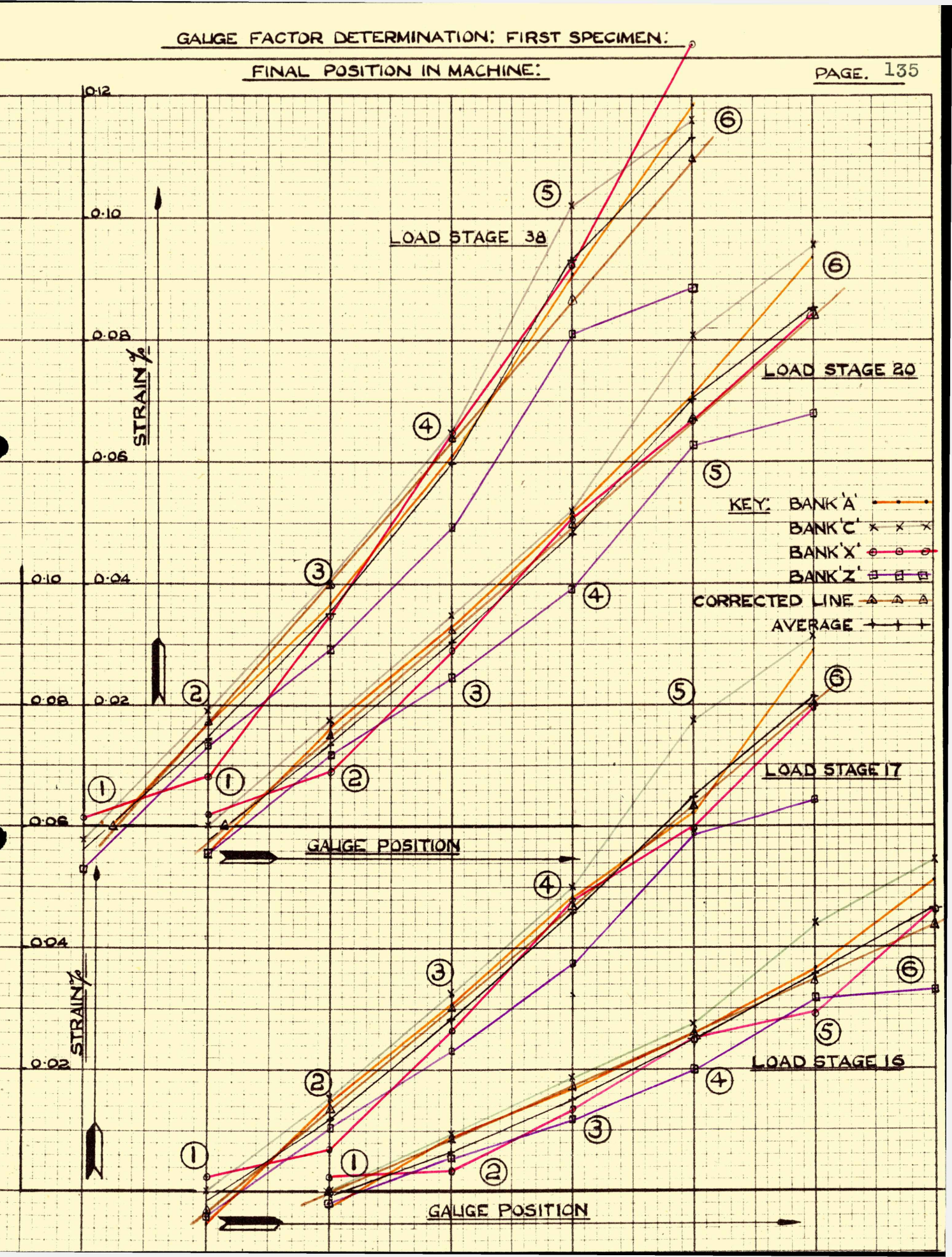
$$\frac{\text{'corrected strain'}}{\text{actual (or 'absolute') strain.}}$$

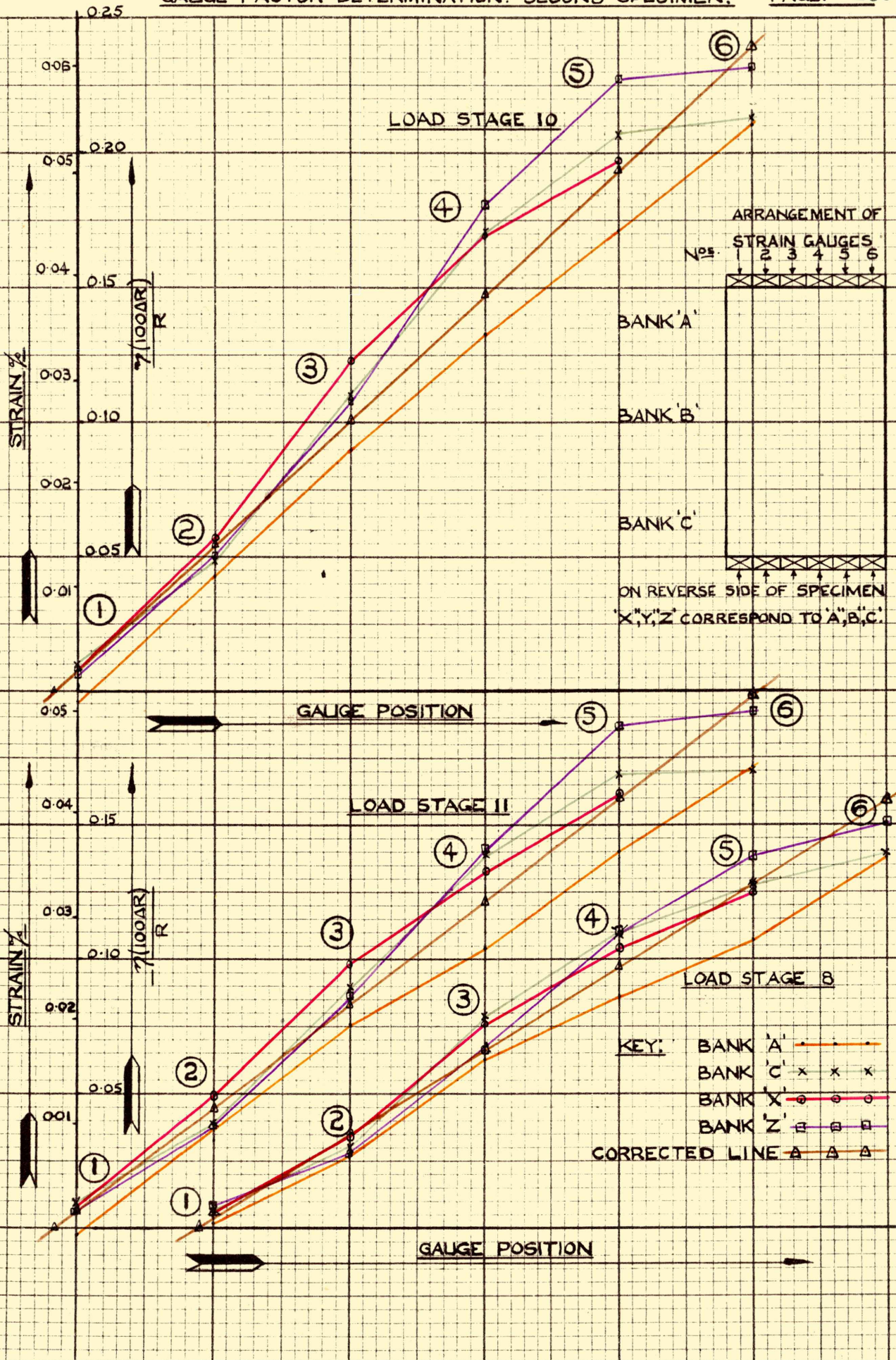
GAUGE FACTOR DETERMINATION: FIRST SPECIMEN:



GAUGE FACTOR DETERMINATION: FIRST SPECIMEN:

FINAL POSITION IN MACHINE:




LOAD STAGE 10
STRAIN %
0·25
0·20
0·15
0·10
0·05
0·08
0·05
0·04
0·03
0·02
0·01
0·005
γ(100ΔR)/R
ARRANGEMENT OF STRAIN GAUGES
Nos. 1 2 3 4 5 6
BANK 'A'
BANK 'B'
BANK 'C'
ON REVERSE SIDE OF SPECIMEN
'X','Y','Z' CORRESPOND TO 'A','B','C'.
GAUGE POSITION
LOAD STAGE 11
0·04
0·03
0·02
0·001
0·15
0·10
0·05
LOAD STAGE 8
KEY:
BANK 'A'
BANK 'C'
BANK 'X'
BANK 'Z'
CORRECTED LINE
GAUGE POSITION

Tables showing the calculated 'gauge factors' are given in Appendix VII p. 208 and the 'gauge factors' can be seen to remain fairly constant at different load stages. (N.B. In the case of the first specimen in its final position in the machine, Bank'X' had reached plasticity by load stage 38.)

Minor adjustments were made to 'gauge factor' values, after all the 'corrected' strain graphs in the elastic zone had been plotted. Thereafter the same factors were used throughout the test.

Application of 'Gauge Factors' to Results.

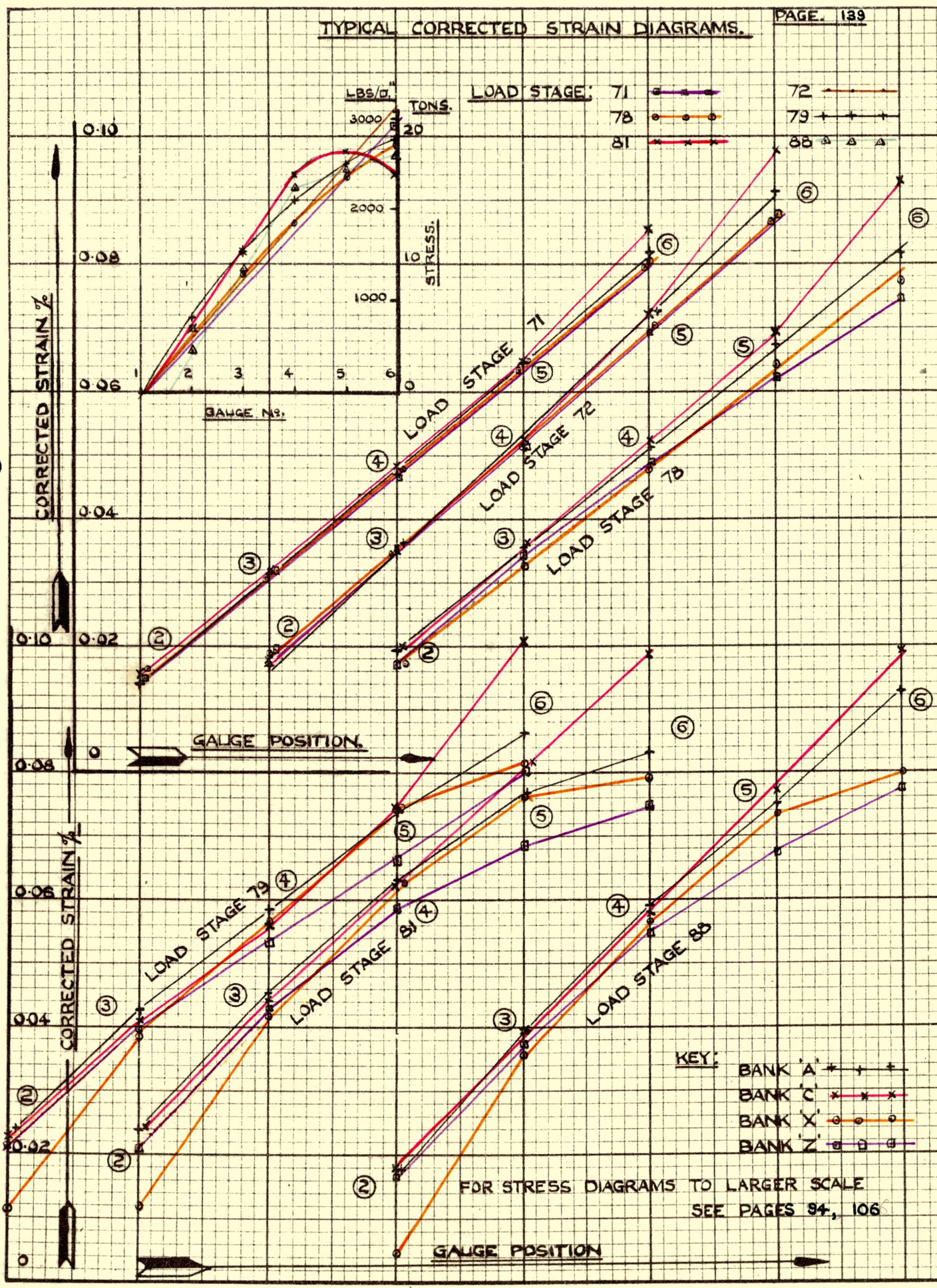
The ideal way of utilising the method of 'gauge factors' which has just been described would be to apply the factors to the strains recorded at each load stage, before applying a further load stage. An estimate of the adjustments required to the stress-distribution to bring the 'corrected' strain line into a straight line would then be made, and hence a further stress-distribution more accurate than the previous one, decided upon. After the next load stage, with this new stress-distribution, the process would be repeated until sufficient accuracy was achieved. This was the system adopted in the test on the second specimen. However, in the case of the first specimen this could not be carried out, as the idea was not evolved until after the test. But selection of the stress-distributions which were in closest agreement with those in operation in a beam could still be

made, by applying the 'gauge factors' to all the strain recordings made in the test and picking out the 'corrected' strain-distributions which were nearest to a straight line. This involved much work, but was rewarded by the selection of five stress-distributions, four of which were in the plastic range, with the 'corrected' strain-distributions of one or more of the four end gauge banks almost perfectly linear. These stress-distributions together with the corresponding 'corrected' strain-distributions are given in the results, p.155 to 159. A few typical graphs showing other 'corrected' strain-distributions are given on p.139. Further examples may also be seen in the chapter dealing with the testing of the second specimen. It was thought unnecessary to burden the thesis with all the 'corrected' strain graphs, since having once been plotted and observed they are of no further use, also, if required they can be obtained from the strain-distributions and gauge factors already in the thesis.

Typical 'Corrected' Strain Diagrams.

On p.139 are shown 'corrected' strain diagrams corresponding to some of the stress-distributions tried out during the test on the first specimen. Up to load stage 70 the 'corrected' strain diagrams were perfectly linear at all gauge banks. The 'corrected' strain-diagrams at load stages 71 and 72, however, (linear stress-distributions) indicate that these stress-distributions are the right ones

TYPICAL CORRECTED STRAIN DIAGRAMS.



FOR STRESS DIAGRAMS TO LARGER SCALE SEE PAGES 94, 106

for banks 'A','X' and 'Z' but that bank'C' has begun to strain under gauge No.6 at a more rapid rate. Stages 78, with a stress-distribution of a slightly curved nature,(convex upward) and 79, even more curved, show in the 'corrected' strain diagrams that these stress-distributions are still not right for bank'C'. (At the same time indication is given that the remaining banks 'A','X' and 'Z' are not being correctly stressed. This is satisfying to see since the different stress-distributions at stages 71 and 72 have already been shown to be the right ones for banks 'A','X' and 'Z'.) Stage 81 gives almost a straight 'corrected' strain diagram for bank'C', but the straining under gauge No2 is a little too small. At stage 88 the 'corrected' strain-distribution for bank 'C' is almost perfectly straight, and the corresponding stress-distribution was therefore taken to be the distribution required.

The stress-distributions with corresponding 'corrected' strain diagrams most nearly linear have all been selected in the same manner as for stage 88. Summaries of these distributions and the 'corrected' strain diagrams are given on pages 160 and 161 in the results.

CHAPTER XII.

Testing of Second Specimen.

The vast amount of experimental work which had been vital for the development of a technique and the discovery of new facts in this recent method of testing concrete specimens and which had been meticulously carried out during the testing of the first specimen, served its purpose well having furnished much valuable information. Not only was the actual test now able to follow certain well defined lines, but also the preparation of the specimen for testing was much simplified. The reasons for the rejection of some of the earlier methods and the adoption of more suitable ones will not be given here as a full account may be found in the chapter dealing with conclusions.

Strain measurement was carried out by electrical means. The author manufactured 3in. electrical strain gauges (as described in preceding pages) for this purpose. A considerable speed-up in the recording of strain readings was attained by wiring the electrical strain gauges up to a Savage and Parsons 50-way unit. "$\frac{7(100\,\Delta R)}{R}$", which is directly proportional to strain, can be read off immediately upon balance of the moving-coil reflecting galvanometer to null-point. The only disadvantage which this box has, when compared with the type used in the first test, is the necessity for wiring one dummy gauge for each active gauge.

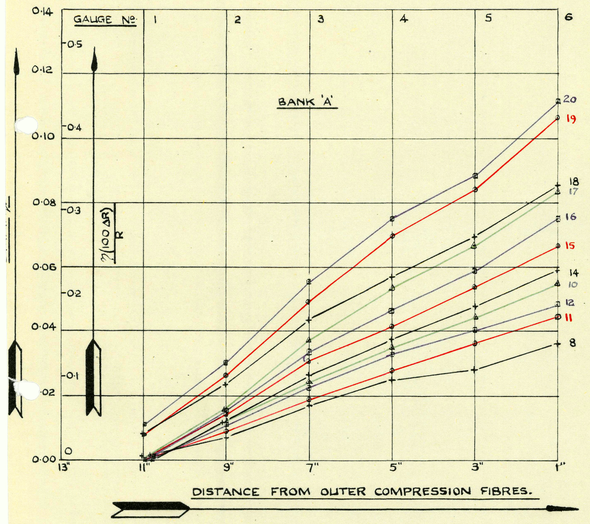
The serviceable gauges remaining on the old specimen were used as 'dummies' for the active gauges on the second specimen, thus eliminating this disadvantage. A detailed description of the Savage and Parsons 50-way unit is given by P.B.Morice,[11] B.Sc. in No.6 Mar. 1951, of the Magazine of Concrete Research, whilst the Wheatstone's Bridge arrangement used in the first test is described by R.D.Binns,[9] B.Sc.,D.I.C., and H.S.Mygind, B.A.,D.I.C. in No.1. Jan. 1949, of the same publication. The reader is referred to these articles for further information. No other method of strain measurement was used in the test on the second specimen.

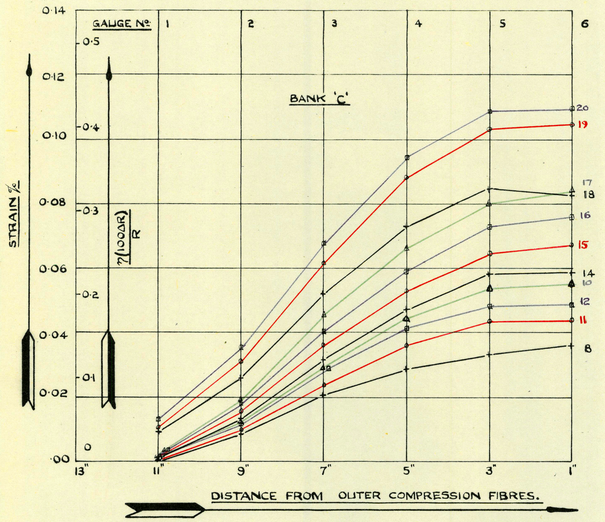
The tensioning frame was not employed, and the depth of the beam element was reduced, as a result, to 12ins.

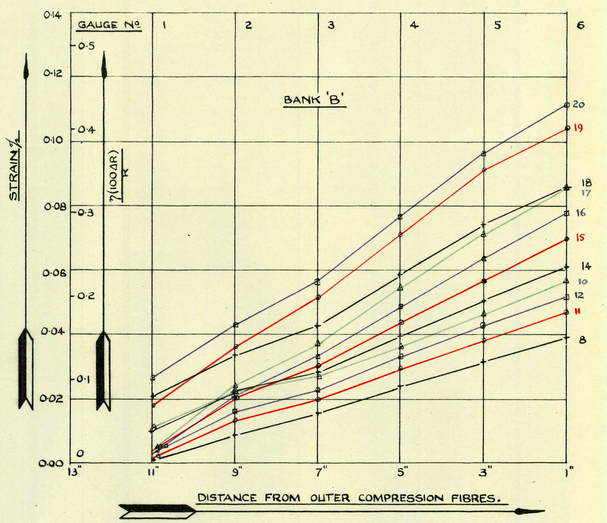
The specimen was subjected in the early stages of the test to stresses of a linear nature, and the strains were recorded and graphed. (See p. 143.) It was observed that for a given loading, the central banks 'B' and 'Y' were straining more than the end banks. Apart from bank 'X', in which gauges NO.4 and 6 appeared erratic, all strain gauges were working well and the variations from perfect straight line straining were repeated at all load stages. At stages Nos. 8, 10, and 11 gauge factors were calculated. (See p. 136 and 209.) These factors were suitably adjusted in the load stages immediately following so that the 'corrected' strain

STRAIN DISTRIBUTION AT ALL SECTIONS OF 2ND SPECIMEN.

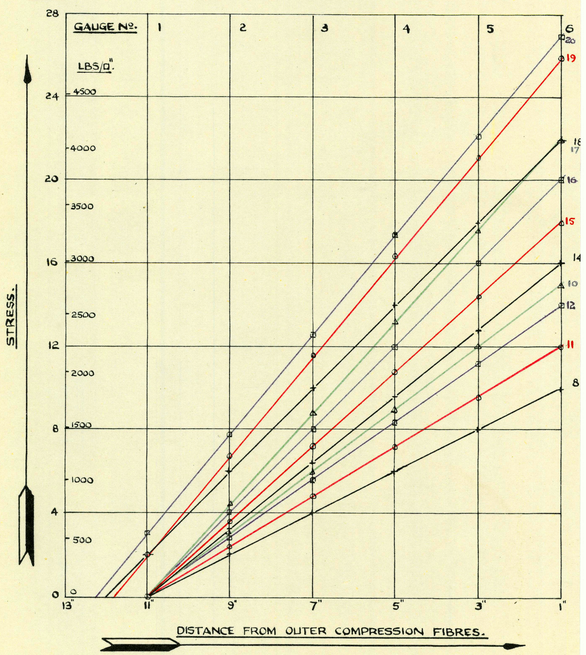
FOR LOAD STAGES UP TO THE PLASTIC ZONE.

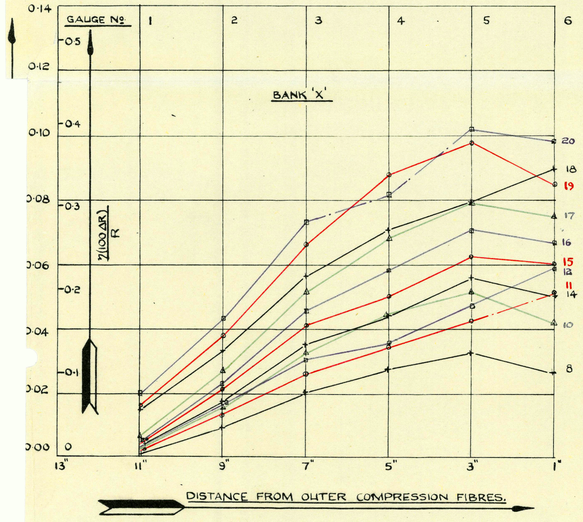


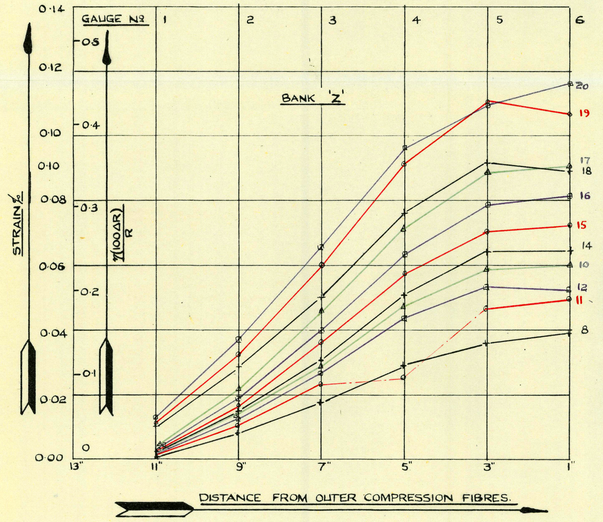


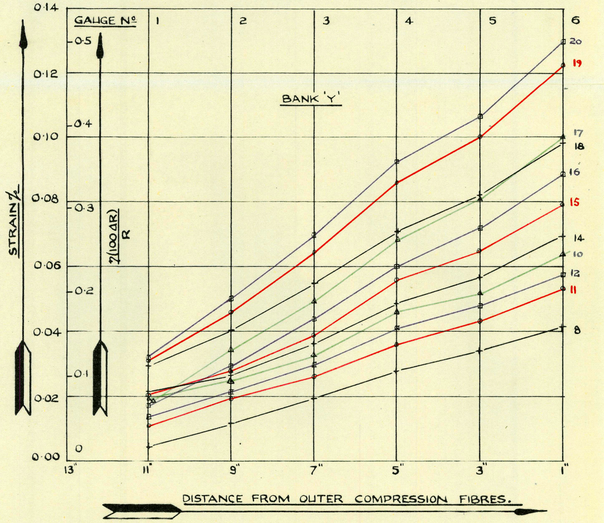


STRESS DISTRIBUTION.



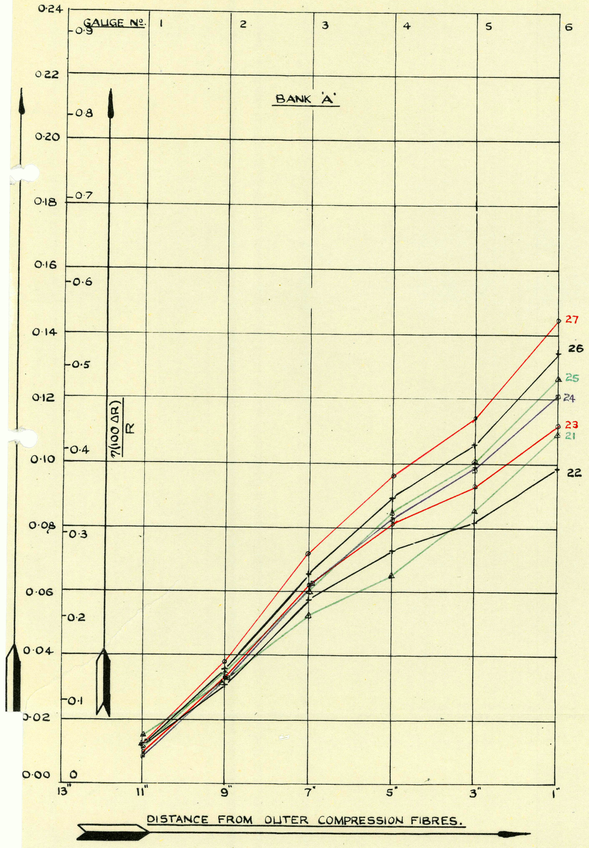


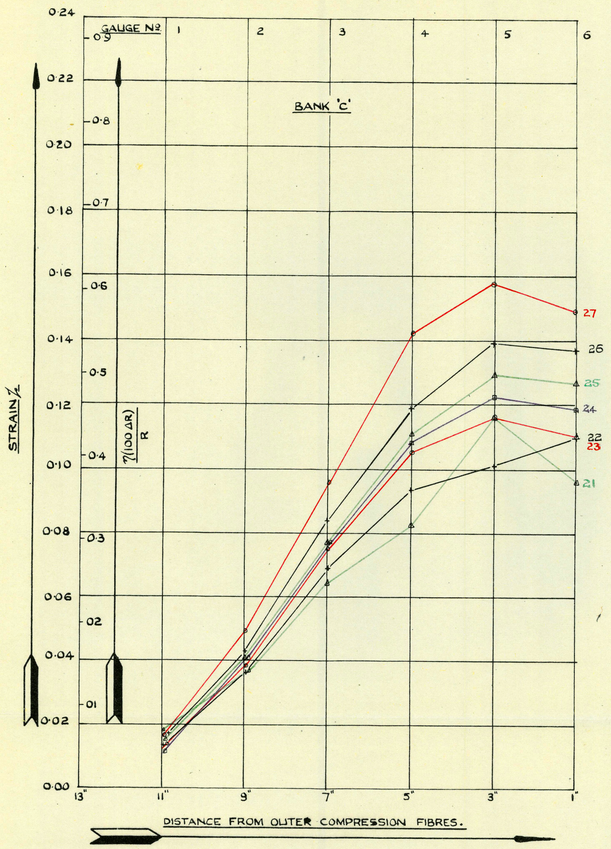


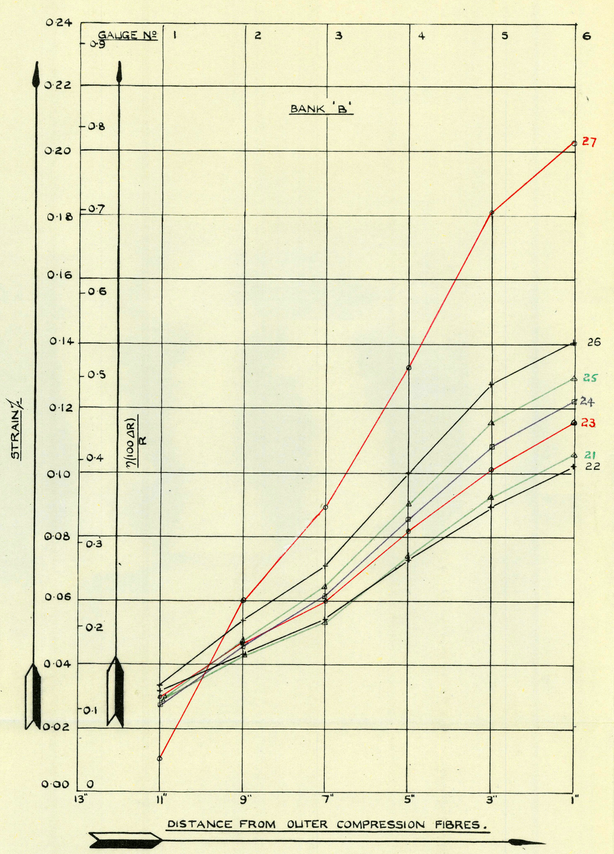


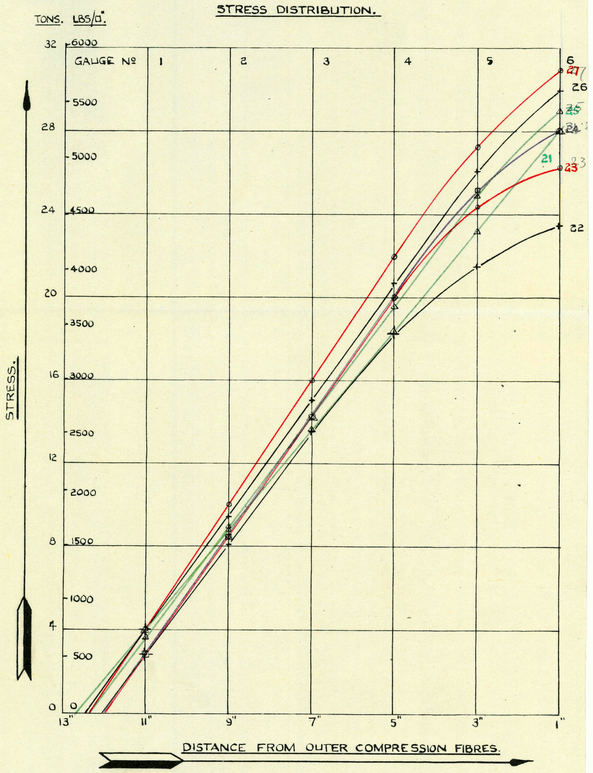
STRAIN DISTRIBUTION AT ALL SECTIONS OF SECOND SPECIMEN.

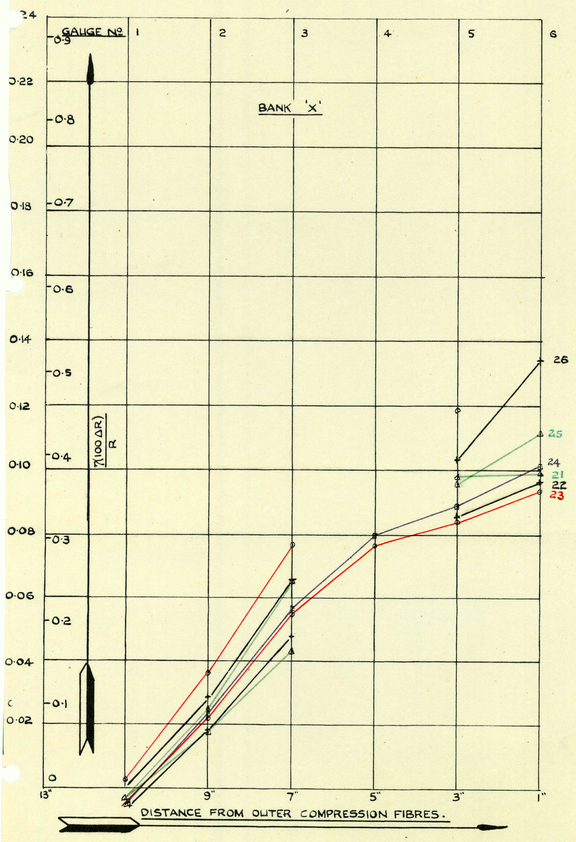
LOAD STAGES IN THE PLASTIC ZONE UP TO FAILURE.

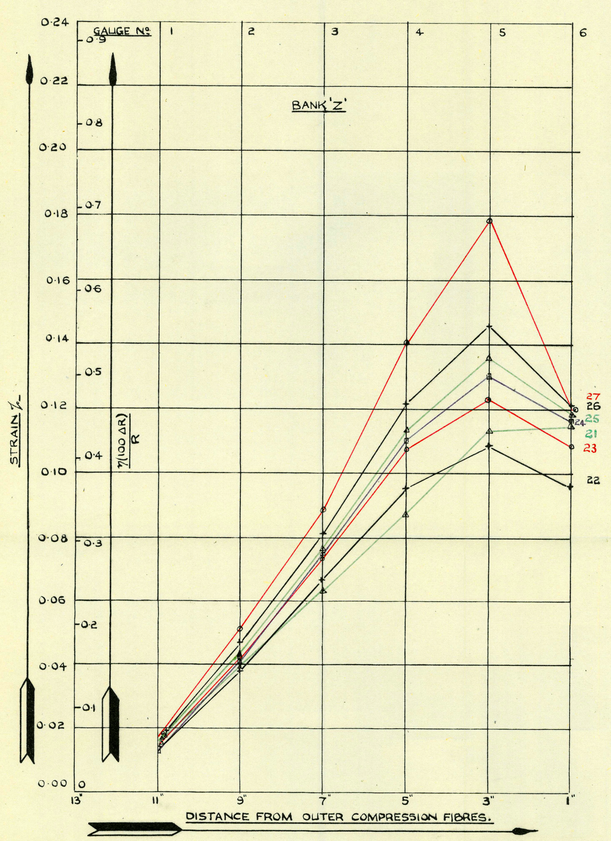


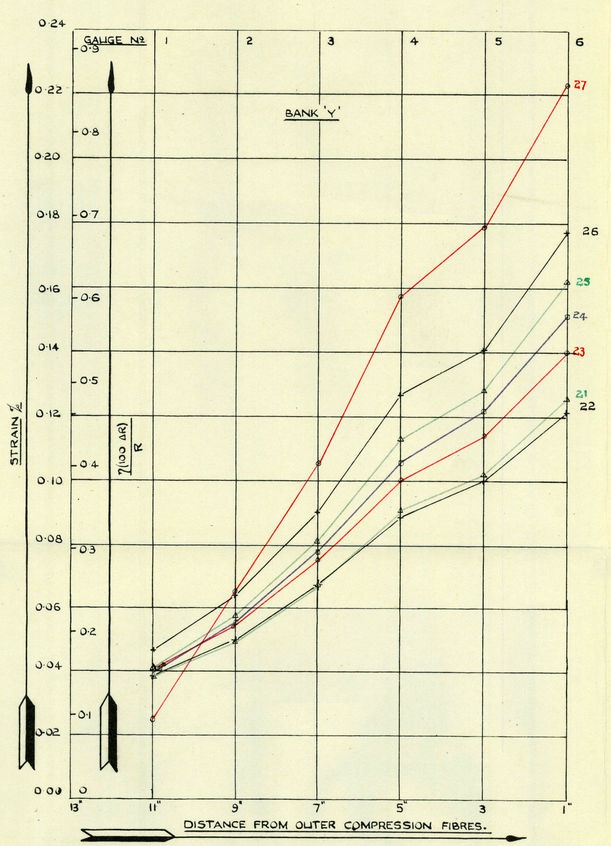




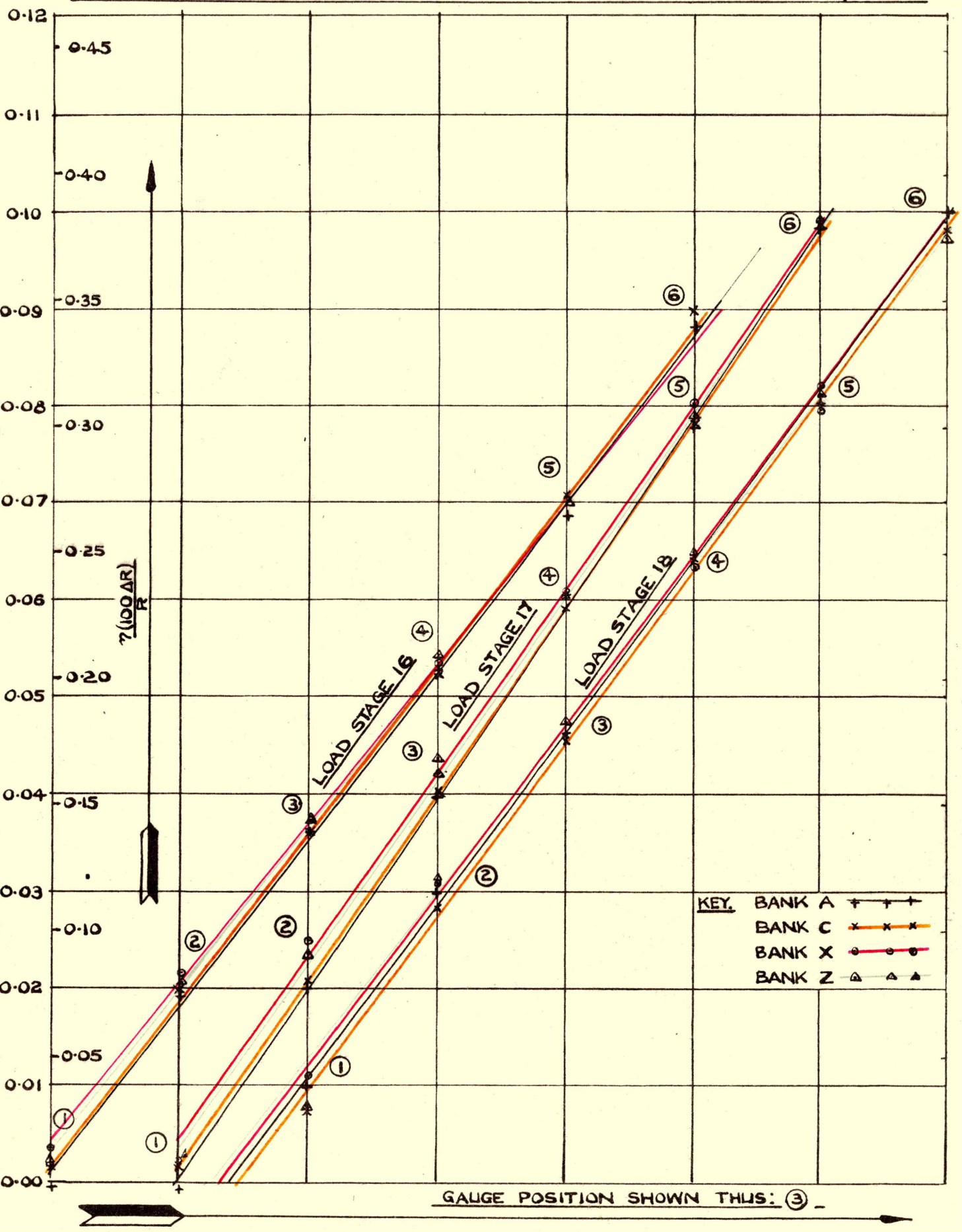




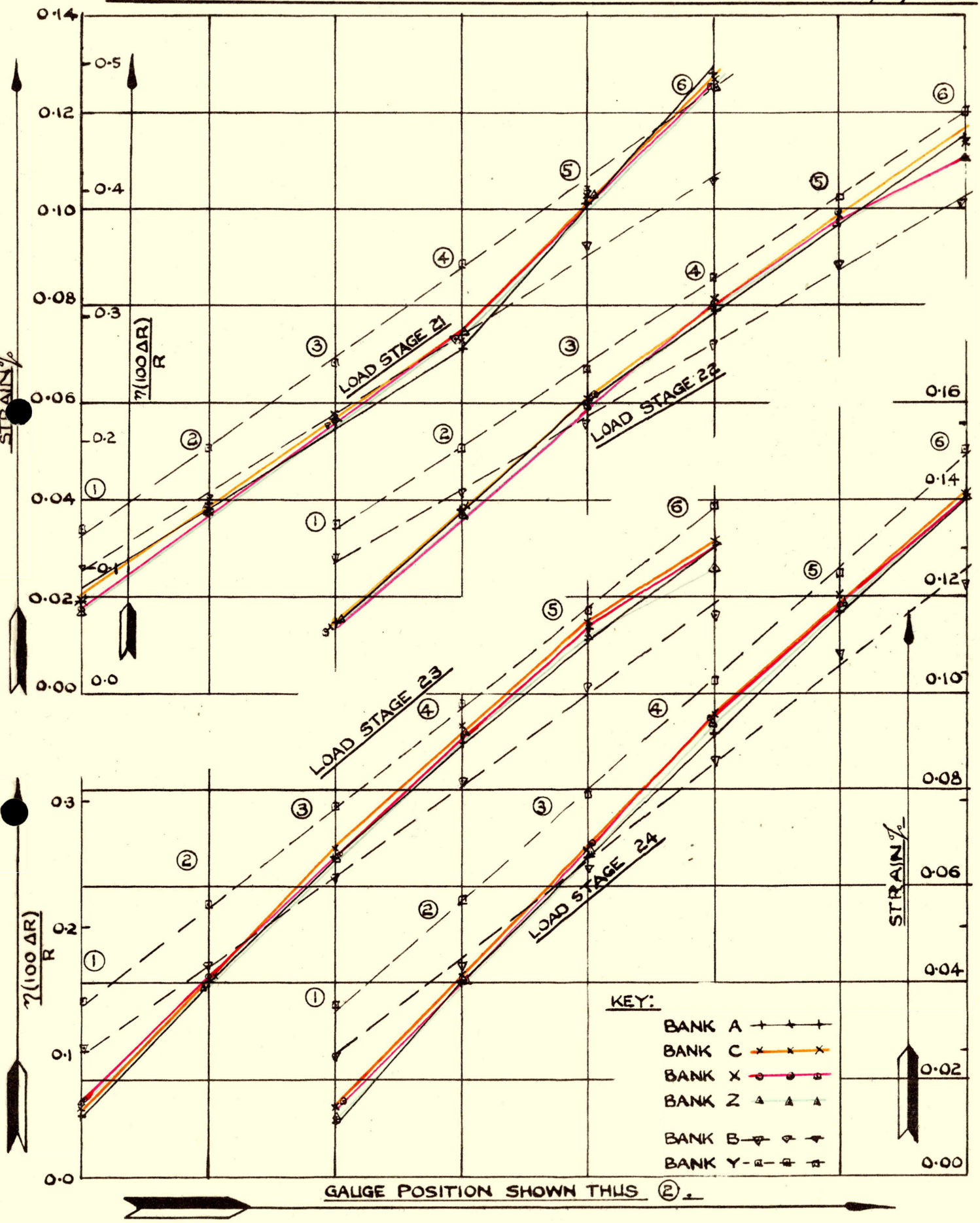




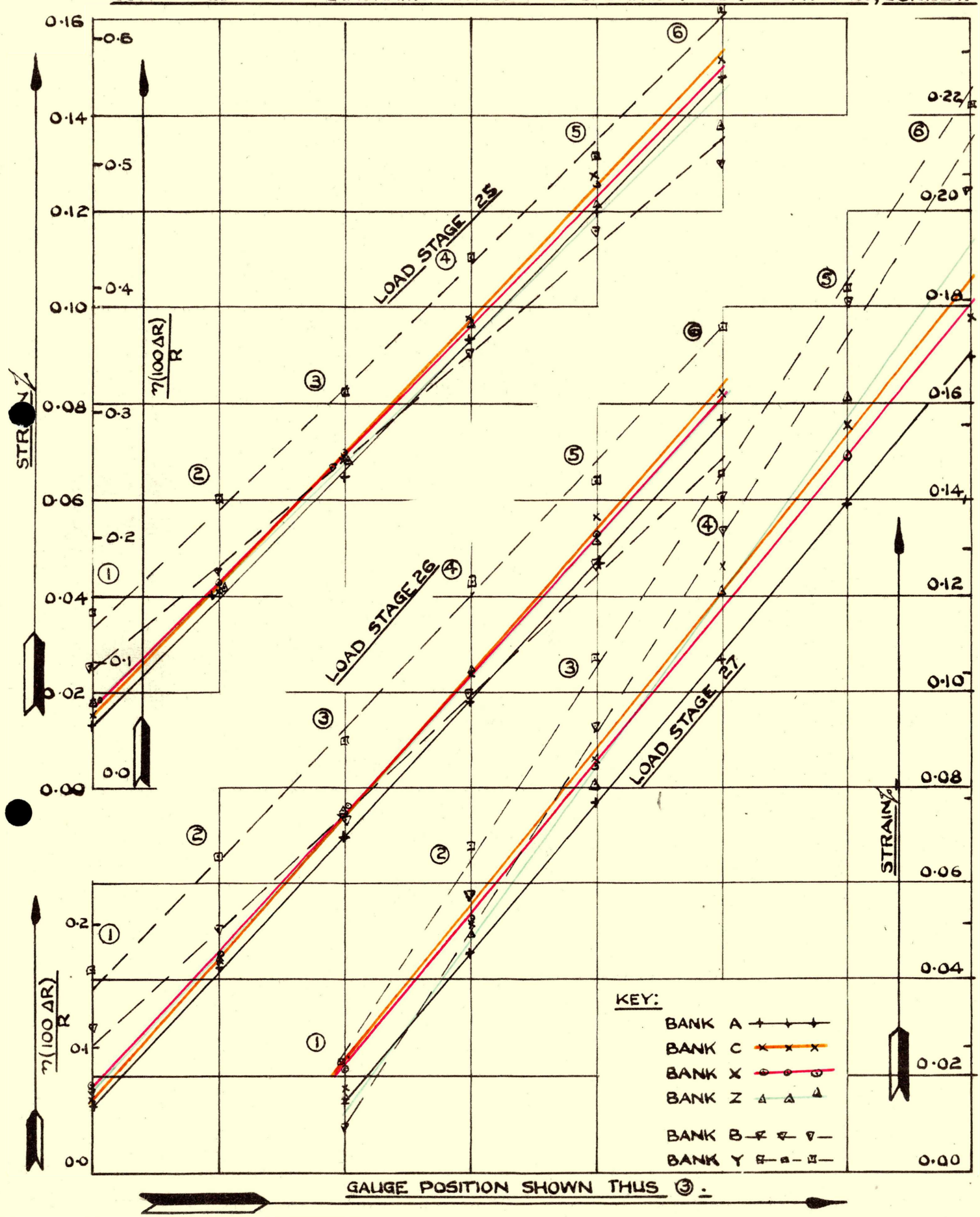
CORRECTED STRAIN DIAGRAMS FOR SECOND SPECIMEN LOAD STAGES 16, 17 AND 18.



CORRECTED STRAIN DIAGRAMS FOR SECOND SPECIMEN. LOAD STAGES 21, 22, 23 AND 24.



CORRECTED STRAIN DIAGRAMS FOR SECOND SPECIMEN. LOAD STAGES 25, 26 AND 27.



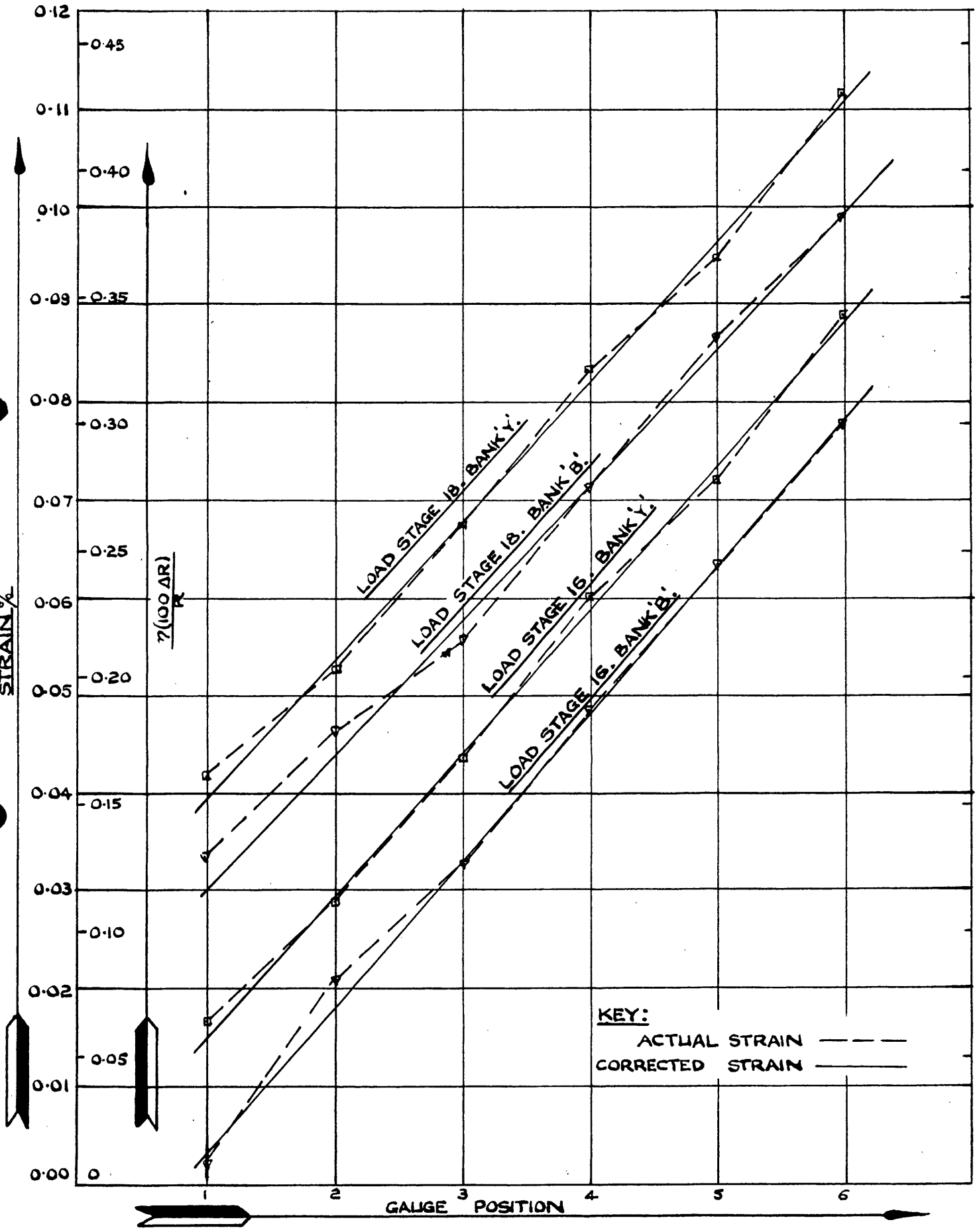
diagrams were sensibly linear, when the specimen was loaded with a linear stress-distribution in the elastic range. From here onwards, 'corrected' strain diagrams were plotted for each set of strain gauge readings. (N.B. The practice of unloading the specimen between each successive loading was continued. This was considered desireable mainly because of the necessity to load from zero for accuracy, and also to eliminate the creep that would ensue if the higher loads were maintained for long periods during the progressive working out of results and the estimation of the next stress-distribution to be applied.) Stress-distributions were increased progressively, but instead of leaving the inmost load-point un-stressed, all six load points were increased, in an attempt to get all the variable loads in operation on the part of the stress-distribution curve which was being investigated. This had the effect, in the portions of the specimen opposite to the end gauge banks, of moving the neutral axis across to the extremity of the specimen. In the test on the first specimen the load point nearest to the tension zone had been unstressed and as a result the number of points on the stress-distribution curve was then one less than the maximum. Pages 145 to 147 show the effect on the 'corrected' strain diagrams of the applied stress-distributions. The stress-distributions are given on p. 143 along with the absolute strain-distributions.

The first indication of the specimen having reached plasticity, was clearly shown by the form of the 'corrected' strain diagram corresponding to load stage 21. (See graphs) Until this stage had been reached, the applied linear stress-distributions had been producing linear 'corrected' strain diagrams. On the application of load stage 21, however, it can be seen that the 'corrected' strain diagram has increased excessively at gauge points Nos. 5 and 6 turning the graph out of its linear form. The 'concave upwards' form of the 'corrected' strain diagram indicated that a reduction of the stresses at gauge points Nos. 5 and 6 was required.

Stress-distribution 22 was thus tried out. The resulting 'corrected' strain diagram showed that the stress reductions had been too severe, witness the 'convex upwards' form of the 'corrected' strain diagram. Various trial stress-distributions were investigated, and finally stages 25, 26 and 27 produced linear 'corrected' strain diagrams and, therefore, could be accepted as applying true stress-distribution.

It has already been pointed out that more straining was occurring at the central portions (gauge banks 'B' and 'Y') of the specimen than elsewhere. This was a matter for concern, because it was believed that in the light of previous experiments no indication of plasticity taking place at the central portion of the specimen would be given by a change in the shape of the strain-

DETERMINATION OF GAUGE FACTORS FOR CENTRAL BANKS OF SECOND SPECIMEN.



distribution there. Previous experiment showed that sensibly linear strain-distribution was produced at the central section of the beam element for any distribution of stress at the load points. To keep as rigid a check as possible on the behaviour of the straining at banks 'B' and 'Y' seperate gauge factors were determined, (see p.150 and 210.) and 'corrected' strain diagrams drawn for banks 'B' and 'Y' independently. Reference to the 'corrected' strain diagrams show no deviation from a straight line form occurring in these gauge banks. Since, at load stage 21, the end gauge banks all indicated that plasticity had been reached in those portions of the specimen, and because the central portion under gauge banks 'B' and 'Y' was straining more than the ends of the specimen, it was clear that plasticity was further advanced in the central portion of the specimen than elsewhere. No method of correlating the straining of the central portion of the specimen with the stress-distribution at the load points was available. Testing continued, see p. 144 , and true stress-distributions for the concrete in the ends of the specimen were obtained during the early plastic stage there. Failure of the specimen at the centre portion, after load stage 27, see p.153 , prevented stress-distributions being determined further than the stage which had then been reached by the concrete in the end sections.

Variation in the strength of the concrete through the specimen, resulted in failure occurring

at that part of the specimen at which stress-distribution cannot be fairly assessed, (i.e. the central portion). A straight forward solution of this difficulty, so that future experimenters in this field may avoid the possibility of this type of failure preventing their assessment of the stress-distribution at and near failure, is given in the conclusions.

---//---

Creep.

A measure of the sum of the 'creep-drift' was always available throughout all tests, from the strain recordings under 'no-load' conditions between each load stage. These figures were found to be quite low, and to be proportional to the strain. Under gauge Y6, where failure occurred in the second specimen and which was the highest strain -0·221%- recorded throughout the tests, the 'creep-drift' strain was 0·007% and only $\frac{3}{100}$ ths. of the total strain. Without the very laborious use of 'drift compensation gauges', it is not possible to differentiate between creep and drift. However, the drift would be practically infinitesmal because of the short time elapsing between the two readings.

---//---



FAILURE OF SECOND SPECIMEN.

CHAPTER XIII.

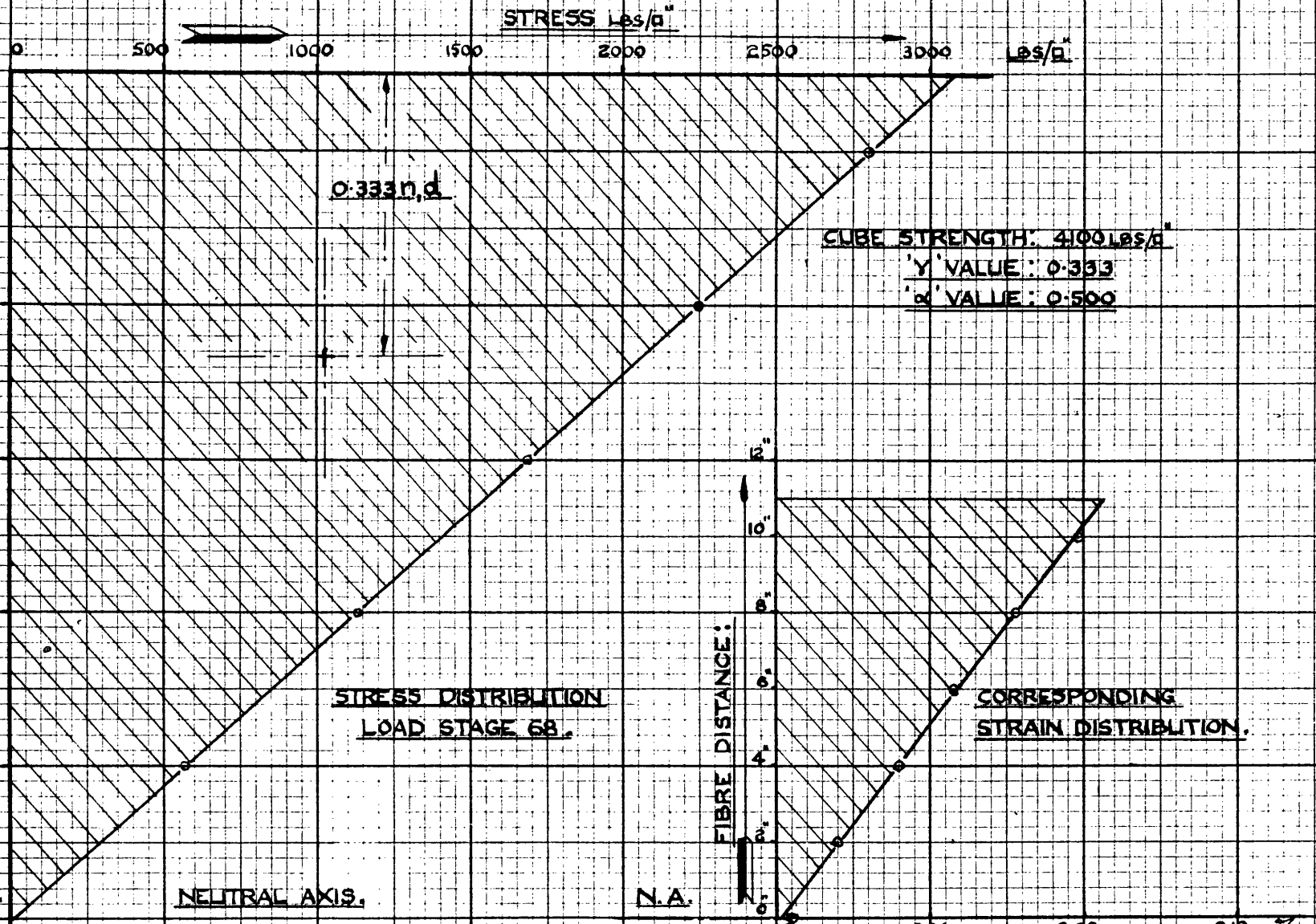
RESULTS AND CONCLUSIONS.

Many of the results and conclusions, developed from individual tests during the course of these progressive experiments, have already been set down in their appropriate chronological places in the body of the thesis, and will not, therefore, be repeated here. Rigorous comparisons have been made between the strain-distributions in beams subjected to bending and the strain-distributions observed under varying conditions of loading in the bending simulation specimens. From these numerous comparisons and tests, the method of applying 'gauge factors' to obtain the 'corrected' strain diagrams was discovered. By this method selections of those stress-distributions, applied to the bending simulation specimens, were made which produced straining conditions precisely the same as those in a beam.

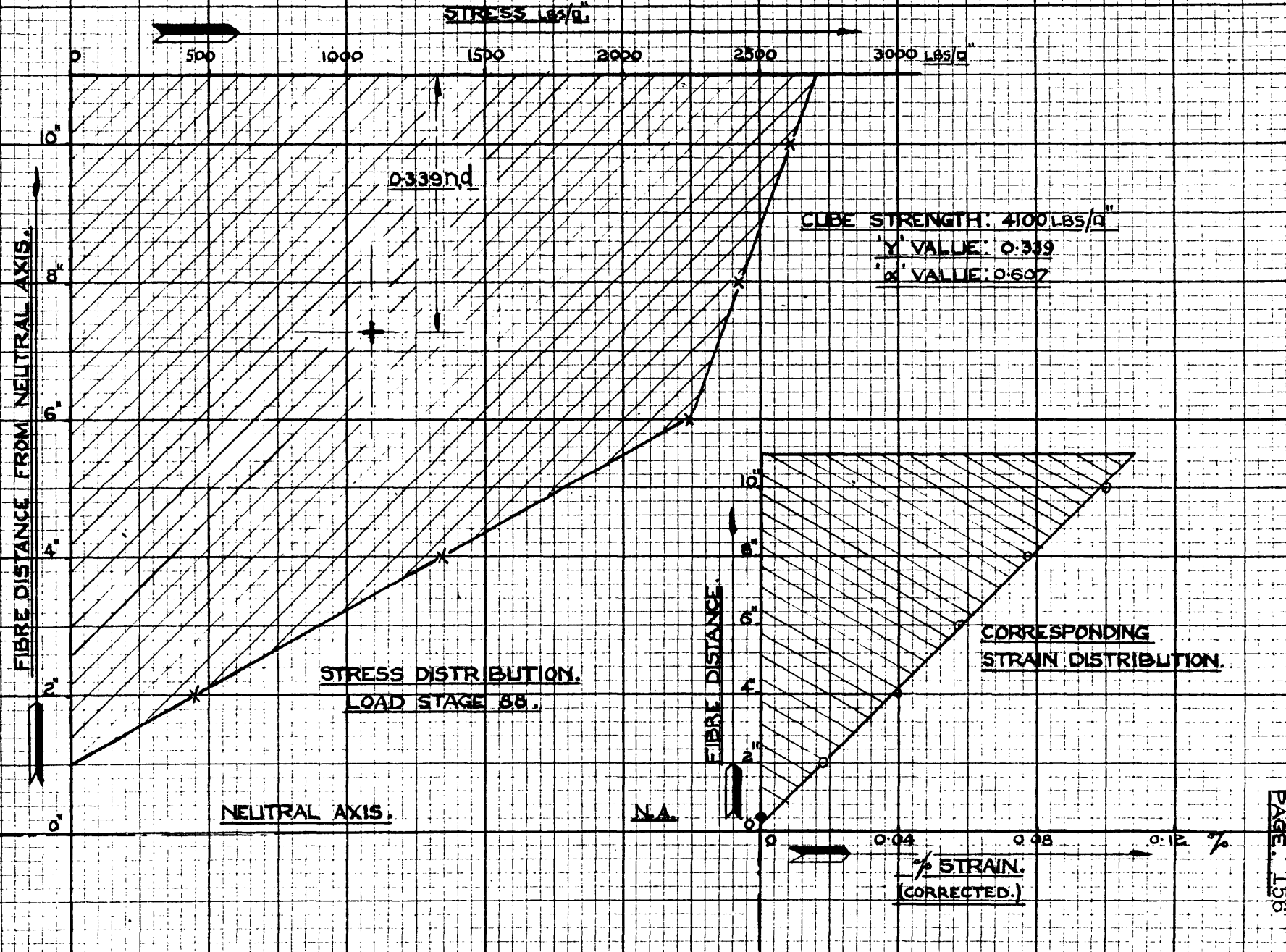
To reproduce here all those results which led to the discovery of this testing procedure or, indeed, to set forth the method itself, would merely repeat what has already been written at length, and so unnecessarily burden the thesis. The first part of this chapter will, therefore, be confined to the presentation of results which have been selected by the application of the 'gauge factor' method, and to relevant discussions. A brief summary of conclusions will then follow.

---//---

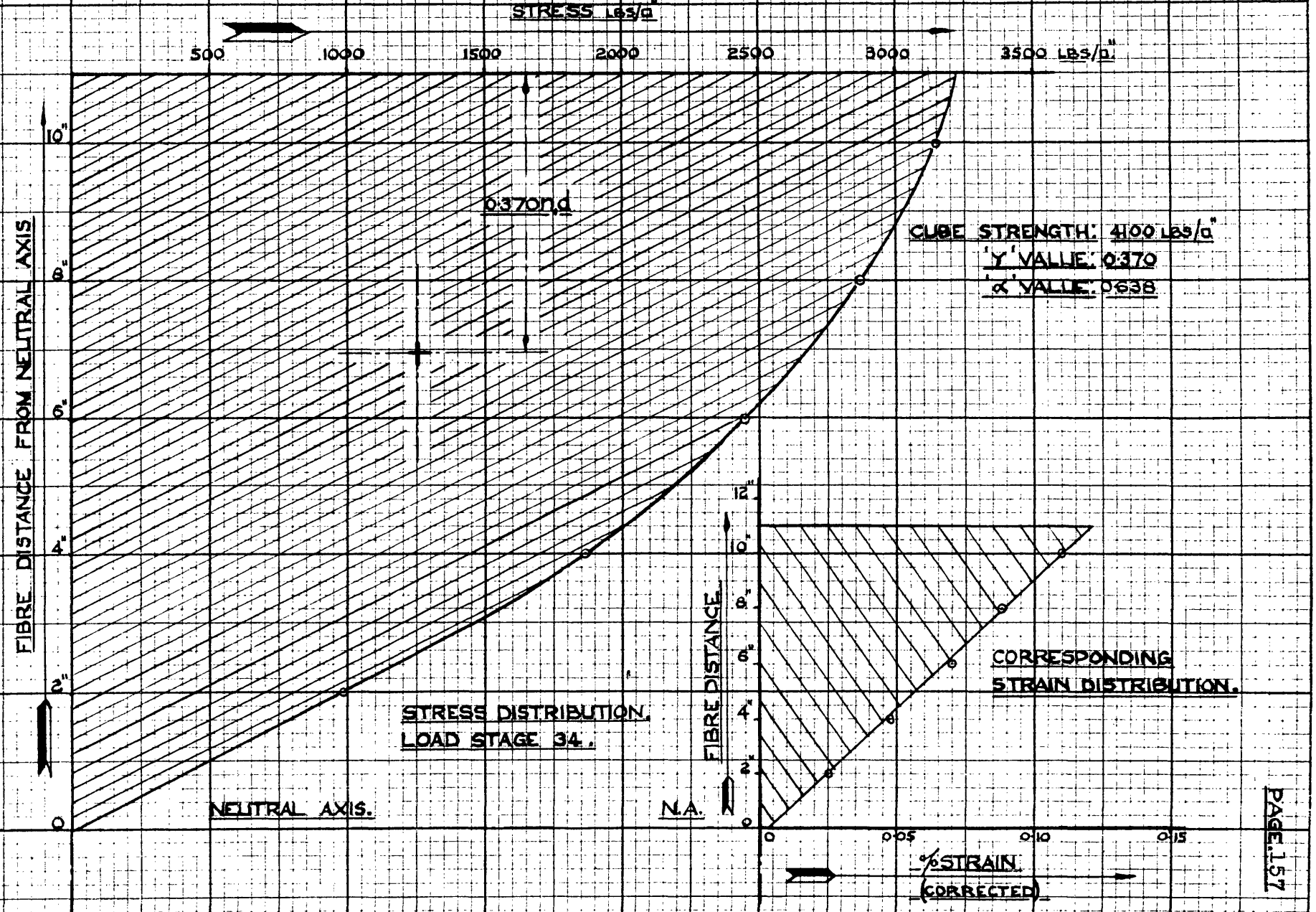
STRESS DIAGRAM AT LOAD STAGE 68: FIRST SPECIMEN:

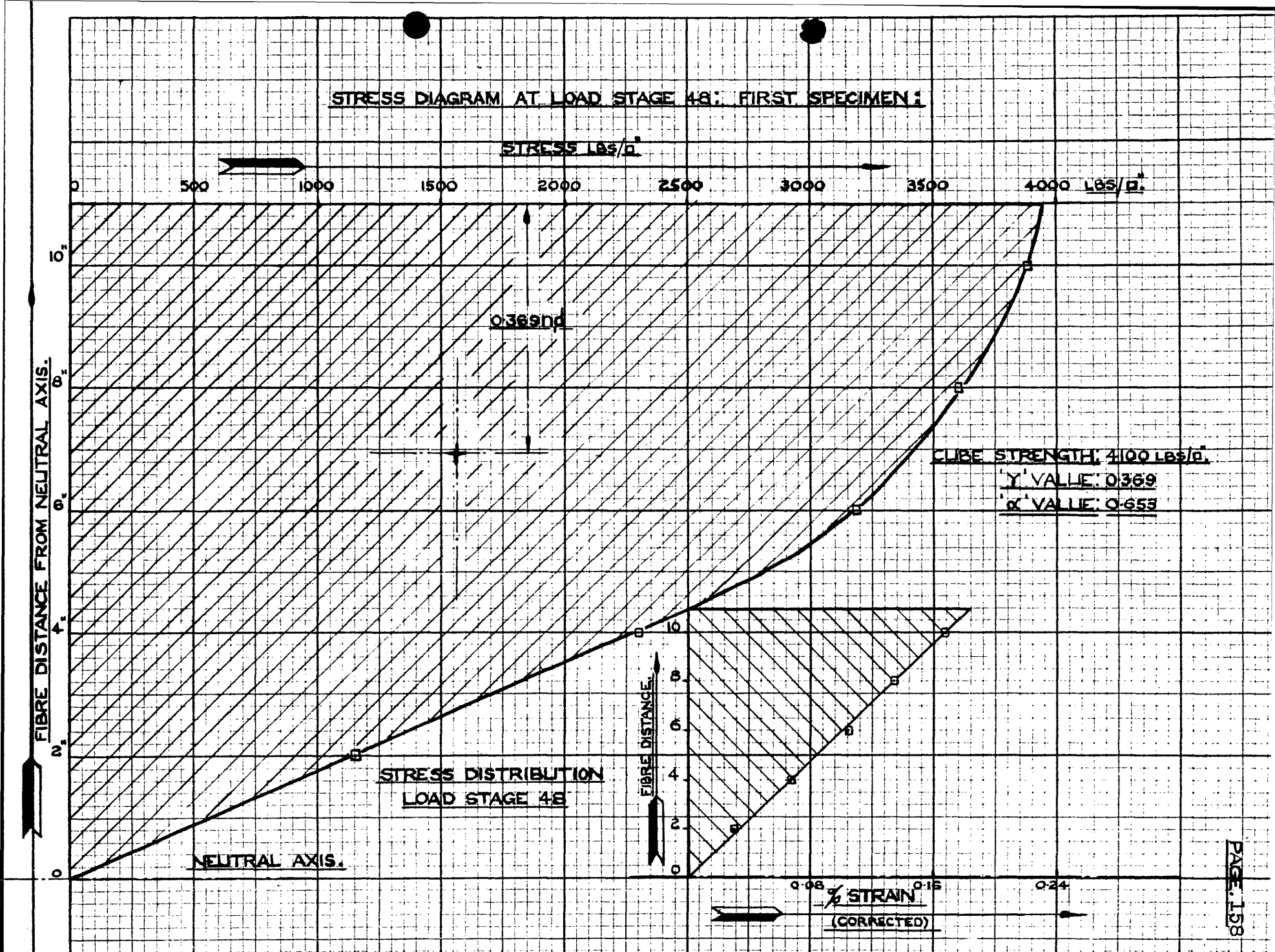


STRESS DIAGRAM AT LOAD STAGE 88: FIRST SPECIMEN:

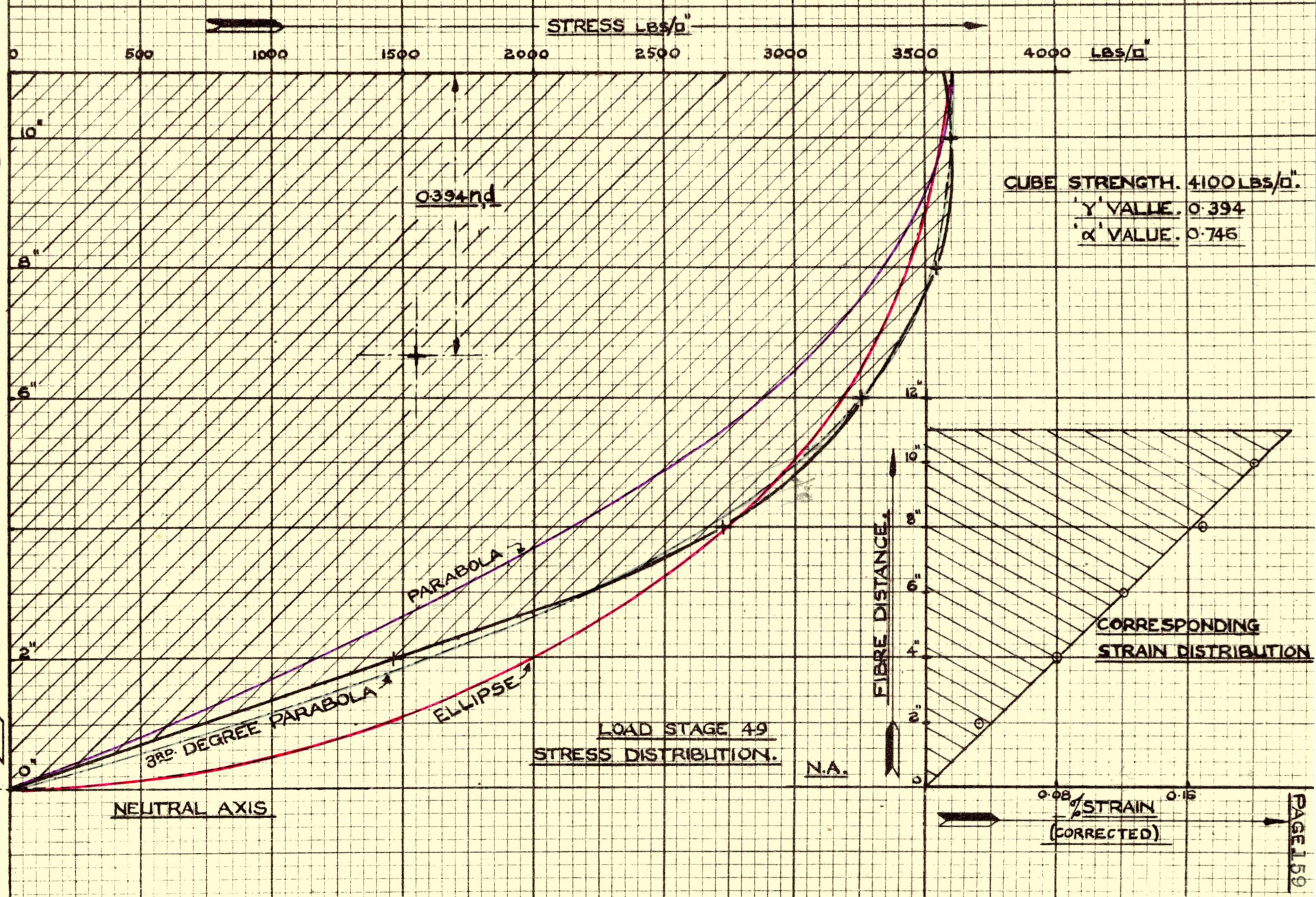


STRESS DIAGRAM AT LOAD STAGE 34: FIRST SPECIMEN:

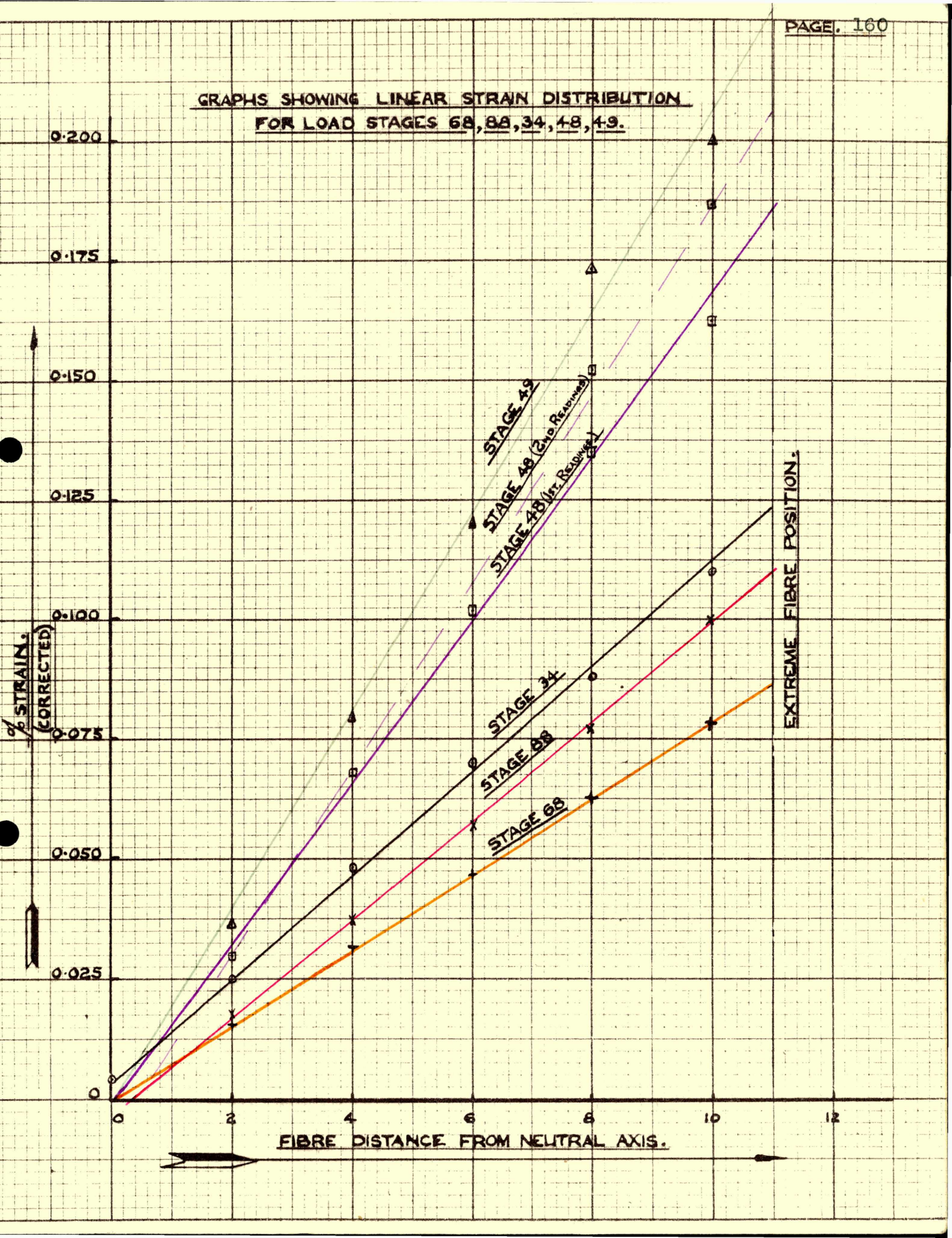



STRESS DIAGRAM AT LOAD STAGE 48: FIRST SPECIMEN:
STRESS LBS/□"
0
500
1000
1500
2000
2500
3000
3500
4000 LBS/□".
FIBRE DISTANCE FROM NEUTRAL AXIS.
10"
8"
6"
4"
2"
0
0.369nd
CUBE STRENGTH: 4100 LBS/□".
'Y' VALUE: 0.369
'α' VALUE: 0.653
STRESS DISTRIBUTION
LOAD STAGE 48
NEUTRAL AXIS.
FIBRE DISTANCE.
10
8
6
4
2
0
0.08
0.16
0.24
% STRAIN
(CORRECTED)

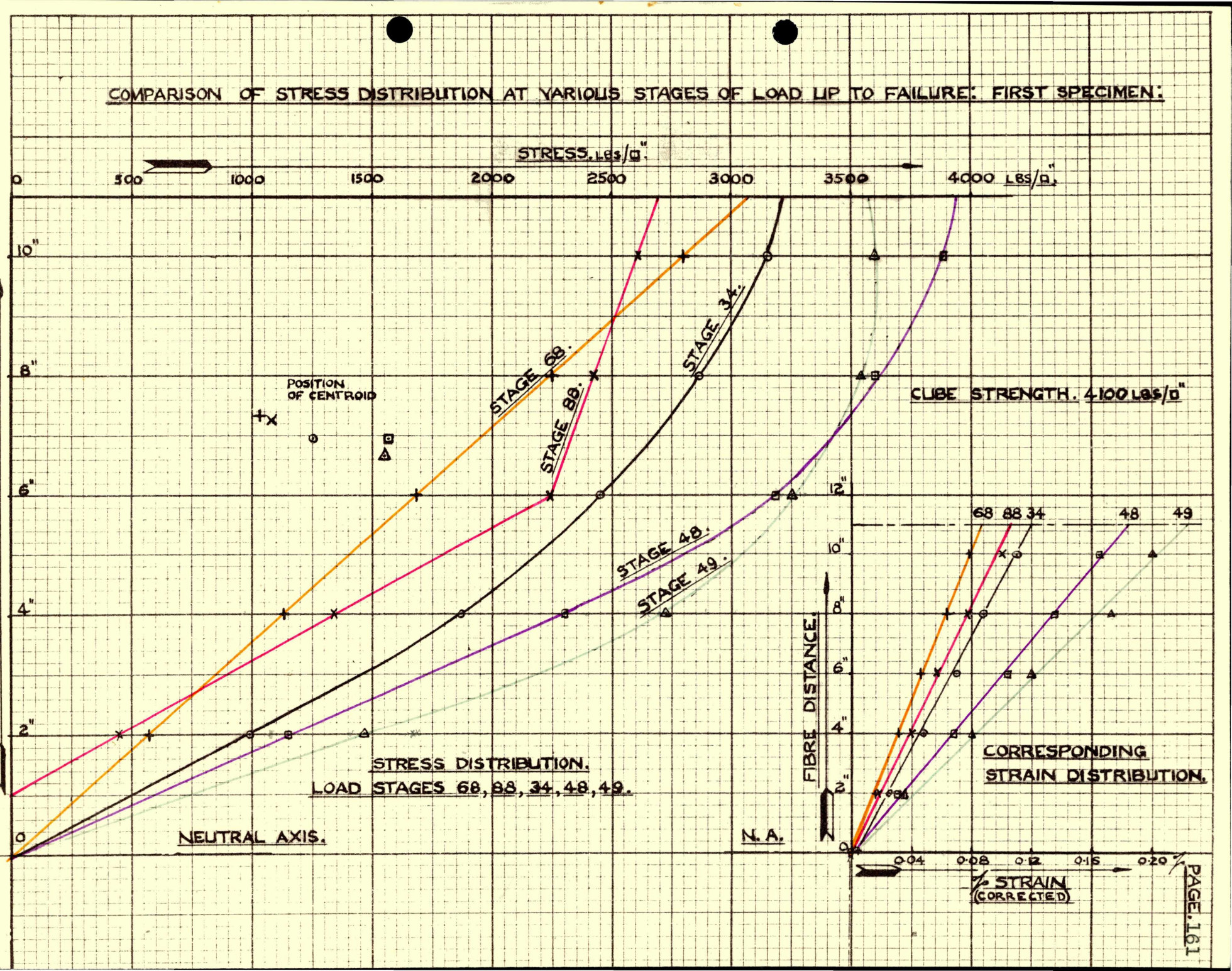
STRESS DIAGRAM AT FAILURE: FIRST SPECIMEN.



GRAPHS SHOWING LINEAR STRAIN DISTRIBUTION FOR LOAD STAGES 68, 88, 34, 48, 49.



COMPARISON OF STRESS DISTRIBUTION AT VARIOUS STAGES OF LOAD UP TO FAILURE: FIRST SPECIMEN:



Stress Distributions Corresponding to Those in a Beam Failing in Compression.

The use of 'gauge factors' and 'corrected' strain diagrams resulted in a selection of less than 10% of the many stress-distributions which had been tried out in the test on the first specimen. These final selections of stress-distributions corresponded to the stress-distributions which would occur in a beam failing in compression, or in an eccentrically loaded column, having the same dimensions and grade of concrete as the elemental specimen. These selected stress-distributions in the element of beam, or column, under test at successive stages, commencing at the end of the elastic range and ending at failure, can be seen on pages 155 to 161.

From these results it is easy to observe the progressive changes occurring in the shape of the stress-distribution during increasing intensities of loading right up to failure of the specimen.

As the load increases, the first change from linear stress-distribution which is prevalent in the elastic range, is a relative falling off in the stress on the two load points nearest to the outer compression fibres. This decrease in the stresses required on the outer fibres to maintain linear strain-distribution spreads, as the load increases, towards the neutral axis, until when failure finally

occurs it covers about two-thirds of the total stress-diagram; i.e. the linear portion of the stress-diagram at failure is reduced to about one-third of the neutral axis depth.

At failure, the maximum stress occurs at the outer compression fibres and is maintained almost at this same value over the outermost quarter of the compression fibres. The maximum strain was recorded under gauge A6 , being 0·214% which corresponds to a strain at the extreme compression fibres of $\frac{11}{10} \times 0{\cdot}214\% = 0{\cdot}235\%$. Values of the constants α and γ for the stress-distribution at failure were 0·746 and 0·394 respectively. The calculations for these figures are given on p. 164 and are typical of the method used in computing α and γ for all load stages.

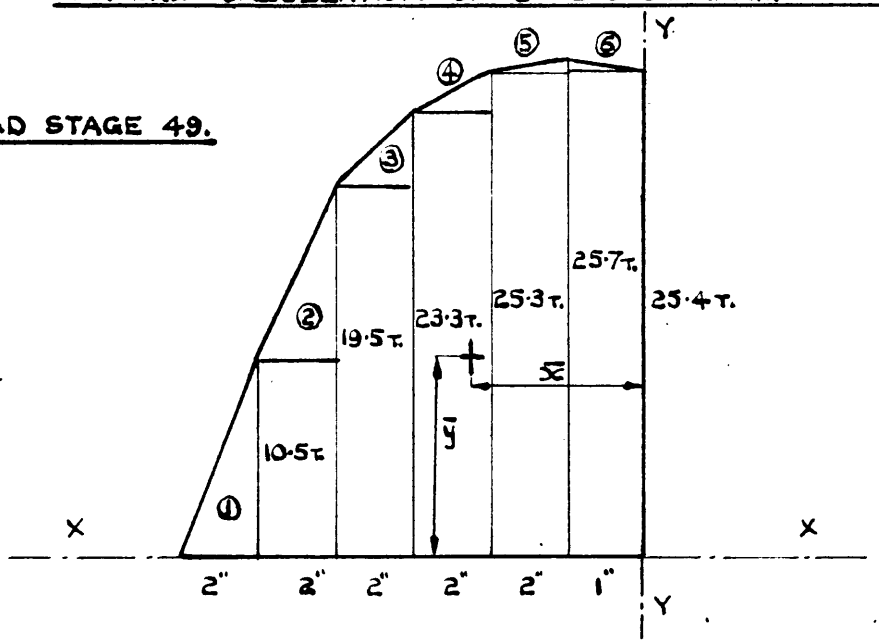
Comparisons between Mathematical Figures and Stress-Distributions.

The constants α and γ have been tabulated, p. 165 , in ascending order of magnitude for both mathematical figures and for stress-distributions. The table commences with a triangle at load stage 68, and finishes with a rectangle.

The stress-distribution can be seen to leave the triangular shape of the elastic range and to approximate progressively (so far as the factors α and γ are concerned) to a hyperbola, a parabola and finally a cubic or third degree parabola. Further up the scale are the quarter ellipse, the

TYPICAL CALCULATION OF STRESS DIAGRAM CONSTANTS.

LOAD STAGE 49.



N.B. STRESS UNITS KEPT IN TONS FOR EASE OF CALCULATION.

PART.	AREA.	DISTANCE OF C.G. FROM Y.Y.	MOMENT ABOUT Y.Y.	DISTANCE OF C.G. FROM X.X.	MOMENT ABOUT X.X.
Δ^{LE} ①	10·5	9·67	101·8	3·50	37
Δ^{LE} ②	9·0	7·67	69·1	13·50	122
Δ^{LE} ③	3·8	5·67	21·6	20·77	79
Δ^{LE} ④	2·0	3·67	7·3	23·97	48
Δ^{LE} ⑤	0·4	1·67	0·6	25·43	10
Δ^{LE} ⑥	0·1	0·67	0·1	25·50	3
RECT^{LE} ②	21·0	8·00	168·0	5·25	110
RECT^{LE} ③	39·0	6·00	234·0	9·75	380
RECT^{LE} ④	46·6	4·00	186·3	11·65	543
RECT^{LE} ⑤	50·6	2·00	101·2	12·65	640
RECT^{LE} ⑥	25·4	0·50	12·7	12·70	322
	208·4 ΣA.		902·7 $\Sigma A\bar{x}$		2294 $\Sigma A\bar{y}$

$$\bar{x} = \frac{902.7}{208.4} = 4.33"$$

$$\bar{y} = \frac{2294}{208.4} = 11.0 \text{ TONS.} = \frac{11.0 \times 2240}{2 \times 8} \text{ LBS/□".}$$

$$Y = \frac{4.33}{11} = 0.394$$

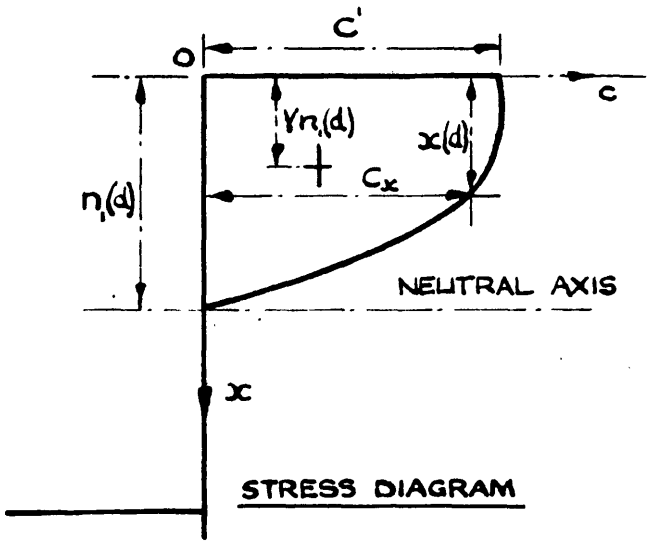
$$\alpha n_1 d_c = 208.4 = 11 \times 25.4\alpha$$

$$\alpha = 0.746$$

$\bar{y} = 1540$ LBS/□".

$Y = 0.394$

$\alpha = 0.746$



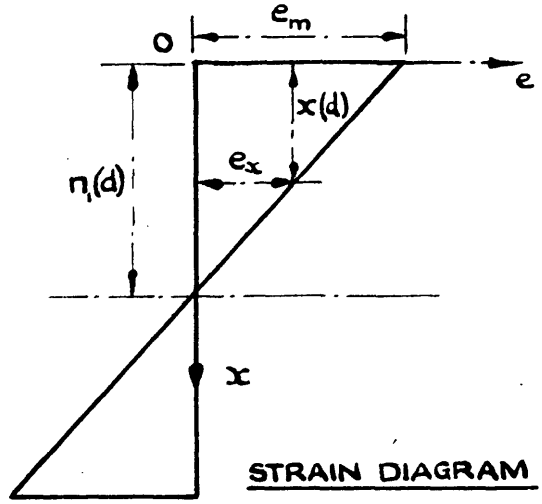


TABLE OF STRESS DISTRIBUTION CONSTANTS.

STRESS DIAGRAM	α SHAPE FACTOR	γ DEPTH OF C.G.
TRIANGLE: LOAD STAGE 68	0·500	0·333
LOAD STAGE 88	0·607	0·339
HYPERBOLA	0·625	0·356
LOAD STAGE 34	0·638	0·370
LOAD STAGE 48	0·653	0·369
PARABOLA	0·667	0·375
FAILURE: LOAD STAGE 49	0·746	0·394
THIRD DEGREE PARABOLA	0·750	0·400
QUARTER-ELLIPSE	0·785	0·425
FIFTH DEGREE PARABOLA	0·833	0·429
RECTANGLE	1·00	0·500

fifth degree parabola and the rectangle.

The shape of the stress-distribution at failure is of great interest, since upon it depend the factors required for plastic theory and the ultimate resisting moment of the beam element. The constants α and γ of the stress-distribution at failure fall between those of a parabola, a third degree parabola and a quarter ellipse. These mathematical figures ~~figures~~ have therefore been plotted to the same scale as the stress-distribution diagram at failure shown on p. 159. Clearly the stress-distribution at failure approximates very closely in shape to a cubic parabola.

Cubic Parabola.

Consider the stress diagram and strain diagram shown on p. 165.

From the stress diagram:

Let C_x be the stress at any point distant x(d) from the outer compression fibres at failure.

With the origin at O:-

$$C_x = C' - \frac{C'}{n_1^3}.x^3 \quad ------ (1).$$

Area of stress-diagram $= \alpha n_1(d)C'$

$$= \int_{x=0}^{x=n_1} C_x.dx = \int_{x=0}^{x=n_1} (C' - \frac{C'}{n_1^3}.x^3).dx$$

$$= \tfrac{3}{4}.n_1(d)C'$$

$$\underline{\alpha = 0.75}$$

Cubic Parabola. (Cont'd.)

Moment of area about extreme fibres $= \int_{x=0}^{x=n_1} x.C_x.dx$

Therefore depth of centre of gravity $= \dfrac{\int_{x=0}^{x=n_1} x.C_x.dx}{\int_{x=0}^{x=n_1} C_x.dx}$

$$\gamma = 0{\cdot}4n_1(d)$$

$$\underline{\gamma = 0{\cdot}4n_1(d)}$$

Hence the figures $\alpha = 0{\cdot}75$ and $\gamma = 0{\cdot}4$ for the cubic parabola can be seen to correspond closely to $\alpha = 0{\cdot}746$ and $\gamma = 0{\cdot}394$, the figures obtained in the stress-distribution at failure.

From the strain diagram.

Let e_x be the strain at any point distant x(d) from the outer compression fibres, and let e_m be the strain at the outer compression fibres.

Then:-

$$\frac{x}{n_1} = \frac{e_m - e_x}{e_m}$$

or, $$x = \frac{n_1}{e_m}.(e_m - e_x) \quad \text{- - - - - - - - (2).}$$

Substituting (2) in (1) and transposing,

$$C_x = C' - \frac{C'}{e_m^3} \cdot (e_m - e_x)^3$$

Which gives the relationship existing between the concrete stress and strain in the compressive fibres at failure. This also is a cubic parabola, and, therefore, the stress-distribution diagram at failure represents the stress-strain relationship in the concrete at failure to a scale such that the length of the principal axis perpendicular to the neutral axis is equal to 'e_m'. The fact that at a given load the stress-distribution diagram represents the stress-strain relation in the concrete at that load, is true for any shape of the stress-distribution diagram, provided the strain is linear.

Calculations Resulting from Stress-Distribution at Failure.

$\alpha = 0{\cdot}746$

$\gamma = 0{\cdot}394$

$C' = 3580$ lbs./sq.in.

$e_m = 0{\cdot}235\%$

Now cube crushing strength, $C_u = 4100$ lbs./sq.in.

Cylinder crushing strength, $C_c = 3500$ lbs./sq.in.

$n_1 d = 11$ ins.

From beam dimensions, $d = 19{\cdot}5$ ins.

$$n_1 = 0{\cdot}564$$

$$b = 8 \text{ ins.}$$

$$\propto C' = 0{\cdot}746 \times 3580 = 2670 \text{ lbs./sq.in.}$$

or, $$\underline{\underline{\propto C' = 0{\cdot}65 C_u}}$$

and, $$\underline{\underline{\propto C' = 0{\cdot}76 C_c}}$$

$$\underline{\underline{E'_c = \frac{C'}{e_m} = \frac{3580}{0\ 235} \cdot 100 = 1{\cdot}53 \times 10^6 \text{lbs./sq.in.}}}$$

A value for E_c, the low stress or elastic value of E'_c, may be determined from the stress-distribution diagram at failure (p. 159.) for the curve leaves its elastic form at a fibre distance of approximately 4·2ins. from the neutral axis the stress then being 2800 lbs./sq.in. and the corresponding strain $\frac{4{\cdot}2}{11} \cdot 0{\cdot}235\% = 0{\cdot}091\%$

Therefore, $$\underline{\underline{E_c = 3{\cdot}07 \times 10^6 \text{lbs./sq.in.}}}$$

This compares well with the value of E_c obtained from the stress-strain relationship, p. 173, derived from gauge A6 (the point at which failure eventually occurred); for, at a strain of 0·091%, the curve is leaving its elastic form and the corresponding stress is again 2800 lbs./sq.in. ,

giving:- $$\underline{\underline{E_c = 3{\cdot}07 \times 10^6 \text{lbs./sq.in.}}}$$

Hence $$E'_c = \frac{1{\cdot}53 \times 10^6}{3{\cdot}07 \times 10^6} \times E_c = 0{\cdot}5\, E_c$$

$$\underline{\underline{E'_c = 0{\cdot}5 E_c}}$$

From equation (5) in the Summary of Professor A.L.L.Baker's plastic theory given in Chapter I.,

$$M' = \alpha C' b n_1 d^2 (1 - \gamma n_1)$$

Hence $M' = 0{\cdot}746 \times 0{\cdot}564 \times C' bd^2 (1 - 0{\cdot}394 \times 0{\cdot}564)$

$$\underline{\underline{M' = 0{\cdot}327\ C' bd^2}}$$

But $C' = 0{\cdot}874\ C_u = 1{\cdot}02 C_c$

$$\underline{\underline{M' = 0{\cdot}335\ C_c bd^2}} \qquad \text{and} \quad \frac{M'}{C_c bd^2} = 0{\cdot}335$$

$$\underline{\underline{M' = 0{\cdot}286\ C_u bd^2}} \qquad \text{and} \quad \frac{M'}{C_u bd^2} = 0{\cdot}286$$

The similarity of these formulae to beam test results, shows that the position of the neutral axis at failure of the specimen, was correct for the true simulation of a compression failure with the same dimensions as the beam element under test. Values of the 'Secant Modulus of Elasticity', E'_c, prior to failure are given in the following table, together with values of $\frac{M'}{C_c bd^2}$ and $\frac{M'}{C_u bd^2}$ at various stages of loading in the plastic range.

The ratio of M' at failure to M' at the commencement of plasticity was 1·67.

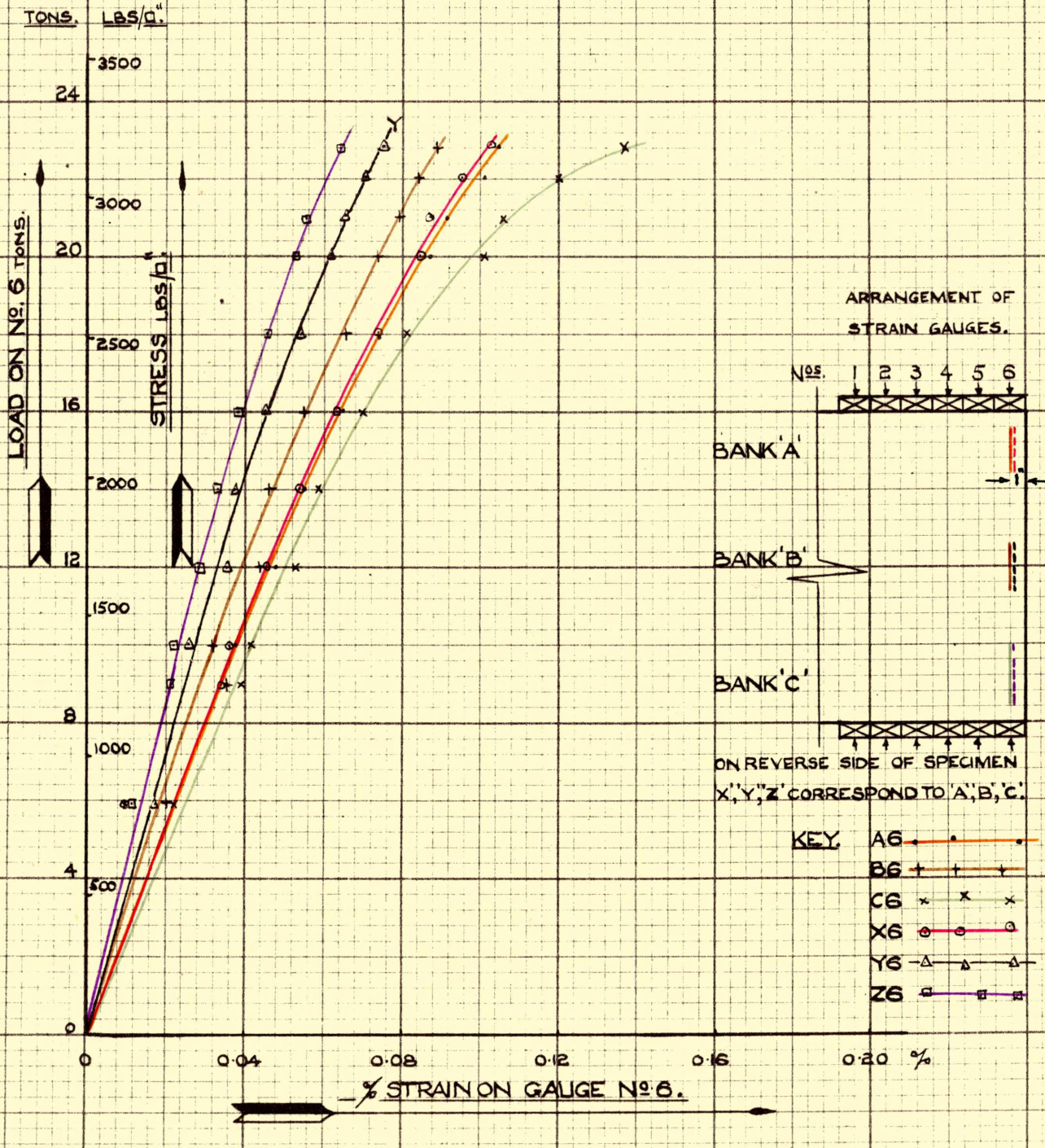
STAGE	α	γ	C'	n_1	'k' in $C'=kC_u$	$\frac{M'}{C_u bd^2}$	$\frac{M'}{C_c bd^2}$	E'_c
68	0·500	0·333	3050	0·564	0·744	0·170	0·200	2·86
88	0·607	0·339	2700	0·564	0·660	0·183	0·214	2·66
34	0·638	0·370	3210	0·564	0·783	0·223	0·262	2·51
48	0·653	0·369	3940	0·564	0·960	0·280	0·328	1·76
FAILURE 49	0·746	0·394	3580	0·564	0·875	0·286	0·335	1·53

Stress-Strain Relationship at Points in the Compression Zone During Varying Load Stages.

Use is still made of the results which have been selected by the 'gauge factor' and 'corrected' strain diagram method.

Firstly, graphs of stress at a given distance from the extreme compression fibres against strain at gauges that same distance from the extreme compression fibres, have been plotted. See p. 172 to 178. Though the strain gauges from which these recordings have been taken are equidistant (for any particular graph) from the extreme compression fibres, they are at different positions on the faces of the specimen. Their exact location is given by the drawing accompanying each graph and headed 'arrangement of strain gauges'. The effect of eccentricity of the loading during the testing carried out with the first specimen in its initial position in the machine can be seen (on p. 172.) by the diverging tendency of the stress-strain curves corresponding to the various gauge banks. The same gauges, p. 173, show less tendency to diverge during testing with the specimen in its second, and final, position in the machine. When allowance is made for those factors, discussed in the thesis, which cause local strain discrepancies to occur, it seems that these curves do tend, in general, to follow the same line as one another.

STRESS/STRAIN CURVES FOR GAUGE No. 6.
1ST. SPECIMEN. INITIAL POSITION IN MACHINE.

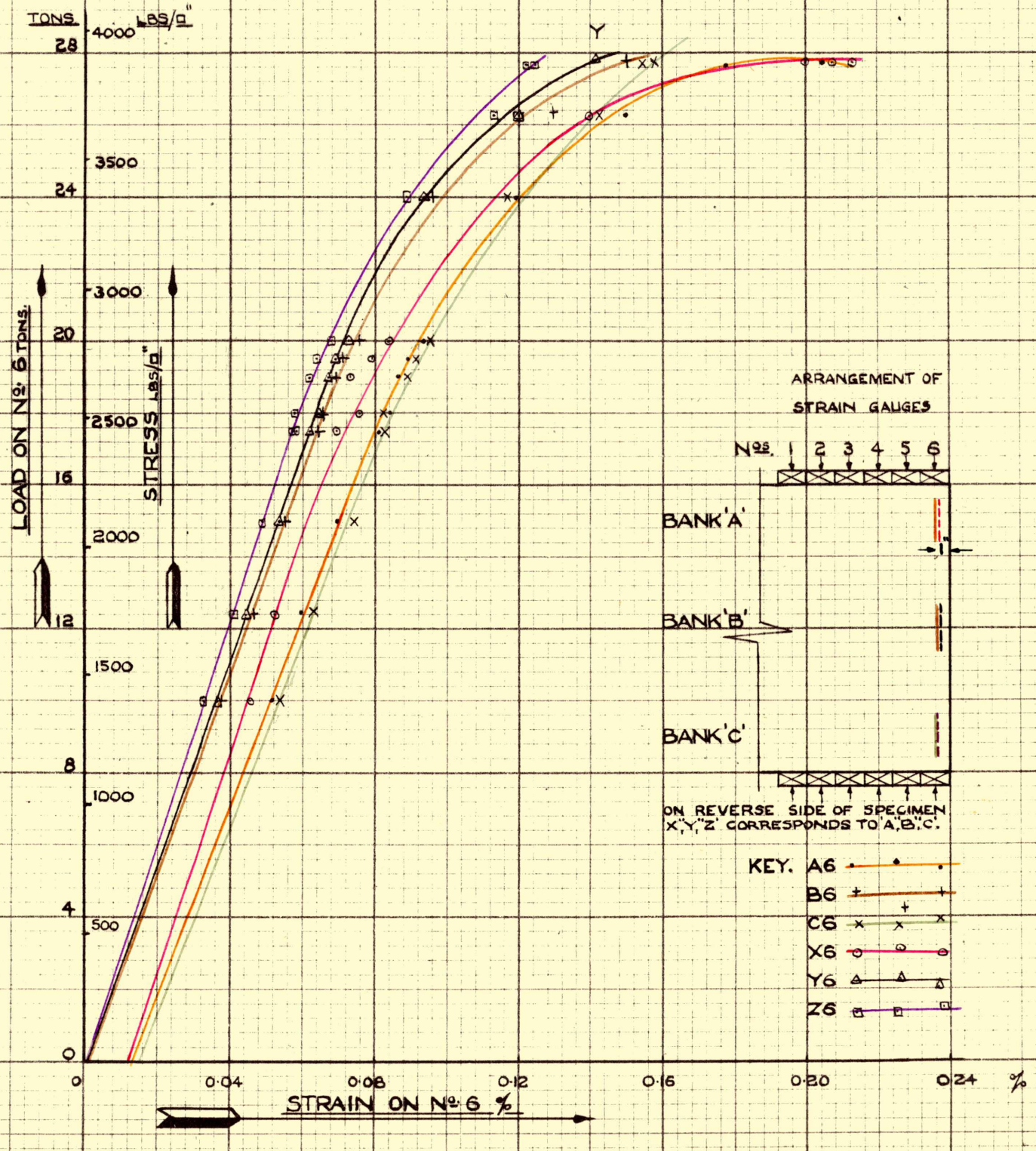


ARRANGEMENT OF STRAIN GAUGES.

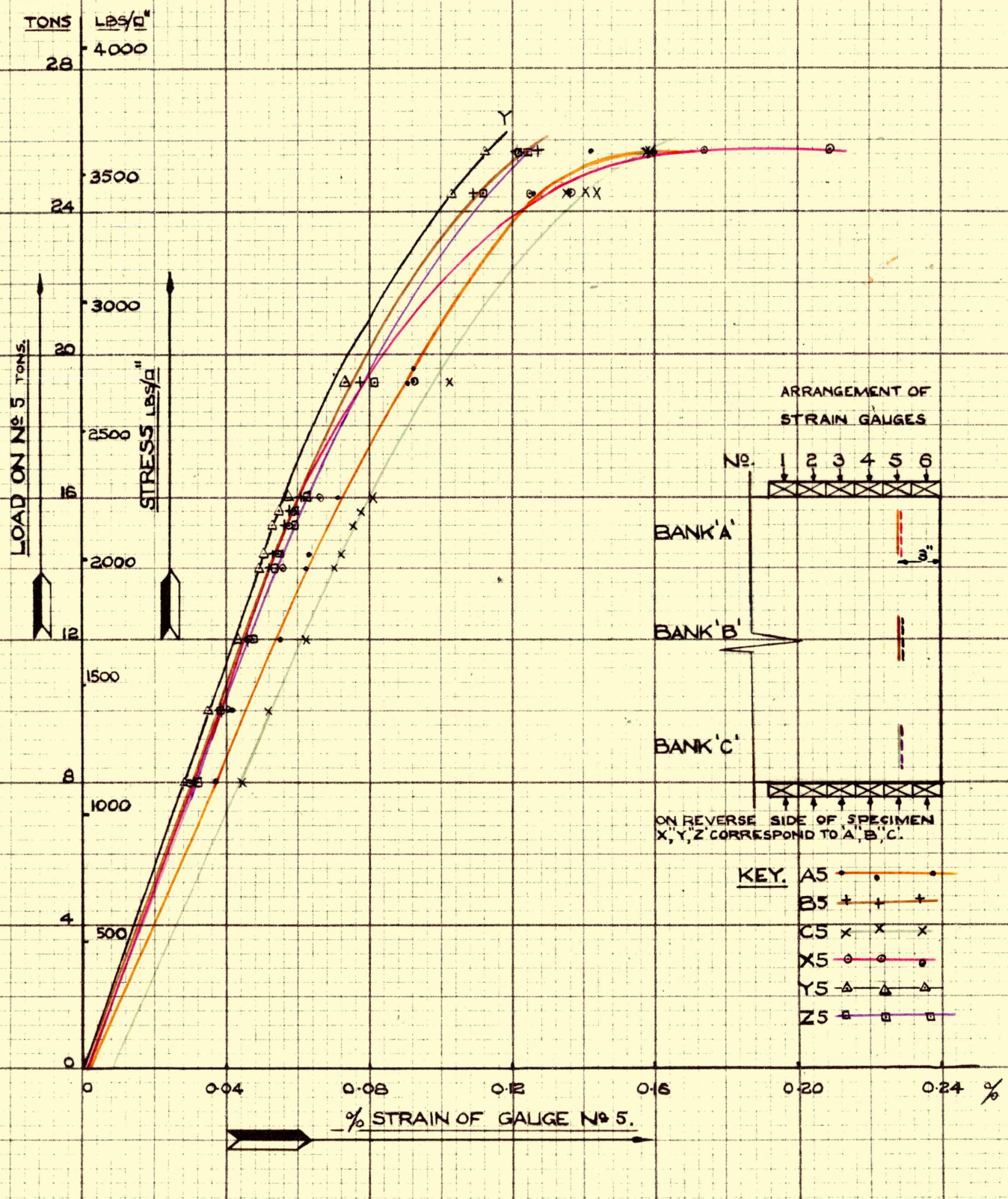
ON REVERSE SIDE OF SPECIMEN
'X','Y','Z' CORRESPOND TO 'A','B','C'.

KEY

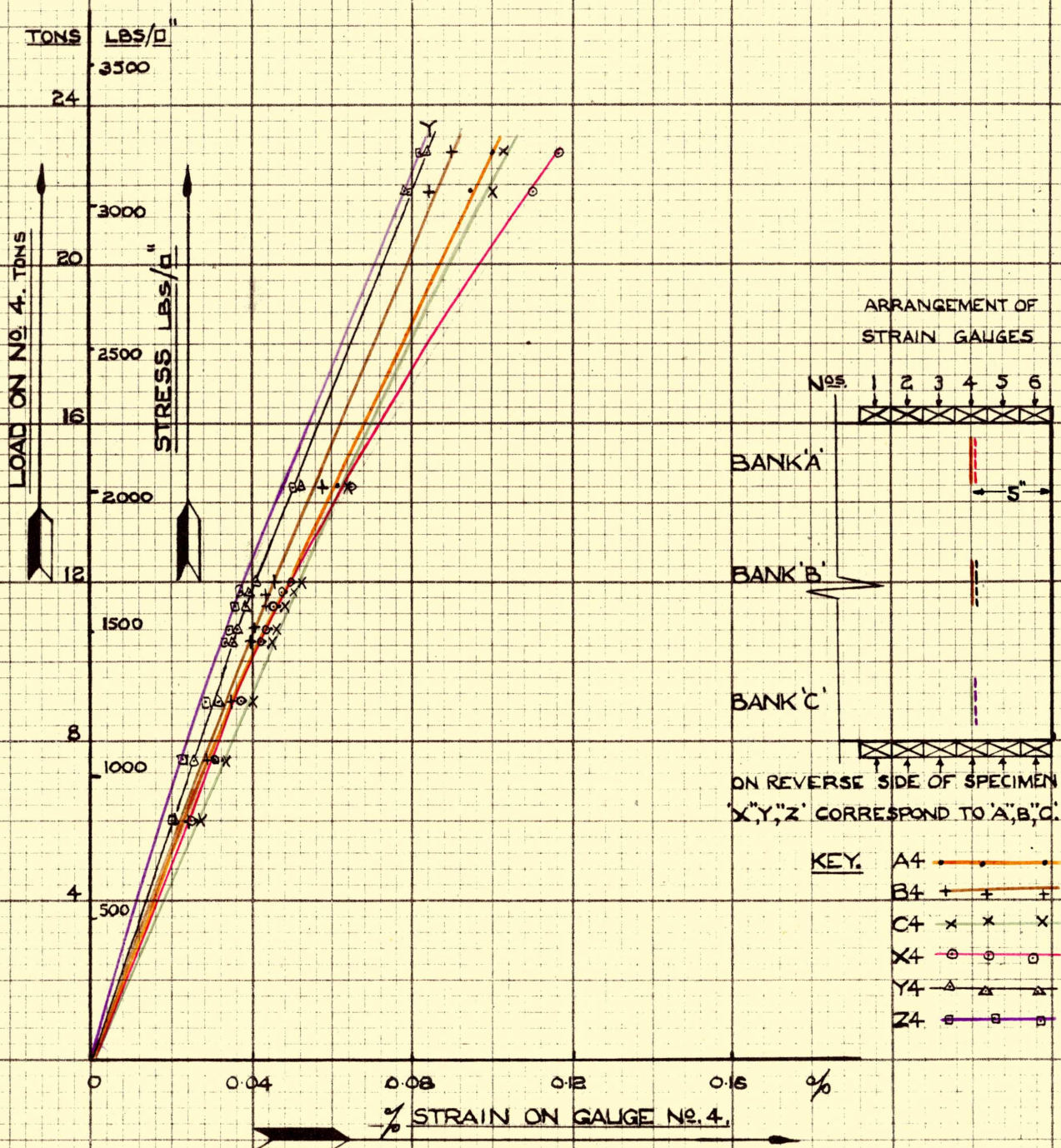
STRESS/STRAIN CURVES FOR GAUGE No. 6.
1ST. SPECIMEN. FINAL POSITION IN MACHINE.



STRESS/STRAIN CURVES FOR GAUGE No. 5.
1ST. SPECIMEN FINAL POSITION IN MACHINE.



STRESS/STRAIN CURVES FOR GAUGE No. 4.
1ST. SPECIMEN. FINAL POSITION IN MACHINE.

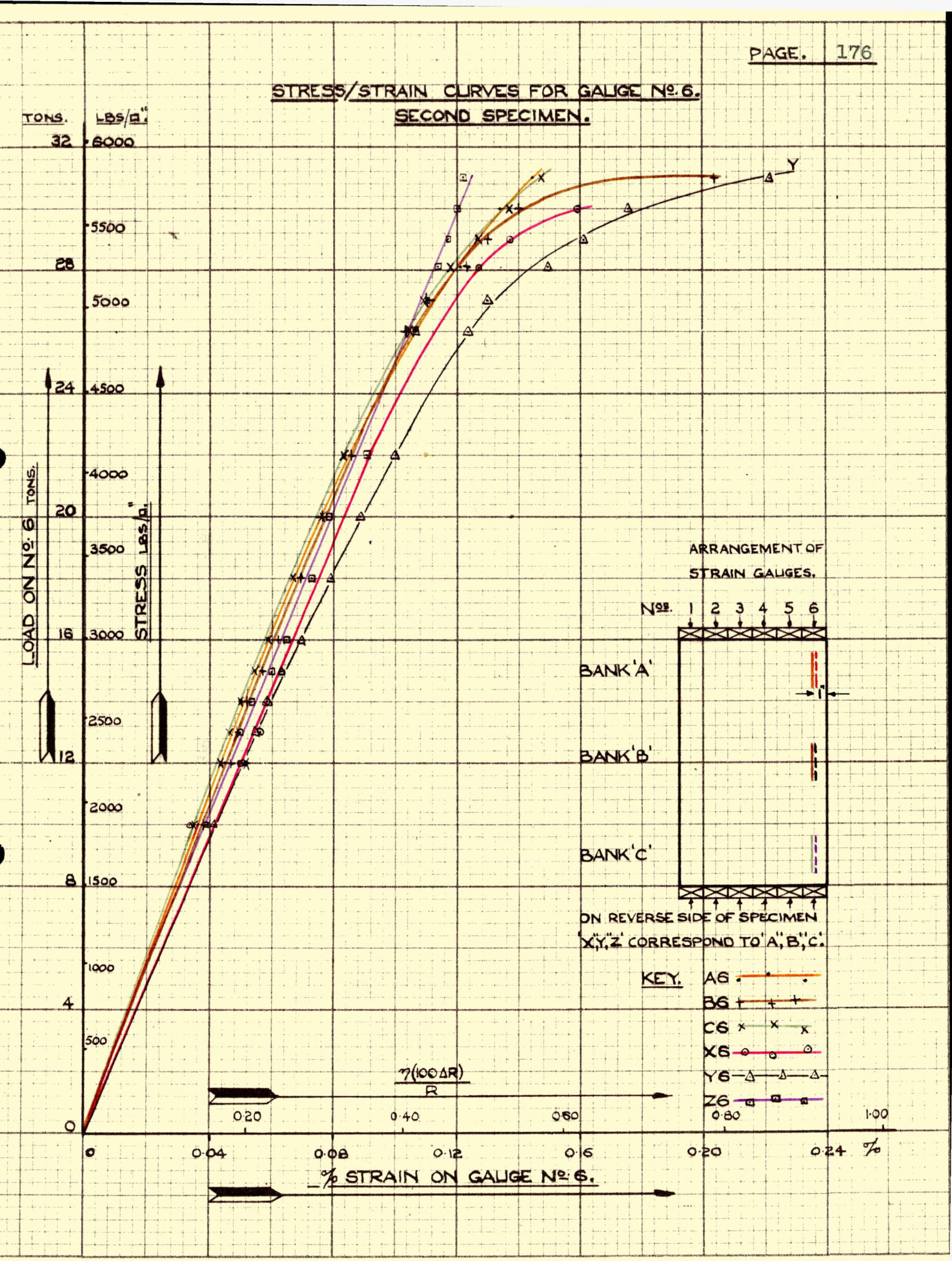


ARRANGEMENT OF STRAIN GAUGES

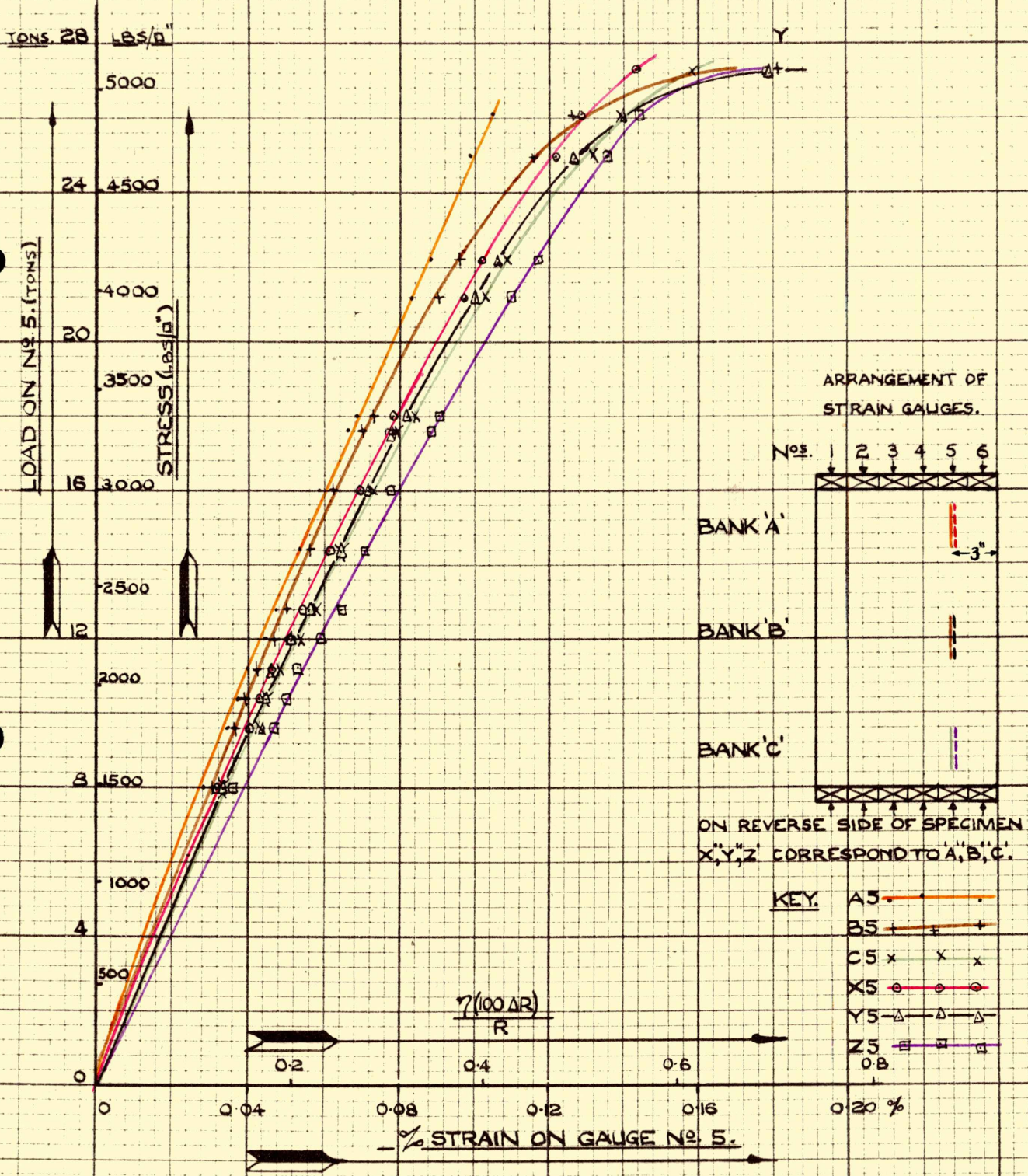
ON REVERSE SIDE OF SPECIMEN 'X','Y','Z' CORRESPOND TO 'A','B','C'.

KEY.

STRESS/STRAIN CURVES FOR GAUGE No. 6.
SECOND SPECIMEN.



STRESS/STRAIN CURVES FOR GAUGE No. 5.
SECOND SPECIMEN.

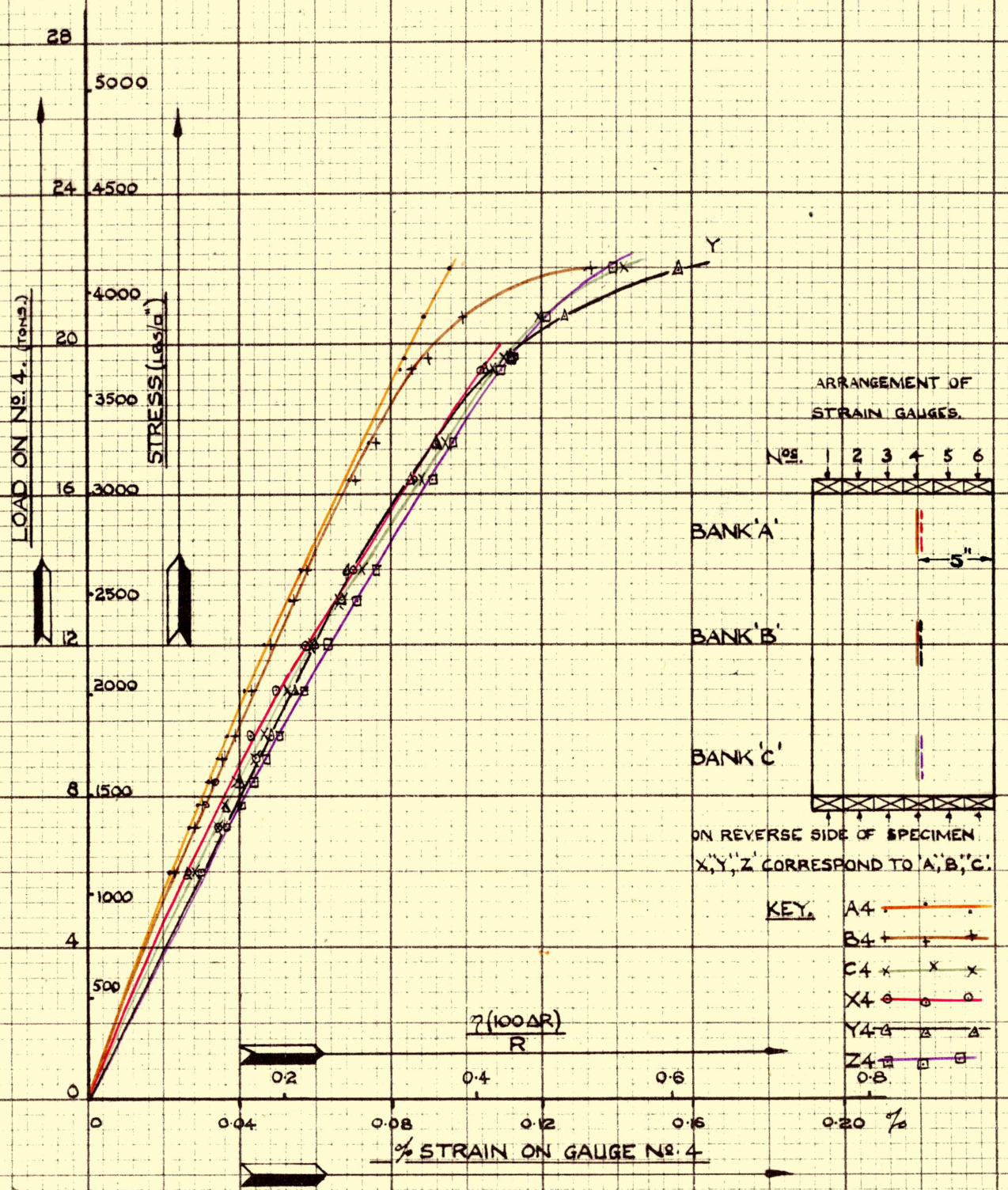


ARRANGEMENT OF STRAIN GAUGES.

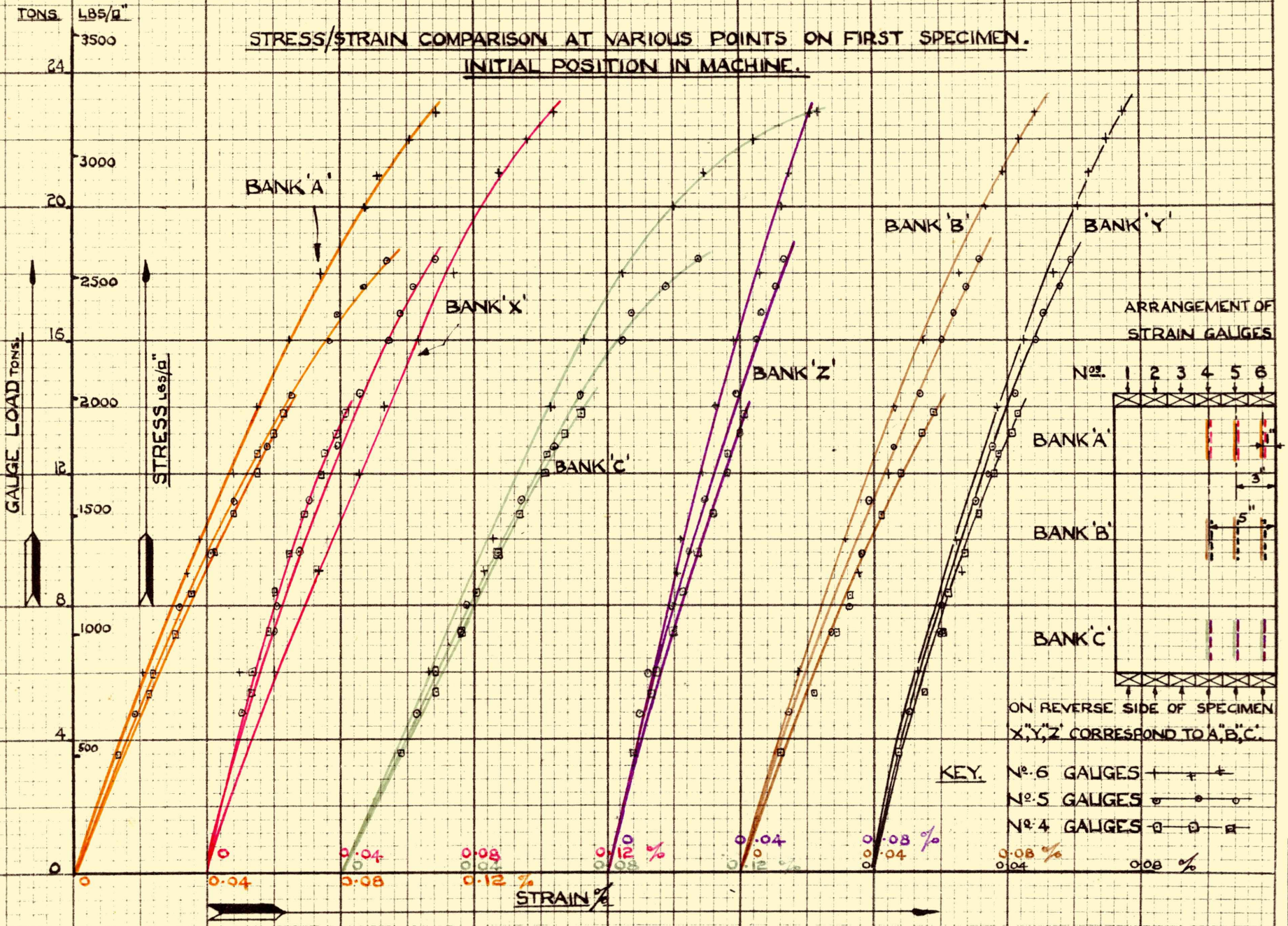
ON REVERSE SIDE OF SPECIMEN
X', Y', Z' CORRESPOND TO 'A', 'B', 'C'.

KEY.

STRESS/STRAIN CURVES FOR GAUGE No. 4.
SECOND SPECIMEN.

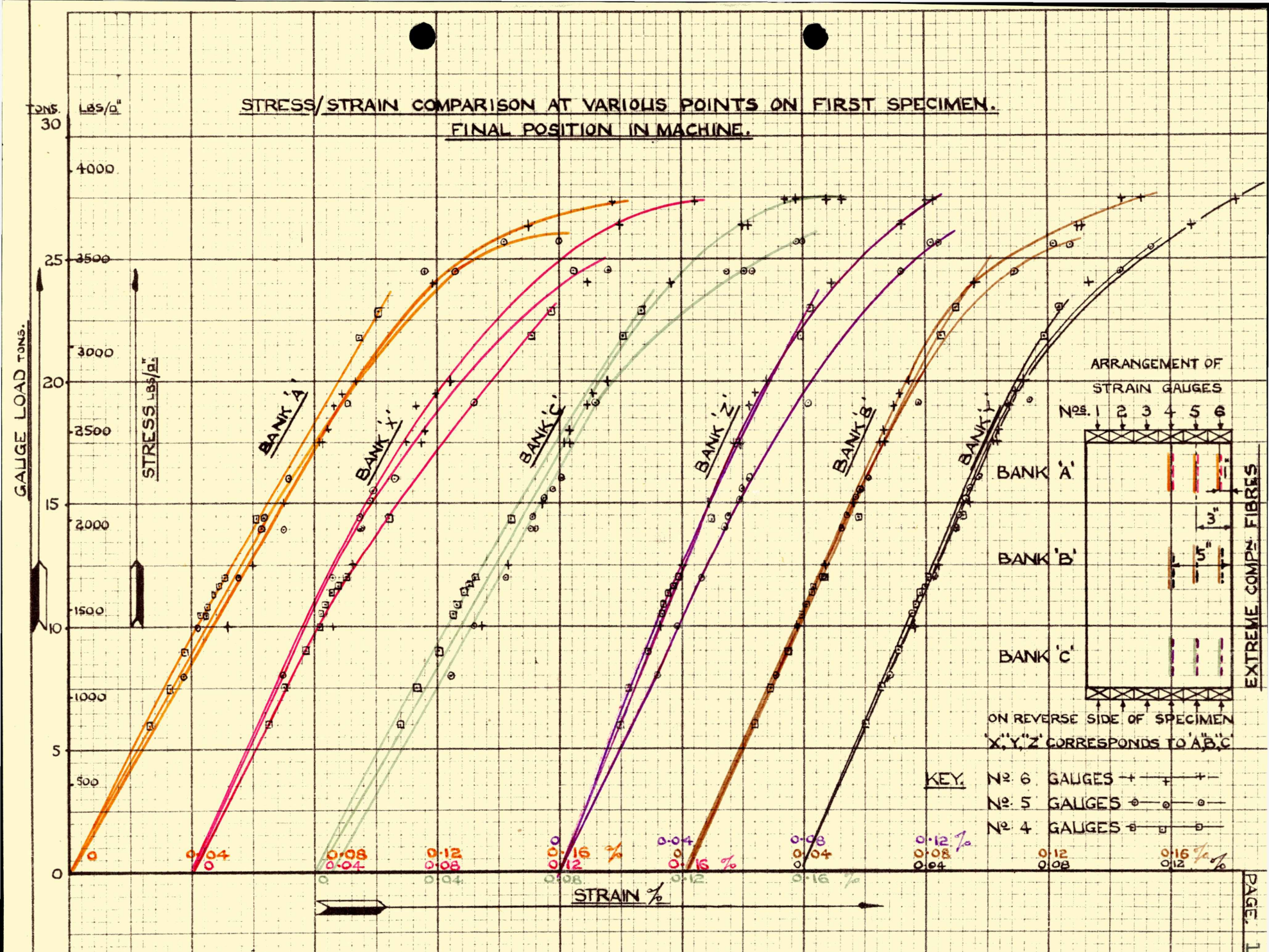


STRESS/STRAIN COMPARISON AT VARIOUS POINTS ON FIRST SPECIMEN.
INITIAL POSITION IN MACHINE.

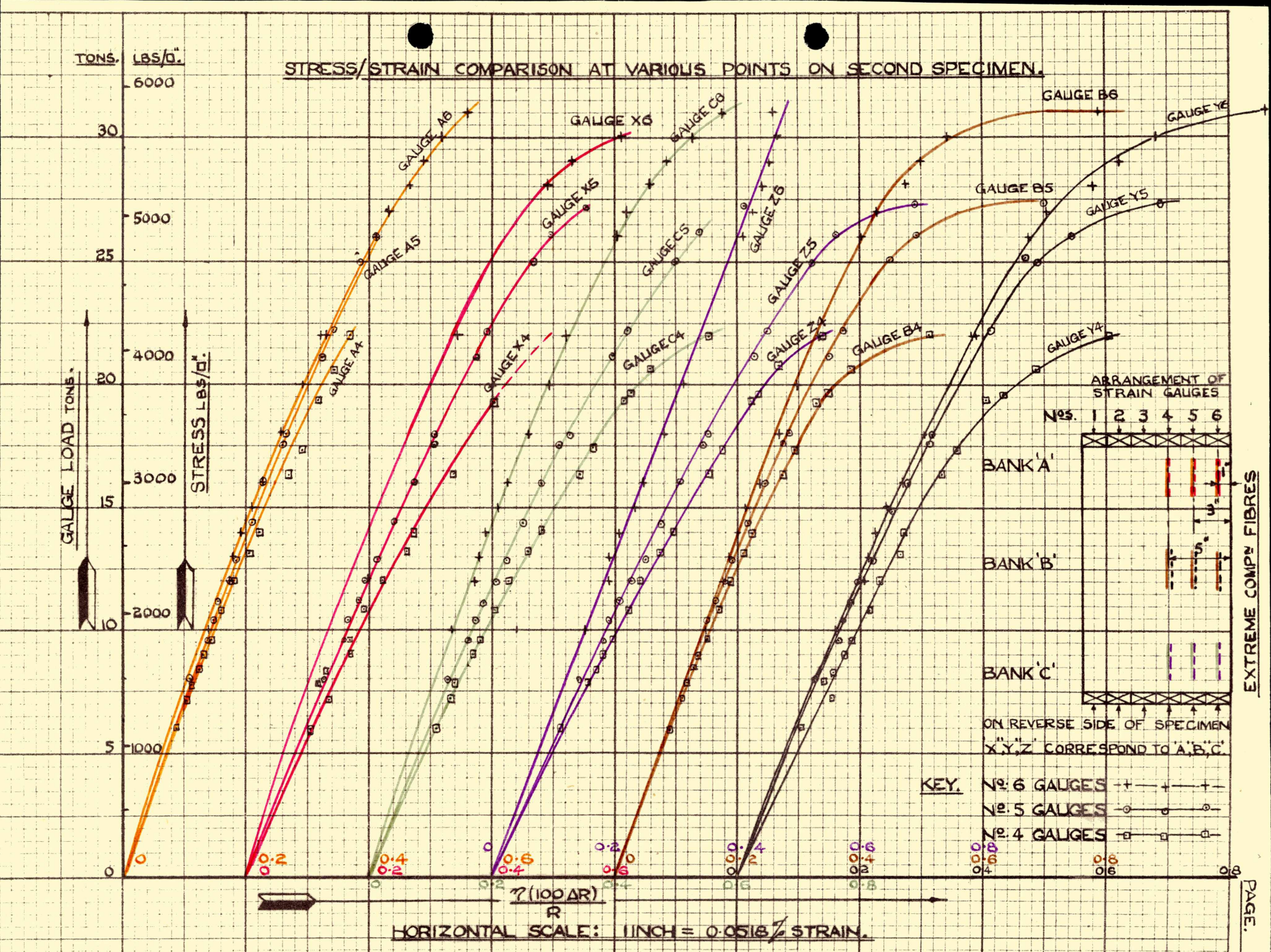


EXTREME COMP^N FIBRES

STRESS/STRAIN COMPARISON AT VARIOUS POINTS ON FIRST SPECIMEN.
FINAL POSITION IN MACHINE.



STRESS/STRAIN COMPARISON AT VARIOUS POINTS ON SECOND SPECIMEN.



Secondly, comparisons of gauge recordings belonging to the same gauge bank, but situated at different distances from the extreme compression fibres, see p.179 to 181 , have been plotted. With the exception of those results obtained in the second specimen about which, as is explained later, the author had justifiable misgivings, the curves traced out by the graphs, particularly during the test on the first specimen in its final and most reliable position in the machine, seem again to follow the same line as one another.

The general form traced out by the graphs which refer to the first specimen are similar to one another and to the stress-distribution at failure of the first specimen. This fact indicates therefore that, provided the true stress-distribution corresponding to that in a beam (as indicated by the method of 'gauge factors') is being maintained during successive stages of loading throughout testing, the stress-strain relationship is the same for all points in the specimen whatever their position or record.

((N.B. This is assumed by J.M.Prentis[12] in his analysis of the stress-distribution in beams subjected to pure bending moment. ...'it is assumed that a given strain may be identified with a specific stress irrespective of the position and history of the element considered.' Data is obtained from test results on an end-anchored prestressed concrete beam tested in the Concrete Technology Department of the Imperial

College, London, on behalf of the D.S.I.R. and under the supervision of Professor A.L.L.Baker. The analysis by Mr. Prentis gives a stress-strain curve which is very similar to the form -cubic parabola- found by the author using bending simulation. The concrete crushing strengths are similar in both cases.))

---//---

Discussions Arising from Test on Second Specimen.

1): Tensioning.

The tensioning frame was not employed during the testing of the second specimen for the following reasons:-

(i). The tensioning device was unable to produce a uniform force, even approaching the magnitude of the total compression force at failure, along the length of the beam element.

(ii). Even when (at low loads) the tension force was of the same order of magnitude as the total compressive force, it had little or no effect upon the strain in the compressive fibres.

(iii). The function of the tension steel in a beam subjected to a pure bending moment is to provide, by virtue of its anchorage in the end portions of the beam, an equal and opposite force to the compressive force in the concrete which together constitute a resisting moment.

In the case of the bending simulation specimen,

the equal and opposite force to the compressive force, in (iii), is produced by the reactions set up in the columns of the bending simulation machine itself, and the only useful purpose which might be served by the tension steel in bending simulation is to assist in the location of the neutral axis. To do this with any degree of accuracy tension must equal compression, and there should be no slip in the concrete linear strain-distribution being maintained across the tensile zone, as well as the compressive zone, of the beam element.

Since tension could not nearly be brought equal to compression, and since slipping was observed even at the comparatively small level of tension force which it was possible to apply, tensioning was omitted in the test on the second specimen. The absence of tensioning will not effect the distribution of strain, or therefore of stress, in the compressive fibres (as indicated in (ii)), but will result in the neutral axis depth being dependent upon the gradient of the stress-distribution applied by the operator, and not upon the linear nature of the strain-distribution right across the width of the specimen. N.B. The author is of the opinion that bending simulation tests are best adapted to the investigations of the constants α , γ , E'_c and C' ; and that the variations in $n_1 d$, the depth of the neutral axis, is best left to beam tests.

2): Type of Failure.

The second specimen failed at the

central, and weaker, portion of the beam element. As mentioned in Chapter XII, no method of correlating the straining at the central portion of the beam element with the stress-distribution at the load poins was available, because, as shown by previous experiment, sensibly linear strain-distributior was produced at the central section of the beam element for any distribution of stress at the load points. This renders the stress measurements recorded on the second specimen highly questionable, for the applied stress-distributions unavoidably lagged behind the true state of affairs occurring at the section most advanced in plasticity.

Saint-Venant's Principle the strains which are produced in a body by the application to a small part of its surface of a system of forces statically equivalent to zero force and zero couple are of negligible magnitude at distances which are large compared with the linear dimensions of the part. The author is of the opinion that this Principle and the following restatement by Professor R.V.Southwell[13] of Saint-Venant's Principle, though referring to elastic materials, gives an indication of the reasons why, in the test on the second specimen, true stress assesment was rendered impossible.

' Forces applied at one part of an elastic structure will induce stresses which except in a region close to that part, will depend almost entirely upon their resultant action, and very little upon their distribution. ' Professor R.V.Southwell

gives this interesting proof of this theorem:-

' Let us consider the case of a long girder, or braced framework, which is loaded at its two ends by forces applied in any given way; and let us employ the symbol A to denote those regions which immediately adjoin the parts at which the forces are applied, and the symbol B for the remainder. The conditions of equilibrium require merely that the resultant action transmitted by B shall have a definite value; but the conditions of continuity (or of compatibility of strains) will not be satisfied unless the total increase of the strain energy stored in A and B has its minimum value. Evidently, then, the equilibrium configuration may be regarded as in the nature of a compromise between the requirements of A and B . To reduce to a minimum the strain energy stored in A, the reactions between A and B would require to distribute themselves in a manner which will depend upon the distribution of the forces applied to A; the requirements of B, on the other hand, will not vary, since there must be some definite distribution of stresses, in an otherwise unloaded body, which will entail the minimum storage of strain energy in transmitting a given resultant action. Thus, in the process of adjustment which results in the actual distribution corresponding to equilibrium, we may picture a contest between the unloaded portions, which strive always after 'standardisation' and the loaded portions, which demand a particular solution for every specified distribution

of the forces acting on them. As we pass from the regions of application of load through successive sections of the unloaded portion B, there will be a steady tendency for the claims of standardisation to prevail. The theorem stated (on the previous page) is an immediate deduction, and we may work back from this, by the principle of superposition, to Saint-Venant's Principle. '

To revert to the bending simulation specimen. The molecules of a body, such as the bending simulation specimen, or indeed of all bodies and alll structures composed of bodies connected in any way whatever, can be regarded as framed structures and will therefore posses the same properties as the particular examples of a 'long girder, or braced framework' selected by Professor R.V.Southwell in his theorem proof. Symbol A, in the proof, corresponds to the end sections of the bending simulation specimen at which loads are applied, whilst Symbol B corresponds to the central section of the bending simulation specimen at which failure occurred.

That the above principles apply both to the plastic as well as to the elastic stage of testing by bending simulation, is comfirmed by the experiences gained by the test on the second specimen. The author therefore concludes that future testing by bending simulation should be carried out with specimens whose lengths are reduced as much as possible.

A reduction in the length of the specimen would have the advantage of increasing the ability of the recorded strain-distributions to indicate the adjustments required to be made to bring the applied stress-distribution into the shape existing in a beam.

In the second specimen test (p.181.) it seems very likely therefore that had a shorter specimen been used, the stresses on the outer (No.6) gauges would have been reduced relative to gauges further towards the neutral axis (e.g. No.4) at an earlier stage of loading than was in fact the case, - and conversely the stresses raised under gauges Nos. 4 and 5 -, without causing a reduction in the gradient of the strain distribution across the specimen. This would have resulted in the stress-strain relationships at various points on the specimen following the same form as one another, as occurred in the first specimen test.

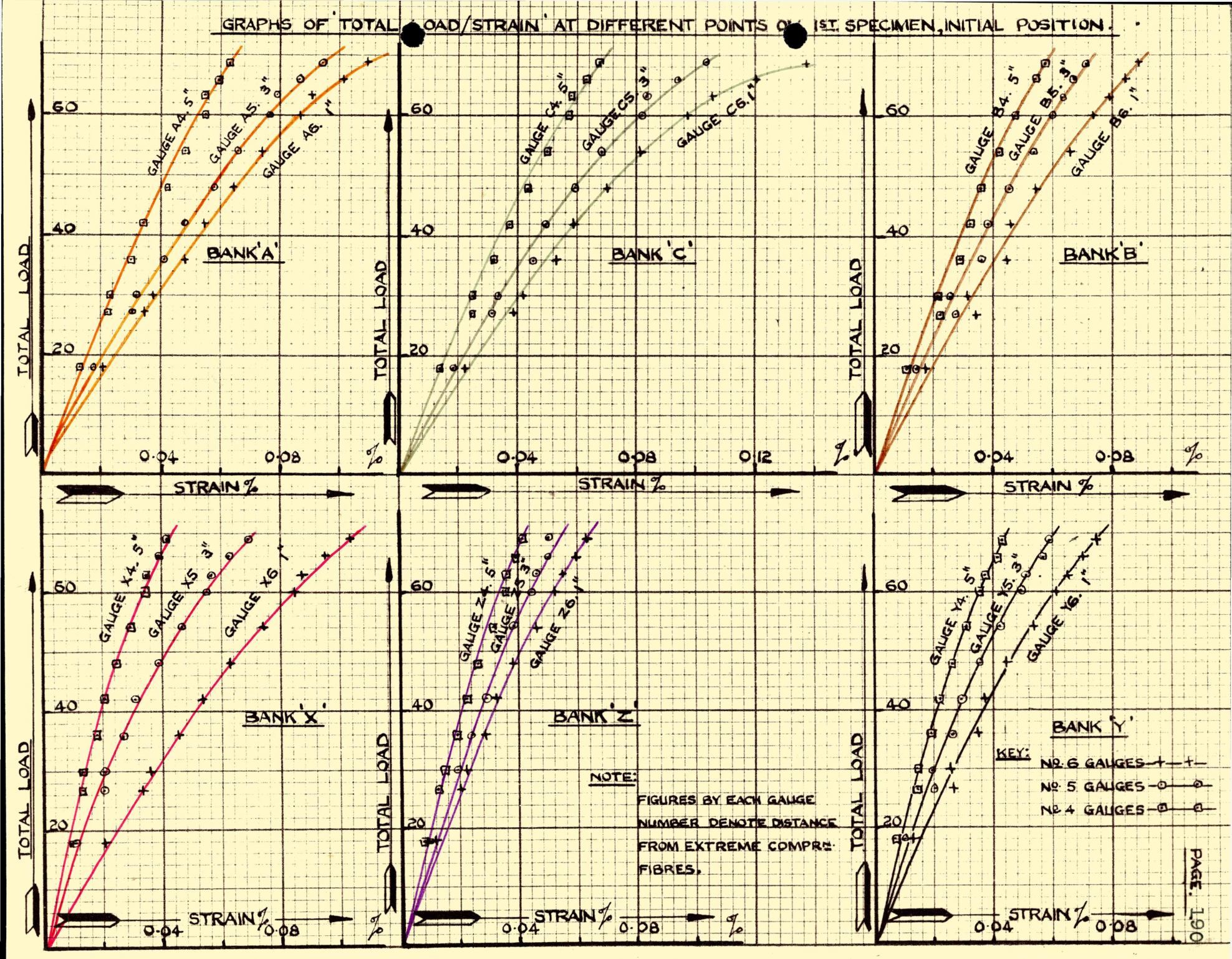
---//---

Total Load against Strain at Different Fibre Depths.

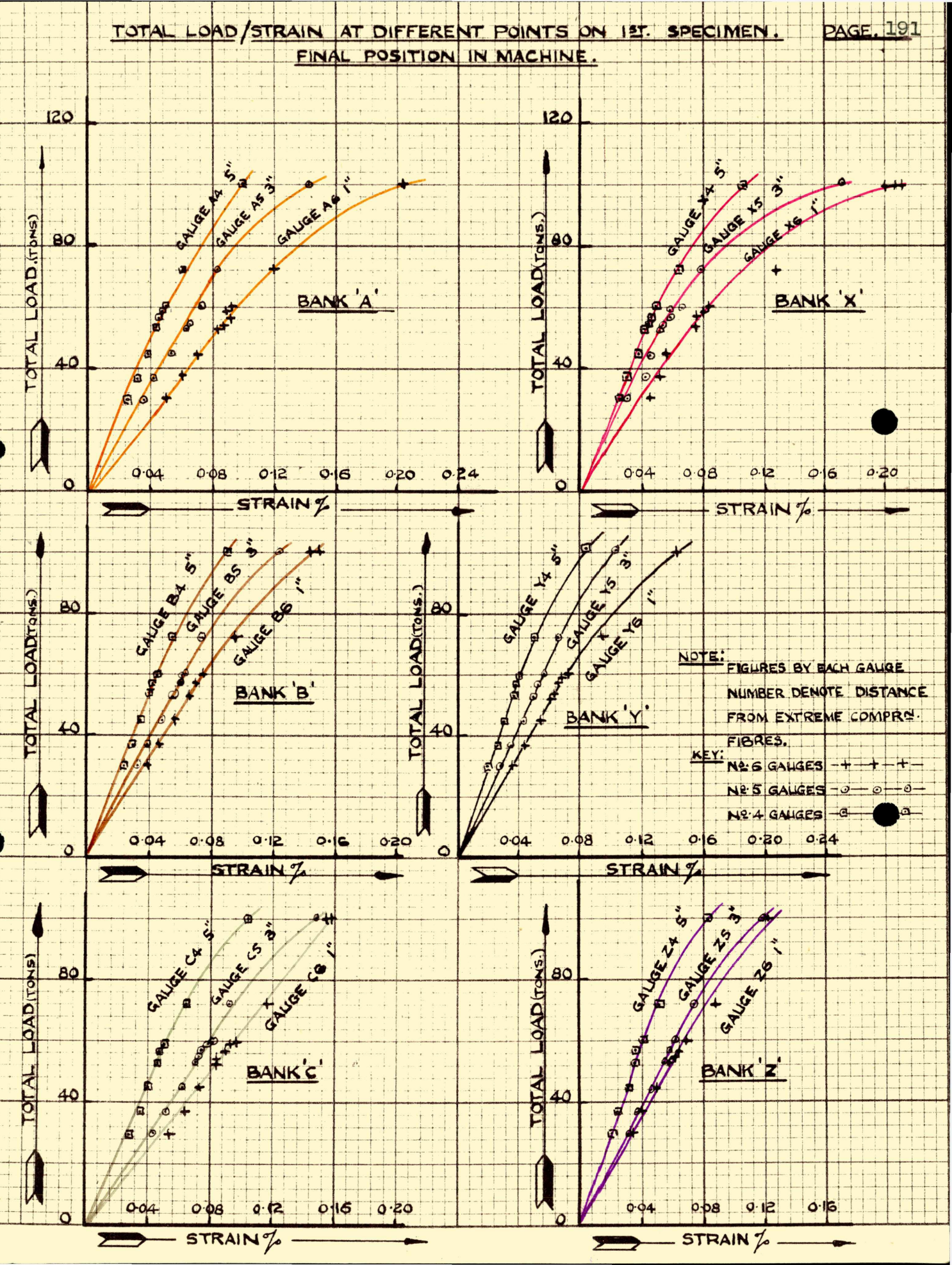
Graphs have been plotted, p.190 to 194 of the total load on the beam element against the strain at different points between the neutral axis and the extreme compression fibres. These results are analagous to curves in beam tests relating load to the corresponding strain at points on the face of the beam at various distances from the extreme compression fibres, or top edge of the beam.

Such graphs from beam tests are given by Professor R.H.Evans in his Paper[10] on the plastic theories for ultimate strength of reinforced concrete beams. Comparison of the results from the bending simulation specimens with those representing a beam failing in compression, i.e. 'Beam No. 14, Compression Failure', shown by Professor R.H.Evans, give good agreement when the scales of the graphs, the dimensions of the beams and the relative positions at which strains are shown, are taken into account.

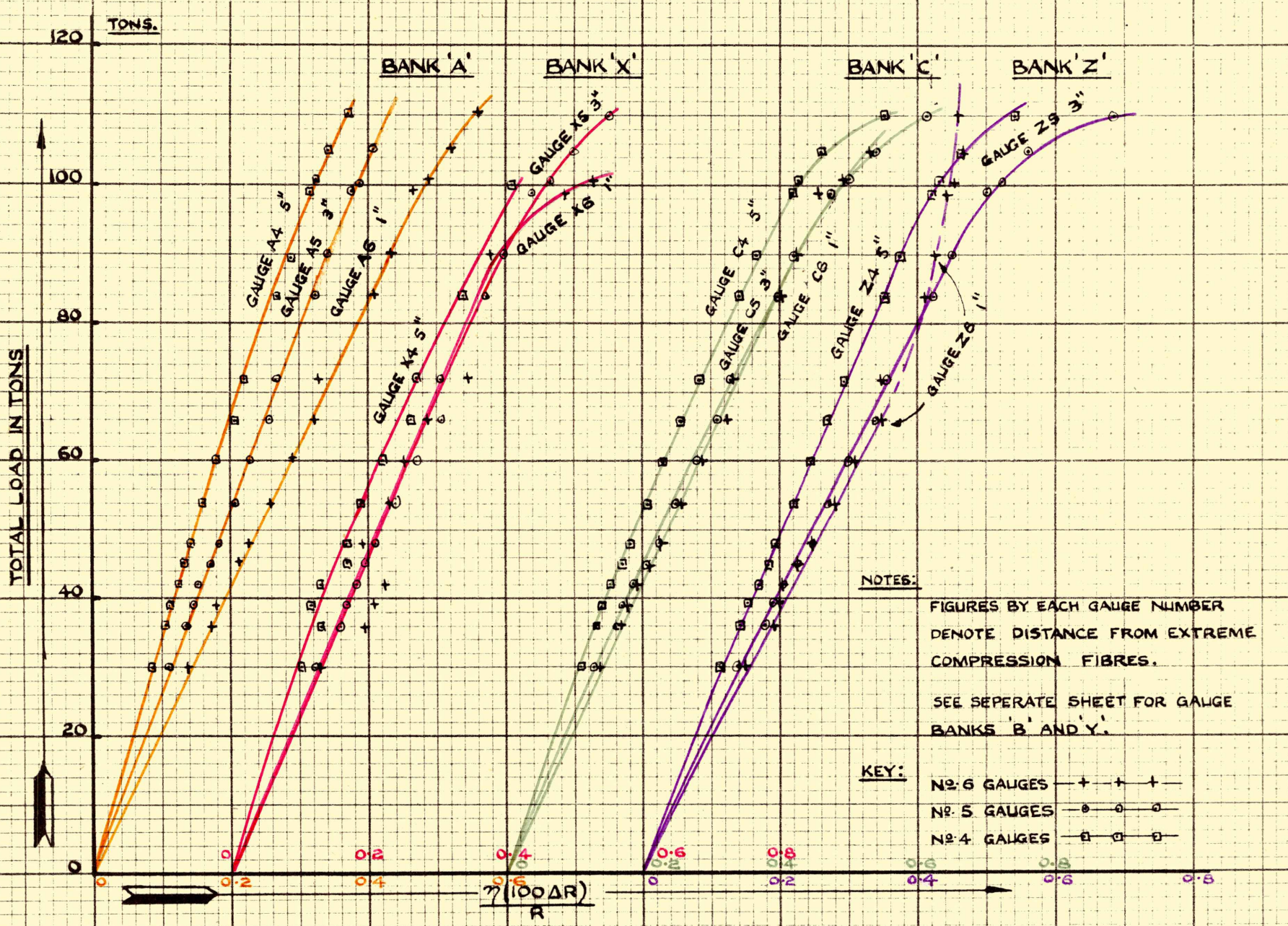
This evidence is brought forward to supplement strain-distribution comparisons, which have already been made, to indicate that, in so far as strict comparisons with beam tests can be made, the bending simulation tests do copy, faithfully, those conditions of straining which exist in beams.


GRAPHS OF 'TOTAL LOAD/STRAIN' AT DIFFERENT POINTS ON 1ST. SPECIMEN, INITIAL POSITION.
TOTAL LOAD
STRAIN %
BANK 'A'
GAUGE A4. 5"
GAUGE A5. 3"
GAUGE A6. 1"
BANK 'C'
GAUGE C4. 5"
GAUGE C5. 3"
GAUGE C6. 1"
BANK 'B'
GAUGE B4. 5"
GAUGE B5. 3"
GAUGE B6. 1"
BANK 'X'
GAUGE X4. 5"
GAUGE X5. 3"
GAUGE X6. 1"
BANK 'Z'
GAUGE Z4. 5"
GAUGE Z5. 3"
GAUGE Z6. 1"
BANK 'Y'
GAUGE Y4. 5"
GAUGE Y5. 3"
GAUGE Y6. 1"
KEY:
No. 6 GAUGES
No. 5 GAUGES
No. 4 GAUGES
NOTE:
FIGURES BY EACH GAUGE NUMBER DENOTE DISTANCE FROM EXTREME COMPRN. FIBRES.
PAGE. 190

TOTAL LOAD/STRAIN AT DIFFERENT POINTS ON 1ST. SPECIMEN. FINAL POSITION IN MACHINE.



TOTAL LOAD/STRAIN AT POINTS IN END SECTIONS OF SECOND SPECIMEN.



NOTES:

FIGURES BY EACH GAUGE NUMBER DENOTE DISTANCE FROM EXTREME COMPRESSION FIBRES.

SEE SEPERATE SHEET FOR GAUGE BANKS 'B' AND 'Y'.

KEY:

No. 6 GAUGES

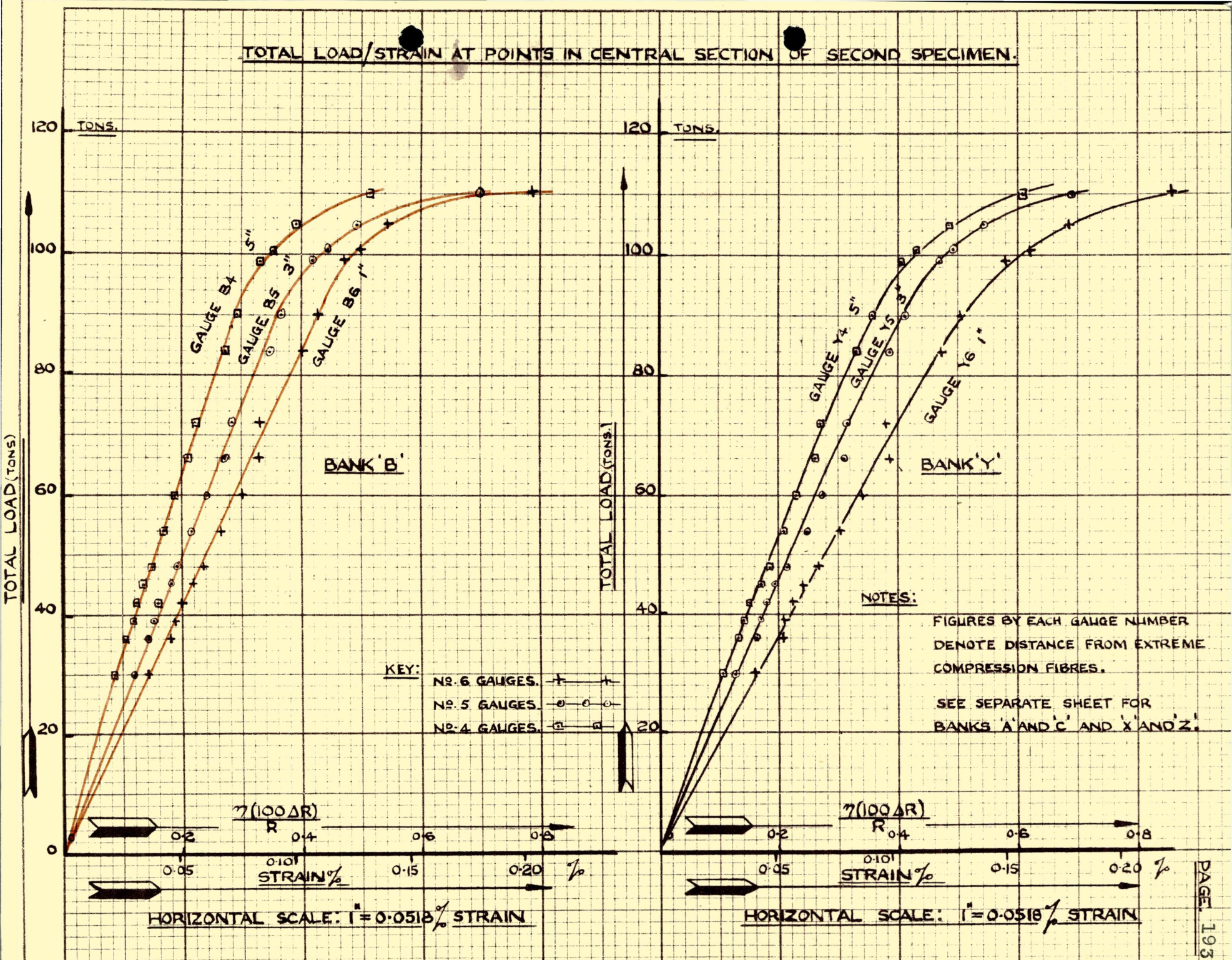
No. 5 GAUGES

No. 4 GAUGES

HORIZONTAL SCALE: 1 INCH = 0·0518% STRAIN.

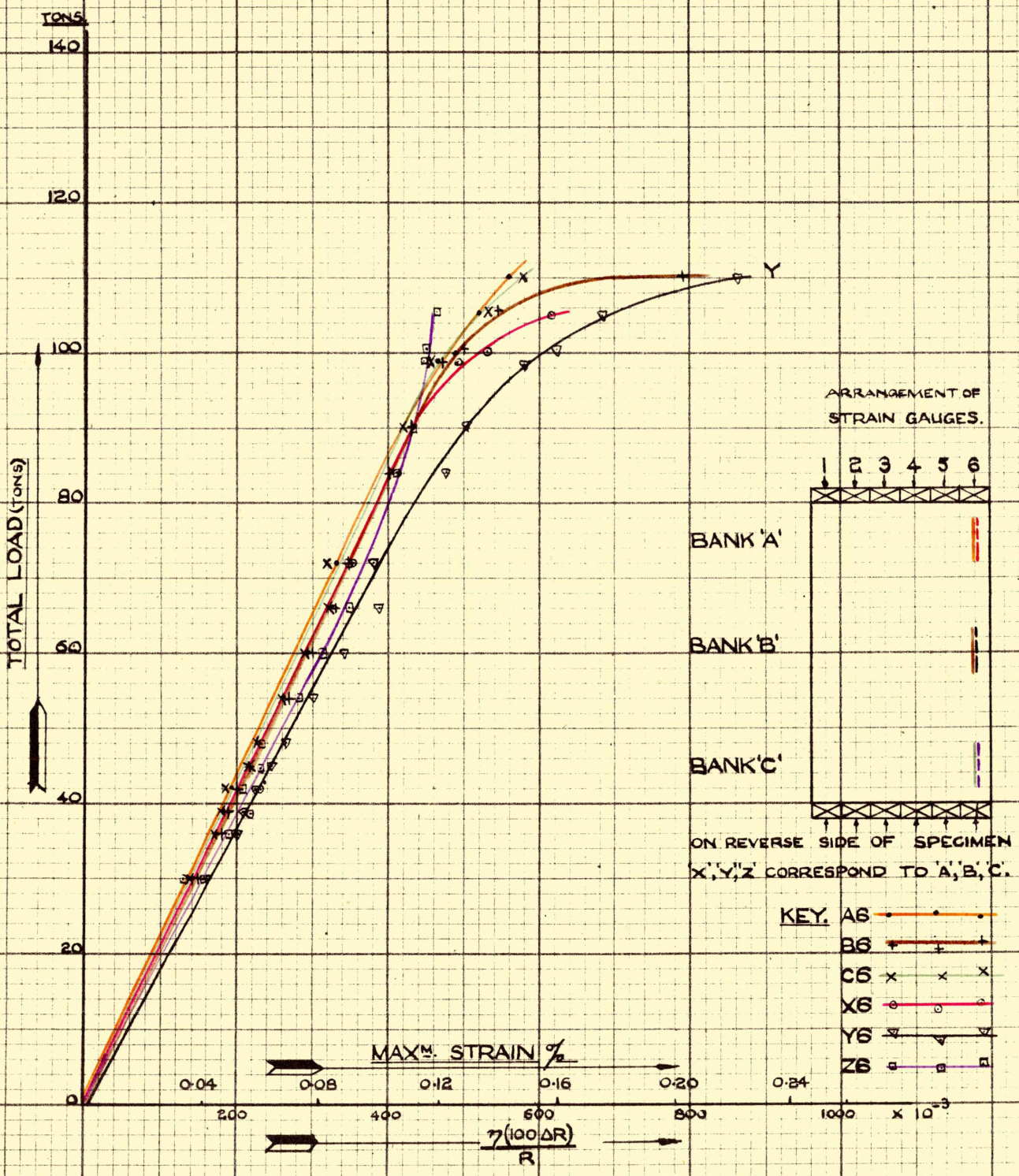
PAGE. 192

TOTAL LOAD/STRAIN AT POINTS IN CENTRAL SECTION OF SECOND SPECIMEN.



PAGE 193

TOTAL LOAD/MAXm. STRAIN CURVES FOR 2nd SPECIMEN.



Brief Summary of Conclusions.

(i) Bending simulation can be used to subject a concrete specimen which is similar to an elemental length of a beam to the same conditions of straining as are present, without question, in the compressive fibres of a beam.

(ii) Measurement of the applied stress-distribution corresponding to the condition in (i) can be made. Use of the following fundamental principle will best enable this to be achieved.

(iii) At all stages of loading, the true strain-distribution on any given gauge bank, which should be aimed at and attained before any corresponding stress-distribution be accepted as representative of beam conditions, is that strain-distribution which follows, exactly, the shape of the strain-distribution existing under linear stress-distribution in the elastic range.

(iv) "Gauge factors" enable the "corrected" strain diagrams to be drawn out and compared. The "corrected" strain diagrams provide a reliable means of selecting with precision those stress-distributions which fulfil the conditions and principles required, and which correspond, therefore, to the stress-distributions present in a beam.

(v) The best type of strain gauge for use with bending simulation specimens is the electrical resistance strain gauge.

(vi). A basic technique for testing by bending simulation has been developed using the foregoing principles. Results obtained using this technique show, on analysis, that for the particular cases tested:-

(a) The stress-distribution corresponding to that in a beam is almost exactly a cubic parabola.

(b) The stress-strain curves at varying distances from the neutral axis are similar to one another. During increasing load they gradually trace out the same shape as the stress-strain relationship at failure, i.e. a given strain may be identified with a specific stress irrespective of the position and history of the element considered.

Conclusions which will be of particular interest to future experimenters in this field are:-

(vii). A reduction in the length of the specimen subjected to test will increase the ability of the recorded strain-distributions to indicate the adjustments required to be made to bring the applied stress-distribution into the shape existing in a beam.

(viii). A steel mould for casting the specimens is absolutely necessary if accurate results are required.

(ix). The specimen should be centred with great care in the machine, and the heavy top-plate should be positioned to lie in the same plane as the base-plate of the machine.

Further Research.

The technique of testing by bending simulation which the author has developed in this work has enabled factors required in plastic theories of design in reinforced concrete to be evaluated for the particular cases tested only. Before any generalisations can be made, many tests are required. It is hoped that future experimenters will, therefore, be encouraged to take advantage of this new and interesting method of testing, and to carry out tests over a wide variety of conditions. Concrete strength and rate of loading appear to be variables worthy of early consideration. Limiting values of these design factors would then become available and so give strong support to those methods of design which are based upon plastic theories and ultimate load.

Author's Note.

All results given in this thesis, unless marked otherwise, have been obtained from the individual researches and experiments carried out by the author. Any results obtained from other sources, and reproduced here as evidence to corroborate ideas, have been clearly marked with the name of their origin.

BIBLIOGRAPHY

1. C.S. Whitney

(a) "Application of Plastic Theory for Reinforced Concrete Design." Journal of the American Society of Civil Engineers. Vol. 66, p.1749.

(b) "Application of Plastic Theory to the Design of Modern Reinforced Concrete Structures." Journal of the Boston Society of Civil Engineers. January, 1948.

2. K. Haynal-Konyi

"The Modular Ratio. A new Method of Design Omitting m." Concrete and Constructional Engineering, 1937, No. 32.

3. K.C. Cox

"Test of Reinforced Concrete Beams with Recommendations for Attaining Balanced Design." Journal of the American Concrete Institute. 1941. 38, 65.

4. L.J. Mensch

Journal of the American Concrete Institute. 1914. 10, 28.

5. H. Kempton-Dyson

"What is the Use of the Modular Ratio?" Concrete and Constructional Engineering. 1922, pp. 330, 408, 486.

6. Professor V.P. Jensen

"The Plasticity Ratio of Concrete and its Effect on the Ultimate Strength of Beams." Journal of the American Concrete Institute. 1943, 14, 6, 565.

7. H.D. Stead

"A Study of Plastic Theories for the Ultimate Strength of Reinforced Concrete Beams in Bending." M.Sc. Thesis. London University, 1949.

8. Professor A.L.L. Baker — "Recent Research in Reinforced Concrete, and its Application to Dsign." Journal of the Institute of Civil Engineers. No. 4, 1951, p. 262.

9. R.D. Binns and H.S. Mygind — "The Use of Electrical Resistance Strain Gauges, and the Effect of Aggregate Size on Gauge Length in Connection with the Testing of Concrete." Magazine of Concrete Research. No. 1. 1949.

10. P.B. Morice — "The C.A.C.A. Structures Laboratory." Magazine of Concrete Research. No. 6, 1951.

11. J.M. Prentis — "The Distribution of Concrete Stress in Reinforced and Prestressed Concrete Beams when Tested to Destruction by a Pure Bending Moment." Magazine of Concrete Research No. 5. 1951.

12. Professor R.V.Southwell — "Castigliano's Theorem of Least Work and the Principle of Saint-Venent." Philosophical Magazine. Vol. XLV, January 1923, p. 193.

13. V.S.M. Ziauddin — "Ultimate Strength of Prestressed Concrete Beams with Reference to the Plastic Theory." M.Sc.(Eng.) Thesis, London University, 1950.

10. Professor R.H.Evans. — 'The Plastic Theories for the Ultimate Strength of R.C.Beams.' Journal of the Inst. of C.Engs. No.2. Dec. 1943.

APPENDIX I.

SENSITIVITY FACTORS OF ELECTRICAL RESISTANCE STRAIN GAUGES.

COMPRESSION.

	1st. Load Application		2nd. Load Application	
	Increasing	Decreasing	Increasing	Decreasing
% Strain at which 'λ' changes GAUGE No.1.	0·14% 1·83 1·71	0·13% 1·93 1·86	0·13% 1·95 1·89	0·11% 1·98 1·89
% Strain at which 'λ' changes GAUGE No.2.	0·13% 1·97 1·81	0·11% 2·03 1·92	0·11% 2·04 1·99	0·11% 2·10 1·95
% Strain at which 'λ' changes GAUGE No.3.	- 1·85 -	0·13% 1·90 1·80	0·13% 1·89 1·86	0·11% 1·97 1·81
% Strain at which 'λ' changes Gauge No.4.	- 1·90 -	0·11% 2·02 1·91	0·14% 2·01 1·96	0·13% 2·08 1·96

TENSION.

	1st. Load Application		2nd. Load Application	
	Increasing	Decreasing	Increasing	Decreasing
% Strain at which 'λ' changes GAUGE No.1.	- 1·85	0·11% 1·99 1·87	0·09% 1·94 1·88	0·13% 1·99 1·88
% Strain at which 'λ' changes GAUGE No.2.	0·06% 1·99 1·92	0·11% 2·03 1·94	0·11% 1·97 1·94	0·09% 2·01 1·92
% Strain at which 'λ' changes GAUGE No.3.	- 1·71	0·09% 1·97 1·76	0·09% 1·86 1·80	0·09% 1·96 1·74
% Strain at which 'λ' changes GAUGE No.4.	0·11% 1·89 1·87	0·11% 2·04 1·91	- 1·96	0·09% 2·02 1·93

APPENDIX II.

Typical Result Sheet from Optical Gauge Tests.

GAUGE No.1.						GAUGE No.2.			
Load in TONS.	Fixed Mirror Reading	Correction $\times 10^{-2}$	Moveable Mirror Reading	Scale Reading ins.	Strain $\times 10^{-5}$	Fixed Mirror Reading	Correction $\times 10^{-2}$	Moveable Mirror Reading	Strain $\times 10^{-5}$
0·0	0·50	-	5·42	5·42	0·0	0·44	--	0·89	00·0
0·2	0·71	-21	5·30	5·09	4·8	0·68	24	1·46	5·0
0·4	0·73	-23	4·92	4·69	10·6	0·70	26	1·82	10·1
0·6	0·75	-23	4·53	4·30	16·3	0·71	27	2·11	15·8
0·8	0·72	-22	4·17	3·95	21·3	0·70	26	2·38	18·5
1·0	0·71	-21	3·79	3·58	26·7	0·70	26	2·63	22·3
1·4	0·70	-20	3·11	2·91	36·4	0·69	25	3·21	31·1
1·8	0·68	-18	2·47	2·29	45·4	0·69	25	3·80	40·0
2·2	0·67	-17	1·83	1·66	54·5	0·68	24	4·41	49·3
2·6	0·64	-14	1·21	1·06	63·2	0·68	24	5·00	58·1
2·4	0·65	-15	1·50	1·35	59·0	0·68	24	4·71	53·8
2·2	0·66	-16	1·81	1·65	54·6	0·68	24	4·42	49·5
2·0	0·66	-16	2·12	1·96	50·1	0·68	24	4·13	45·0
1·8	0·68	-18	2·43	2·25	45·9	0·68	24	3·84	40·7
1·4	0·70	-20	3·08	2·88	36·8	0·69	25	3·33	33·0
1·0	0·70	-20	3·69	3·49	28·0	0·70	26	2·74	23·9
0·6	0·71	-21	4·32	4·11	19·0	0·70	26	2·16	15·2
0·4	0·71	-21	4·64	4·43	14·4	0·70	26	1·87	10·8
0·2	0·71	-21	5·01	4·80	9·0	0·67	23	1·57	6·8
0·1	0·65	-15	5·25	5·10	4·6	0·62	18	1·40	4·9

APPENDIX III.

Pressure Gauge Calibration.

Example Sheet for Gauge No.4.

Pressure Gauge (TONS)	Proving Ring	Ring Load (TONS)	Pressure Gauge (TONS)	Proving Ring	Ring Load (TONS)	Pressure Gauge (TONS)	Proving Ring	Ring Load (TONS)
5·3	1045	5·69	5·25	1042	5·68	5·4	1024	5·59
10·1	1953	10·7	10·2	1981	10·8	10·1	1946	10·6
15·1	2929	15·9	15·0	2926	15·8	15·1	2918	15·8
20·0	3818	20·7	20·0	3810	20·7	20·0	3807	20·7
25·1	4686	25·5	25·0	4700	25·6	25·1	4695	25·6
30·2	5468	29·8	30·4	5509	30·0	30·4	5510	30·0
36·0	6325	34·6	35·5	6260	34·2	35·6	6292	34·4
40·0	6824	37·2	39·8	6862	37·5	39·0	6745	36·8
35·1	6273	34·2	35·1	6286	34·3	35·0	6317	34·5
30·0	5206	28·4	30·0	5250	28·7	30·0	5280	28·8
25·0	4234	23·0	25·0	4263	23·2	25·0	4299	23·4
20·0	3246	17·6	20·0	3264	17·7	20·0	3289	17·8
14·9	2340	12·7	14·9	2352	12·7	14·9	2375	12·8
10·0	1500	8·18	10·0	1508	8·22	10·0	1530	8·34
4·95	732	4·00	5·0	733	4·01	5·0	746	4·08

APPENDIX IV.

Table of Trial Run on Pressure Gauge No.2. Showing Comparison Between Estimated Load and Actual Load Given by Proving Ring.

Pressure Gauge (TONS)	Proving Ring Reading	Estimated Correction	Estimated Load (TONS)	True Load (TONS)
00-0	-	-	-	-
25·3	4507	-0·6	24·7	24·5
27·3	4904	-0·6	26·7	26·7
29.9	5380	-0·6	29·3	29·4
15·0	2650	-0·6	14·4	14·4
16·0	2725	-1·1	14·9	14·7
16·9	2842	-1·3	15·6	15·4
15·0	2658	-0·6	14·4	14·4
14·0	2443	-0·5	13·5	13·2
24·7	4358	-0·7	24·0	23·7
25·7	4554	-0·6	25·1	24·8
27·3	4881	-0·5	26·9	26·6
26·0	4792	+0·5	26·5	26·1
25·0	4629	+0·4	25·4	25·2
26·3	4700	-0·4	25·9	25·6
25·0	4627	+0·3	25·3	25·2
26·3	4692	-0·5	25·8	25·6
36·9	6814	+0·3	37·2	37·1
36·0	6713	+0·6	36·6	36·5
37·9	6834	-0·6	37·3	37·2
38·7	6977	-0·7	38·0	38·1
37·5	6943	+0·6	38·1	37·9
0·0	-	-	-	-

APPENDIX V.

Example Sheet.

CUT-OUT SETTING (TONS)	PRESSURE GAUGE INDICATOR READINGS.					
	GAUGE.1.	GAUGE.2.	GAUGE.3.	GAUGE.4.	GAUGE.5.	GAUGE.6.
5·0	6·0	4·8	5·5	5·8	5·2	6·1
	5·9	4·9	5·3	5·8	5·1	6·1
	6·0	4·9	5·2	5·7	5·0	6·1
	6·0	4·9	5·3	5·8	5·3	6·1
10·0	10·7	10·3	10·4	10·5	10·4	11·1
	11·1	10·1	10·4	10·5	10·4	11·2
	10·9	10·1	10·5	10·9	10·4	11·2
	11·0	10·3	10·6	10·7	10·6	11·2
15·0	15·6	15·5	15·7	15·7	16·0	16·0
	15·8	15·6	15·7	15·6	16·0	16·0
	15·7	15·8	15·6	15·9	15·7	16·3
	15·7	15·7	15·7	15·9	16·0	16·2
20·0	20·2	20·8	20·9	20·9	21·0	20·5
	20·3	20·9	20·7	20·8	20·8	20·5
	20·2	21·0	20·9	20·9	20·9	20·7
	20·3	20·9	20·9	20·8	20·9	20·6
25·0	25·0	26·1	26·0	26·0	26·1	25·0
	25·0	26·2	25·7	26·0	26·0	25·4
	25·0	26·3	25·9	26·0	26·1	25·1
	25·1	26·4	25·9	26·0	26·0	25·0

N.B. Similar tables were drawn up for loads up to 40tons.

APPENDIX VI.

Results of Eccentricity Test Using Two Proving Rings.

LOAD BLOCK No.6.

Position of Top Plate	Pressure Gauge (Tons)	Ring'A'. (Tons)	Ring'B'. (Tons)	Ratio of Loads	Total Load (Tons)	Difference for Calibration
No specific position.	4·0	1·75	2·13	+1·21	3·88	-0·1
	8·0	3·51	4·10	+1·17	7·61	-0·4
	12·0	5·33	5·94	+1·11	11·27	-0·7
	16·0	7·15	7·80	+1·09	14·95	-1·0
Side'B' raised half a turn	4·0	2·10	1·67	-1·26	3·77	-0·2
	8·0	4·02	3·52	-1·14	7·54	-0·4
	12·0	5·89	5·41	-1·09	11·30	-0·7
	16·0	7·70	7·26	-1·06	14·96	-1·0
Side'B' lowered again a half turn	4·0	1·70	2·01	+1·18	3·70	-0·3
	8·0	3·51	3·92	+1·12	7·43	-0·6
	12·0	5·36	5·85	+1·09	11·20	-0·8
	16·0	7·14	7·66	+1·07	14·80	-1·2

N.B. Positive sign before 'load ratio' means that proving Ring'B' carries the heavier load.

Negative sign before 'load ratio' means that proving Ring'A' carries the heavier load.

APPENDIX VI.(Cont'd.)

Results of Eccentricity Test Using Two Proving Rings.

LOAD BLOCK No.1.

Position of Top Plate	Pressure Gauge (Tons)	Ring'A' (Tons)	Ring'B' (Tons)	Ratio of Loads	Total Load (Tons)	Difference for Calibration
Horizontal	4·0	1·64	1·44	-1·14	3·08	-0·9
	8·0	3·62	3·29	-1·10	6·91	-1·1
	12·0	5·55	5·14	-1·08	10·69	-1·3
	16·0	7·65	7·16	-1·07	14·81	-1·2
Parallel to plane of base plate	4·0	1·59	1·73	+1·09	3·32	-0·7
	8.0	3·62	3·81	+1·05	7·43	-0·6
	12·0	5·60	5·77	+1·03	11·37	-0·6
	16·0	7·59	7·79	+1·03	15·38	-0·6

LOAD BLOCK No.2.

Position of Top Plate	Pressure Gauge (Tons)	Ring'A' (Tons)	Ring'B' (Tons)	Ratio of Loads	Total Load (Tons)	Difference for Calibration
Horizontal	4·0	1·87	1·62	-1·15	3·49	-0·5
	8·0	3·74	3·46	-1·08	7·20	-0·8
	12·0	5·71	5·25	-1·09	10·96	-1·0
	16·0	7·65	7·21	-1·06	14·86	-1·1
Parallel to plane of base plate	4·0	1·76	1·62	-1·09	3·38	-0·6
	8·0	3·74	3·58	-1·04	7·32	-0·7
	12·0	5·66	5·43	-1·04	11·09	-0·9
	16·0	7·53	7·33	-1·03	14·86	-1·1

N.B. The above type of test was carried out on all the load blocks.

APPENDIX VII.

Gauge Factors for 1st. Specimen, Initial Position in Machine.

LOAD STAGE	GAUGE	1	2	3	4	5	6
60	A	-	0·79	0·76	0·80	0·80	0·95
	C	-	0·80	0·82	0·81	0·79	0·85
	X	-	1·84	1·67	1·36	1·18	0·95
	Z	-	1·28	1·24	1·26	1·44	1·57

LOAD STAGE	GAUGE	1	2	3	4	5	6
66	A	-	0·85	0·85	0·82	0·81	0·89
	C	-	0·87	0·82	0·81	0·77	0·81
	X	-	2·09	1·65	1·35	1·15	0·89
	Z	-	1·37	1·27	1·26	1·35	1·44

LOAD STAGE	GAUGE	1	2	3	4	5	6
67	A	-	0·92	0·93	0·85	0·81	0·90
	C	-	0·93	0·86	0·83	0·77	0·81
	X	-	2·44	1·71	1·36	1·14	0·91
	Z	-	1·58	1·36	1·30	1·38	1·46

LOAD STAGE	GAUGE	1	2	3	4	5	6
68	A	-	0·90	0·93	0·85	0·81	0·94
	C	-	0·91	0·84	0·82	0·76	0·80
	X	-	2·34	1·69	1·35	1·13	0·91
	Z	-	1·50	1·34	1·31	1·38	1·47

FINAL SELEC-TION	GAUGE	1	2	3	4	5	6
	A	-	0·90	0·92	0·84	0·81	0·90
	C	-	0·91	0·84	0·83	0·77	0·81
	X	-	2·34	1·68	1·35	1·14	0·91
	Z	-	1·50	1·34	1·30	1·38	1·46

APPENDIX VII.(Cont'd.)

Gauge Factors for 1st. Specimen, Final Position in Machine.

	GAUGE	1	2	3	4	5	6
LOAD STAGE 16	A	-	1·08	1·06	1·01	0·95	0·88
	C	-	1·01	0·94	0·95	0·80	0·81
	X	-	2·65	1·29	1·04	1·19	0·95
	Z	-	1·70	1·45	1·30	1·10	1·34

	GAUGE	1	2	3	4	5	6
LOAD STAGE 17	A	-	0·96	1·01	0·98	1·01	0·91
	C	-	0·88	0·94	0·94	0·82	0·87
	X	-	1·97	1·15	0·99	1·08	1·01
	Z	-	1·34	1·33	1·27	1·07	1·25

	GAUGE	1	2	3	4	5	6
LOAD STAGE 20	A	-	0·92	0·99	0·99	0·94	0·91
	C	-	0·86	0·93	0·95	0·82	0·88
	X	-	1·67	1·11	0·98	1·01	1·00
	Z	-	1·24	1·30	1·27	1·07	1·24

	GAUGE	1	2	3	4	5	6
LOAD STAGE 38	A	-	1·05	1·10	1·05	0·94	0·95
	C	-	0·95	1·00	0·99	0·85	0·95
	X	-	2·20	1·15	0·99	0·94	0·86
	Z	-	1·34	1·36	1·28	1·00	1·24

	GAUGE	1	2	3	4	5	6
FINAL SELEC-TION	A	-	1·03	1·08	1·03	0·95	0·92
	C	-	0·86	0·93	0·95	0·82	0·87
	X	-	1·67	1·11	0·99	1·05	1·00
	Z	-	1·24	1·30	1·27	1·07	1·25

APPENDIX VII. (Cont'd.)

Gauge Factors for Second Specimen.

	GAUGE	1	2	3	4	5	6
LOAD STAGE 8	A	1·67	1·33	1·06	1·14	1·19	1·15
	C	0·83	1·16	0·86	0·89	1·01	1·16
	X	0·71	1·06	0·87	0·95	1·03	-
	Z	0·71	1·29	1·01	0·88	0·93	1·06

	GAUGE	1	2	3	4	5	6
LOAD STAGE 10	A	-	1·25	1·10	1·11	1·12	1·14
	C	0·78	1·07	0·90	0·86	0·93	1·14
	X	0·78	0·95	0·81	0·86	0·98	-
	Z	1·00	1·08	0·93	0·81	0·85	1·03

	GAUGE	1	2	3	4	5	6
LOAD STAGE 11	A	-	1·37	1·09	1·14	1·16	1·15
	C	0·75	1·13	0·91	0·90	0·96	1·17
	X	0·86	0·96	0·86	0·90	0·99	-
	Z	0·86	1·16	0·96	0·86	0·88	1·04

	GAUGE	1	2	3	4	5	6
FINAL SELEC-TION	A	-	1·32	1·08	1·13	1·16	1·15
	C	0·79	1·12	0·89	0·88	0·97	1·16
	X	0·78	0·99	0·85	0·90	1·00	-
	Z	0·86	1·17	0·97	0·85	0·89	1·04

APPENDIX VIII.

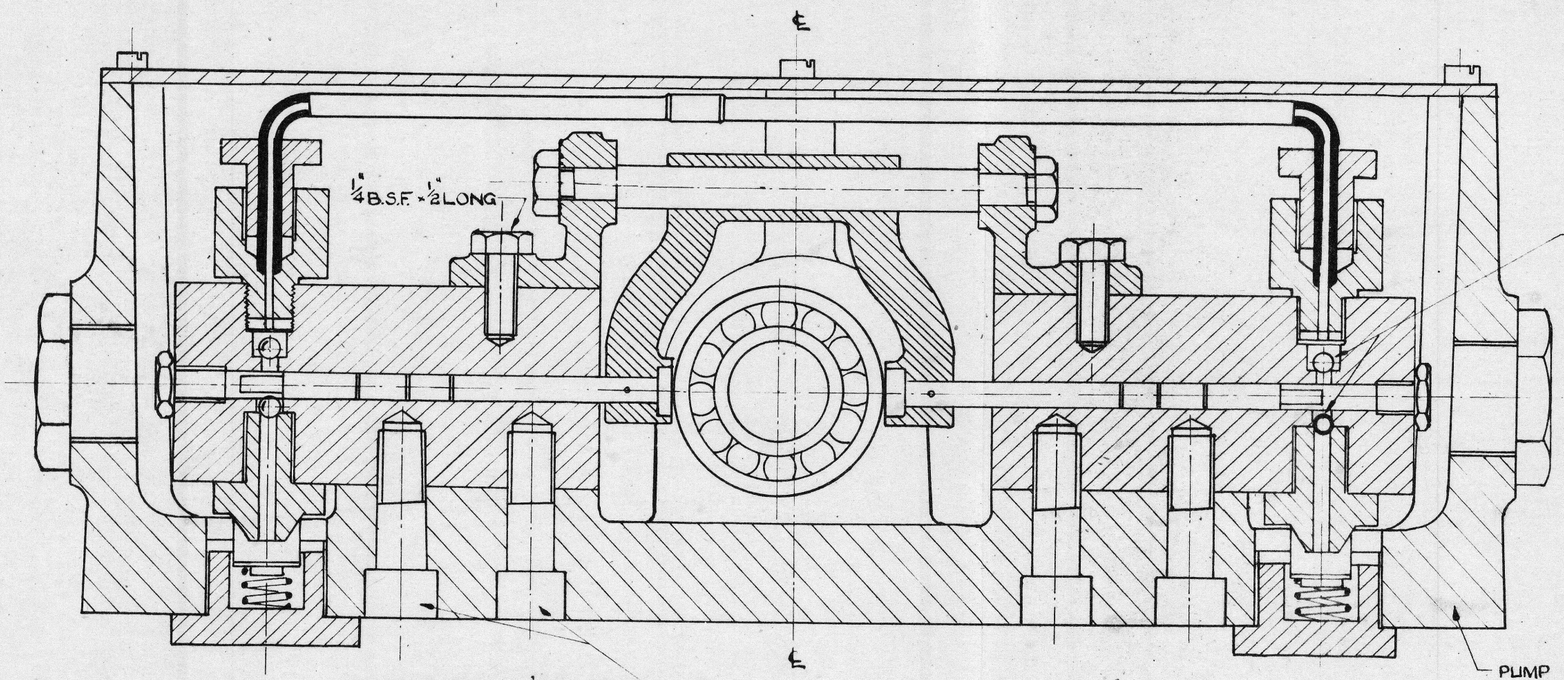
Gauge Factors for Central Banks of Second Specimen.

	GAUGE	1	2	3	4	5	6
LOAD STAGE 16	B	1·62	0·87	1·00	0·99	1·00	1·00
	Y	0·91	1·02	1·01	0·97	1·01	0·99

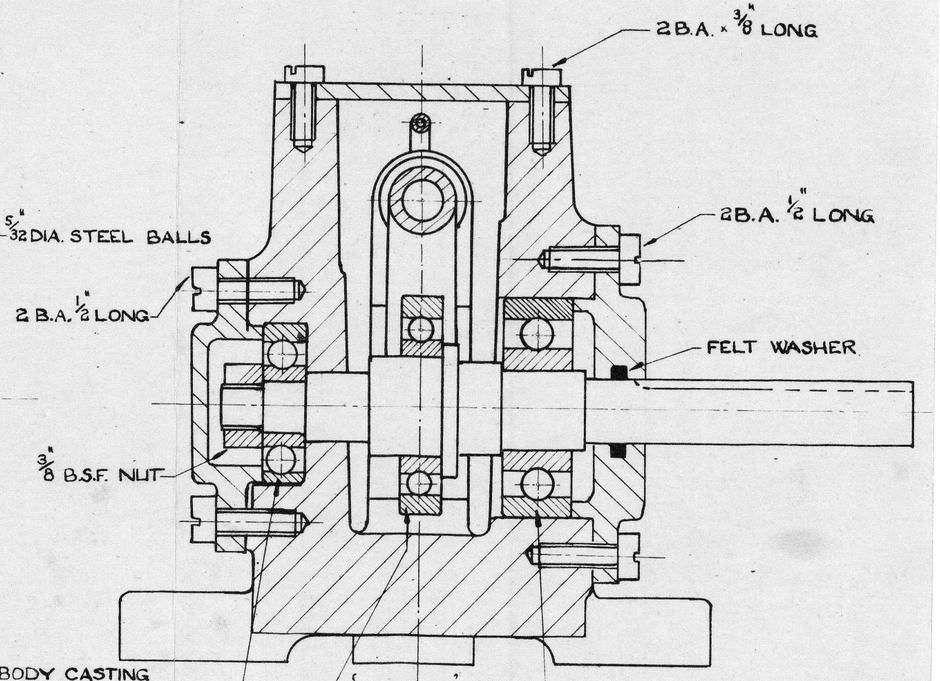
	GAUGE	1	2	3	4	5	6
LOAD STAGE 18	B	0·84	0·92	1·05	1·00	0·98	1·15
	Y	0·91	1·02	1·00	0·98	1·02	1·12

	GAUGE	1	2	3	4	5	6
LOAD STAGE 20	B	0·91	0·97	1·05	1·00	0·99	1·01
	Y	0·93	1·06	1·03	0·98	1·03	0·99

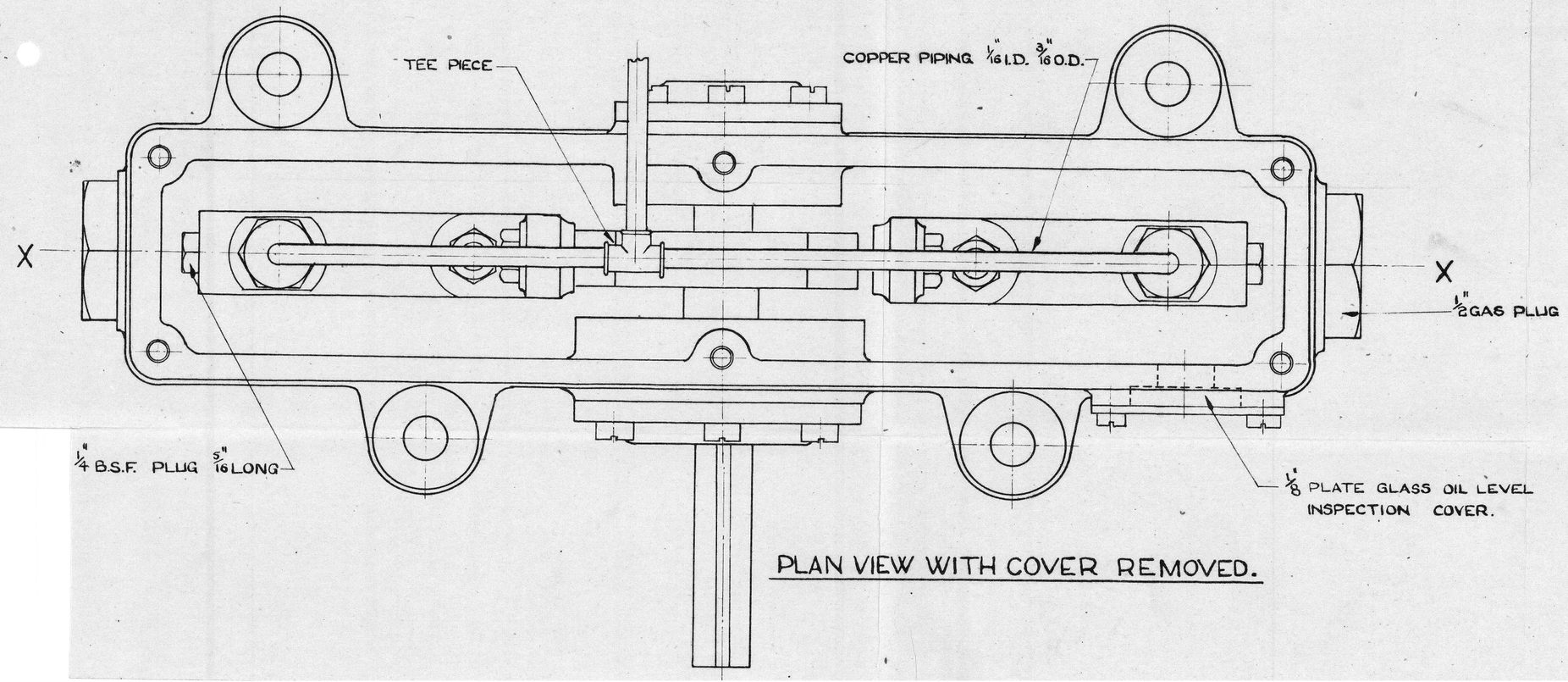
	GAUGE	1	2	3	4	5	6
FINAL SELEC-TION.	B	0·91	0·95	1·04	1·00	1·00	1·00
	Y	0·92	1·05	1·02	0·98	1·03	1·00



SECTIONAL ELEVATION ON 'XX.'

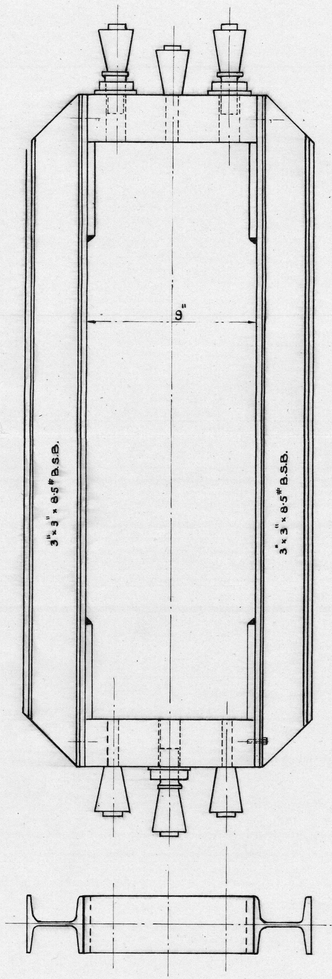


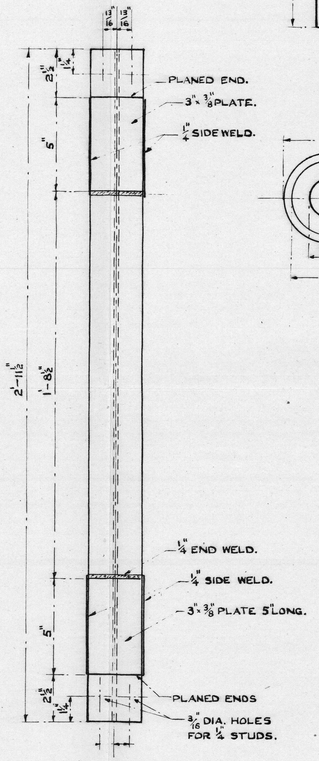
SECTION ON ℄.



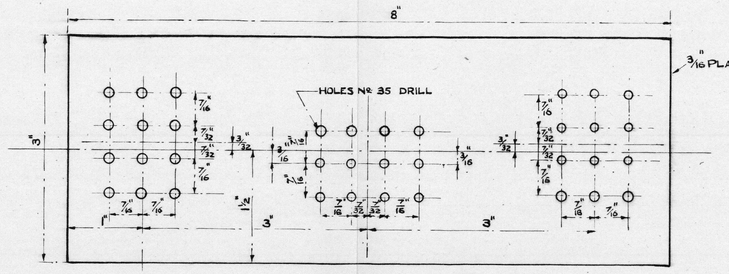
PLAN VIEW WITH COVER REMOVED.

MAT'L	CASTINGS ETC.	CIVIL ENGINEERING DEPARTMENT CITY AND GUILDS COLLEGE EXHIBITION RD. LONDON S.W.7	
DRN. BY	R.W.S.		
No OFF	6	SCALE	FULL SIZE
GENERAL ASSEMBLY H.P. PUMP.			
DATE: 25.10.50		DRG. No.	

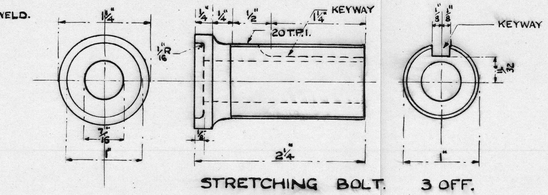




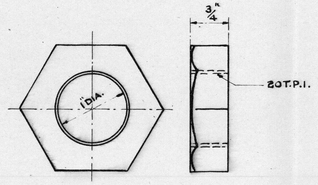
STRECHING FRAME ASSEMBLY.



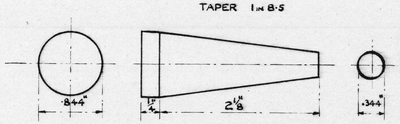
WIRE SPACING PLATE.
TWO OFF.



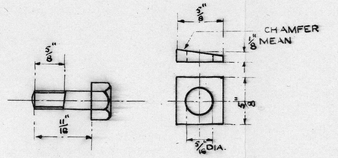
STRETCHING BOLT. 3 OFF.



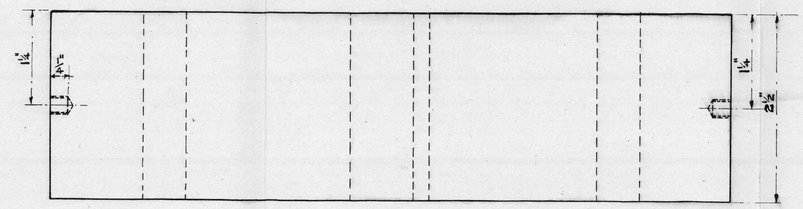
1" DIA. NUT AND WASHER
3 OFF.

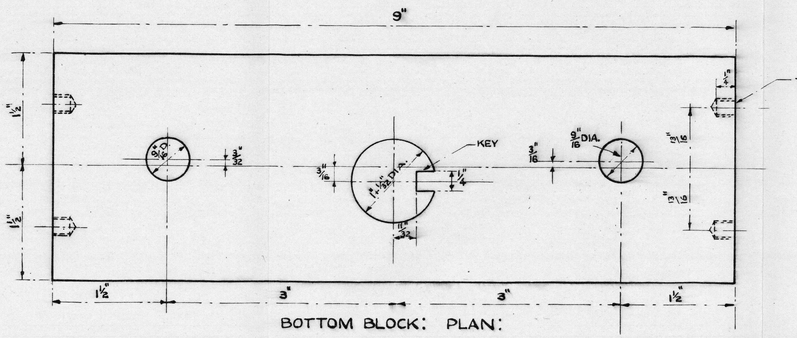


CASE HARDENED WEDGES.
6 OFF.

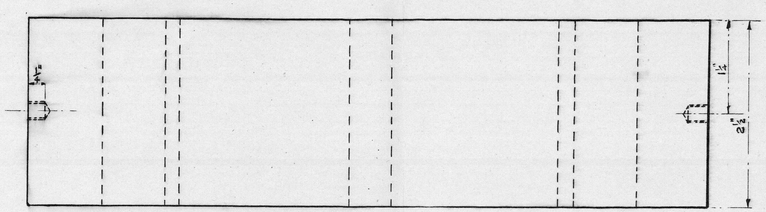


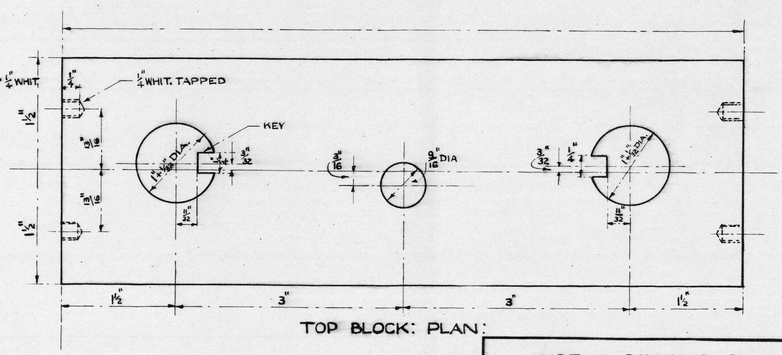
8 No. 1/4 WHIT. STUDS AND WASHERS.





BOTTOM BLOCK: PLAN.





TOP BLOCK: PLAN.

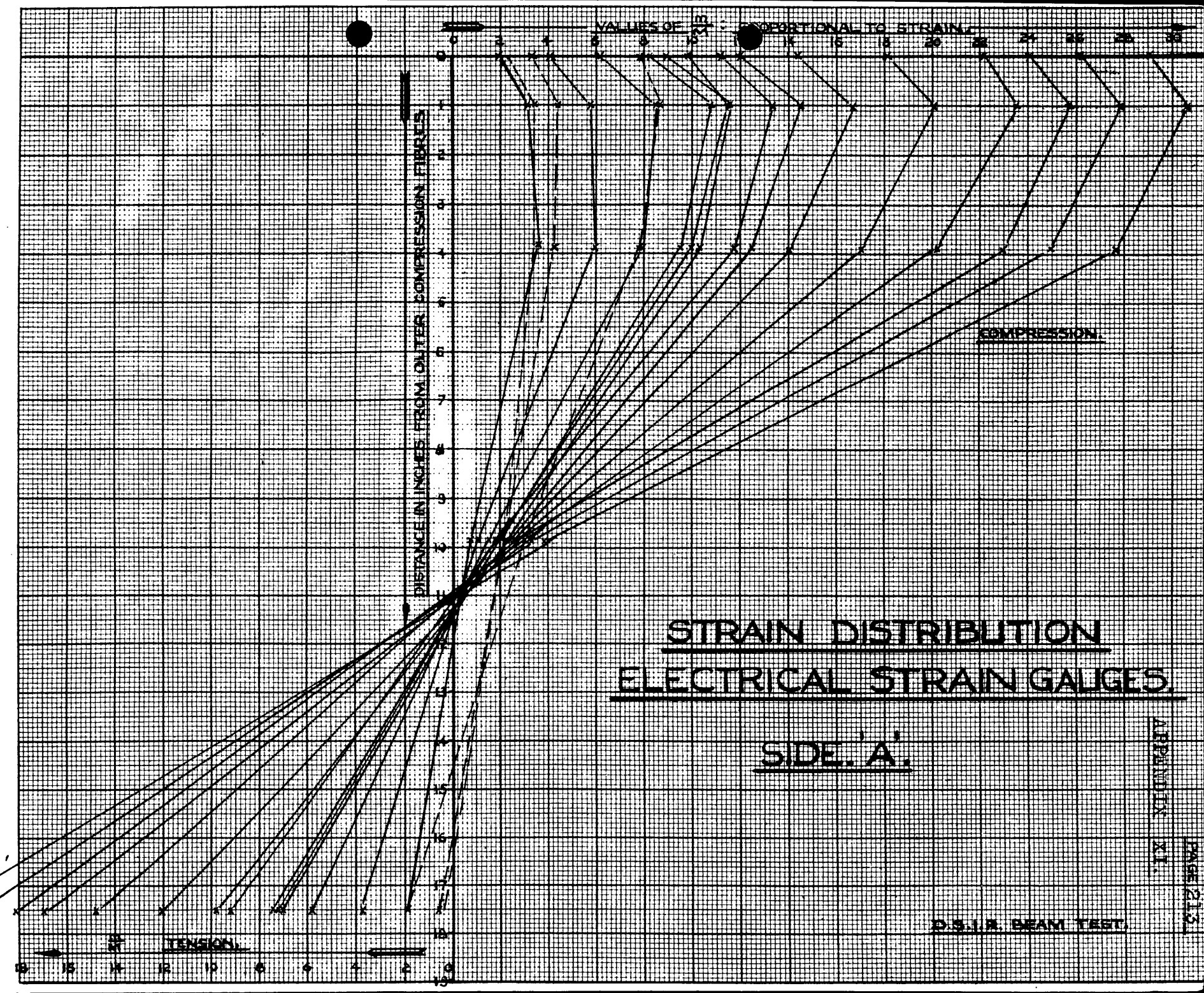
WIRE STRECHING FRAME

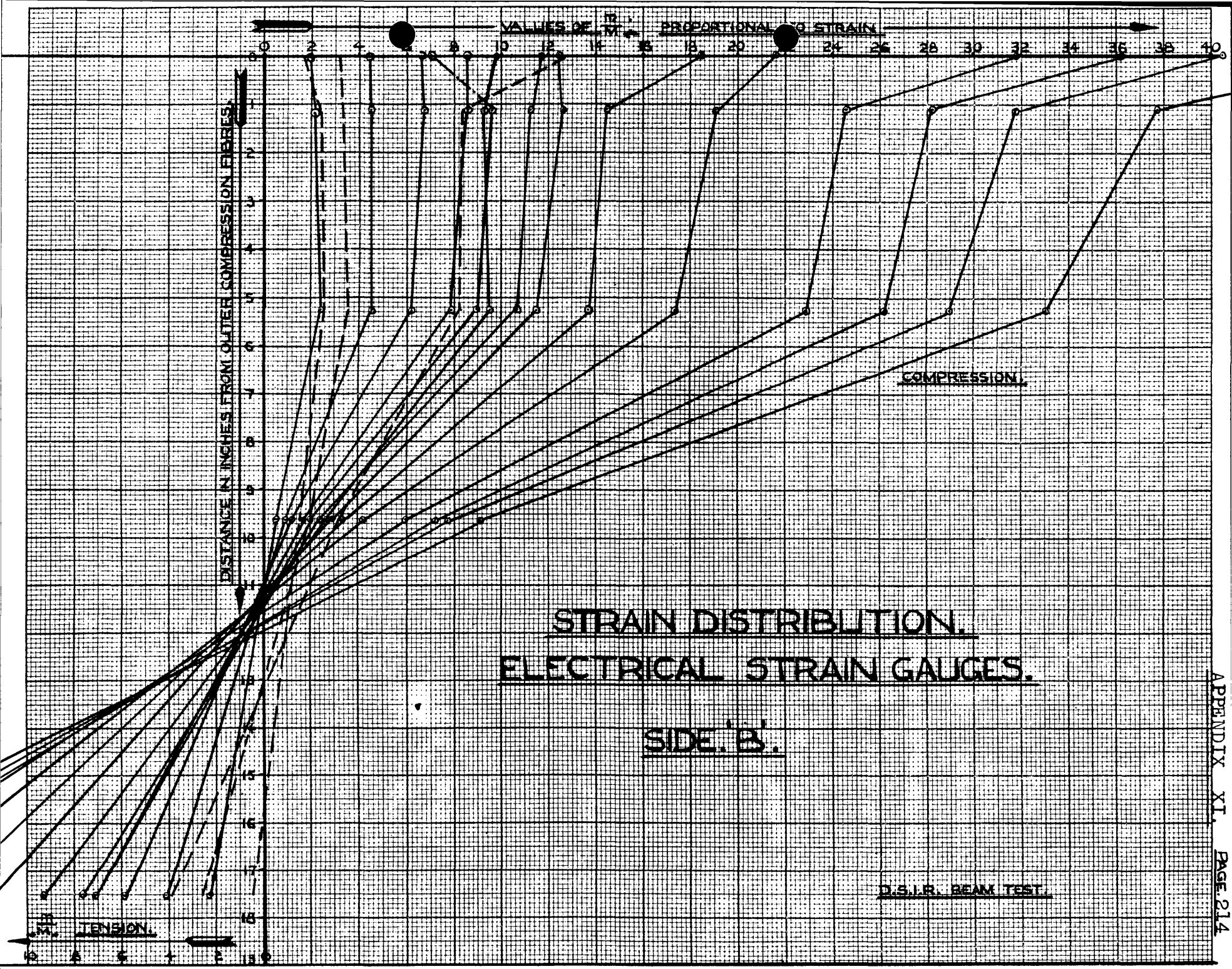
DRAWN BY: R.W. SMITHIES. DATE: JUNE 1950

SCALES: 1/4 AND FULL SIZE:

CIVIL ENGINEERING DEPT. CITY AND GUILDS COLLEGE.

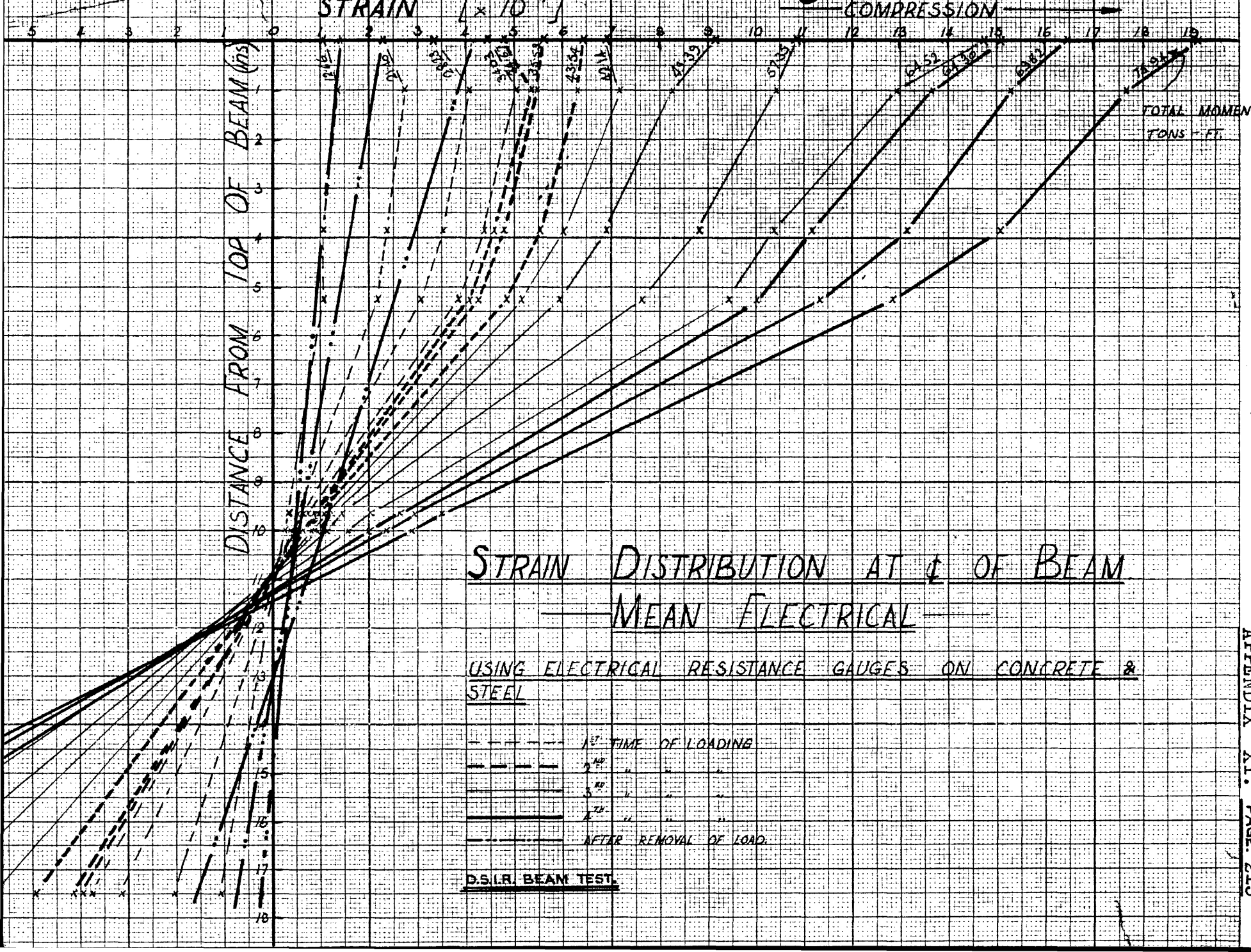
EXHIBITION ROAD. LONDON. S.W.7.

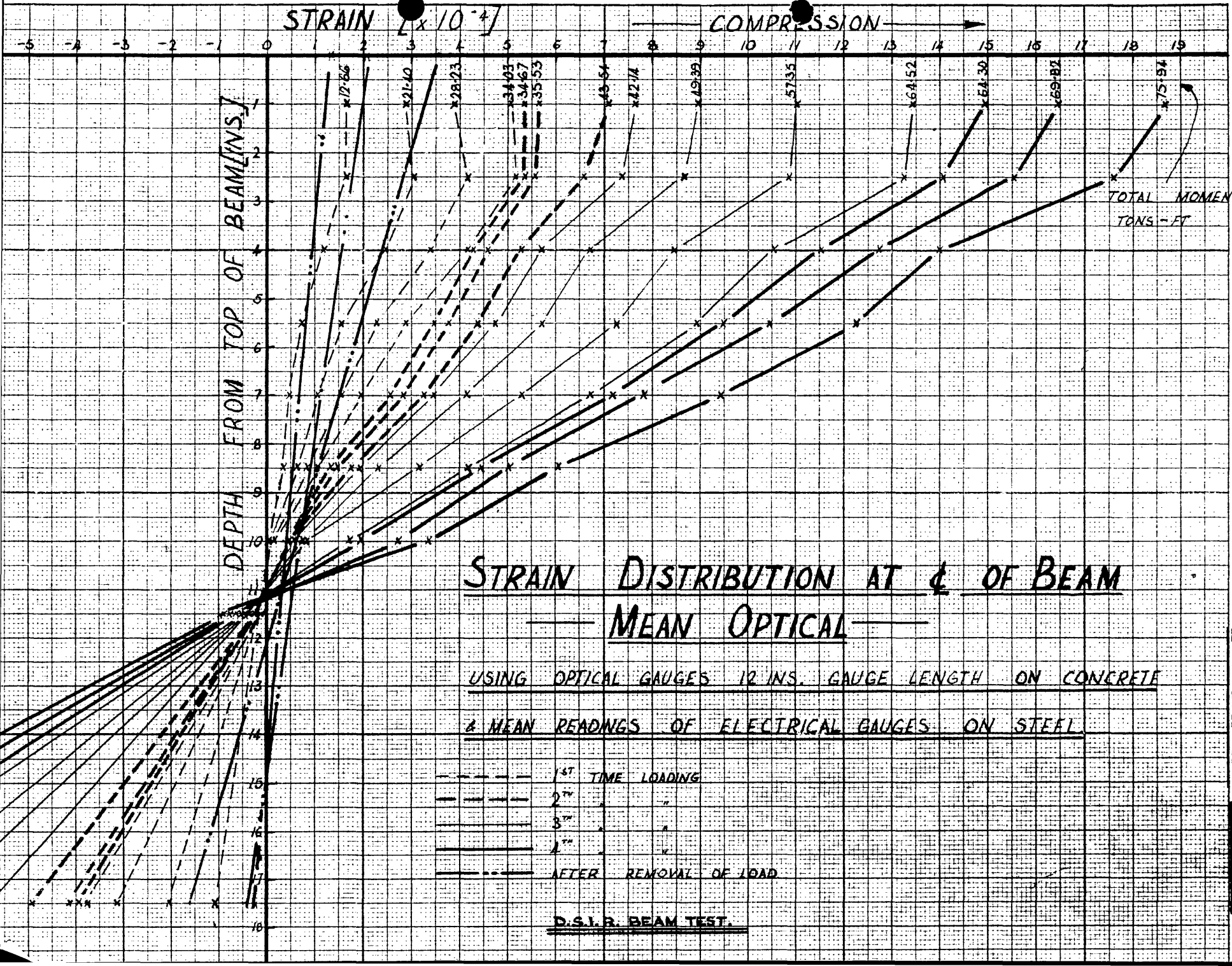

VALUES OF $\frac{M}{I}$ PROPORTIONAL TO STRAIN
DISTANCE IN INCHES FROM OUTER COMPRESSION FIBRES
COMPRESSION.
TENSION.
$\frac{M}{I}$
STRAIN DISTRIBUTION
ELECTRICAL STRAIN GAUGES.
SIDE 'A'.
D.S.I.R. BEAM TEST.
FIG. 21.
PAGE 213.

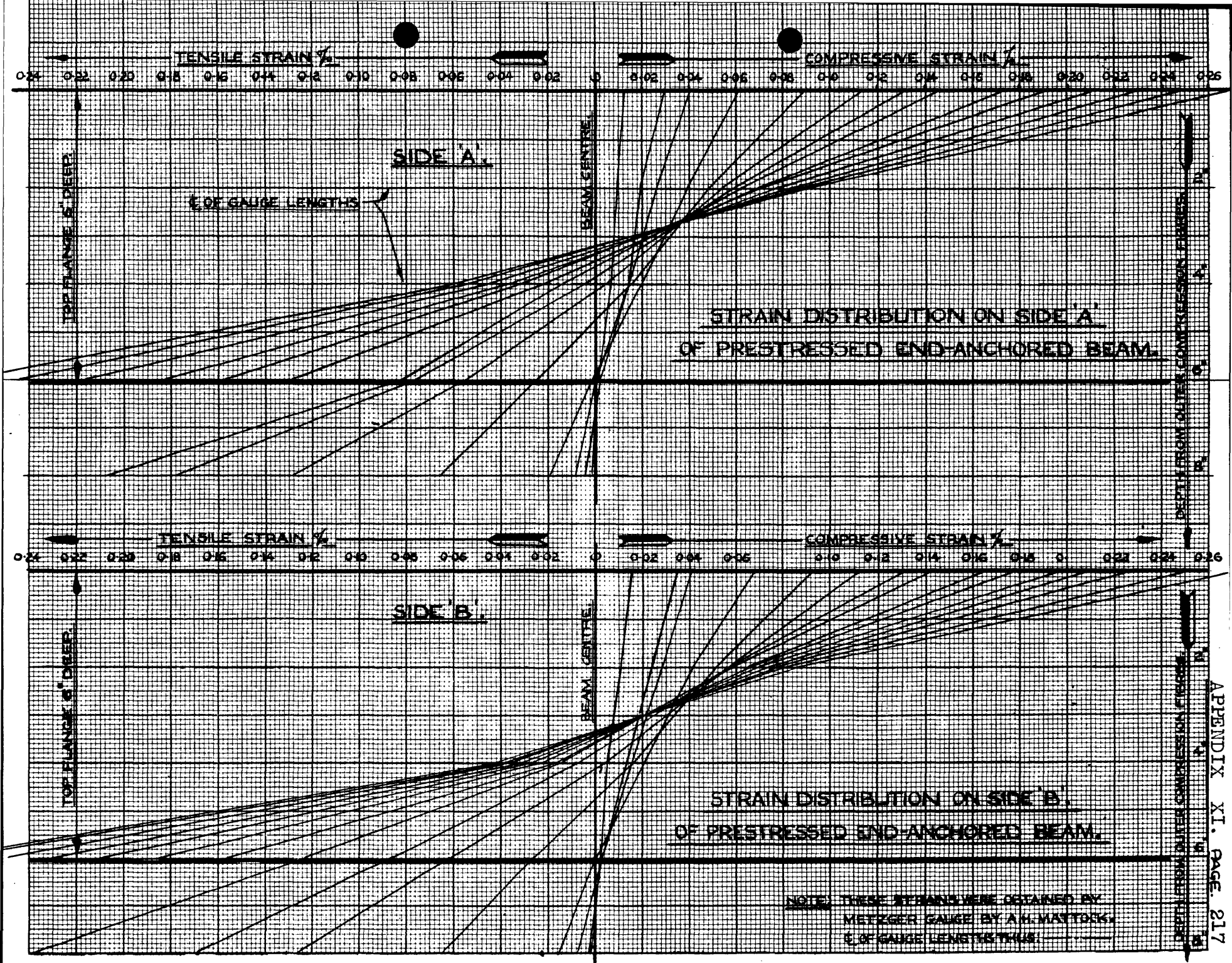


STRAIN DISTRIBUTION.
ELECTRICAL STRAIN GAUGES.
SIDE 'B'.

D.S.I.R. BEAM TEST.


STRAIN { x 10⁻⁶ }
COMPRESSION
TOTAL MOMENT TONS - FT.
DISTANCE FROM TOP OF BEAM (ins)
STRAIN DISTRIBUTION AT ℄ OF BEAM
MEAN ELECTRICAL
USING ELECTRICAL RESISTANCE GAUGES ON CONCRETE & STEEL
1ST TIME OF LOADING
2ND " " " "
3RD " " " "
4TH " " " "
AFTER REMOVAL OF LOAD.
D.S.I.R. BEAM TEST.


STRAIN [x 10⁻⁴]
COMPRESSION
DEPTH FROM TOP OF BEAM [INS.]
TOTAL MOMENT TONS-FT
×12·26
×21·40
×28·23
×34·03
×34·67
×35·53
×43·54
×42·14
×49·39
×57·35
×64·52
×64·30
×69·82
×75·84
STRAIN DISTRIBUTION AT ℄ OF BEAM
— MEAN OPTICAL —
USING OPTICAL GAUGES 12 INS. GAUGE LENGTH ON CONCRETE
& MEAN READINGS OF ELECTRICAL GAUGES ON STEEL
1ST TIME LOADING
2ND " "
3RD " "
4TH " "
AFTER REMOVAL OF LOAD
D.S.I.R. BEAM TEST.


TENSILE STRAIN %
COMPRESSIVE STRAIN %
SIDE 'A'.
℄ OF GAUGE LENGTHS
TOP FLANGE 'A' DEEP
BEAM CENTRE
DEPTH FROM OUTER COMPRESSION FIBRE
STRAIN DISTRIBUTION ON SIDE 'A'
OF PRESTRESSED END-ANCHORED BEAM.
TENSILE STRAIN %
COMPRESSIVE STRAIN %
SIDE 'B'.
TOP FLANGE 'B' DEEP
BEAM CENTRE
DEPTH FROM OUTER COMPRESSION FIBRE
STRAIN DISTRIBUTION ON SIDE 'B'
OF PRESTRESSED END-ANCHORED BEAM.
NOTE: THESE STRAINS WERE OBTAINED BY
METZGER GAUGE BY A.H. MATTOCK.
℄ OF GAUGE LENGTHS THUS: ——

TENSILE STRAIN %

COMPRESSIVE STRAIN %

0·24 0·20 0·16 0·12 0·08 0·04 0·00 0·04 0·08 0·12 0·16 0·20 0·24

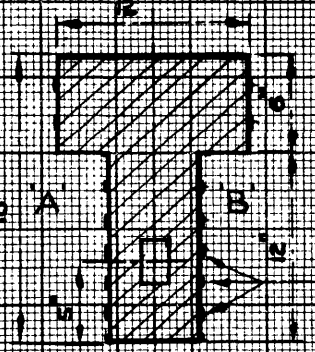
TOP "A" AND "B" BEAM

DEPTH FROM TOP OF BEAM IN INCHES

0" 2" 4" 6" 8" 10" 12" 14" 16" 18"

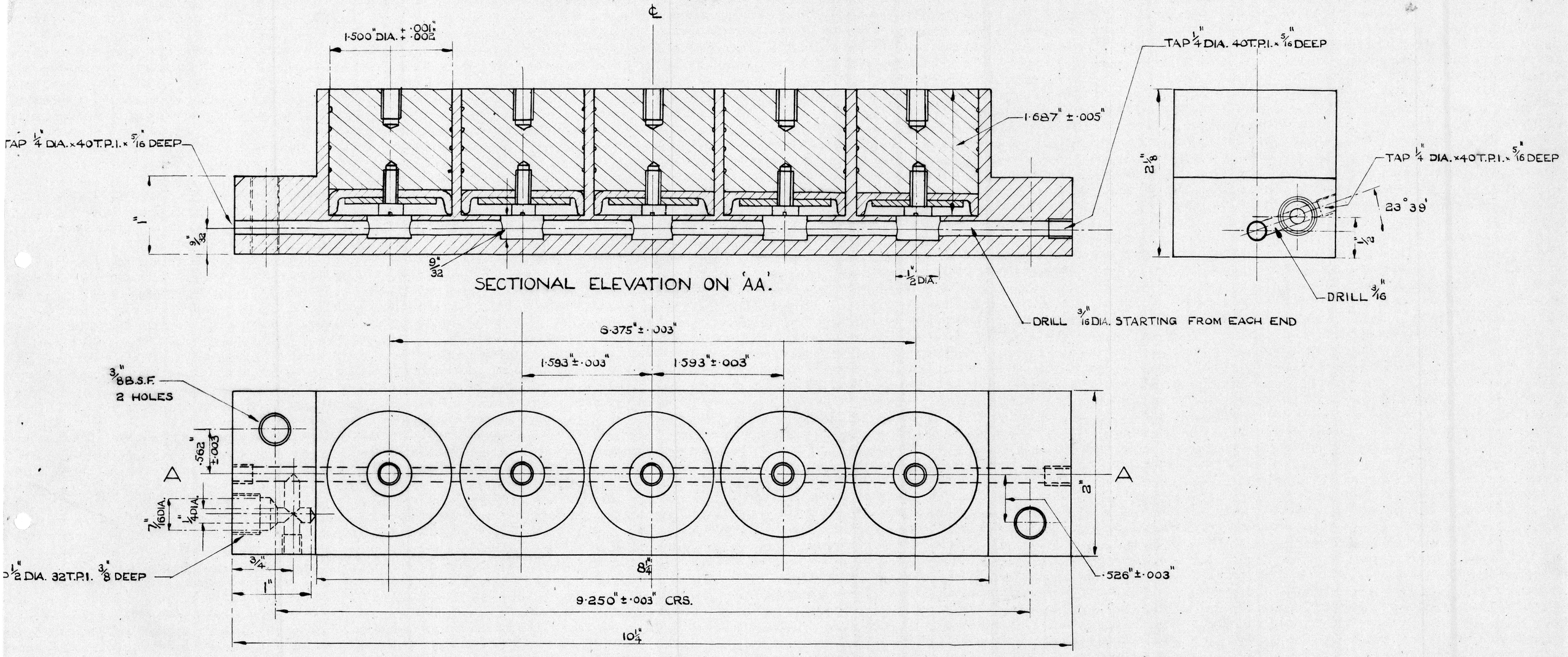
MID-SPAN

MEAN STRAIN DISTRIBUTION FOR END-ANCHORED PRE-STRESSED BEAM.



MID-SPAN CROSS-SECTION.

NOTE: THESE STRAINS WERE OBTAINED BY METZGER GAUGE BY A.H. MATTOCK. ℄ OF GAUGE LENGTHS THUS ——



MAT'L	EN. 16 OR ST. S.	CIVIL ENGINEERING DEPARTMENT
DR'N BY	R.W.S.	CITY AND GUILDS COLLEGE
		EXHIBITION RD. LONDON S.W.7.

TABLE 6 : 1

Name of Dam	Green Mountain		Anderson Ranch			Granby		Alcova		
Zone	1	2	1	2	3	1	3	1	2	3
Clay fraction %	8.5	5.9	13.8	3.5	3.5	8.2	1.0	14.0	-	-
- 200 mesh %	20.7	12.3	35.2	10.5	3.6	27.1	2.0	45.3	38.3	-
- ¼ in. %	64.8	49.2	89.9	57.5	40.1	72.8	48.0	97.2	95.1	-
Maximum size - inches	3	3	5	5	5	5	12	5	12	-
Dry density (- ¼") lb/cu. ft	132.2	126.6	120.4	125.0	116.2	126.8	-	122.9	122.6	126.3
Water content %.	8.4	9.4	12.4	10.7	9.9	9.1	-	10.8	10.1	7.9
Permeability ft/year	0.09	35.1	0.05	177.0	240.0	0.08	163.0	0.24	6.50	50.0
Specific gravity	2.71	2.66	2.63	2.63	2.63	2.66	2.61	2.63	2.63	-
Weight as placed - lb/cu. ft	151.9	153.3	138.7	150.1	150.7	146.0	150.3	137.0	136.5	-
c' lb/sq. ft	800	-	800	-	-	1,280	-	930	-	-
tan Ø'	0.70	0.70	0.70	0.70	0.70	0.66	0.66	0.68	0.68	-
F (lowest value)	1.31		1.90			1.52		1.67		
Pore pressure as % of weight of bank	45.3		38.2 - 39.1			35.4 - 39.2		26.0		